AD-764 114

PEOPLE SURVIVABILITY IN A DIRECT EFFECTS ENVIRONMENT AND RELATED TOPICS

A. Longinow, et al

IIT Research Institute

Prepared for:

Defense Civil Preparedness Agency

May 1973

IIT RESEARCH INSTITUTE

PEOPLE SURVIVABILITY IN A DIRECT EFFECTS ENVIRONMENT AND RELATED TOPICS

Final Report

DCPA Contract DAHC 20-68-C-0125
Work Unit 2614D

May 1973

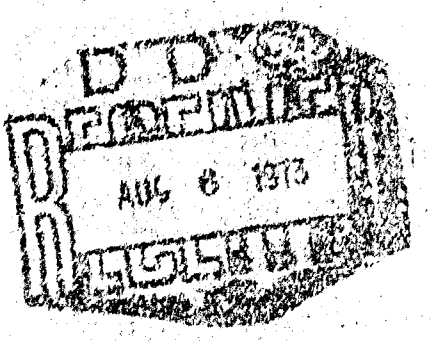

Approved for public release;
distribution unlimited.

SUMMARY

1. INTRODUCTION

This report contains a description of a deterministic, computerized method (simulation model) for predicting the survivability (relative safety) of people located in conventional (NFSS) buildings when subjected to the direct effects of nuclear weapons. Effects considered include: thermal radiation, prompt nuclear radiation, primary blast and secondary blast, i.e., the effects of flow velocities and debris. This is an operational tool which has been applied to the analysis of existing buildings which were surveyed in detail.

The report also contains a description of the physical basis supporting this computer program, its computational structure and limits of application. The use of the program is illustrated by means of example problems representing real situations.

Related topics considered in this study include: distribution of blast-initiated debris, shelter-cost and effectiveness comparisons and survivability of people in special permanent and expedient shelters.

2. PEOPLE SURVIVABILITY PREDICTION MODEL

The reason for developing this model is to provide a quick and reliable means for estimating the protection afforded by conventional buildings when subjected to the direct effects of nuclear weapons. The reason for emphasizing conventional buildings is that these structures constitute the only significant, current sheltering resource, not only against the effects of nuclear weapons, but also against natural disasters such as tornados and hurricanes. It is therefore important to have a firm understanding of their protective capabilities.

The current model is a deterministic simulation procedure which is capable of considering buildings in substantial detail

and of predicting numbers of survivors. Its detailed formulation allows the user to consider several data categories, i.e., weapon environment, building characteristics, bodily positions, and distribution of personnel. As such it is useful in determining what building characteristics and modes of evasive action are important in maximizing the numbers of survivors.

The simulation model consists of five parts:

- Data input routine
- Weapon effects generator
- Dose prediction routines
- Casualty estimation routines
- Output routines

Typical input includes the physical description of the building analyzed, i.e., geometry, number of stories, typical room lengths, percent window openings, sill heights, and wall strengths. People may be assumed to be uniformly distributed in standing and/or prone body positions in all or selected portions of the building. The weapon environment is specified by providing the weapon size, height of burst, and range from ground zero. The latter set of data is used by "weapon effects generator" routines to determine the free-field intensity of each effect at the location of the building in question. Each of the free-field effects is then modified by the presence of the building taking into account its geometry and physical properties. The modified free-field effects provide the basis for determining dose relationships for each of the effects considered. Doses predicted are then compared with casualty criteria to determine number of survivors.

The simulation model uses mortality data only and therefore survivors include both the injured and uninjured personnel. Very generally, survivors include those persons who are expected to survive (live) at least one week after the event provided that basic rescue operations are carried out.

This is continuing study, and although the simulation model is operational an attempt is being made to improve its capabilities in several areas. The most important of these is to provide a capability for separating survivors into injured and uninjured categories.

This simulation model was applied to a people survivability analysis of 25 existing buildings which were surveyed in detail.* Sample results of this analysis effort are included in the report. Results indicate the importance of collecting appropriate building data and the taking of evasive action by the building occupants.

3. DISTRIBUTION OF BLAST-INITIATED DEBRIS

Combustible (burning) building debris located over or in proximity to basement shelters may constitute a major hazard to shelter occupants. In such an environment casualties may be produced as a result of flame exposure, smoke, toxic gases, and temperature gradients. Duration and intensity of these effects at any given location depends on the composition, size, and distribution of the ignited debris pile.

Currently very little usable information exists on realistic distributions of urban debris. Studies performed to date can be divided into two categories, i.e., those which were primarily concerned with gross distributions of debris, taking into account large urban areas and numerous building types and those concerned with specific cases of debris information. The latter category includes numerous experimental (field) studies. Although many debris studies have been performed in the past, none of these were concerned with the specific makeup of debris piles at the local level, i.e., in the vicinity of various buildings containing shelters.

*Longinow, A. and Ojdrovich, G., "Survivability in a Direct Effects Environment (Analysis of 25 NFSS Buildings)" Contract DAHC 20-72-C-0318, IIT Research Institute Project J6271, January 1973.

A portion of this study was devoted to the task of predicting the distribution of building debris including structural components and building contents.

The analysis method uses a deterministic free-flight model which traces the trajectory of each debris piece from the time of separation (rupture) to the time it comes to rest downrange from its original position. The primary mechanism producing horizontal transport is due to aerodynamic forces generated by the blast wind. Vertical motion results from aerodynamic lift forces and gravity. The model considers impact with ground surface, the possibility of bounce and subsequent free flight. This is the first debris transport model capable of treating buildings in detail. As such it is also useful in predicting overall debris profiles for the purpose of determining the extent of debris clearance operations.

This model was applied to the analysis of a two-story frame building located at the 5 psi range of a 1 MT nuclear weapon. Results of the analysis are described in Chapter 3. In this particular example, structural debris became distinctly segregated from the building contents.

4. COST AND SURVIVABILITY ANALYSIS

Chapter 4 contains a cost and people survivability comparison between a slanted basement and a corresponding abovegrade shelter. Both shelters have equal floor areas and are assumed to be located in identical buildings which were completely designed and costed in the course of this study. The two parent buildings are one-story steel frame and masonry structures commonly used as small office buildings or medical centers. Cost and people survivability estimates are given for these four cases:

- Conventional buildings without basement
- Conventional building (no basement) with a 15 psi (design) dual-use shelter integral with the parent structure.
- Conventional building with a partial basement
- Conventional building with a dual-use partial basement shelter - 15 psi (design).

Results indicate that the hardened basement shelter is less costly and survivabilitywise superior to the aboveground hardened shelter.

5. ANALYSIS OF SPECIAL PERMANENT AND EXPEDIENT SHELTERS

In the context of this discussion special permanent shelters are defined as those which may be constructed by individuals with direct effects and/or fallout radiation protection in mind. This may include a concrete block basement shelter, a wooden lean-to basement shelter or a small neighborhood shelter separate from private dwellings.

Expedient shelters may be defined as those structures which are capable of being constructed within a relatively short period of time by unskilled or semiskilled labor using little or no specialized equipment. Such shelters are important in an evacuation mode. However their effective use requires a substantial preplanning and prestocking effort.

A fair number of different shelter concepts in both categories exist at this time. Eight of these were chosen and analyzed in the course of this study. Analytic results are described in Chapter 5 of this report.

IIT Research Institute
10 West 35th Street
Chicago, Illinois 60616

IITRI Project J6144

Final Report

PEOPLE SURVIVABILITY IN A DIRECT EFFECTS ENVIRONMENT AND RELATED TOPICS

Contract DAHC 20-68-C-0126
DCPA Work Unit 1614D

by

A. Longinow
G. Ojdrovich
L. Bertram
A. Wiedermann

Approved for Public Release;
Distribution Unlimited

DCPA Review Notice

"This report has been reviewed in the Defense Civil Preparedness Agency and approved for publication. Approval does not signify that the contents necessarily reflect the views and policies of the Defense Civil Preparedness Agency."

for

Defense Civil Preparedness Agency
Washington, D.C. 20310

May 1973

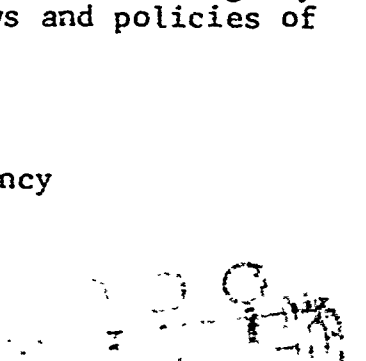

FOREWORD

This is the final report on IITRI Project J6144 entitled "People Survivability in a Direct Effects Environment and Related Topics." The work reported herein was performed for the Shelter Research Division, Defense Civil Preparedness Agency under Contract DAHC 20-68-C-0126, Work Unit 1614D. It was monitored by Mr. C. D. Kepple, Mr. G. N. Sisson and Mr. D. A. Bettge of the Shelter Research Division, DCPA.

The study was conducted in the Structural Analysis Section, Engineering Mechanics Division of IIT Research Institute (IITRI). IITRI personnel involved in this study include A. Longinow, G. Ojdrovich and A. Wiedermann. Outside consultants include Dr. L. Bertram of the Department of Mechanics, Iowa State University, who developed the methodology for predicting the blast loading on building occupants (Appendix B); and Mr. G. A. Kennedy of George A. Kennedy and Associates, Inc., Chicago, Ill., who provided cost data and environmental systems designs for the comparative study reported in Chapter 4.

Respectfully submitted,
IIT RESEARCH INSTITUTE

A. Longinow
Manager
Structural Analysis

APPROVED:

M. R. Johnson
Assistant Director
Engineering Mechanics Division

ABSTRACT

This report describes a deterministic, computerized methodology for predicting the survivability (relative safety) of people located in conventional (NFSS) buildings when subjected to the direct effects of megaton range nuclear weapons. Individual effects considered include thermal radiation, prompt nuclear radiation, primary and secondary blast and debris. The computational process is described and illustrated by means of example problems.

Related topics include: distribution of blast-initiated debris, analysis of special permanent and expedient shelters relative to blast effects and a cost and survivability comparison of above- and below-grade shelters.

CONTENTS

CONTENTS (Contd)

CONTENTS (Contd)

CONTENTS (Concl)

ILLUSTRATIONS

ILLUSTRATIONS (Contd)

ILLUSTRATIONS (Concl)

TABLES

CHAPTER 1

STUDY BASIS

1.1 INTRODUCTION

This chapter provides the basis for and a discussion of IITRI Project J6144, DCPA Work Unit 1614D, whose primary objective was to develop a computerized simulation model capable of predicting the survivability (relative safety) of people located in conventional buildings when subjected to the direct effects of nuclear weapons. Subsidiary, related topics considered in this study include:

- Distribution of Blast-Initiated Debris
- Shelter Cost and Effectiveness Comparisons
- People Survivability in Expedient Shelters

All of these topics are discussed briefly in this chapter and are presented in detail in succeeding chapters of this report.

1.2 DEVELOPMENT OF PEOPLE SURVIVABILITY PREDICTION MODEL

1.2.1 Development Basis

The reason for developing this model is to provide a quick and reliable means for assessing the protection afforded by conventional buildings and primarily by those which contain substantial numbers of people for significant portions of the day. This latter category includes most if not all of the National Fallout Shelter Survey (NFSS) structures.

The reason for emphasizing conventional buildings is that these structures constitute the only significant current sheltering resource. Each of them has some level of inherent ability in providing protection, not only against the effects of nuclear weapons, but also against natural disasters such as tornados and hurricanes. It is therefore important to have a firm grasp of their protective capabilities. Although much of the methodology developed in this study is applicable to the

evaluation of the sheltering potential of buildings against natural hazards, the current emphasis is on direct effects which occur in the Mach region of nuclear weapons.

The ultimate usage of results is to provide for reliable on-site assistance at the local level. Results of this study would take the form of a concise building classification scheme which would be used for the rating of buildings in terms of their inherent protective capabilities and thus for the optimum distribution of the local population within them before and after the event.

This simulation model is also capable of performing damage assessment studies and should therefore be used by agencies engaged in such work. The model is a deterministic simulation procedure which is now capable of considering buildings in substantial detail and of predicting people survivability. Its detailed formulation allows the user to consider several data categories (weapon environment, building characteristics, bodily positions and dispersal of personnel). As such it is useful in determining what parameters need to be considered and to what degree of accuracy.

Aside from the input and output portions, this model consists of three parts which can be described as follows:

- Weapons Effects Generator
- Dose Prediction Routines
- Casualty Estimation Routines

For a given weapon size, height of burst and range, the "Weapon Effects Generator" determines the free field intensity of each effect at the location of the building in question. Each of these is then modified by the presence of the building taking into account its geometry, physical properties and bodily positions of personnel. This is done using the various "Dose Prediction" routines. Doses predicted are then compared with casualty criteria to determine percent survivors. The operation of this model is discussed and illustrated by means of examples in Chapter II.

The model uses mortality data only and therefore survivors include both the injured and the uninjured. Very generally, survivors include those persons who are expected to survive (live) at least one week after the event provided that basic rescue operations are carried out.

The current model is a direct outgrowth of an earlier analytic model entitled Shelter Evaluation Program (SEP) (Ref. 1) which was developed for the purpose of evaluating the effectiveness of NFSS buildings against the direct effects of nuclear weapons. In applying the SEP code in this study to a comparative analysis of buildings which were surveyed in detail it was discovered that results were insensitive to certain distinct structural and geometric building variations which should have produced corresponding variations in people survivability. An examination of the code was performed and it was concluded that the formulation of the casualty estimation portion of the SEP code was too crude for a sufficiently detailed evaluation of inherent building protection. It therefore became necessary to introduce certain modifications.

It must be noted that for the time period (1967-1968) in which the SEP code was developed it was certainly within the state of the art. However, significant technical progress was made since then in several important areas; computer simulation of people response (Ref. 2), failure characteristics of masonry walls (Refs. 3 and 4), debris mechanics (Ref. 5), shock wave interaction (Ref. 6), and therefore modifications were both warranted and desirable.

Modifications were undertaken in conjunction with a detailed examination and documentation of the original SEP code. A write-up of the documentation is provided as an annex to this report. Routines earmarked for revision are described as follows.

Blast Filling (Loading) Routine: The function of this routine is to determine the time-dependent blast loading experienced by personnel located in various parts of buildings as a function

of free field conditions and building geometry. The original version assumes the loading to be that of the free field reduced by a factor which is a function of window area to wall area.

People Translation Routine: The function of this routine is to determine magnitudes and types of impact experienced by personnel when subjected to blast loading. The original version simulates a building occupant as a single, rigid block capable of rotating about the base and translating horizontally but restrained from vertical motion.

Debris Casualty Routine: The function of this routine is to determine types and magnitudes of debris impacts experienced by building occupants produced by the breakup of building walls. In its treatment of this problem the SEP code neglects the relative motion of people and debris. Also, only exterior portions of buildings can be analyzed with any degree of accuracy.

Prompt Nuclear Radiation Dose Prediction Routine: The function of this routine is to predict whole body nuclear radiation doses experienced by building occupants as a function of building mass and geometry. As a result of recent findings (Ref. 7) the dose rate data contained in this routine are out of date.

Specific modifications performed in the course of the current effort are described in the following paragraphs.

1.2.2 Blast Loading Routine

The modified version is a two-dimensional model which can consider buildings having any reasonable number of stories and rooms located on each story. Rooms need not be of the same size. Walls separating them can have any number of openings and different strengths. Should the loading be such that the strength of any exterior wall or interior partition is exceeded in the loading process, the routine is capable of considering the corresponding failure process (time variation of opening produced by the failing wall) and its influence on the loading (pressures and velocities) of adjoining rooms. Individual wall strengths and response times are provided as part of input data.

The routine computes diffraction impulses and dynamic pressures at various locations in any given room as a function of time and geometric and physical building characteristics, i.e., height above ground surface, area of openings and their location, room size (height, length and width), building geometry, wall strengths and times to wall failure. These loadings can then be applied to individual building occupants for casualty estimation.

Since the routine has the capability of considering different room sizes and wall strengths it provides a means for estimating the relative advantages of placing people in exterior rooms, interior rooms, corridors or in some proximity relative to stairwell and elevator shafts.

The major disadvantage is its two-dimensional character. For a given building the model neglects cross-flow between adjacent, parallel bays and between adjacent stories. Thus, when a large rectangular multistory building is subjected to blast normal to one of its sides, then results of this model apply directly to its central portion and approximately to the end portions provided all bays running parallel to the direction of blast are essentially the same. For most buildings of interest this is approximately true.

The dominant direction of flow is expected to be in the direction of blast propagation and thus the omission of cross flow for the purpose of estimating translation casualties is not considered to be serious for most structures of interest. This feature can be added in the future provided it is deemed necessary after this model is sufficiently exercised and evaluated. It will be recalled that this (two-dimensional) model represents a significant improvement over the model previously used.

In the course of this effort the blast loading model was formulated, programmed and checked out. However due to time constraint it was not possible to perform the needed parametric

sensitivity studies and incorporate them within the main body of the overall simulation model. The physical basis and the corresponding formulation of this routine is described in Appendix B.

1.2.3 Translation Survivability Routine

As presently modified, this routine is a self-contained model consisting of seven subroutines. The model accepts data on the weapon environment, body positions of personnel and building characteristics. On this basis it determines those areas in any given room which are unaffected by the blast jet. People located in such areas are assumed not to be subjected to blast translation as long as external walls remain in place.

A given building occupant is simulated by means of a plane, rigid rectangular block having three degrees of freedom. Depending on specific conditions of loading and room geometry, the occupant may impact the floor and/or the far wall in several different ways, i.e., head, foot or whole body impact.. Impact type magnitudes are then compared with casualty criteria to determine levels of survivability. The formulation of this routine is described in Appendix A.

Appendix A also describes a translation simulation routine which treats the occupant as an articulated man consisting of three rigid masses (head, thorax, lower limbs) interconnected by means of nonlinear springs. This representation was found to be superior to the single mass model described above. After undergoing the necessary sensitivity analysis, this model will be incorporated within the body of the translation survivability routine.

With the exception of the blast loading portion, the current, operational version of the translation survivability routine is a complete reformulation of the one originally contained in the SEP code, both in its dose prediction and casualty estimation. It admits of more detail and is more representative of real situations.

For the time being, the loading experienced by personnel still consists of the free field diffraction and drag, modified (knocked down) by a factor (ratio) which is a function of window opening area to wall area. For most problems of interest this loading is considered to be conservative. Just how conservative this is will be established when this loading approach is replaced by the one described in Appendix B in conjunction with the articulated man model.

1.2.4 Current Operational People Survivability Model

The current operational model is considerably more detailed, compact and efficient than the original version. Existing portions of the SEP code were documented, verified and corrected as necessary. Several of the routines earmarked for revision were reformulated, programmed and checked out as described previously. This included:

- Blast loading routine
- Translation survivability routine
- Articulated man routine

For the present effort these were considered to be more important than the debris and prompt nuclear radiation routines which were left in the original form.

When it concerns mortality estimates, the current model is considered to be adequate. In its present form it applied very well to multistory framed buildings with "weak" walls and "weak" (studwall) interior partitions, i.e., buildings which do not produce significant, casualty level debris when interacting with the blast wave. As long as exterior walls remain in place it applies quite adequately to most "strong wall" framed and load-bearing buildings.

Debris is an important casualty producer in the remaining categories of shelter space and especially when it becomes necessary to separate survivors in injured and uninjured categories. For this reason it becomes useful to reformulate the current debris casualty prediction routine.

1.3 BUILDING ANALYSIS EFFORT

A substantial portion of the total effort described in this report was devoted to the survivability analysis of two categories of buildings. This included the Detroit-Greensboro buildings (Ref. 8,9) and a set of "special" buildings.

Detroit-Greensboro buildings were ten NFSS structures which were surveyed in detail by Research Triangle Institute (RTI). Their data formed the basis for the recently completed "all effects" survey. They were analyzed using the original version of the SEP code. Although these structures were different in many respects, these differences were not reflected in survivability results obtained. On the basis of these results it became necessary to examine and modify the SEP code as described previously.

The set of "special" buildings analyzed were existing structures not of the NFSS category and represented an operational analysis effort. Thirty-three such buildings were analyzed in substantial detail using hand calculation procedures for the most part. This analysis effort formed the basis for the various SEP code modifications discussed previously.

1.4 DISTRIBUTION OF BLAST-INITIATED DEBRIS

Combustible (burning) building debris located over or in proximity to basement shelters may constitute a major hazard to shelter occupants. In such an environment casualties may be produced as a result of flame exposure, smoke, toxic gases and temperature gradients. Duration and intensity of these effects at any given location depends on the composition, size and distribution of the ignited debris pile.

When designing fire experiments for the purpose of studying the effectiveness of various safety measures which may be used by shelter occupants to mitigate the effects of fires, it is necessary to use realistic compositions and distributions of representative building debris. Currently very little usable information exists on realistic distributions of urban debris.

Studies performed to date can be divided into two categories, i.e., those which were primarily concerned with gross distributions of debris, taking into account large urban areas and numerous building types (Refs. 10,11,12) and those concerned with specific cases of debris formation (Ref. 13). The latter category includes numerous experimental (field) studies. Although many debris studies have been performed in the past, none of these were concerned with the specific makeup of debris piles at the local level, i.e., in the vicinity of various buildings containing shelters.

A portion of this study was devoted to the task of predicting the distribution of building debris including structural components and building contents. This was done in support of fire experiments conducted under DCPA Work Unit 1135A.

The analysis method uses a deterministic free-flight model which traces the trajectory of each debris piece from the time of separation (rupture) to the time it comes to rest downrange from its original position. The primary mechanism producing horizontal transport is due to aerodynamic forces generated by the blast wind. Vertical motion results from aerodynamic lift forces and gravity. The model considers impact with ground surface, the possibility of some degree of bounce and subsequent free flight. This is the first debris transport model capable of treating buildings in detail. As such it is also useful in predicting overall debris profiles for the purpose of determining the extent of debris clearance operations.

This model was applied to the analysis of a two-story framed building located at the 5 psi range of a 1 MT nuclear weapon. Results of the analysis are described in Chapter 3. In this particular example, structural debris became distinctly segregated from the building contents.

1.5 COST AND SURVIVABILITY ANALYSIS

Chapter 4 contains a cost and people survivability comparison between a slanted basement and a corresponding above grade shelter. Both shelters have equal floor areas and are assumed to be located in identical buildings which were completely designed and costed in the course of this study. The two parent buildings are one-story steel frame and masonry structures commonly used as small office buildings or medical centers. Cost and people survivability estimates are given for the following four cases:

- Conventional building without basement
- Conventional building (no basement) with a 15 psi (design) dual-use shelter integral with the parent structure
- Conventional building with a partial basement
- Conventional building with a dual-use partial basement shelter - 15 psi (design).

Results indicate that the hardened basement shelter is less costly and survivability-wise superior to the aboveground hardened shelter.

1.6 ANALYSIS OF SPECIAL PERMANENT AND EXPEDIENT SHELTERS

In the context of this discussion special permanent shelters are defined as those which may be constructed by private individuals with direct effects and/or fallout radiation protection in mind. This may include a concrete block basement shelter, a wooden lean-to basement shelter or a small neighborhood shelter separate from private dwellings.

Expedient shelters may be defined as those structures which are capable of being constructed within a relatively short period of time by unskilled or semiskilled labor using little or no specialized equipment. Such shelters are important in an evacuation mode. However their effective use requires a substantial preplanning and prestocking effort.

A fair number of different shelter concepts in both categories exist at this time. Eight of these were chosen and analyzed in the course of this study. Analytic results are described in Chapter 5 of this report.

REFERENCES

1. Feinstein, D. I., et al, "Personnel Casualty Study" for Office of Civil Defense, Contract OCD-PS-64-201, Work Unit 1125A, Subcontract B-10923 (4949A-24)-US, IIT Research Institute, July 1968.

2. Huston, R. L. and Passerello, C. E., "On the Dynamics of A Human Body Model," Journal of Biomechanics, Vol. 4, pp 369-378, Pergamon Press, 1971.

3. Gabrielsen, B. and Wilton, C., Shock Tunnel Tests of Wall Panels, for Defense Civil Preparedness Agency, Contract DAHC-20-71-C-0223, Work Unit 1123G, URS Research Company, January 1972.

4. Whiele, C. K. and Bockholt, J. L., Existing Structures Evaluation, Part IV. Two-Way Arching Walls, Stanford Research Institute, September 1970 (AD 719 306).

5. Wiedermann, A. and Nielsen, H., Debris and Fire Environment from Soft Oil Storage Tanks under Nuclear Attack Conditions, IIT Research Institute, for U.S. Army Engineer Division, Huntsville Corps of Engineers, Contract DACA 87-70-C-0001, 1971.

6. Dodoni, A. and Pandolfi, M., "Interaction of Traveling Shock Waves with Orifices inside Ducts," Int. J. Mech. Sci., 13(1), pp 1-16, 1971

7. Auxier, J. A., et al, Recommended Standard Free Field Environment for Initial Radiation Shielding Calculations, Initial Radiation Working Group, Radiation Shielding Subcommittee, Advisory Committee on Civil Defense, National Academy of Science, February 1971 (Preliminary Draft).

8. Wiehle, C. K. and Bockholt, J. L., Existing Structures Evaluation, Part V: Applications, Stanford Research Institute, for Office of Civil Defense), Menlo Park, California, July 1971 (AD 733 343).

9. Wiehle, C. K. and Bockholt, J. L., Blast Response of Five NFSS Buildings, Stanford Research Institute, for Office of Civil Defense, Menlo Park, California, October 1971 (AD 738 547).

10. Edmunds, J. E., "Structural Debris Caused by Nuclear Blast," United Research Services Corporation, for Office of Civil Defense, Contract OCD-PS-64-19, October 1964.

11. Feinstein, D. I., "Debris Distribution," IIT Research Institute, for Office of Civil Defense, Contract OCD-PS-64-50, Subtask 3322B, August 1964.

12. Barnett, R. L., et al, "Debris Formation and Translation," IIT Research Institute, for Office of Civil Defense, Contract OCD-PS-64-201, November 1966.

13. Byrnes, J. B., "Effects of an Atomic Explosion on Two Typical Two-Story and Basement Wood Frame Houses," Operation UPSHOT-KNOTHOLE, WT 792, Federal Civil Defense Administration, Washington, D.C., September 1953.

CHAPTER 2

ANALYSIS OF PEOPLE SURVIVABILITY IN CONVENTIONAL (NFSS) BUILDINGS

2.1 INTRODUCTION

The objective of this chapter is to describe a computer simulation model (program) developed for the purpose of predicting the survivability (relative safety) of people located in conventional (NFSS) buildings when subjected to the direct effects of nuclear weapons. This analytic tool was developed (and is in a continuing state of refinement) as part of a study whose ultimate aim is to provide for reliable on-site assistance at the local civil defense level.

This model is a direct outgrowth of the SEP code (Ref. 1) which has been modified as described in the previous chapter. In its present operational form the model, although greatly simplified and refined over that of its original version is still too complex and technical to find wide, general application by nontechnical personnel.

The envisioned, final result of this model would take the form of a concise building classification scheme which could easily and reliably be used at the local civil defense level for the rating of buildings in terms of their protective capabilities and thus for the optimum distribution of the local population within them before and after the event.

At present the computer program is both a research tool and an operational device. As an operational device it has been applied to a fairly modest sample of buildings which included the Detroit-Greensboro buildings, 33 "special buildings" and 25 all-effects survey buildings. As a research tool it is hoped that sufficient exercising of this model together with recommended updates and revisions, on a sufficiently wide spectrum, of buildings will produce reliable data upon which a simplified building classification scheme may be built.

This chapter discusses the formulation of this computer program, its physical basis and usage. Some representative results are illustrated by means of example problems.

2.2 DESCRIPTION OF THE MODEL

2.2.1 Scope of the Model

As discussed in the previous chapter, the primary emphasis of the study which resulted in the formulation of this computer program, is on conventional (NFSS) buildings. Generally these are large, framed (reinforced concrete and steel) and load-bearing structures which contain substantial numbers of people for significant portions of the day. In its present state of development the model is capable of considering low and high-rise framed buildings (with or without basements) with a high degree of confidence. Very generally such buildings are for the most part diffraction sensitive, i.e., when interacting with a blast wave the walls are expected to fail and be removed early in the loading with the frame remaining essentially intact. In such buildings the major hazard is the translation and the "sweeping out" of people by the high velocity winds.

The model is not capable of treating load-bearing buildings with the same degree of confidence. For the most part such buildings are expected to collapse catastrophically once the exterior (load-bearing) walls fail. Although in buildings having large and moderate apertures (windows), translation of personnel will pose a serious hazard, debris casualties produced by the breakup and collapse of the structure are expected to be at least as significant if not more so. In its present stage of development this simulation model does not contain a rational procedure for estimating casualties produced by the collapse of a load-bearing building.

The current model considers only the direct (prompt) effects which occur in the Mach region of nuclear weapons. These effects and the corresponding casualty-producing mechanisms are listed in Fig. 2.1 in the order of the event.

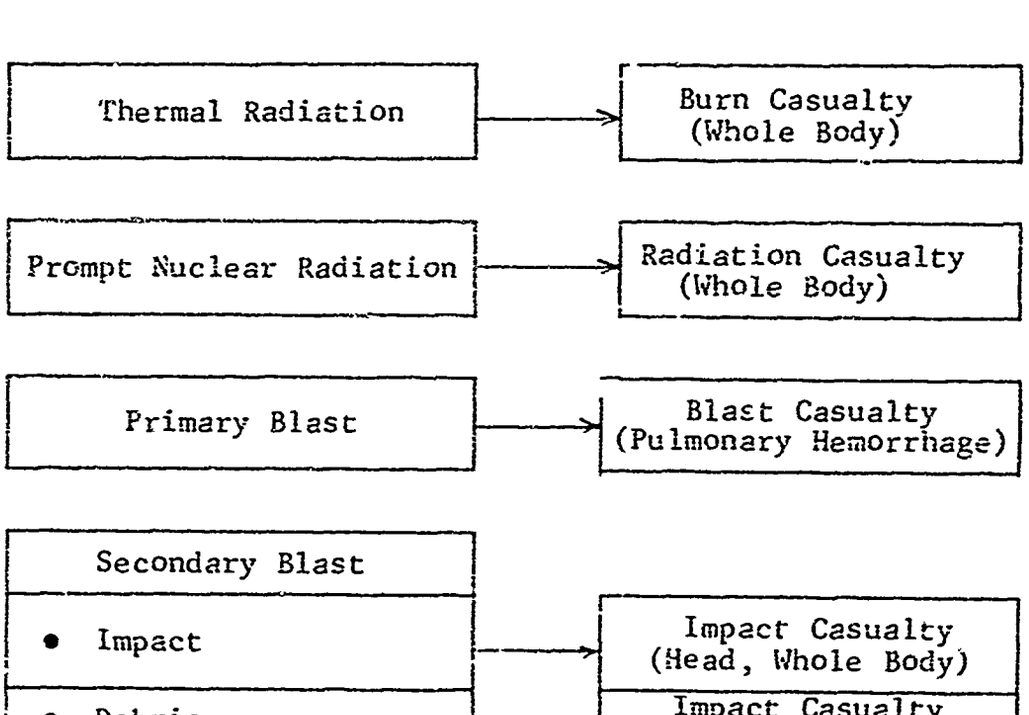

Fig. 2.1 Effects and Casualty-Producing Mechanisms Considered in the Operational Simulation Model

The correspondence between effects and casualty mechanisms is for the most part self-explanatory.

As mentioned in the previous chapter this simulation model uses casualty data which make no distinction between injured and uninjured in the conventional sense. It predicts numbers of survivors based on several general though major categories of trauma (see Fig. 2.1). On this basis, survivors include those persons who are expected to live (survive) at least one week after the event provided basic rescue operations are carried out.

Although currently available casualty data are very limited, they are nonetheless capable of being categorized so to allow for at least a crude distinction between the injured and uninjured. Since the current effort is a first detailed study of people survivability in a direct effects environment, the complexity which would have been introduced by the task of categorizing casualty data did not appear warranted especially since several of the dose prediction models (debris casualty prediction routine for example) are still too crude to justify the effort.

The influence of fires which may occur subsequent to prompt effects is not considered in this simulation model. In a fire environment casualties can occur as a result of flame exposure, smoke, toxic gases and temperature gradients. The task of evaluating the sheltering potential of buildings against blast induced fire effects is significantly different from that of prompt effects and requires the results of a prompt effects analysis. For a given attack condition the occurrence, distribution and intensity of fires is dependent on the fire load and the manner in which the ignited pieces become distributed and intermixed among the resulting debris piles. An initial investigation into the makeup of debris piles both for the fire problem and the people-debris interaction problem is reported in Chapter 3.

Fire hazard is also dependent on secondary contributions such as the existence of heating fuels, broken gas lines, etc. Further, the extent to which a given fire is capable of producing

casualties in a building depends on the ability of its occupants in mitigating its effects, i.e., putting it out, reducing its intensity by removing debris, evacuating the building, etc. The formulation of the fire problem for the purpose of evaluating the sheltering potential of buildings is being considered in another study (Ref. 2) on an experimental basis.

2.2.2 Description

The computer program is a deterministic procedure which is capable of considering buildings in substantial detail and of predicting the relative safety of people located within when subjected to the direct effects of nuclear weapons. The detailed formulation allows the user to consider many categories of data (weapon environment, building characteristics, body positions and dispersal of personnel) and to determine the importance of each variation on the inherent safety.

As mentioned in the preceding chapter, the model consists of a series of routines with appropriate updates and revisions from the original SEP code (Ref. 1) In its most basic form it consists of the following parts.

1. Input: The input routine accepts data on the weapon size, height of burst and range from ground zero. Building description is input in terms of geometry and physical properties. This includes data on window sizes, sill heights, type of window covering, failure overpressure levels for exterior and interior walls, debris size distributions, etc. The program also requires data on personnel, i.e., where they are located and in what initial bodily positions -- prone or standing. Basements and upper stories are treated separately.

In its present stage of development in order to arrive at an estimate of people survivability in a given building, a structural analysis of its walls, floor systems and if necessary, frame must be performed beforehand. Analytic results sought include collapse overpressures, modes of and times to collapse of

each pertinent structural component. These results are then used by the computer program along with known building geometry and weapon data to arrive at the survivability estimate for each of the effects tabulated earlier.

2. Dose Prediction Routines: This set of routines determines the intensities of individual effects and casualty mechanisms that are experienced by personnel in subject building.

- Thermal Radiation -- This routine modifies the intensity of free field thermal energy for each room facing the direction of blast by the presence of window glass, curtains, window sills, neighboring buildings, etc. Resulting intensities are applied uniformly to the room occupants.
- Prompt Nuclear Radiation -- This routine modifies the intensity of free field nuclear radiation for each room by the use of building mass and geometry. Resulting intensities are applied uniformly to room occupants.
- Blast Filling -- By making use of building geometry, sizes of window openings, room geometries, failure overpressure levels for exterior and interior walls, this routine determines the time dependent dynamic pressure intensities within each room analyzed.
- Blast Translation and Impact Routine -- Using the loading determined in the blast filling routine, this routine applies it to simulated personnel located in respective rooms to determine the type and intensity of impact velocities. Impacts can be on the floor, walls or on the ground surface. It may be a head or a whole body impact.
- Acceleration Routine -- This routine monitors dynamic pressure intensities experienced by personnel in respective rooms. Body accelerations produced by dynamic pressures are capable of producing incapacitating trauma without the aid of translation and impact (Ref. 3).
- Debris -- This routine makes use of a free-flight rigid body (debris) model to determine types and intensity of debris impact on personnel. Only structural debris as occurs from the breakage of walls is considered.

3. Casualty Estimation Routines: A routine is provided to relate each of the computed dose intensities to corresponding casualty criteria. These criteria are contained within the body of the program and are described in Appendix C. A flow chart of the computational process is shown in Fig. 2.2.

The simulation model does not consider synergistic effects in the strict sense of the term. Biomedical data capable of being used for this purpose simply do not exist. For want of a better approach the model combines casualty probabilities (P_i) for each of the effects considered to arrive at a total casualty probability (P) as follows:

$$P = 1 - \prod_{i=1}^{i=n} (1 - P_i)$$

The current simulation model is in two distinct forms. The first form consists of routines comprising the simulation of the process dependent on detailed input and followed by a step by step solution of the problem. In this form parameters such as weapon yield, height of burst, specific location of people in building, wall density and thickness, fragment size distribution, translation mechanics, etc. are considered using the established computational algorithm.

The second form of the model (see Appendix C) is a simplified operational version in which standardization of weapon parameters and assumption of uniform distribution of people within the building allowed tabularization of survivability results based upon the previous exercising of the first form. By using standardized results and then appropriately modifying them for specific buildings, survivability estimates can be made with a fraction of the time and effort originally required. For a specifically defined (nontypical) area in a building whose sheltering potential is to be investigated, the first form of the program would apply. For average results for a series of buildings the second form is very adequate.

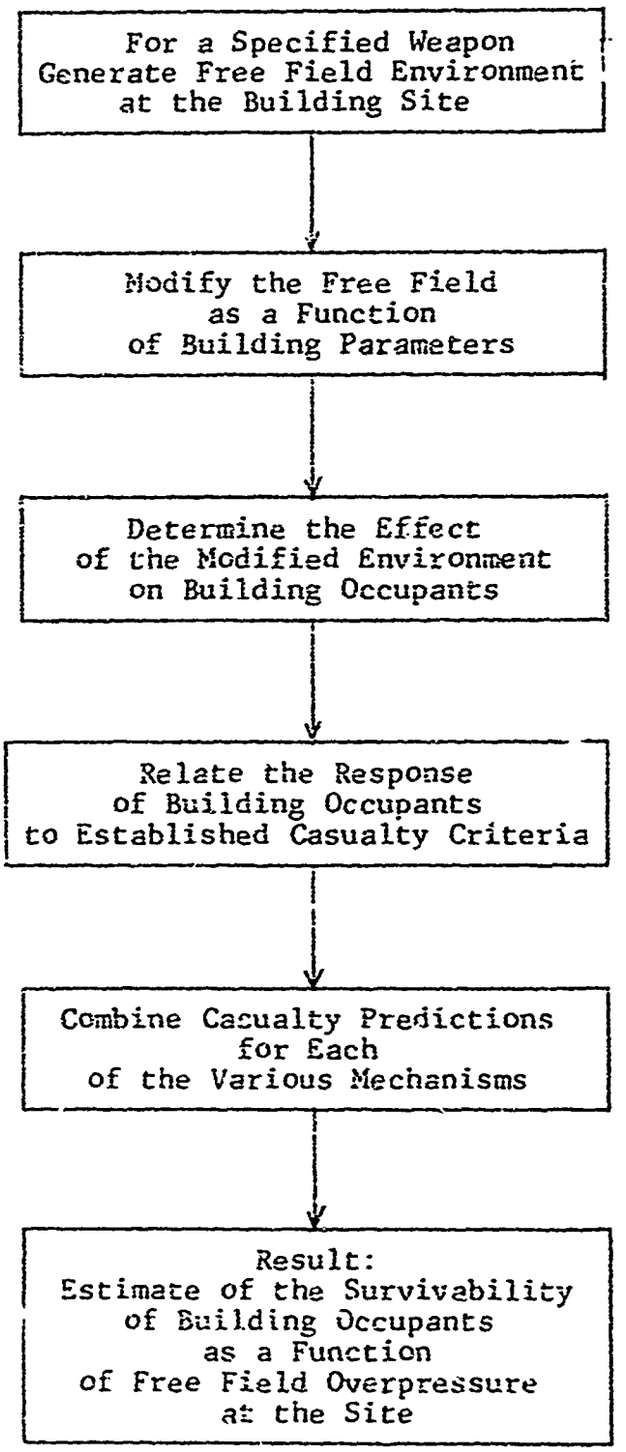

Fig. 2.2 General Computational Process

Survivability of people located in upper stories is analyzed for all of the previously mentioned effects using the first or the second form of this simulation model. Basements are treated separately because most often the primary casualty mechanism involved is the debris from the collapse and breakup of the overhead floor system. The following section illustrates the operation of the model using a simplified example. Results for several existing buildings are described in succeeding sections.

2.3 ILLUSTRATION OF PROGRAM USAGE

2.3.1 Typical Problem

This section illustrates the usage of this simulation model in terms of data requirements and the type of results that are produced. The model is applied to a building shown in Fig. 2.3 with the requirement of determining people survivability (upstairs and in the basement) when subjected to the prompt effects of a single megaton range nuclear weapon.

Figure 2.3 shows an elevation view of a two-story reinforced concrete frame building (with a basement) which is located in the open and away from other buildings. All of the necessary geometric data are given in the figure. This is a section through a long building which is three bays wide. The bays are 16 ft along the short direction and 24 ft along the long direction. Windows are large and represent 50 percent of the total front wall area and are completely screened by means of blinds. Strength (incipient collapse overpressure) of exterior walls is estimated at 6 psi. Sill height is 2 ft. Interior partitions are studwalls (not shown) and have an inherent strength of approximately 0.5 psi. Studwall debris is assumed not to produce mortality level casualties.

The slab over the basement is 8 in. thick and has one-way action. It is continuous over the interior beams and columns and is simply-supported along the peripheral walls. Analysis results indicate that the center span will experience yielding at 12.6 psi and collapse at 14.8 psi. Outside spans are expected to yield at 9.5 psi and collapse at 11 psi.

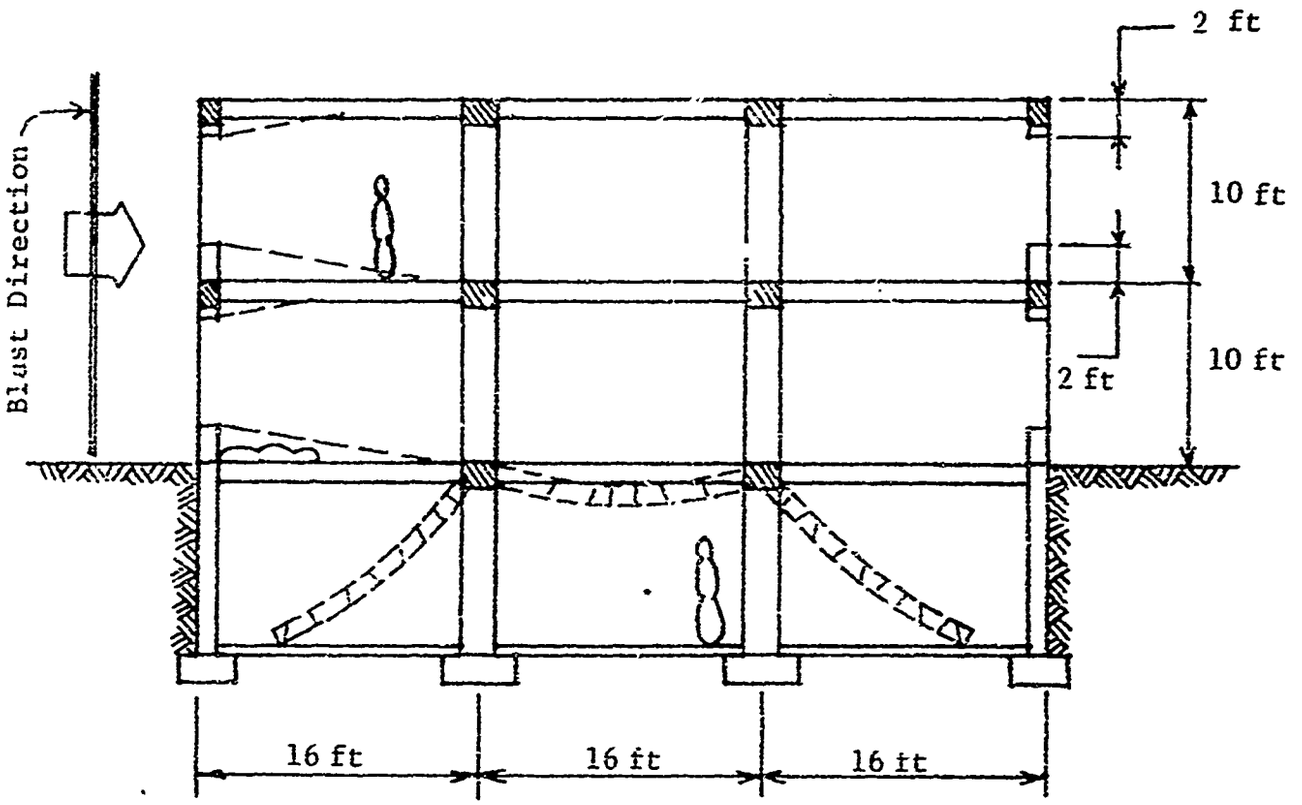

a. Building Elevation

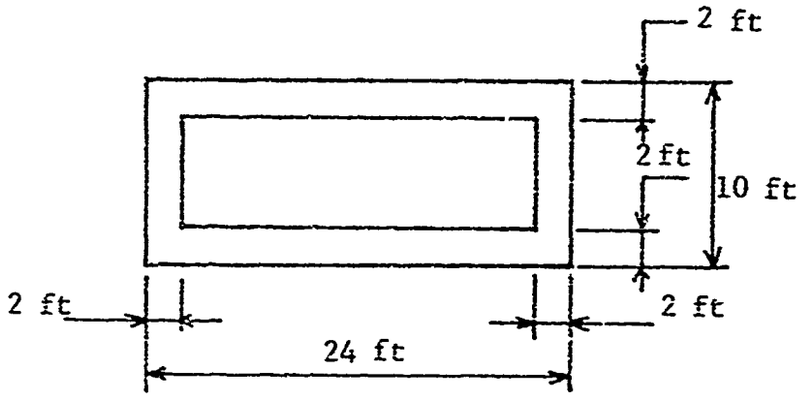

b. Front Wall Elevation

Fig. 2.3 Sample Building

People are assumed to be uniformly distributed at approximately 10 sq ft per person and both the standing and the prone cases are investigated herein. Data described are necessary and sufficient to perform the required analysis. The results are given in Fig. 2.4.

This is a framed building with "weak" walls and is primarily diffraction sensitive. For the range of overpressures of interest (0 to 16 psi) the walls will fail leaving the frame (beams, columns, roof, second story slab) essentially intact. Since windows are large and interior partitions weak, building debris will not be a major casualty producer in the upper stories.

Results given in Fig. 2.4 represent total (combined) survivability estimates for all effects described earlier as a function of overpressure for several different people location and body positions. Each overpressure level is produced by a single (1 MT yield) nuclear weapon. In the upstairs portions, the major casualty mechanism is people translation and impact produced by the high velocity winds. In the basement, the primary casualty mechanism is debris produced by the breakup and collapse of the overhead (reinforced concrete) slab.

The worst case is that of standing second story occupants. The same case for the first story is slightly better since these people do not experience free fall from a higher level. The most favorable case is that of prone first story occupants which is distinctly different from that of the worst case. The basement provides the best protection up to the point at which yielding is produced. After that significant casualties are produced at a faster rate than that of upper stories.

The basement overhead slab is assumed to fail in the manner shown in Fig. 2.3. Failure is initiated at 9.5 psi in the edge spans. They pull off the supports and rotate about the interior columns forming "tents" at about 11 psi. Complete collapse of the edge spans occurs at 12 psi leaving 33 percent survivors.

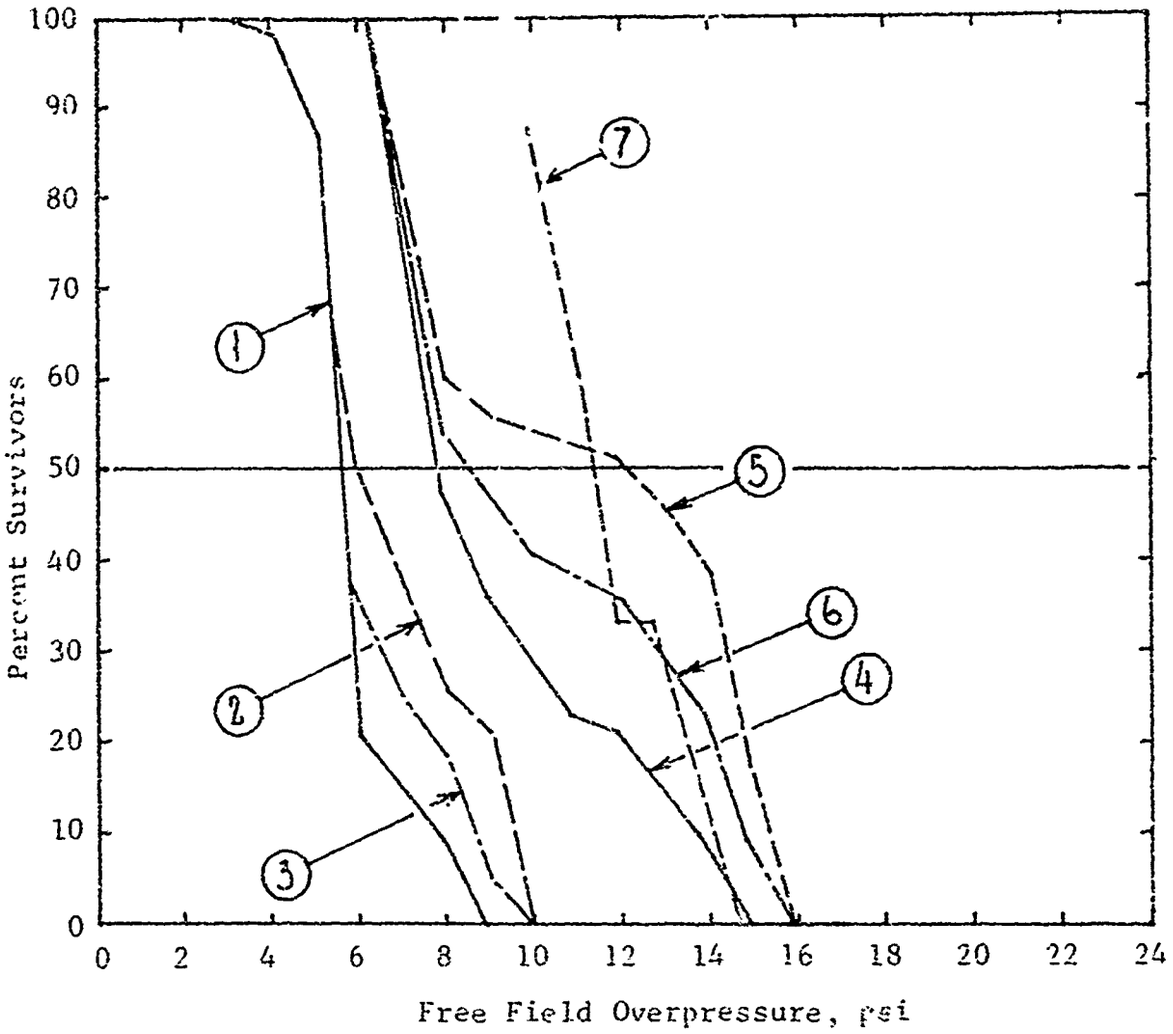

1. Second story (standing occupants)
2. First story (standing occupants)
3. First and second story - average (standing occupants)
4. Second story (prone occupants)
5. First story (prone occupants)
6. First and second - average (prone occupants)
7. Basement

Fig. 2.4 People Survivability Estimate, Sample Building (Fig. 2.3)

The center span yields at 12.6 psi and collapses at 14.8 psi leaving zero survivors. People are uniformly distributed in the basement and whether they are standing or prone is not an important consideration as far as this particular casualty mechanism is concerned. The collapse of the slab is considered in predicting the survivability of people on the first story.

Although in the range of 13 to 16 psi the first story (see curve 5, Fig. 2.4) provides the best shelter space in this building if all occupants are prone, it should be noted that survivors include injured and uninjured personnel. Due to fewer casualty mechanisms manifest in the basement (see curve 7), this shelter area would contain a greater percentage of uninjured survivors than would upper stories.

Some factors affecting people survivability in upper stories and basements are described in the following sections using some results from the "all-effects" survey analysis.

2.3.2 Survivability of People Located in Upper Stories

Analysis of upper stories (using the program described in Appendix C) results in curves showing percent of building occupants surviving all prompt effects as a function of free field overpressure at the site. Two curves are produced for each building analyzed; the first, showing survivability if all people are initially standing, the second, if all people are initially prone.

Many factors enter into a building's potential as shelter. Of primary importance are exterior wall strength and percentage apertures of the walls. Figures 2.5 and 2.6 show results for two buildings with non-load-bearing arching walls. Below are comparative data for the two buildings:

	Building 13	Building 204
Typical wall strength (psi)	27.9	11.6
Percentage apertures	75.0	10.0
Overpressure for 50 percent survivors (psi)		
Standing	6.0	11.5
Prone	14.9	12.4

Frame Type: Steel
Plan Dimensions: 100' x 125'
Height: 81'
Number of Floors: 5
Exterior Wall Type: Two-way reinforced NLBW with arching action
Material: 8" stone/8" brick/12" brick
Typical Strength: 27.9 psi
Aperture Percent: 75
Interior Partitions: 8" brick/6" clay tile/4" wood studwalls

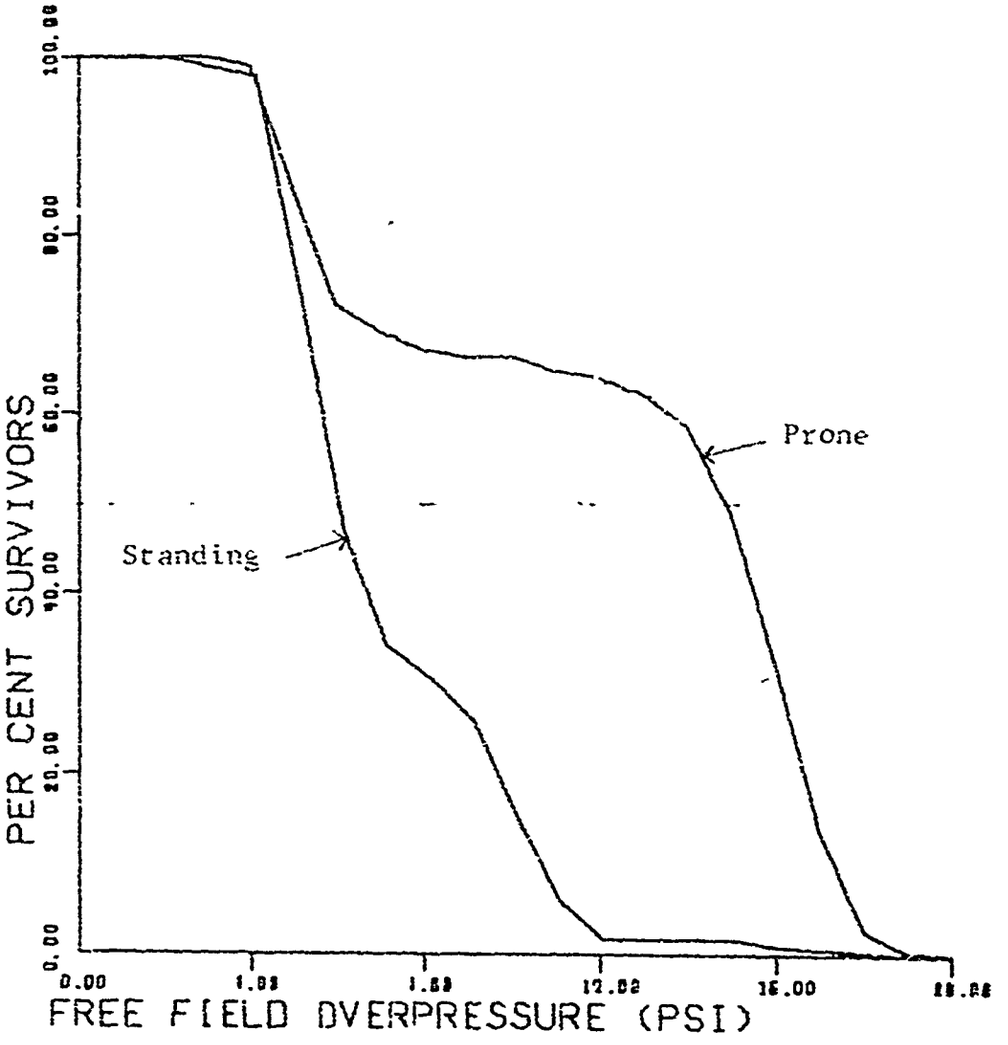

Fig. 2.5 Upper Floor Survivability Estimates
Building 13, Leavitts Department Store

Frame Type: Reinforced concrete
Plan Dimensions: 53' x 140'
Height: 69'
Number of Floors: 6
Exterior Wall Type: Two-way unreinforced masonry NLBW with arching action
Material: 4" brick, 8" structural clay tile
Typical Strength: 11.6 psi
Aperture Percent: 10
Interior Partitions: Clay tile/wood studwalls

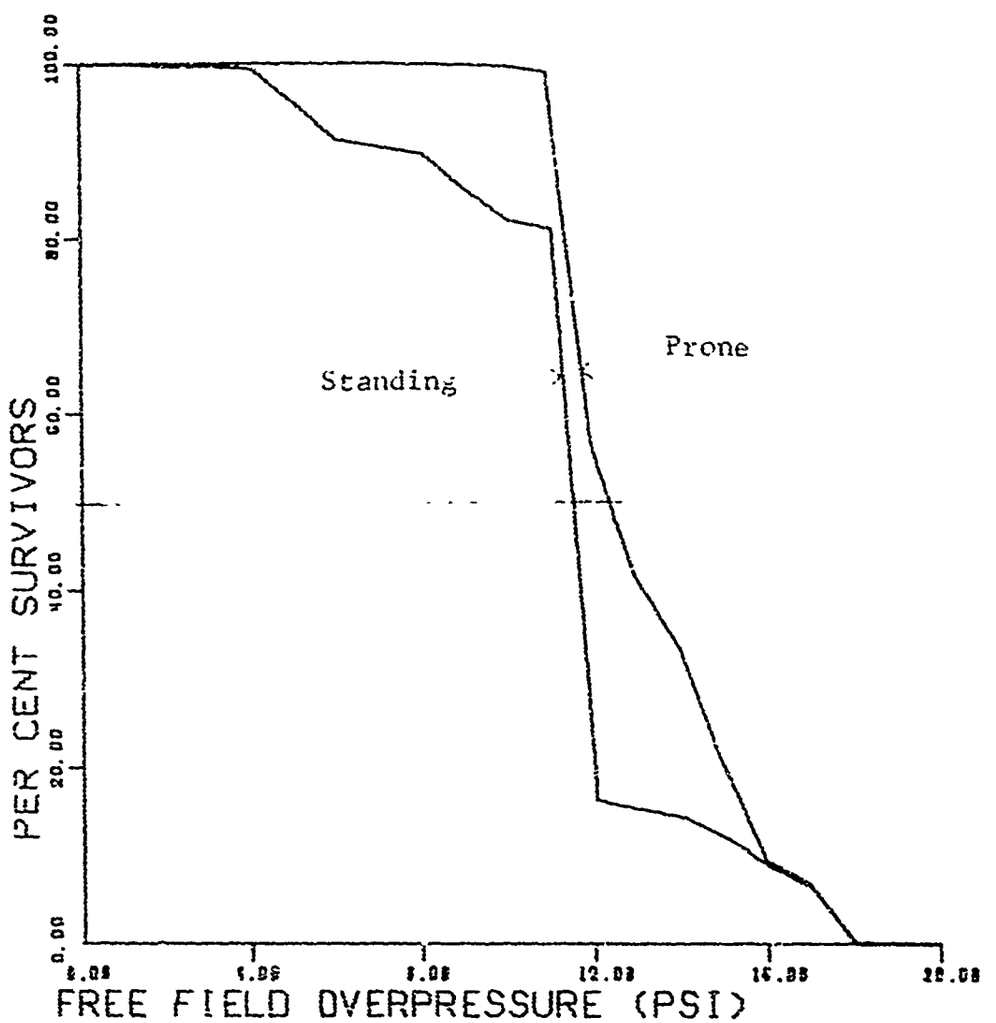

Fig. 2.6 Upper Floor Survivability Estimates
Building 204, Brady Moving and Storage Building

These results (and all other results to date) indicate that shelter occupants taking an initially prone position will have a considerably better chance of surviving. Additionally, although building 13 has walls twice as strong as building 204, it has significantly greater window area. The disadvantage of the window area nullifies many advantages the very strong wall panels have. Figures 2.7 through 2.10 show survivability estimates for four buildings of differing construction, wall strengths, and window percentage. Below are some comparative data for these buildings:

Buildings	63	132	146	195
Wall construction type	Nonarching	Load Bearing	Arching	Load Bearing
Typical wall strength (psi)	1.0	3.5	4.4	4.7
Percentage apertures	50.0	25.0	85.0	20.0
Overpressure for 50 percent survivors (psi)				
Standing	5.8	5.3	6.1	5.7
Prone	9.2	6.2	7.8	8.6

The survivability estimates for people initially standing are very similar for all of the four buildings even though wall construction types, wall strengths, and window percentage are very different. Note that the wall failure overpressures although different are comparatively low with a range from 1.0 psi to 4.7 psi. The comparisons made in the above examples tend to indicate: first, with wall strengths in the higher overpressure ranges the amount of window area has considerable influence on survivability; second, with wall strengths in the low overpressure ranges any number of structure variations make little difference in survivability.

2.3.3 Survivability of People Located in Basements

Analysis of people survivability in basements is done separately from upper floor survivability analysis, because in the vast majority of cases only one casualty mechanism dominates, i.e., debris from the collapse of the overhead floor system. In this analysis, people are assumed to be uniformly distributed throughout the basement area, and once the floor system collapses into the basement all occupants are considered casualties.

Frame Type: Steel
Plan Dimensions: 76' x 349'
Height: 34'
Number of Floors: 3
Exterior Wall Type: One-way cantilever unreinforced masonry NLBW
Material: 4" brick, 2" cavity, 4" concrete block
Typical Strength: 1.0 psi
Aperture Percent: 50
Interior Partitions: 6" concrete block

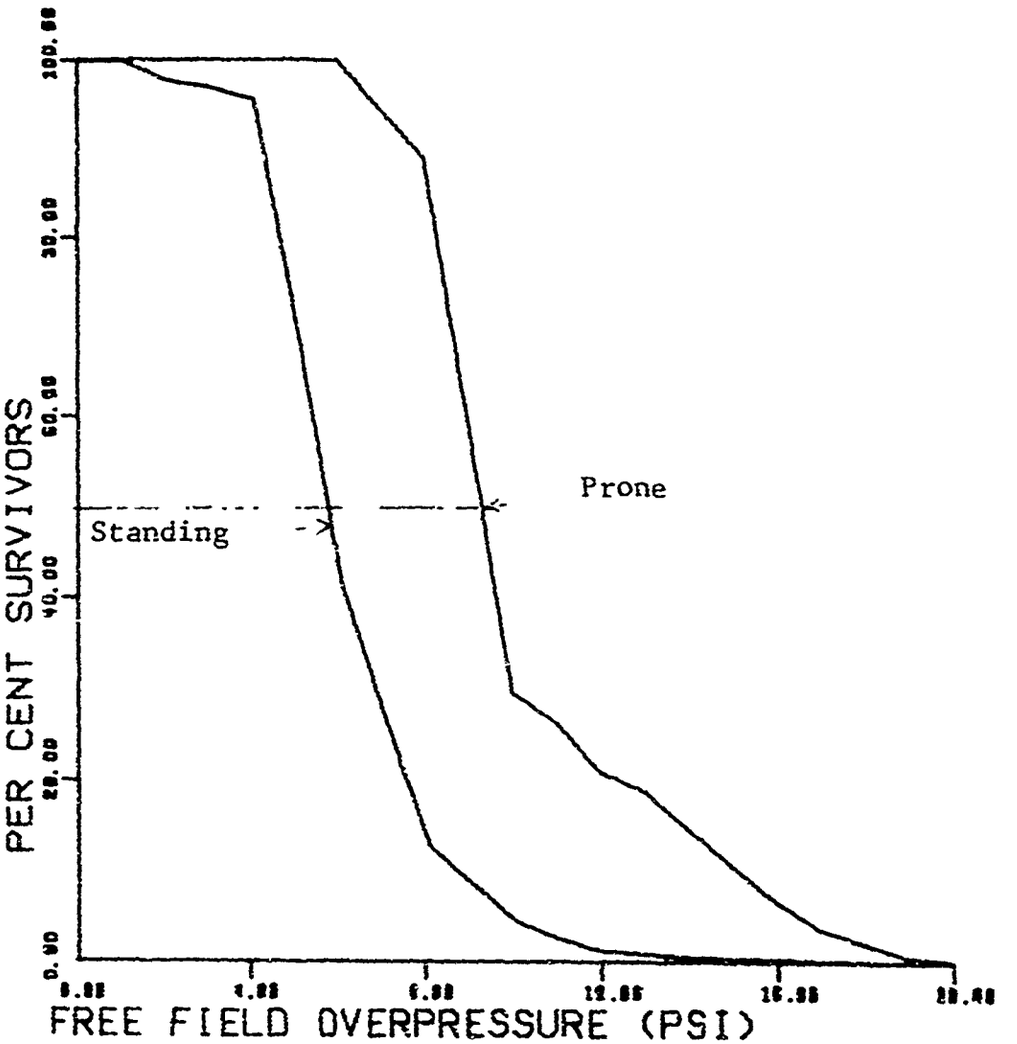

63. AMITYVILLE JUNIOR H. S.

Fig. 2.7 Upper Floor Survivability Estimate
Building 63, Amityville Jr. High School

Frame Type: Exterior bearing wall/interior steel
Plan Dimensions: 78' x 121'
Height: 71'
Number of Floors: 4
Exterior Wall Type: One-way reinforced masonry LBW with horizontal arching action
Material: 4" brick, 12" concrete block/33" to 42" stone
Typical Strength: 6.5 psi
Aperture Percent: 25
Interior Partitions: 4" or 12" unreinforced concrete block

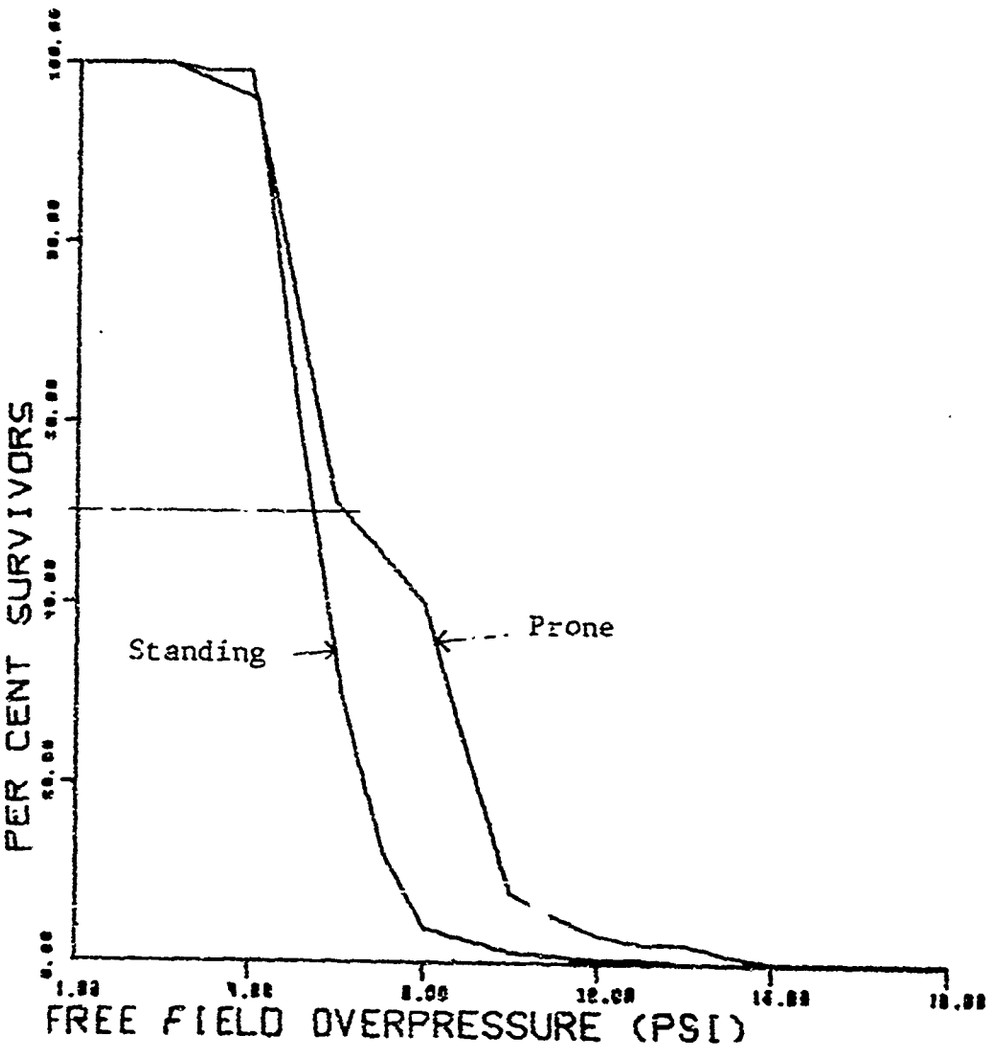

Fig. 2.8 Upper Floor Survivability Estimates
Building 132, Jackson Hill Church

Frame Type: Reinforced concrete

Plan Dimensions: 103' x 200'

Height: 192'

Number of Floors: 20

Exterior Wall Type: One-way unreinforced masonry NLBW with arching action

Material: 4" brick, 4" concrete block

Typical Strength: 4.4 psi

Aperture Percent: 85

Interior Partitions: 4" to 8" concrete masonry/5.5" steel studwalls/ 2" solid plaster

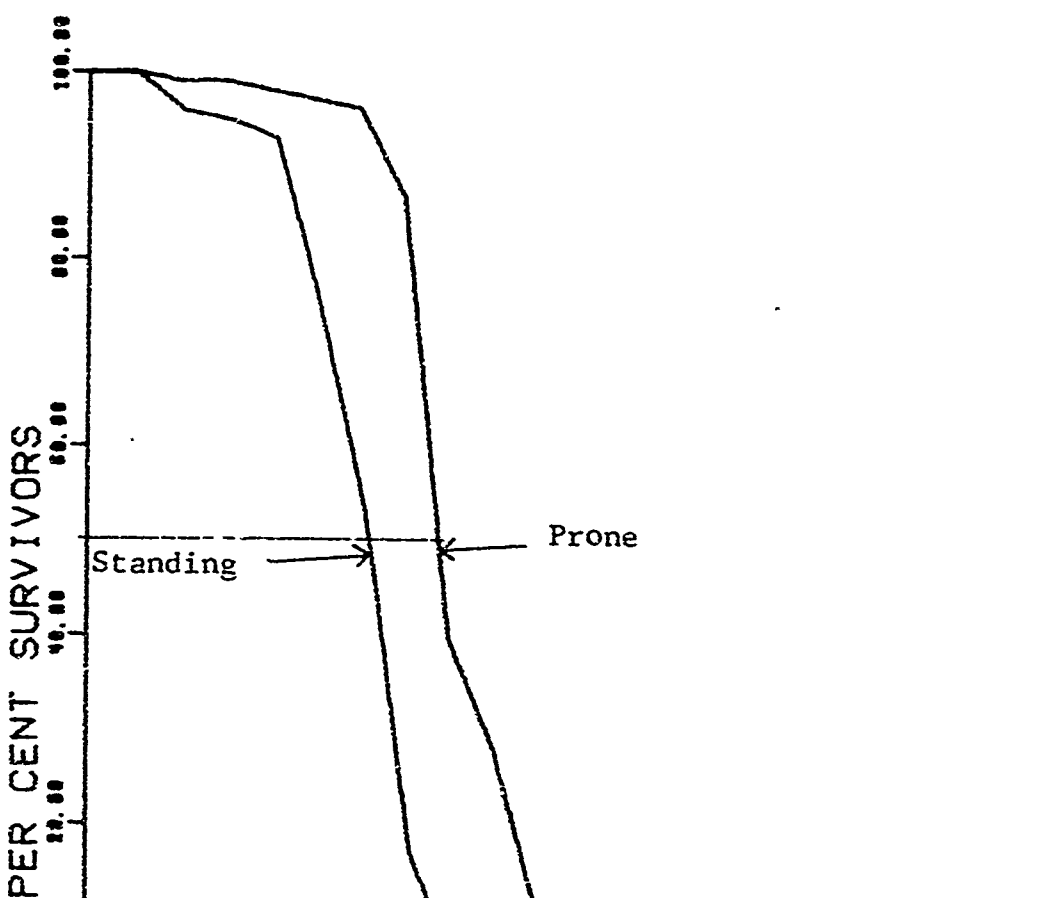

Fig. 2.9 Upper Floor Survivability Estimate Building 146, Marine Drive Apartment

Frame Type: Exterior bearing wall/interior reinforced concrete
Plam Dimensions: 194' x 255'
Height: 24'
Number of Floors: 1 with partial second story
Exterior Wall Type: One-way propped cantilever LBW
Material: 10" reinforced concrete
Typical Strength: 1.9 psi
Aperture Percent: 20
Interior Partitions: 8" concrete block/4" wood studwalls

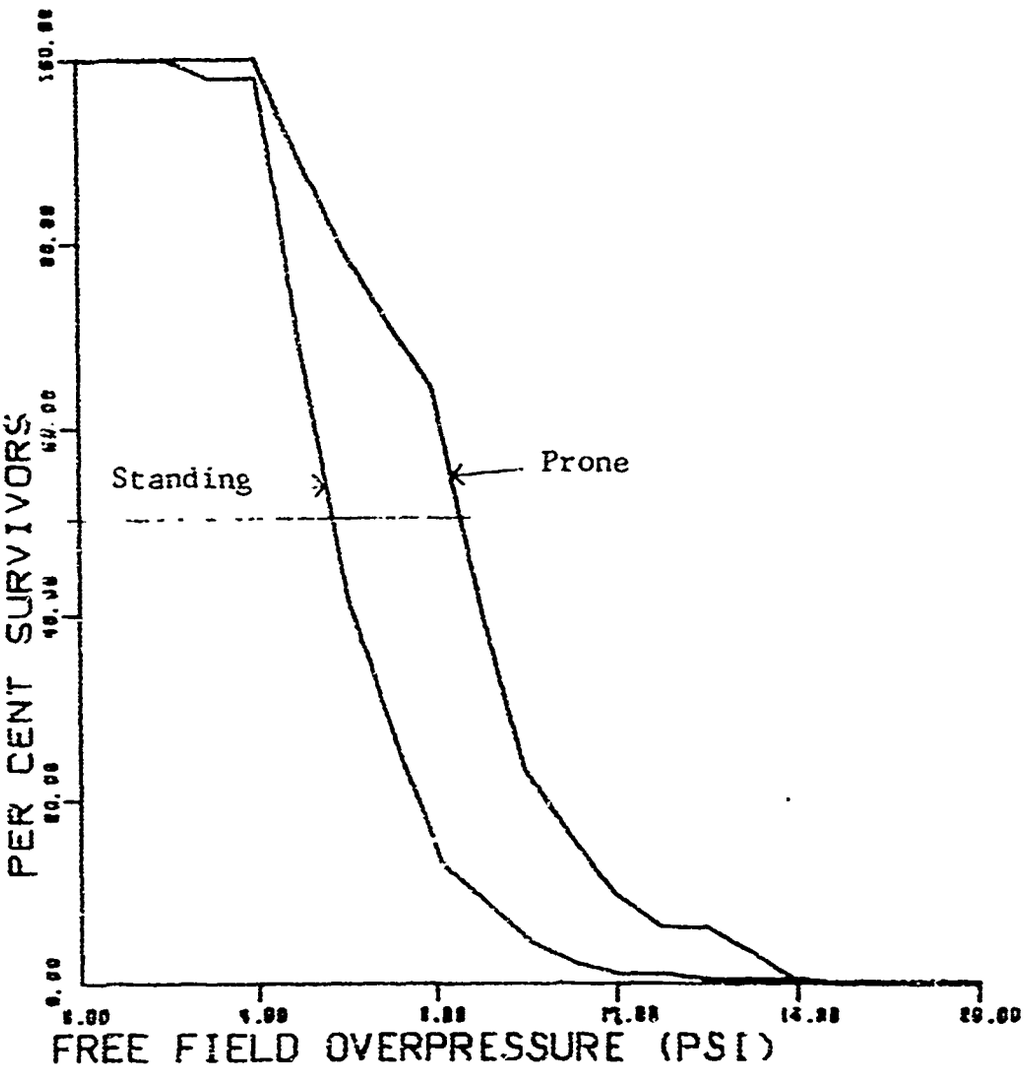

Fig. 2.10 Upper Floor Survivability Estimates
Building 195, May Advertising Building

However, different modes of failure are possible in which an initial collapse does not endanger all personnel. This type of failure, called "tenting", is shown in an idealized way in Fig. 2.11. A floor slab after failing may still provide some protection for people near the walls of the basement, until a greater overpressure than that producing initial collapse causes further failure of the slab in the tented position. At this point all personnel are assumed fatalities.

Survivability in basements such as shown in Fig. 2.11 is completely controlled by the strength of the overhead floor, and, to a lesser extent on the possibility (depending on failure mode and geometry) of tenting action. Thus, the problem in estimating people survivability in basements is considerably simpler than for the upper floors provided the failure mechanism of the slab can be accurately estimated. Typical results for several buildings are shown in Figs. 2.12 through 2.14. In these examples differences in construction type, span length, etc. do not directly reflect the variation in strength of floor systems. Buildings 84 and 204 (see Figs. 2.13 and 2.14) are of the same type of construction, however vast differences in the level of protection exist.

For buildings with very strong floors (>20 psi) the effects of initial nuclear radiation are considered. Building 204, for example, would have an MLOP of 38 psi if floor strength alone governed; initial nuclear radiation reduces this to 19.5 psi.

The use of a building may be significant in making qualitative judgments of its sheltering potential. For instance, building 204 was designed for heavy warehouse loads, while the same type of floor in building 84 was designed for light office loads. Figure 2.12 is included to show the range of sheltering potential. In all cases the effect of fire is not considered although it may be significant if evasive action is not possible.

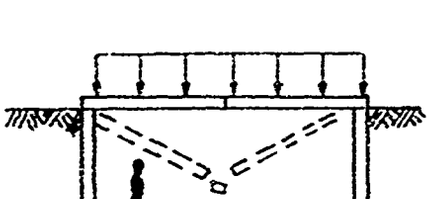

a. Midspan flexural failure

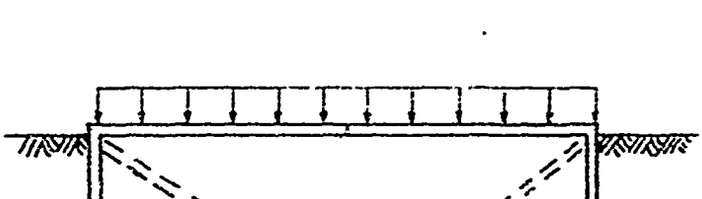

b1. Midspan flexural failure with subsequent "tenting"

b2. Complete failure of "tenting"

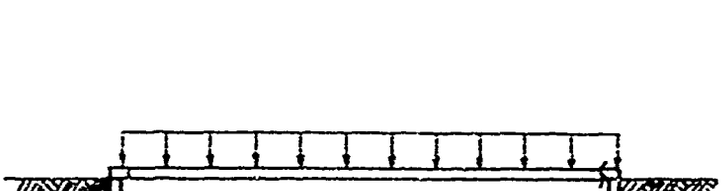

c. Shear failure (no tenting)

Fig. 2.11 Idealized Failure of Slabs over Basements

First Floor - Type: Reinforced concrete slab on reinforced concrete joists

Thickness: 2.5"

Failure Overpressure: 4.5 psi

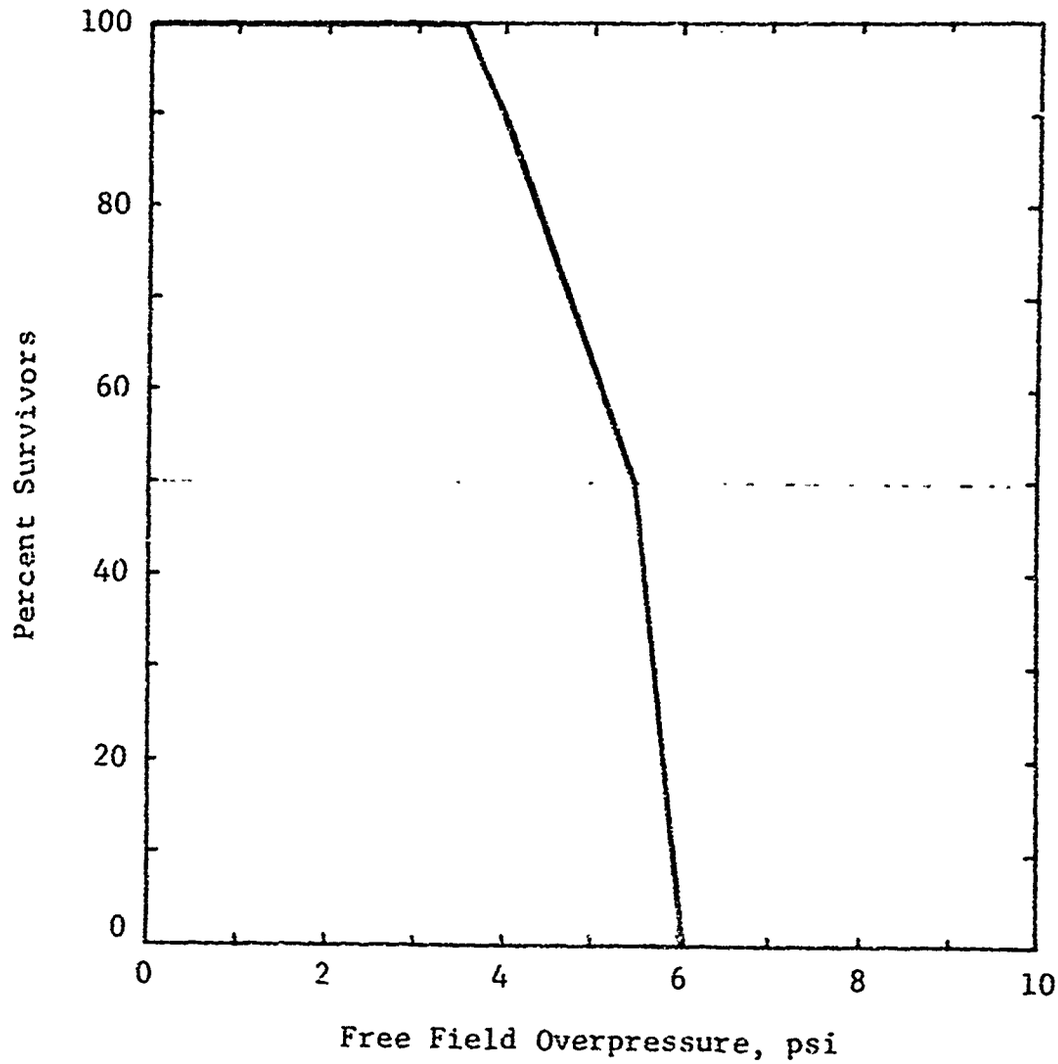

Fig. 2.12 Building 81 Federal Office Building Basement

First Floor - Type: Reinforced concrete slab
Thickness: 10"
Failure Overpressure: 7.5 psi

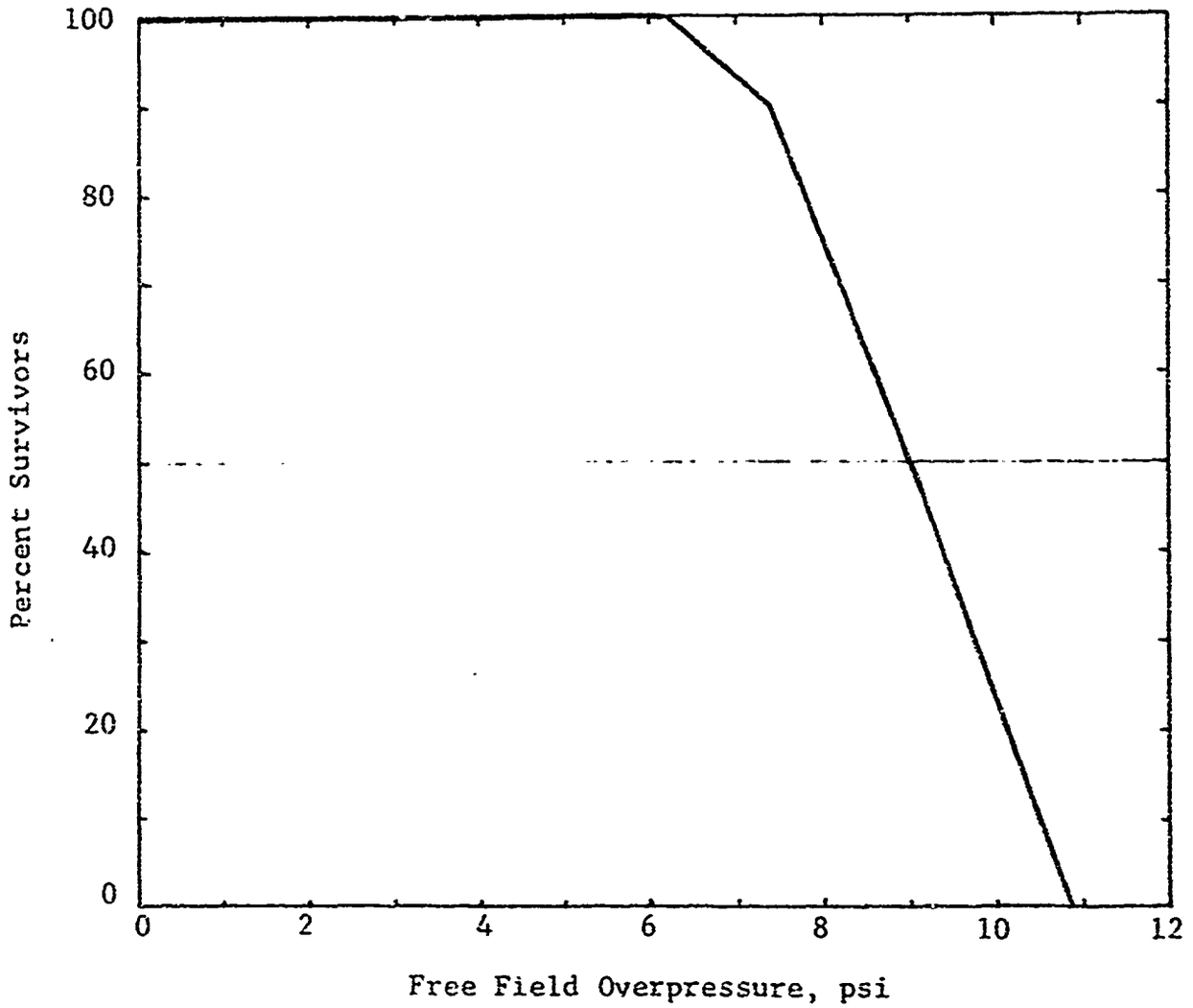

Fig. 2.13 Building 84 Saratoga Municipal Building Basement

First Floor - Type: Reinforced concrete flat slab
Thickness: 8"
Failure Overpressure: 54.1 psi

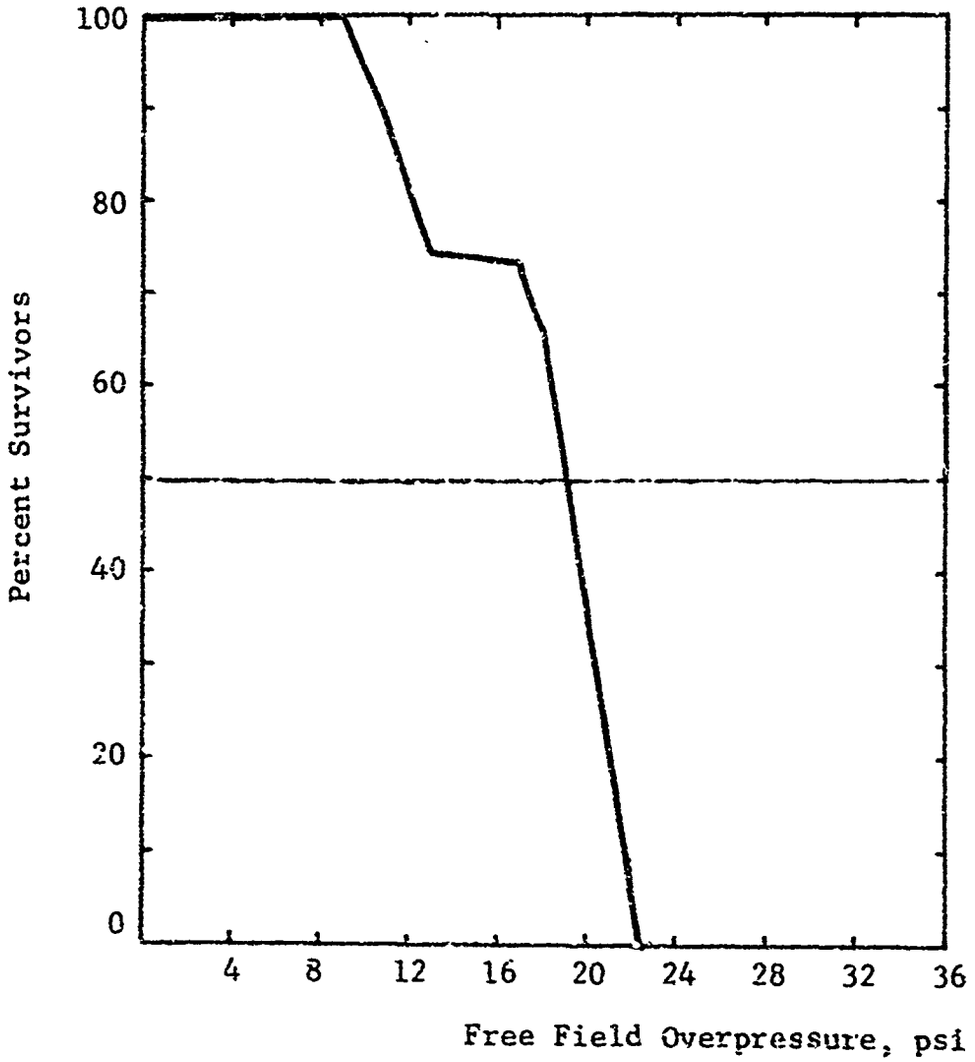

Fig 2.14 Building 204 Brady Moving and Storage Company Building Basement

2.4 CONCLUSIONS

In its present form the methodology for estimating the survivability of people in buildings in a nuclear weapon environment is being used to survey a number of buildings for their sheltering potential. In this sense, it is presently a valuable tool. Further improvements in the model will make it more so.

Since translation of people in the blast wind is from all present evidence the most critical item affecting survivability, a more refined model of the process would lead to better estimates. This improved program would include implementation of a better mathematical model of a man (i.e., the articulated man described in Appendix C). In addition, a more realistic loading model, the blast filling routine (see Appendix B) would be used. In this manner, the reliability of the survivability estimates would be greatly improved.

At present, the degree of nonfatal injuries is not considered in the program, primarily because of the lack of specific, authoritative data. The capability exists for predicting the severity of the mechanisms which could cause injury; and implementation of injury criteria in their present form or, hopefully, with improved data could be done. Addition of injury predictions would provide a better estimate of a building's sheltering potential.

The ultimate aim of improving the present program and the exercising it enough would be to develop a store of experience and knowledge of the problem from which a simplified, reliable building classification scheme could be built. The advantages of such a tool to local civil defense planners would be significant: it would result in the best possible use of the nation's only significant sheltering resource, existing buildings, in the event of nuclear disaster.

REFERENCES

1. Feinstein, D. I., et al, Personnel Casualty Study, IIT Research Institute for Office of Civil Defense, July 1968.

2. Takata, A. N. and Waterman, T. E., "Fire Laboratory Tests - Phase II Interaction of Fire and Simulated Blast Debris, IIT Research Institute for Office of Civil Defense, Contract DAHC 20-70-C-0406, Work Unit 1135A, February 1972.

3. Glaister, D. H., "The Effects of Acceleration of Short Duration," from A Textbook of Aviation Physiology, ed. J. A. Gillies, Pergamon Press, Chapter 26, pp 746-795, 1965.

CHAPTER 3
DISTRIBUTION OF BLAST-INITIATED DEBRIS

3.1 INTRODUCTION

The objective of the study described in this chapter was to determine the probable distances that structural and nonstructural (building contents) debris will travel due to a specific nuclear weapon attack condition, and the probable mixes of debris that would occur at various ranges from the source. The purpose of information generated is to provide guidance for the design of debris fire experiments. The ultimate objective of experimental results is to develop guidance for shelter occupancy, evasive action and the siting of shelters.

3.2 DISCUSSION OF THE DEBRIS PROBLEM

The task of predicting debris distributions for the purpose of developing specific survivability guidance is complex. The salient aspects of the problem that need to be considered in any analysis effort can be described in terms of the general environment as follows.

The detonation of a nuclear weapon will generate a thermal pulse, a transient blast pressure and wind which will interact with surface structures. The extent of primary ignitions in buildings will depend on exposed materials, finishes, types and density of building contents, area of window openings, shielding provided by neighboring buildings, weapon yield and range from the burst point. Depending on the strength of the given building, it may break up under dynamic loads and the resultant pieces (structural debris and contents) will be transported downwind by associated dynamic forces. The extent of primary fires generated downrange will depend on where the ignited pieces end up provided they are not extinguished by the passage of the blast wave or while in transit.

Debris profiles in the direct vicinity of any given building will depend on certain characteristics of the neighborhood i.e., types of neighboring buildings, their strengths, relative positions and separation distances, sizes, fire loads, direction and intensity of blast and range from the burst point.

If the building of interest does not fail while other buildings in its vicinity fail catastrophically, it may serve as an accumulator for some portion of upstream debris which will pile up on its windward side and possibly inside the building itself. Should this building contain a basement shelter with an air intake vent located on the ground level at the windward side, such accumulation could block the vent. Also, depending on the composition and state (burning, smoldering) of the resulting debris pile, primary fires may be produced.

The composition of a debris pile depends on a number of different parameters. Among these are the flight characteristics of individual debris and the extent to which they interact with each other while in transit. Thus at a given accumulator, the debris from an upwind building may be segregated; with light, combustible debris at the bottom and heavy combustibles intermixed with noncombustible debris at the top of the pile. One can also postulate a situation in which the debris from the breakup and contents of a given building is essentially completely segregated in terms of combustibles and noncombustibles.

On the basis of this discussion, parameters that need to be considered in a local debris distribution analysis of a single building or a group of buildings can be categorized as follows:

1) Building and neighborhood geometry (building heights, plan areas, separation distances, occupancy, etc.)
2) Net, time dependent loading on building components and contents
3) Failure characteristics of building and components (failure modes, failure loading, time to failure -- collapse or separation)
4) Debris characteristics (weight, size, shape)
5) Aerodynamic characteristics of debris (drag, lift and moment coefficients)

A review of a number of previous studies in this area indicated that the objectives of this study cannot be met by simply extracting or scaling information obtained in previous work. In this study

we are dealing with the debris problem at a local level. For a given attack condition we are concerned with determining what types of debris piles can be expected to be deposited at a given building in terms of composition and size. This requires consideration of the immediate neighborhood in fairly substantial detail.

Previous studies on the distribution of building debris can be divided into two categories i.e., those which were primarily concerned with gross distribution of debris, taking into account large urban areas and numerous building types (Ref. 1, 2, 3) and those concerned with specific cases of debris formation (Ref. 4). The latter category includes experimental (field) studies.

Some of the earlier analytic studies were severely hampered by the lack of available information on the failure of conventional buildings in a blast environment. This problem is still a formidable stumbling block, however it has been lessened to a fair extent. Full-scale experiments on masonry walls (Ref. 5,6) served to verify their failure modes and corresponding initial debris characteristics. Essentially full-scale tests on reinforced concrete floor systems (Ref. 7,8) provide some of the needed basic information on this class of components. Considering that many of the old and new buildings make extensive use of masonry externally and internally, the experimental information obtained provides a useful input to the analysis of debris transport and distribution.

3.3 ANALYTIC METHOD FOR PREDICTING THE DISTRIBUTION OF BLAST INITIATED DEBRIS

In the previous section, parameters that need to be considered in a debris distribution analysis were discussed and categorized. The purpose of this section is to describe the analytic procedure which was used in the course of this study. This process is described in general terms and is illustrated in the following section by means of a simple application. It consists of two parts:

- Loading and Response Analysis
- Debris Trajectory Analysis

3.3.1 Loading and Response Analysis

An exact analysis of conventional buildings for the purpose of determining their collapsed states (debris distributions) when subjected to a nuclear weapon environment is a practical possibility only when (1) the building in question is sufficiently simple, (2) the behavior of its components from initial yielding to ultimate collapse is known, and (3) the load-time variation, both internal and external is well defined. Actual structures and loadings ordinarily do not satisfy all of these conditions. For this reason, and in order to produce usable results in the shortest possible time, the building analysis process is generally a step by step procedure which considers only the dominant modes of response and relies heavily on experimental data. An analytic process capable of determining the "incipient collapse" state of a structure and subsequently its characteristic, transportable debris is illustrated in Fig. 3.1. This process can be described as follows.

Given a nuclear weapon attack condition, the first step is to determine the free field airblast environment at the location of subject building. In this step the ideal airblast wave is modified as need be by considering the influence of local terrain features such as neighboring buildings or other obstructions. Pressure-time histories acting on the external portions (walls, doors, roof, etc.) of the building are determined by further modifying the local blast environment as this is influenced by the building geometry.

Since conventional buildings contain numerous apertures then it is reasonable to expect that the various structural components will be subject to a combined external overpressure and internal fill-pressure loading. At any given instant of time the net loading on any portion of the building will depend on the relative strength of individual components. A practical, computerized method for determining average fill pressures and flow velocities in rooms having simple geometries is established in Appendix B.

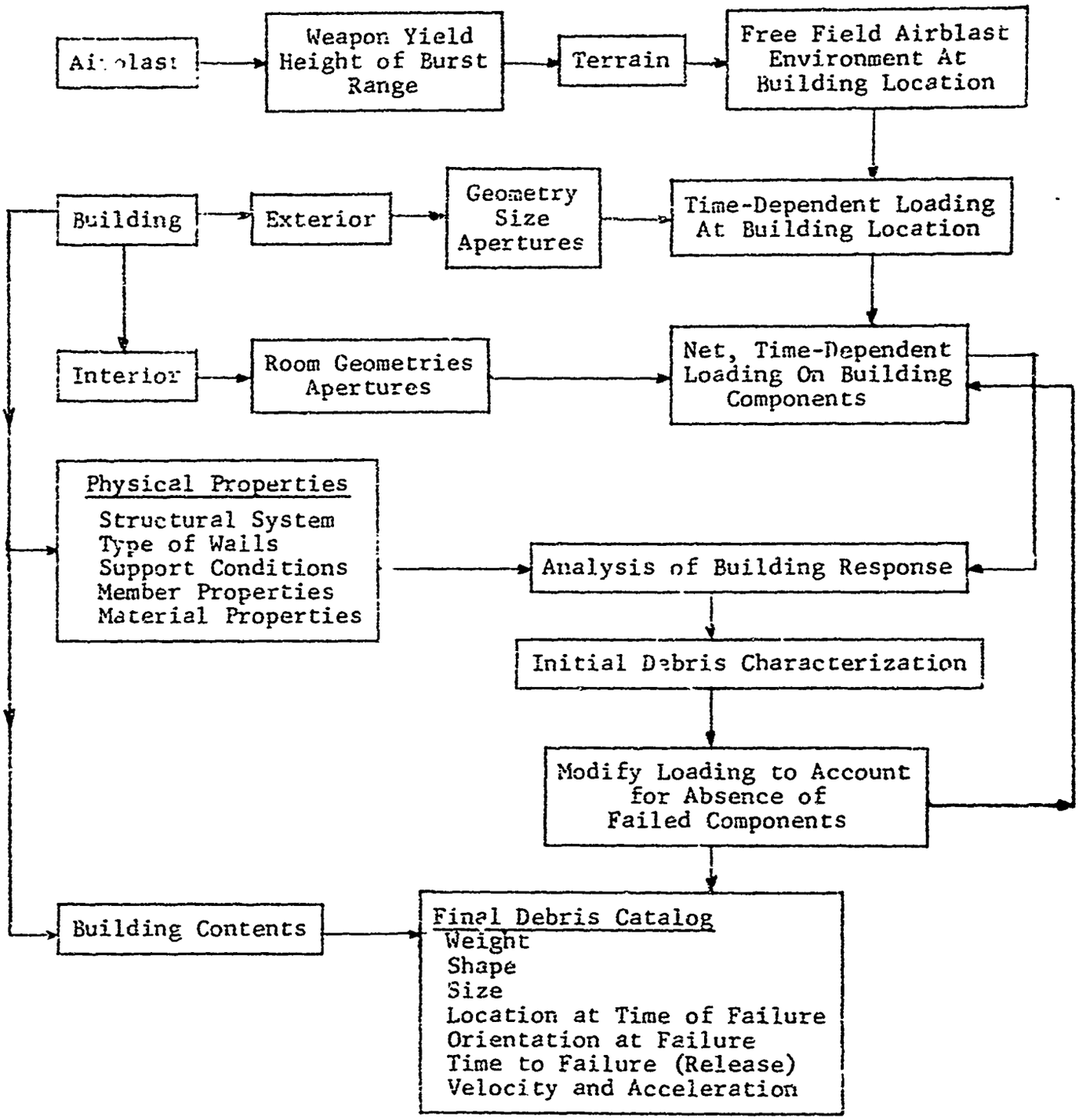

Fig. 3.1 Loading and Response Analysis

Having determined the time dependent net loading on the building as a whole and in particular that on its individual components (external walls, interior partitions, etc.), the next step involves a response analysis.

Conventional buildings consist of closed networks of beam, column, and plate elements. As mentioned previously, an analysis of structural, dynamic response of such a network as a continuous structure is currently a practical possibility only for sufficiently simple geometries and loadings, and then only if elastic response is sought. For this, readily available computer programs exist and can be applied. Computer programs capable of analyzing the dynamic response of structural networks from initial yielding to ultimate, catastrophic collapse do not exist at this time on any practical level. In fact, the quantity of experimental data on the static behavior of individual building components from initial yielding to ultimate catastrophic collapse is as yet fairly limited. This is not to imply that the structural response problem cannot be handled with a fair degree of confidence. The following general approach can produce useful results.

In this approximate approach, the subject building is decomposed into its principal and subsidiary components. Subsidiary components are those which do not affect the response of the building as a whole but are still debris-producing. These are handled separately. The principal components are loaded using the net, time-dependent loading determined as described previously. Support conditions are simulated to correspond to that of the actual, combined structure. The response analysis proceeds on a component by component, time step by time step basis. Since the loading acting on each component in this chain depends on the net loading and response of the ones adjoining to it, the analysis is necessarily an iterative procedure as indicated in Fig. 3.1. Its end result would consist of a debris (size, weight, quantity) distribution to be used in the transport-trajectory analysis together with building contents.

The degree of complexity at the detailed level of analysis depends greatly on the physical makeup of the building (structure) being analyzed. Conventional, single-story wood frame buildings are at one end of the spectrum. When subjected to the blast effects of a large (MT) nuclear weapon at the 2 to 3 psi range, such buildings are expected to be severely damaged (racked and broken) in the diffraction phase of the loading, and dismembered and translated off the site in the drag phase due to the long duration winds. Building failure is expected to be essentially uniform, i.e., the building will fail at all primary connection points at essentially the same time. A dynamic analysis concerned with the behavior of such buildings would concentrate primarily on the overall response rather than on the response of individual components.

The problem is somewhat different when dealing with reinforced concrete and steel framed structures. In this case, building failure is not expected to be uniform. The collapse of internal partitionsand concentration of building contents against one side is expected to precede the failure of the roof system and exterior walls. In this instance the analysis process would be concerned with the sequential collapse of individual building components on a step by step basis. Although other dyramic response analyses are possible, the one described herein is considered to be practical and capable of producing very reasonable state of the art results.

3.3.2 Debris Trajectory Analysis

The debris transport aspect of the analytic process uses a deterministic free-flight model similar to the one described in Ref. 9. This is a two-dimensional (vertical plane) trajectory model which includes both the translational and rotational motions of a given piece of debris which are induced by the aerodynamic forces generated by the blast winds. The input data or information required for the trajectory analysis are described in Fig. 3.2. These include a physical description of the debris, such as its size, weight and geometry, and any other pertinent characteristic of the debris which can be determined, such as its

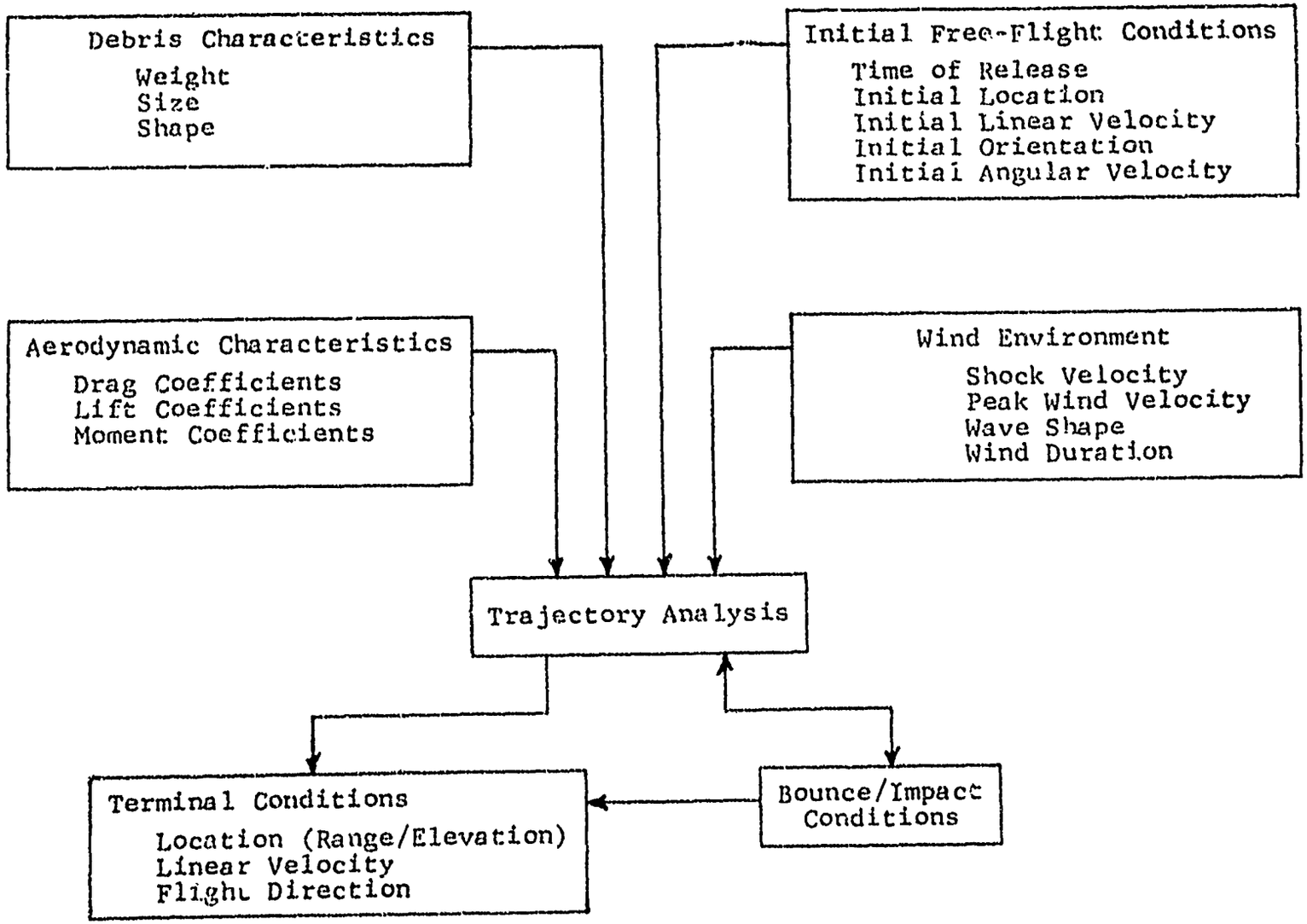

Fig. 3.2 Debris Transport/Trajectory Analysis

moment of inertia. Secondly, the initial free-flight characteristics of the debris must be established. These data include the time of release of the piece of debris into the blast environment, its location at the time of release, and all such initial motion data as are treated in the model. These first two categories of input data are generated in part from the specific response analyses discussed in the preceding section, or estimated from experimental data.

Some of the initial parameters are not influential in the trajectory calculation and thus the number of parameter value groupings and hence the number of trajectory calculations needed to cover the range of parameter values can be limited. In particular, the initial linear velocity of the fragment or piece of debris will always be much smaller than the wind velocity at the time of release such that a single value (probably a value of zero) can often be used. The initial aerodynamic drag force will be proportional, in part, to the square of the difference in these two velocities, hence the force is largely determined by the blast intensity.

The trajectory calculation also requires aerodynamic data on the class of debris shapes encountered. These data include drag, lift, and moment coefficients, each as a function of orientation angle (angle of attack). The data must include all orientations since most pieces of debris will be expected to tumble and rotate as they are transported through the air.

The blast wind is the primary driving force in the transport problem (which also includes gravitational effects) and a satisfactory treatment or approximation of this variable has already been developed (Ref. 9) and is used herein.

It should be noted that any piece of debris which impacts with the ground plane during the early portion of the blast environment may bounce, i.e., not be captured, and even if much momentum is lost as a result of the impact the aerodynamic forces will generally be sufficiently large to loft the piece of debris and cause it to be transported some additional distance. The

piece of debris will acquire additional momentum as a result of this process and again represent a hazard. This bounce phenomenon is included in the analysis process. The analytic process is described in Appendix A. Its application to a practical problem is described in the following section.

3.4 ANALYSIS OF DEBRIS DISTRIBUTION

3.4.1 Introduction

This section demonstrates the applicability of the analytic method described to the analysis of distribution of blast-initiated debris. The demonstration problem considers a conventional, reinforced concrete frame building located at the 5 psi range of a 1 MT nuclear weapon. Debris includes building walls (external and internal) and furniture. The trajectory of each debris item is traced from the time of separation to the time it comes to rest within the building or on the ground plane outside the building. The problem assumes that the building is located in open terrain and therefore the transport of debris is unobstructed. This is not a necessary assumption. The method as formulated is capable of considering the influence of obstructions such as other buildings located within the transport distance. It is also assumed that there is no interaction between individual debris items while in transit. For the specific building considered this assumption is reasonable and should not introduce significant errors in the final debris distribution. As presently formulated, the analysis method is not capable of considering in-flight interaction between several debris items.

3.4.2 Building Description

The subject building is illustrated in Fig. 3.3 which provides its basic geometry. A typical floor plan is shown in Fig 3.4. The structural system is a reinforced concrete, beam and column. frame. Roof and intermediate floor consist of one-way reinforced concrete slabs supported on longitudinal beams and columns. Exterior cladding, in the long direction, consists of unreinforced concrete masonry and window walls arranged in a staggered pattern (see Fig. 3.3). Exterior walls in the short direction consist of concrete

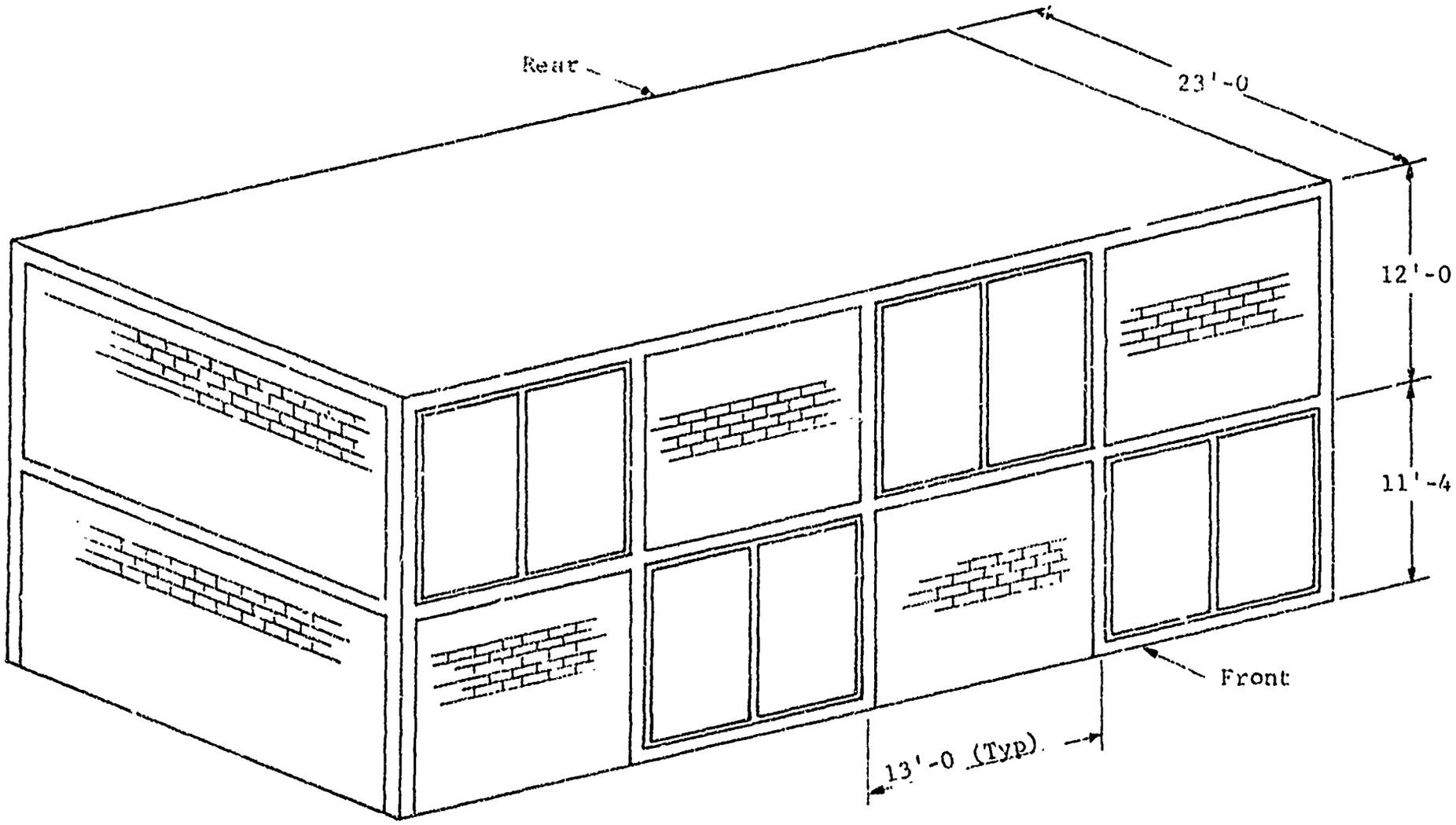

Fig. 3.3 Building Geometry

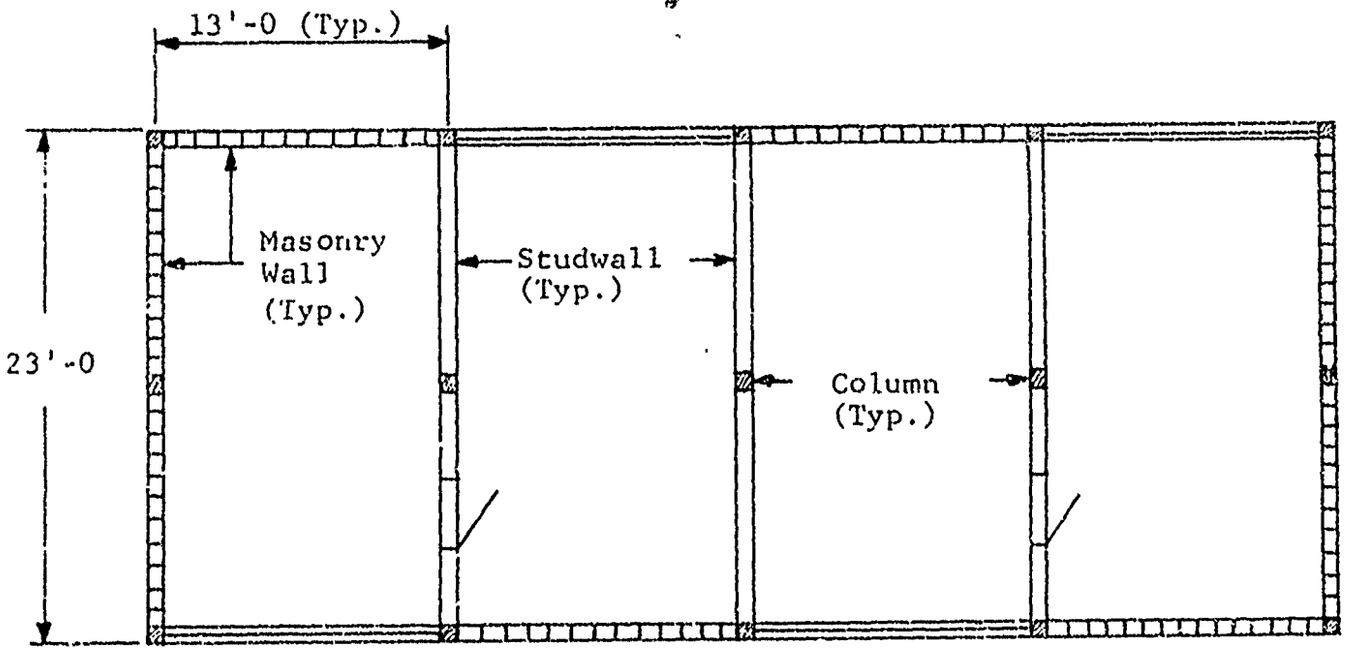

Fig. 3.4 Typical Floor Plan

masonry without windows. Interior partitions are of standard studwall construction, i.e., 2 in.by 4 in. studs at 16 in. centers with plasterboard.

The basic building module has plan dimensions of 13 ft by 23 ft. This particular building consists of eight basic modules. It can be extended on this basis to any practical length and/or height.

3.4.3 Building Contents

For purposes of studying debris distribution, each module of this building is assumed to contain a set of furnishings which are arranged as shown in Fig. 3.5. The geometry and weight of each of these items is given in Fig. 3.6. Their positions from the front wall of the room are given in the following table. The total weight of furnishings per room is 635 lbs.

	Furniture Item	Distance from Front Wall (ft) (See Fig. 3.5)
1.	Sofa	8.0
2.	Table	11.0
3.	Armchair	14.0
4.	Chair No.1	1.0
5.	Chair No.2	14.0
6.	Chair No.3	20.0
7.	Desk	2.0

3.4.4 Weapon Environment and Building Response

This building is assumed to be located at the 5 psi range of a 1 MT nuclear weapon. Its front wall is oriented at right angles to the direction of the blast wave. At this range the longitudinal masonry walls, which have an incipient collapse overpressure of 0.5 psi, will fail catastrophically as will the transverse studwalls. The structural frame including floor and roof slabs and the transverse masonry walls will remain in place. Debris will consist of broken, longitudinal masonry walls, transverse studwalls and furniture items.

The analysis performed takes into consideration the loading history that this building would experience, i.e., reflected pressure experienced by the front wall, time to wall response (approximately 0.04 sec) and the time required for the wave to engulf the building and build up on the other side. The debris transport analysis is performed on this basis.

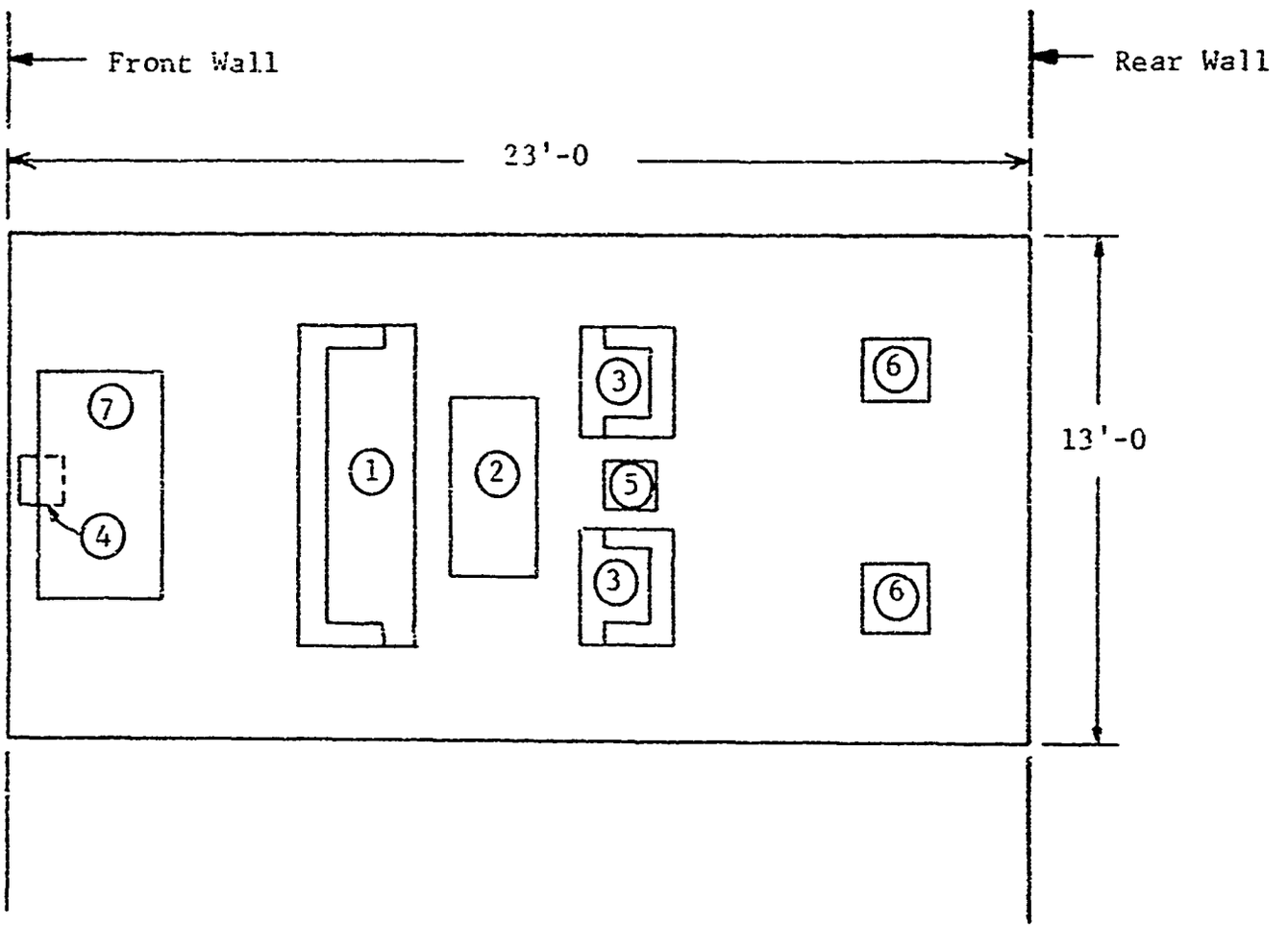

Fig. 3.5 Typical Furniture Layout

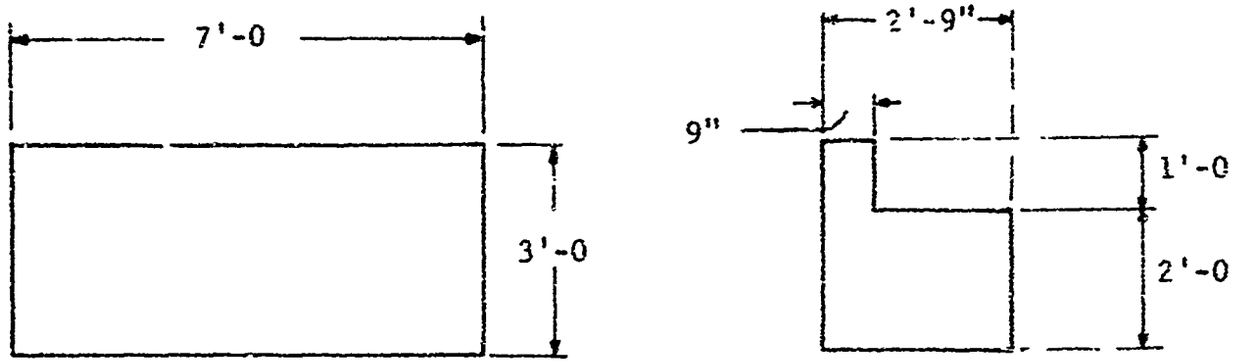

a. Sofa Weight 250 lbs

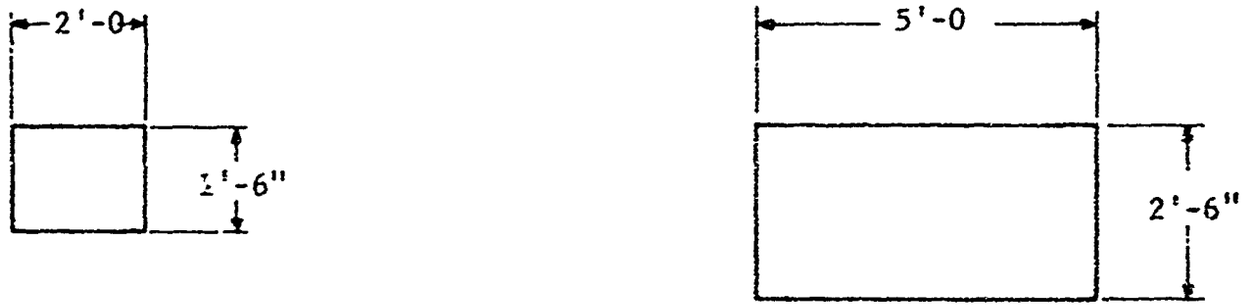

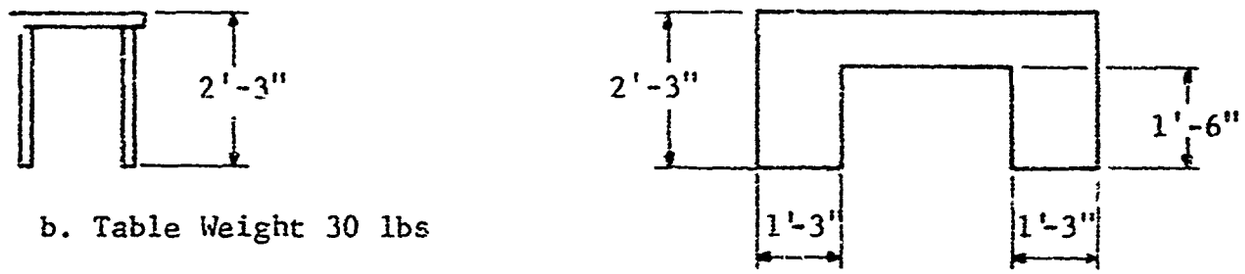

b. Table Weight 30 lbs

c. Desk Weight 150 lbs

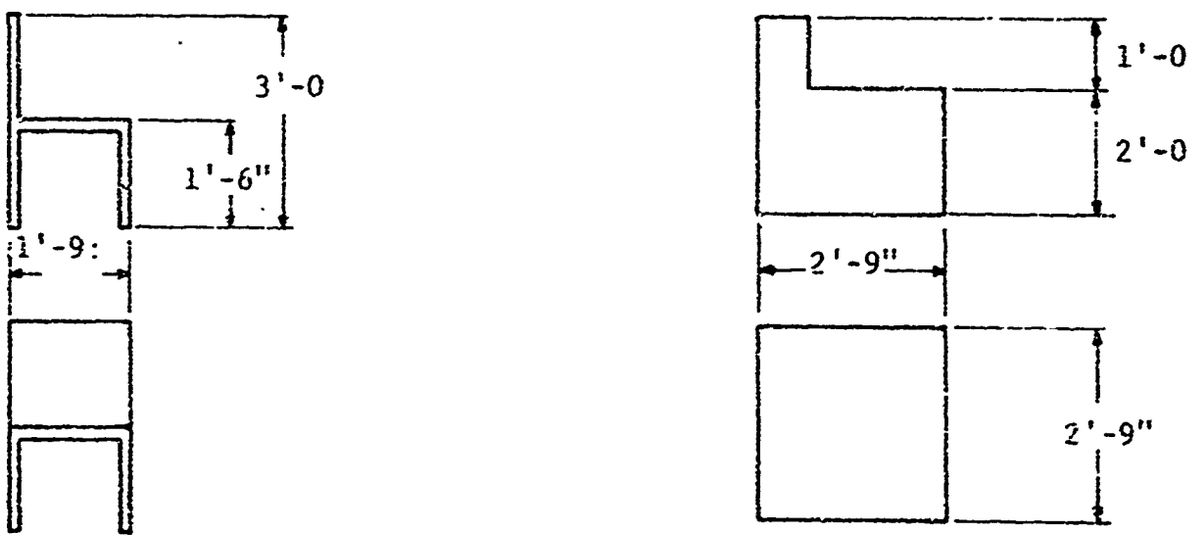

d. Chair Weight 35 lbs

e. Armchair Weight 100 lbs

Fig. 3.6 Furniture Items

Before a debris transport analysis can be performed, it is first necessary to determine the number and size of primary pieces of debris that will be produced when a given wall interacts with the blast wave and the number and size of secondary pieces that will result when a primary piece impacts the floor, wall or any other obstruction. The task of producing such information analytically is extremely difficult and at least for the present must be generated on the basis of an experiment.

The initial crack pattern chosen for the longitudinal masonry walls is shown in Fig. 3.7 and corresponds to an experimental result (Ref. 5) of a simply-supported wall having the same dimensions. This figure shows the primary pieces produced when the wall interacts with the blast wave. An assumed secondary debris pattern is shown in Fig. 3.8. Each primary piece is assumed to break up in pieces having four different sizes, i.e., one-, two-, three- and four-block sizes. These sizes correspond approximately to those obtained in the URS shock tunnel for similar walls. Physical properties of all structural debris used in the transport calculations are given in Table 3.1. In this table the primary debris pieces are designated A, B, C, D and E as in Fig. 3.7. Secondary pieces are designated as BL-1, 2, 3, 4 corresponding to the four block sizes. Each wall is assumed to break up into 58 secondary pieces after impact with the horizontal plane.

Results of the transport analysis are given in the following section. In this analysis each piece of debris (debris particle) is treated separately and individual results are combined at the end. The progress of primary wall pieces is traced from the time the wall first interacts with the blast wave to the time the particle impacts on a horizontal surface. At this time the primary particle is assumed to break in the manner shown in Fig. 3.8.

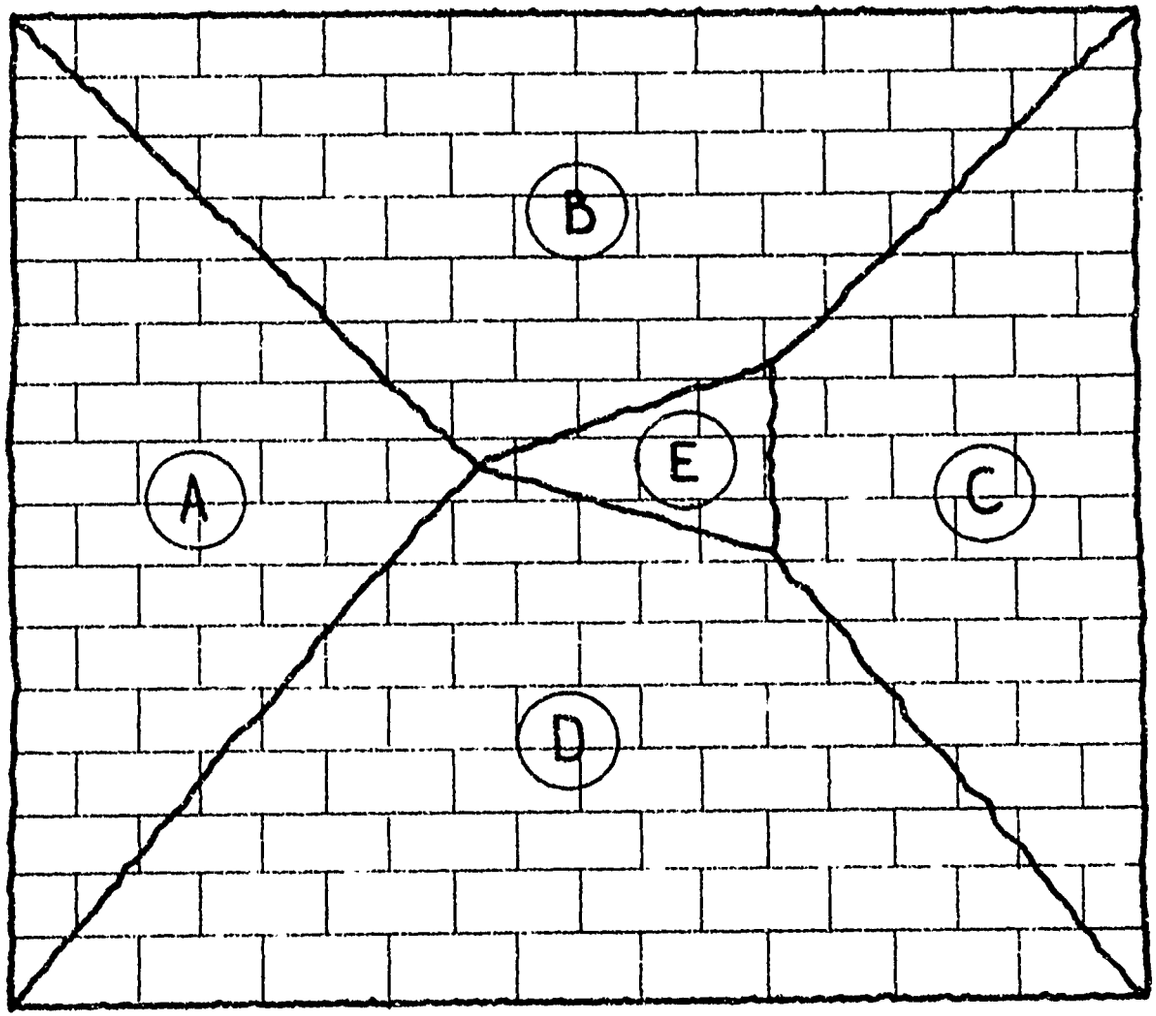

Fig. 3.7 Wall Failure Pattern

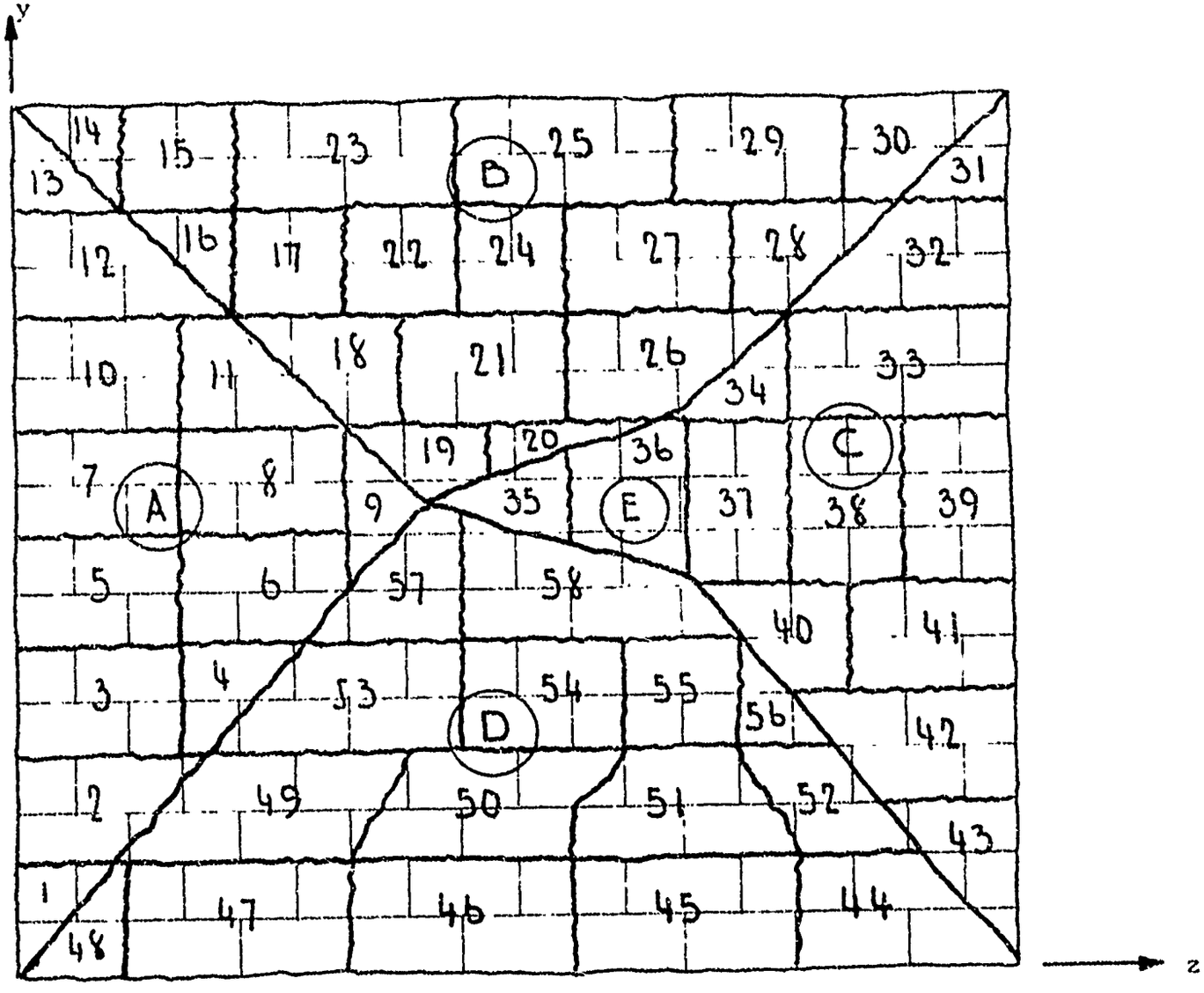

Fig. 3.8 Secondary Debris Pattern

Table 3.1

PHYSICAL PROPERTIES OF STRUCTURAL DEBRIS

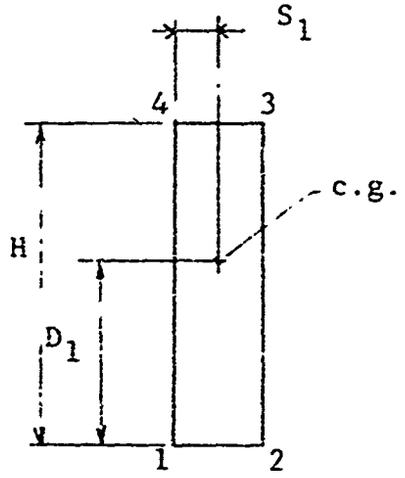

Particle	Weight (lbs)	I* (lbs-sec^2-ft)	H (ft)	D_1 (ft)	S_1 (ft)	W** (ft)
A	1050	82	11.00	5.50	0.33	4.50
B	1290	80	5.50	3.50	0.33	5.50
C	988	77	11.00	5.50	0.33	4.50
D	1580	98	5.50	2.00	0.33	5.50
E	114	1	2.00	1.00	0.33	1.00
BL-1	34	0.08	0.67	0.34	0.33	1.33
BL-2	68	0.39	1.33	0.67	0.33	1.33
BL-3	102	0.59	1.33	0.67	0.33	2.00
BL-4	136	0.78	1.33	0.67	0.33	2.67
Wall Stud	10	0.65	5.00	2.25	0.17	0.17
Plasterboard	2	0.005	1.00	0.50	0.021	1.00

*Moment of Inertia

**Maximum dimension of debris particle normal to the plane of the paper.

At this point the analysis assumes that the vertical center of gravity (c.g.) position, velocity and acceleration of each constituent particle is the same as that of the c.g. of its primary (parent) particle at the time of impact. With these initial conditions the analysis continues to trace the progress of each constituent particle until it comes to rest.

3.4.5 Results of the Debris Transport Analysis

Some initial results on the behavior of the primary debris particles are indicated in Figs. 3.9 through 3.12. Figure 3.9 shows the motion history of particle A (see Fig. 3.7) for the front wall, first story as viewed from the side. The motion is given in equal increments of time. Corresponding velocity histories for several points on the particle are shown in Fig. 3.10. The particle reaches its terminal position at 0.604 sec after arrival of the blast wave. Total (resultant)impact velocity experienced by point 4 is 45.6 ft/sec and that by point 1 is 22.6 ft/sec.

A combined motion history for particles B, D and E produced by a front wall at the first story is shown in Fig. 3.11. It will be noted that there is no interaction between these particles in the course of their motion. Thus at least for the initial part of this problem the assumption that no interaction occurs between individual debris particles appears to be reasonable.

Velocity history for particle B (front wall, first story) is shown in Fig. 3.12. Its corresponding motion history is shown in Fig. 3.11. The reason for the decrease in the velocity of point 1 is due to the tumbling action of this debris piece.

The motion history of a secondary debris particle is shown in Fig. 3.13. This particle is designated as BL-1-A and corresponds to a single block size produced by the breakup of primary particle A. For this particular example the particle was originally located in a front wall on the second level. The primary particle reached its terminal (impact) position at 0.604 sec after the arrival of the blast wave (see Fig. 3.9) at which time it broke up into 13 secondary pieces (see Fig. 3.8).

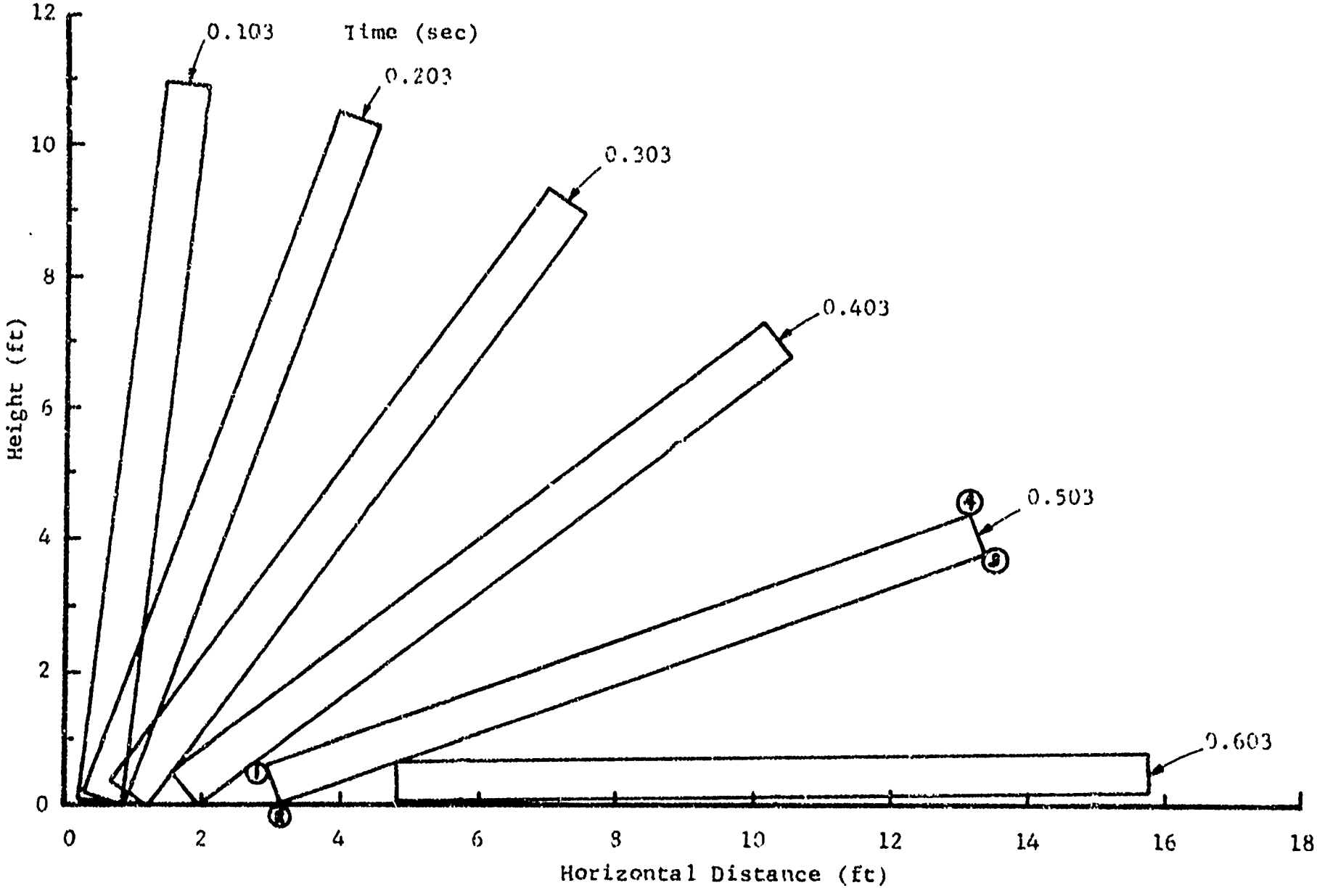

Fig. 3.9 Motion History of Particle A (Front Wall, First Story)

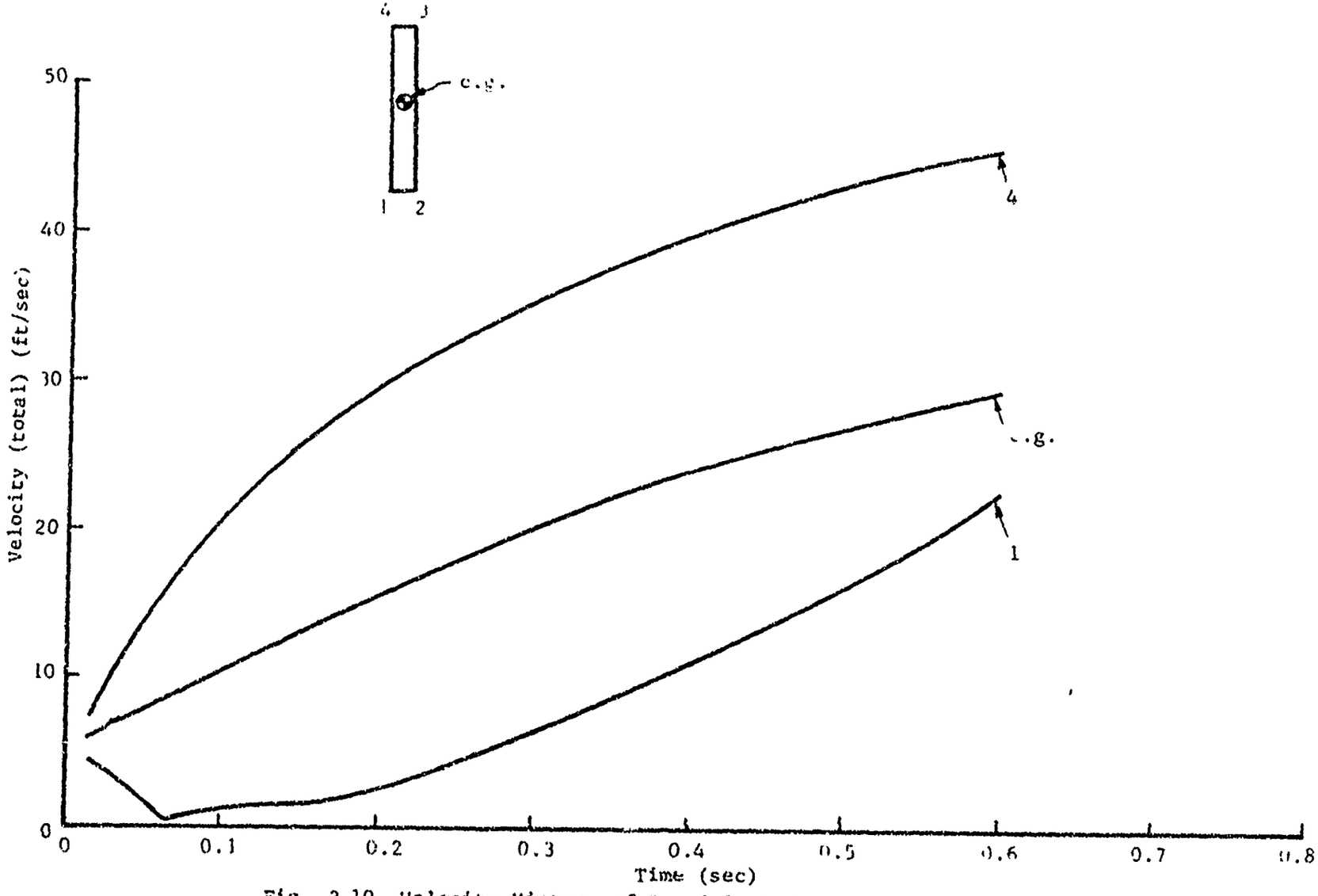

Fig. 3.10 Velocity History of Particle A (Front Wall, First Story)

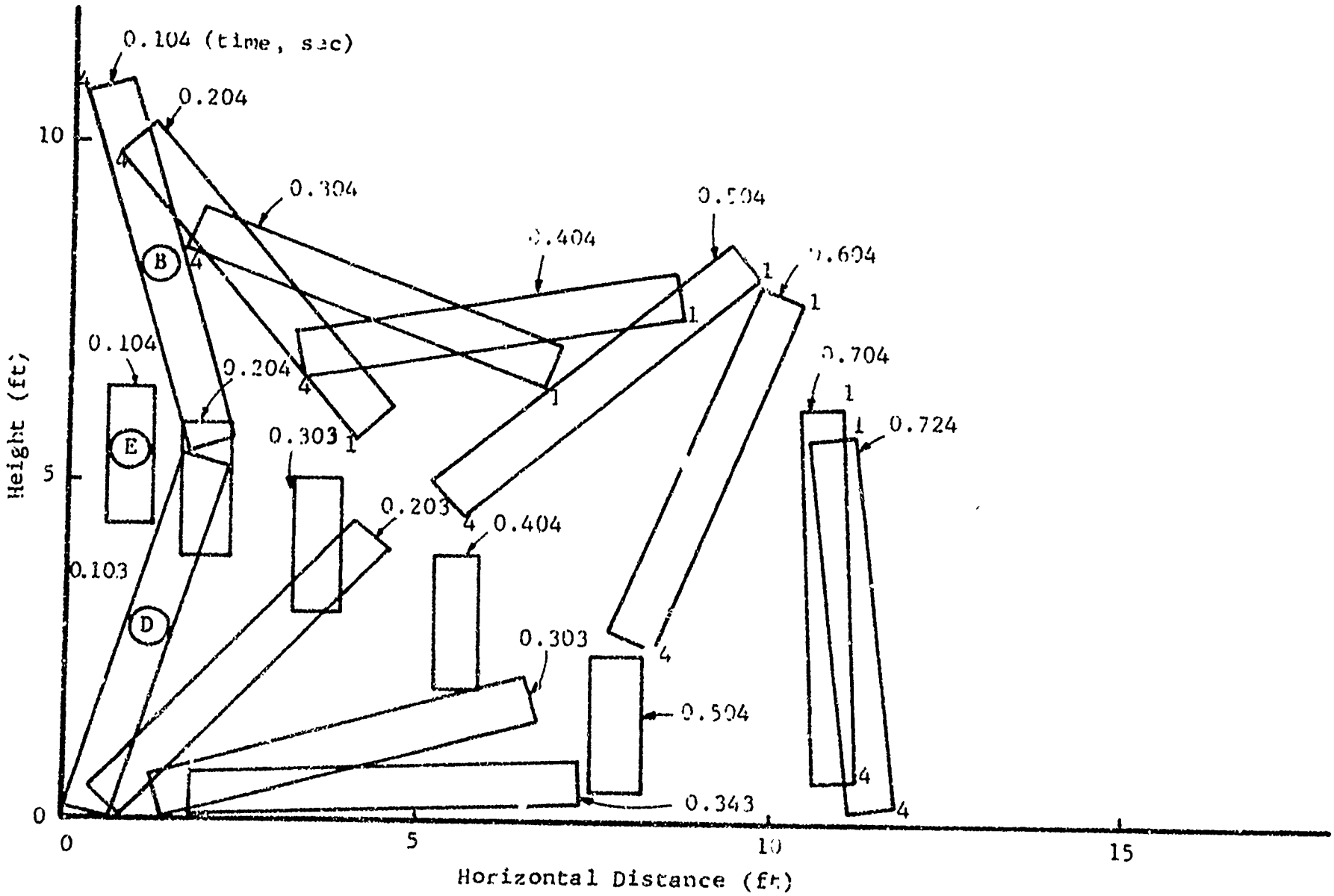

Fig. 3.11 Motion History of Particles B, D and E (Front Wall, First Story)

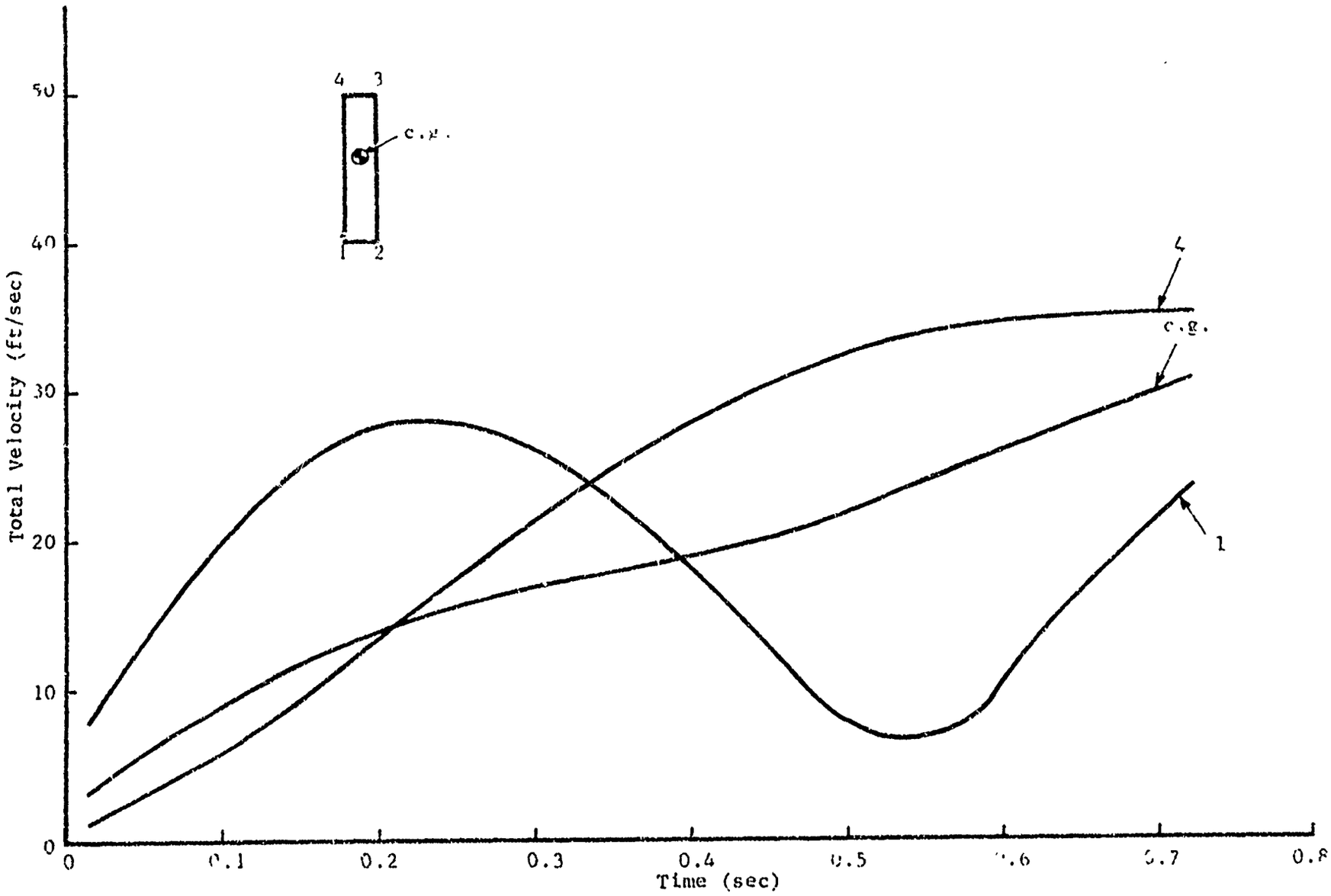

Fig. 3.12 Velocity History of Particle B (Front Wall, First Story)

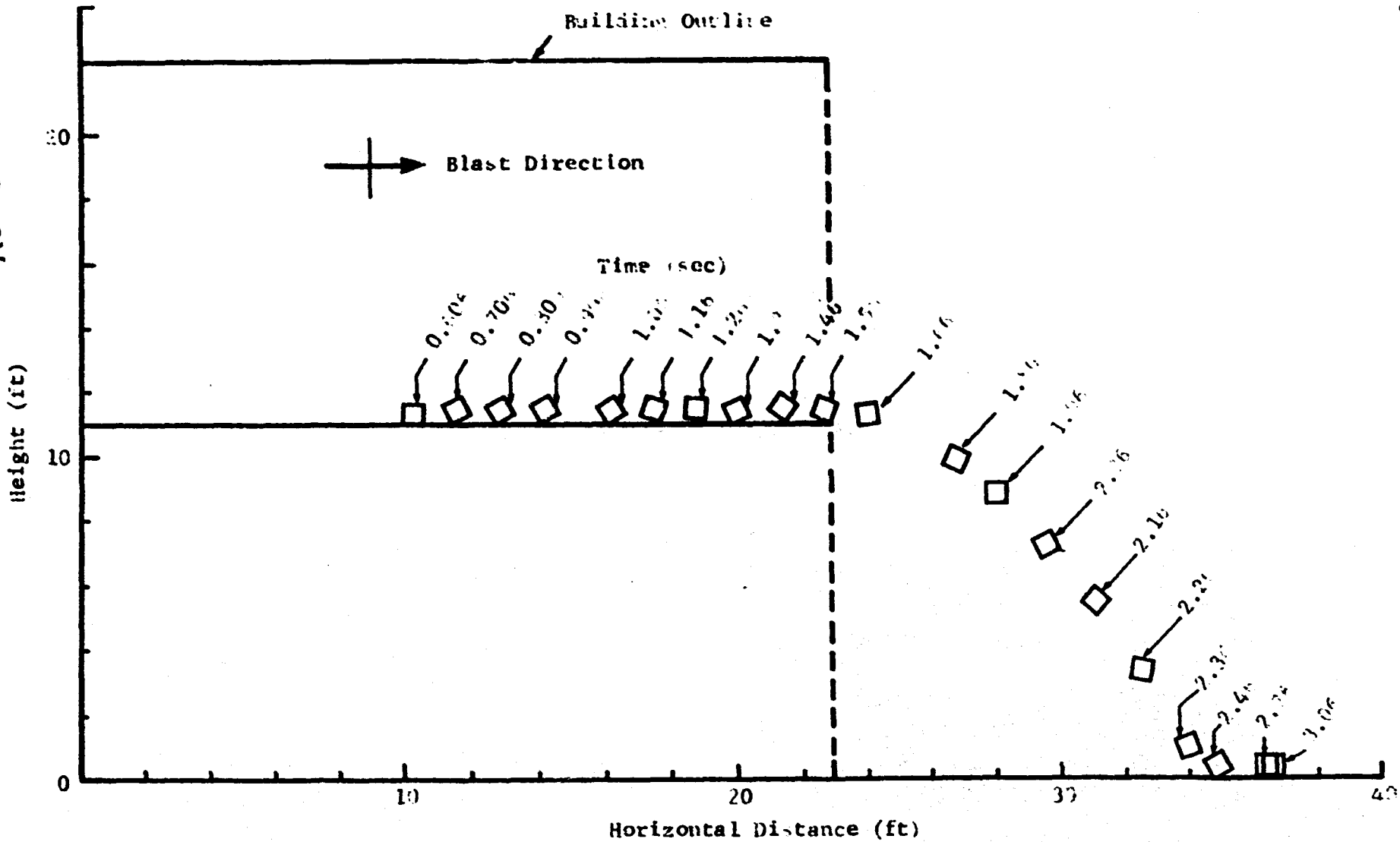

Fig. 3.1[illegible] Motion History of Particle BL-1-A ' Front Wall, Second Story)

Figure 3.13 traces the motion of one of these pieces to its terminal position which is reached 3.06 sec after the arrival of the blast wave. It will be noted that for this example the significant motion of this particle ceases 0.56 sec after the end of the positive phase for overpressure. The positive phase duration at the range of 5 psi from a 1 MT surface burst is 2.5 sec.

Final positions and arrival times for all debris particles produced by one wall (front, first story) are given in Table 3.2. These are c.g. coordinates. The coordinate system used is indicated in Fig. 3.8. Final distribution of wall debris produced by a representative portion (four modules) of this building is shown in Fig. 3.14. A corresponding weight-distance relationship along the horizontal is given in Fig. 3.15. Only masonry wall debris is included in these two figures. Furniture items and studwall debris traveled significantly greater distances and for this reason are not included in these distributions.

Horizontal coordinates (x-distance) of the final positions of furniture items and studwall debris are given in Table 3.3 together with arrival times. Velocity histories for furniture items for the first and second floors are shown in Figs. 3.16 and 3.17 respectively. For the most part these curves are not smooth and contain numerous jumps. These jumps indicate impacts with the ground surface. Second floor debris (see Fig. 3.17) experienced many more bounces before coming to rest than did the first floor debris.

3.4.6 Discussion of Results and Conclusions

In this particular problem the building debris became segregated, i.e., heavy noncombustibles remained relatively close to the building while lighter combustible debris were translated significantly further. This result was in part forced by the conditions of the problem. The building was assumed to be located in the open and sufficiently away from other buildings. It was also assumed that no interaction occurs between individual particles while in transit. For this problem interaction between light and heavy pieces should not alter the results significantly.

Table 3.2

FINAL COORDINATES AND TIME OF ARRIVAL
OF SECONDARY WALL DEBRIS (FRONT WALL, FIRST STORY)

Particle	Size*	z** (ft)	x** (ft)	Time (sec)
1	A-1	-3.7	42.9	2.91
2	A-3	-1.0	25.7	1.41
3	A-3	-1.2	27.1	1.41
4	A-1	-1.9	45.4	2.91
5	A-3	-1.2	28.4	1.41
6	A-3	0.8	28.4	1.41
7	A-3	-1.2	29.9	1.41
8	A-3	0.8	29.9	1.41
9	A-1	0.2	47.9	2.91
10	A-3	-1.2	31.2	1.41
11	A-2	0.3	31.2	1.41
12	A-3	-1.1	32.6	1.41
13	A-1	-3.7	52.1	2.91
14	B-1	1.0	48.5	2.98
15	B-2	2.0	40.8	2.03
16	B-1	2.3	48.5	2.98
17	B-2	3.4	40.8	2.03
18	B-2	4.1	40.8	2.03
19	B-1	5.1	48.5	2.98
20	B-1	6.3	48.5	2.98
21	B-3	5.8	48.4	2.63
22	B-2	4.6	40.8	2.03
23	B-4	4.0	40.8	2.03
24	B-2	6.0	40.8	2.03
25	B-4	6.6	40.8	2.03
26	B-3	7.6	48.4	2.63
27	B-3	7.8	48.4	2.63
28	B-2	9.4	40.8	2.03
29	B-3	9.0	48.4	2.63
30	B-2	10.8	40.8	2.03
31	C-1	15.8	52.3	2.91
32	C-3	13.7	32.8	1.41
33	C-4	13.3	31.4	1.41
34	C-1	13.1	49.5	2.91
35	E-1	6.2	46.3	2.13
36	E-2	7.5	52.4	2.38
37	C-3	11.2	29.8	1.41
38	C-3	12.5	29.8	1.41
39	C-3	13.8	29.8	1.41
40	C-2	12.0	28.0	1.41
41	C-3	13.6	28.0	1.41
42	C-3	13.6	26.6	1.41
43	C-2	14.0	25.2	1.41
44	D-3	10.5	13.6	1.20
45	D-4	8.0	13.6	1.20
46	D-4	5.5	13.6	1.20
47	D-4	2.7	13.6	1.20
48	D-1	1.0	25.9	1.95
49	D-4	3.3	14.9	1.20
50	D-4	5.5	14.9	1.20
51	D-3	8.0	14.9	1.20
52	D-2	9.7	14.9	1.20
53	D-4	4.3	16.4	1.20
54	D-3	6.5	16.4	1.20
55	D-2	8.0	16.4	1.20
56	D-1	9.2	28.5	1.95
57	D-2	4.8	17.9	1.20
58	D-4	6.5	17.9	1.20

*The letter refers to the primary particle - A, B, C, D or E (see Fig. 3.7). The number refers to the size, i.e., 1-, 2-, 3- or 4- concrete blocks.

**Coordinate system is indicated in Fig. 3.8.

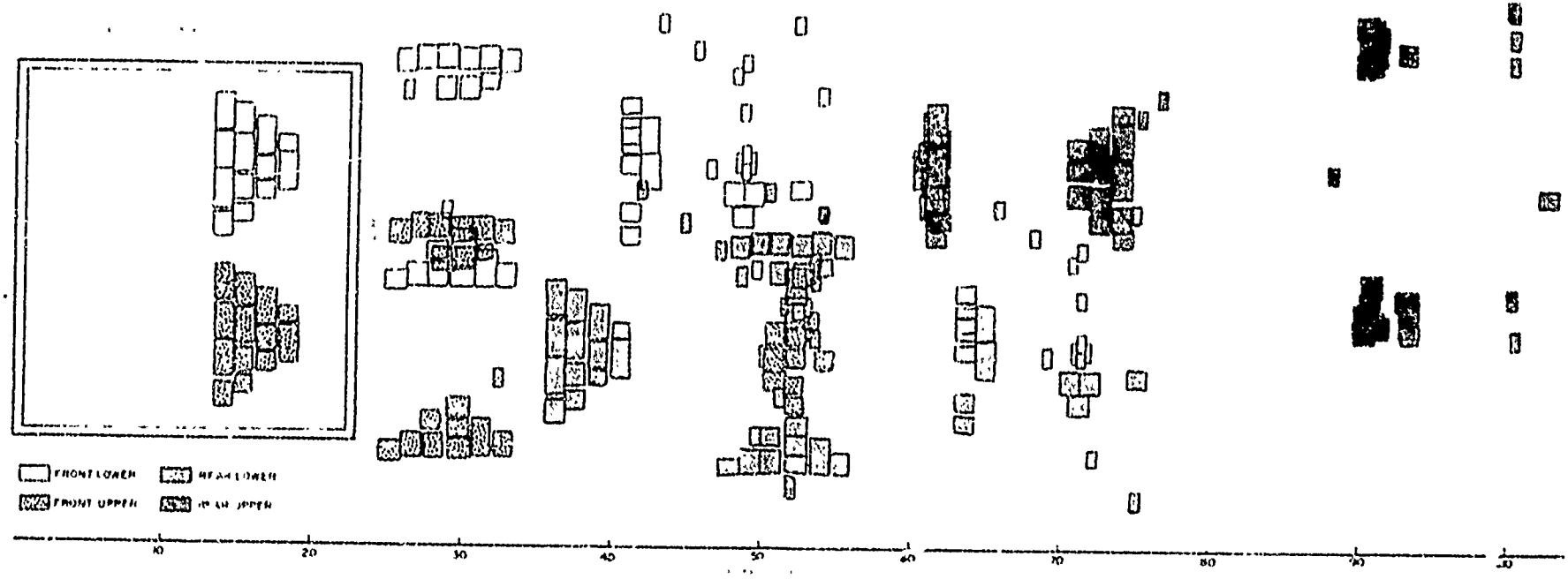

Fig. 3.14 Distribution of Wall Debris

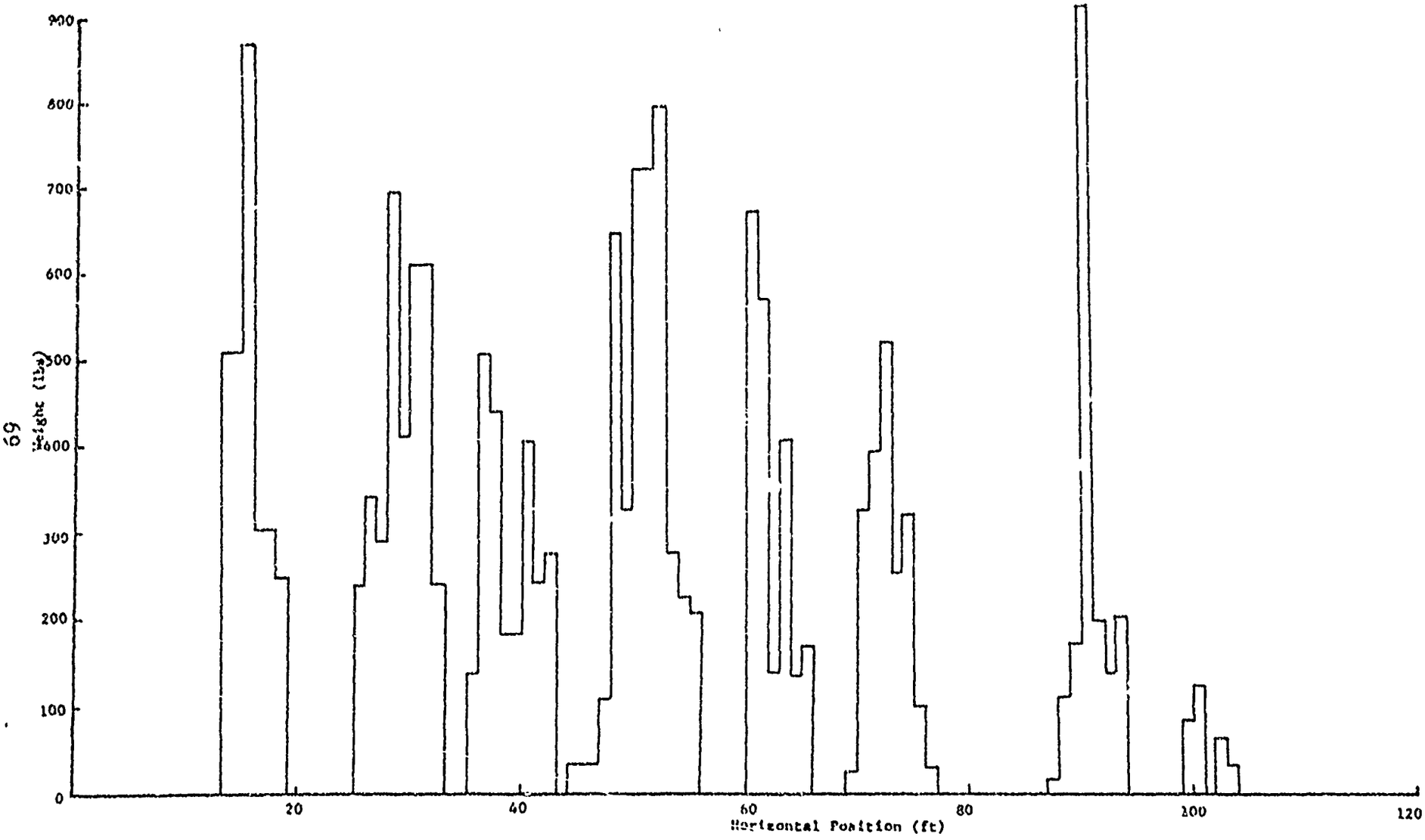

Fig. 3.15 Weight-Distance Relationship of Wall Debris

Table 3.3

FINAL POSITIONS AND TIMES OF ARRIVAL
OF FURNITURE ITEMS AND STUDWALL DEBRIS

	Item	x_i^* (ft)	x_f^{**} (ft)	t_f^{***} (sec)
First Floor	Sofa	8.0	210	5.8
	Table	11.0	328	5.0
	Armchair	14.0	259	7.1
	Chair No.1	1.0	189	5.8
	Chair No.2	14.0	202	5.8
	Chair No.3	20.0	198	5.7
	Desk	2.0	238	6.0
Second Floor	Sofa	8.0	221	5.8
	Table	11.0	373	6.7
	Armchair	14.0	263	6.0
	Chair No.1	1.0	188	5.7
	Chair No.2	14.0	212	5.8
	Chair No.3	20.0	224	5.8
	Desk	2.0	246	6.0
	Plasterboard	11.5	350	6.0
	Stud	11.5	282	6.0

$^*x_i$ - initial position

$^{**}x_f$ - final position

$^{***}t_f$ - time of arrival

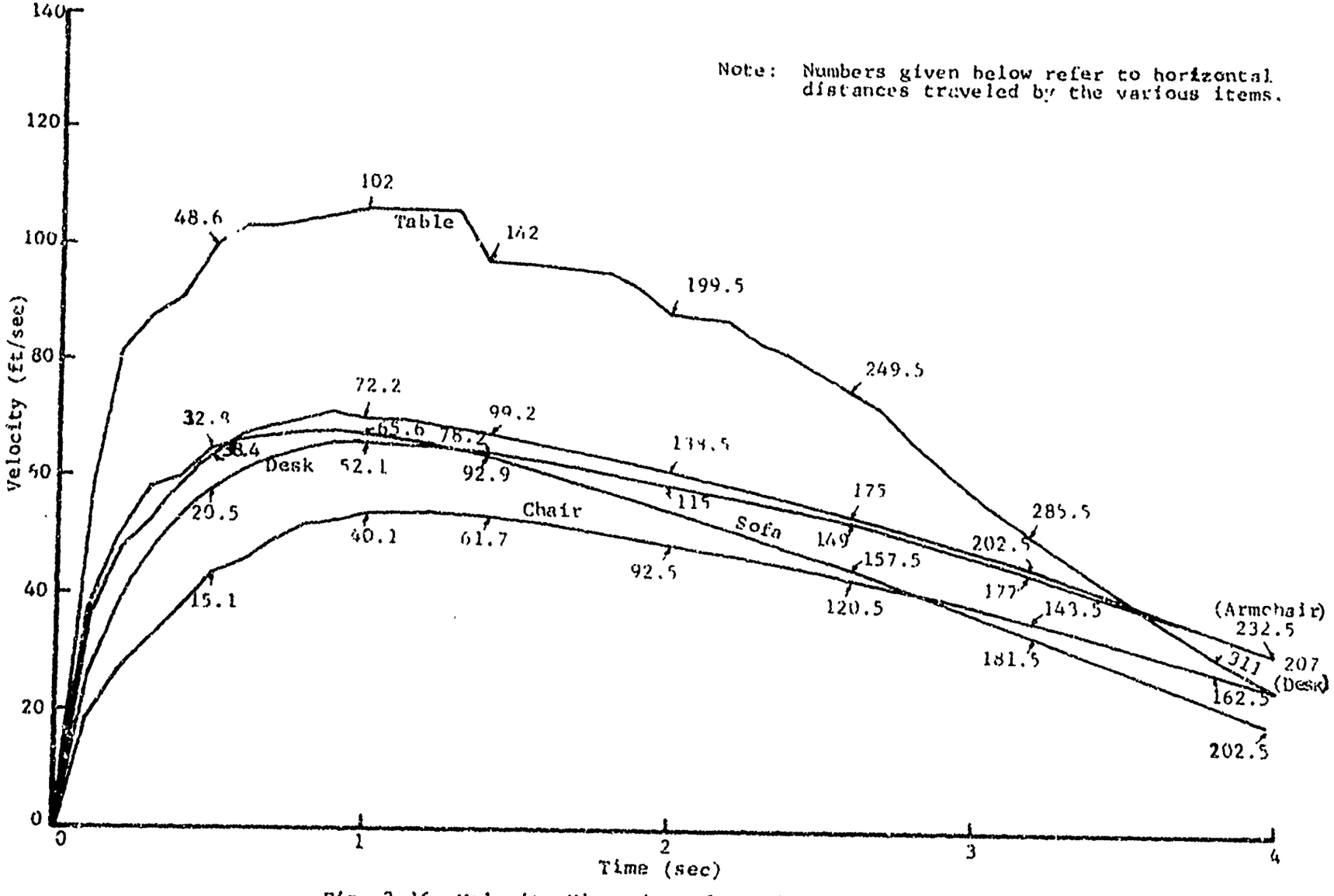

Fig. 3.16 Velocity Histories of Furniture Items (First Floor)

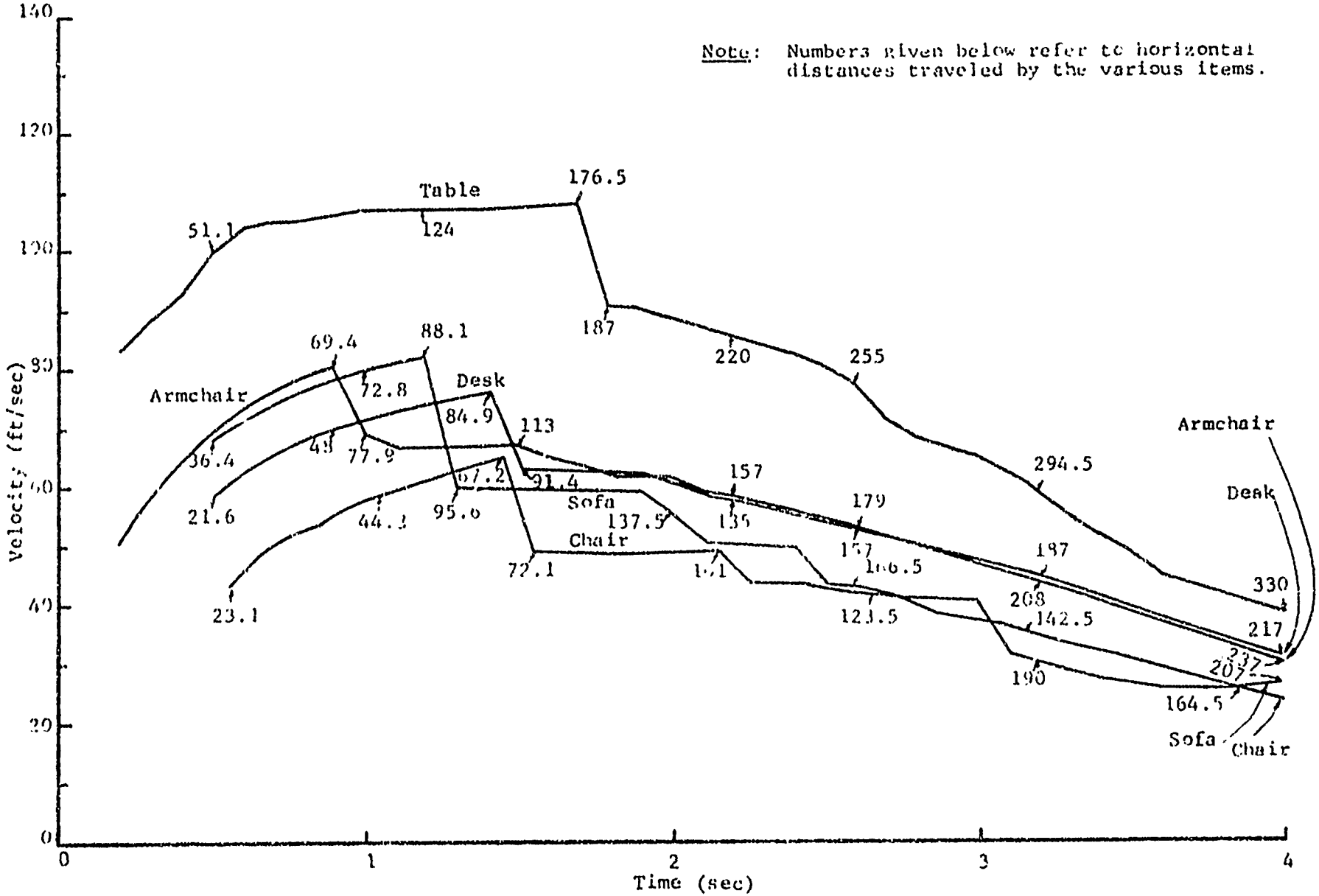

Fig. 3.17 Velocity Histories of Furniture Items (Second Floor)

If interactions occur, they will most likely occur in the early part of the loading, i.e., while the various items are still in the building or close to it. At that time the wind velocity is still sufficiently high and its duration still sufficiently long to loft and segregate the debris in these two categories, i.e., mostly combustibles and mostly noncombustibles. If such segregation does indeed occur in most practical situations then it should be of interest to the designer and planner of shelter systems since this occurrence provides an insight into possible patterns of postattack fires. The problem is one of blast-fire interaction.

The computational model developed provides a basis for determining realistic debris distributions for many practical situations. At the present time it is capable of considering the presence of neighboring buildings, their breakup and contribution to the total debris pile. The model is capable of tracing the progress of individual debris pieces and their interaction with nonmoving obstructions. However, it is not capable of considering the interaction between several pieces of debris while in transit. Should this be an important consideration, such influence can certainly be included. For the present, the model should be exercised parametrically on similar problems as described herein in order to isolate parameters and their significance to the overall problem. Such parameters should include:

- Building geometry (plan, height)
- Differential strength of walls
- Numbers and sizes of wall debris
- Size of window openings
- Differences in soil-spring coefficients
- Differences in aerodynamic coefficients
- Proximity of neighboring buildings
- Differential strengths of neighboring buildings
- Geometry of neighboring buildings
- Ranges of furniture items
- Interaction between several debris pieces while in transit

Although the problem described herein represents a simple, special case of the overall debris problem it was nonetheless treated in necessary detail.

REFERENCES

1. Edmunds, J. E., "Structural Debris Caused by Nuclear Blast", United Research Services Corporation, for Office of Civil Defense, Contract OCD-PS-64-19, October 1964.

2. Feinstein, D. I., "Debris Distribution", IIT Research Institute, for Office of Civil Defense, Contract OCD-PS-64-50, Subtask 3322B, August 1964.

3. Garnett, R. L., et al, "Debris Formation and Translation", IIT Research Institute, for Office of Civil Defense, Contract OCD-PS-64-201, November 1966.

4. Byrnes, J. B., "Effects of an Atomic Explosion on Two Typical Two-Story-and-Basement Wood Frame Houses", Operation UPSHOT-KNOTHOLE, WT 792, Federal Civil Defense Administration, Washington, D.C., September 1953.

5. Edmunds, J. E., "Experiments to Determine Debris Formation From Corrugated Steel and Brick Walls", URS Research Company, for Office of Civil Defense, Contract DAHC 20-69-C-0129, Work Unit 3313 C, January 1970.

6. Wilton, C. and Gabrielsen, B., "Shock Tunnel Tests of Wall Panels", URS Research Company, for Defense Civil Preparedness Agency, Contract DAHC 20-71-C-0223, Work Unit 1123 G, January 1972.

7. Denton, D. R., "A Dynamic Ultimate Strength Study of Simply-Supported Two-Way Reinforced Concrete Slabs", TRI-789, U.S. Army Engineer Waterways Experiment Station, Vicksburg, Miss., July 1967.

8. "Design and Testing of Blast Loaded Reinforced Concrete Slab System", for Office of Civil Defense, U.S. Army Engineer Waterways Experiment Station, Vicksburg, Miss., July 1967.

9. Wiedermann, A. and Nielsen, H., "Debris and Fire Environment from Soft Oil Storage Tanks Under Nuclear Attack Conditions", IIT Research Institute, for U.S. Army Engineer Division, Huntsville Corps of Engineers, Contract DACA 87-70-C-0001, 1971.

CHAPTER 4

COST AND PEOPLE SURVIVABILITY COMPARISON OF PERSONNEL SHELTERS LOCATED ABOVE AND BELOW GRADE

4.1 INTRODUCTION

The objective of the effort described herein was to determine differences in cost and protective capabilities of two shelters having identical geometry and design hardness levels, except that one is to be located at grade (first story), the other below grade (basement).

In order to have a reasonable basis for comparison, four buildings were designed from the same basic floor plan (Fig. 4.1). The four buildings are

(1) Basic building, no basement, no shelter.
(2) Basic building with blast shelter at grade.
(3) Basic building with basement area, no shelter.
(4) Basic building with shelter below grade.

For purposes of this study the basic building was designed as a small one floor office building. The building dimensions are 84 ft by 150 ft, with a floor area of 12,600 sq ft. Under conventional use the building might serve as a typical small professional structure. For direct, nuclear weapon effects protection, a section approximately 50 ft by 37 ft (corresponding to two 25 ft by 37 ft office spaces) was chosen for the shelter area. The shelter was designed to withstand the blast effects at the range of 15 psi free field overpressure resulting from an MT size nuclear weapon. Structural requirements for blast resistance in reinforced concrete (R/C) provide a fallout radiation protection factor in excess of 100.

The shelter was first designed at grade within the basic building. Its location was chosen to utilize most effectively the protection existing walls and partitions of the parent building might possibly provide. Next, a shelter was designed in the same position as the first, but below grade. The basic conventional building and

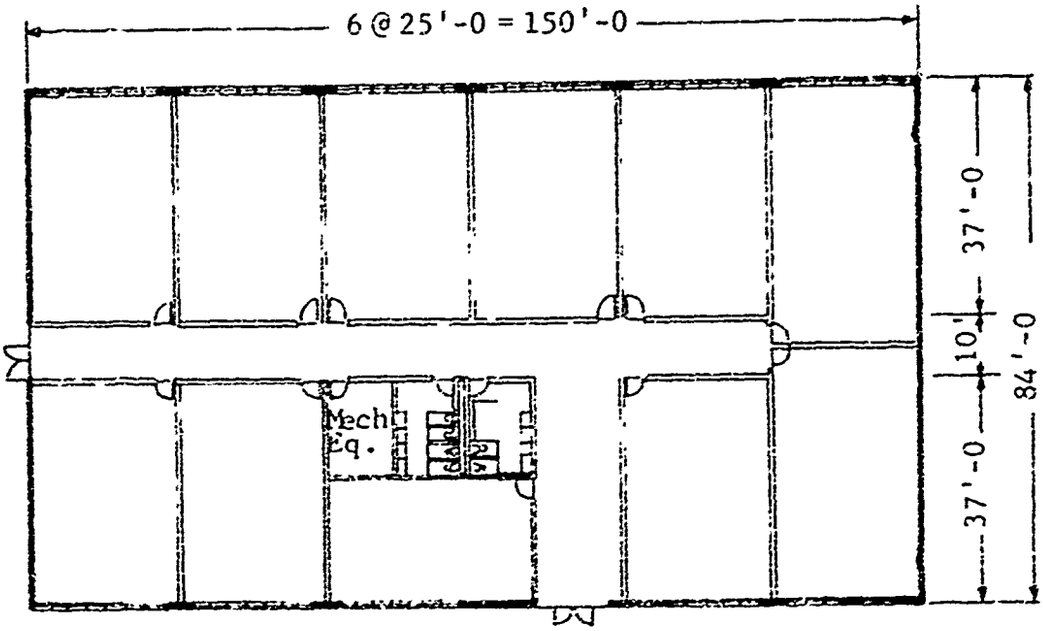

Fig. 4.1a Basic Building Plan

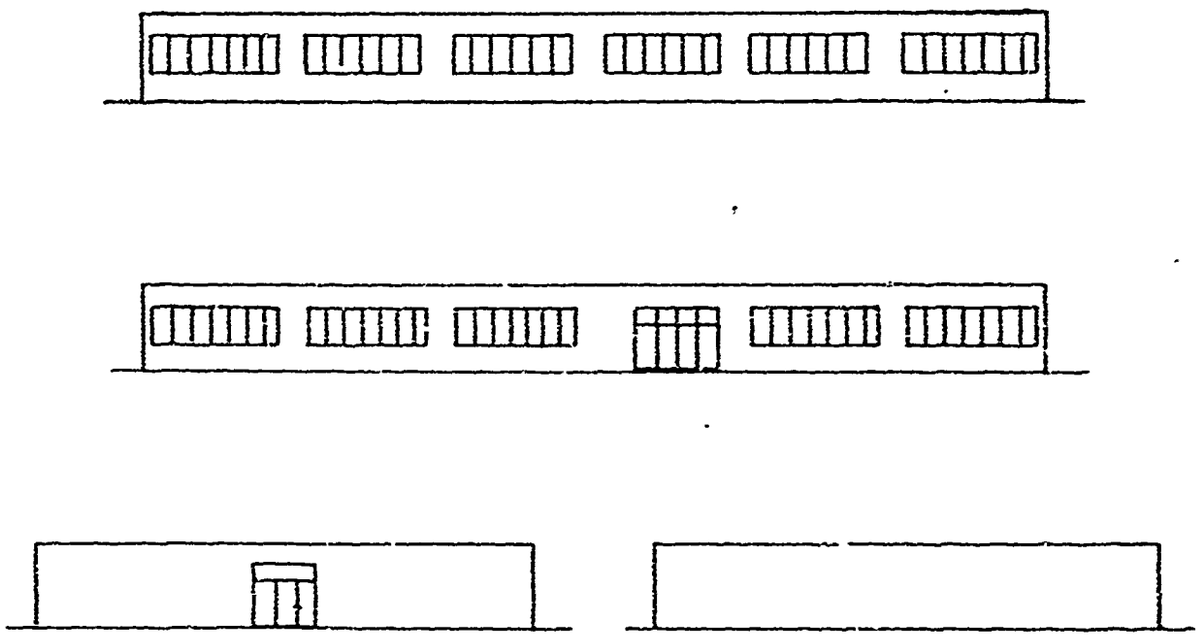

Fig. 4.1b Basic Building Elevations

the same building with a 50 ft by 37 ft conventional basement were designed for comparison with the shelter designs. Although the at-grade shelter occupies two offices it is expected that it (as well as the below grade shelter) will serve dual purposes, that is, conventional use may be made of them in addition to emergency occupancy. The below grade shelter increases the basic building floor area by 1850 sq ft.

Cost estimates* for the four designs are based on new construction, with the shelters being an originally planned part of the building, and not as additions to an existing structure. Conditions typical to the Chicago area were used for both design and cost estimating.

4.2 ARCHITECTURAL

The basic building, planned as a small office structure, has an occupancy under conventional use of approximately 95 people. Typical occupancy would probably be less. The shelter areas, based on an allowance of 10 sq ft per person have an emergency occupancy of 180 people. Sanitary facilities are provided with at least minimum provisions as specified by the Chicago Building Code. However, no emergency sanitation was provided for the blast shelter. Normal equipment such as telephone outlets, lighting, heating and air conditioning are included. The interior partitions are 8 in. hollow concrete block walls, and being nonload bearing, the office layout and plan may be varied depending on specific needs. The inside finishing consists of asphalt tile floor, suspended ceiling system, and painted concrete block walls.

Both shelter variations are divided by a concrete bearing wall for reasons of structural support of the top slab, and for partitioning under conventional use. The below grade shelter has a

*Unit costs appearing in this report were provided by George Kennedy & Associates, Inc., 75 East Wacker Drive, Chicago, Ill., who were employed as consultants for costing and design of mechanical and electrical systems in the course of this study.

clear inside height of 8 ft-3 in. which provides more than the minimum required volume per person under emergency use. The above grade shelter is taller, with 9 ft-4 in. clear ceiling height, in order to conform to the remainder of the building.

4.3 MECHANICAL

The mechanical system for the building includes ventilation and air conditioning capabilities. Based on an occupancy of 95 people, the basic building air supply system provides for 162 cfm per person of which 24 cfm are fresh air, the remainder being recirculated. This air supply results in 7.9 air changes per hour in the basic building plan. The shelters (either variation) have emergency air handling equipment protected inside the shelter area and capable of supplying 15.5 cfm per person for an emergency shelter occupancy of 180 people. All of this air supply is fresh. Ductwork and hardened exhaust and inlet shafts were provided. The emergency shelter air supply results in 9.6 air changes per hour. The basic office areas are air conditioned, but the shelter was not given any emergency air conditioning. Standard air filters are used for the office areas, while CBR filters were provided for the shelter air supply.

Additional equipment for the basic building and shelter variations include fire protection with a sprinkler system having one sprinkler head for every 100 sq ft of floor area. The sprinkler heads would be integral with the suspended ceiling system.

4.4 ELECTRICAL

Since normal commercial power may be assumed lost, an emergency 15 KW generator for the shelter is included. Lighting fixtures giving 100 ft candles of illumination for the office areas and corridors are provided. The emergency motor-generator, in addition to driving the ventilation system, can provide for a minimum of 10 foot candles illumination in the shelters. Additional equipment includes wall outlets, switches, wiring, and telephone outlets.

4.5 STRUCTURAL

The structural system of the basic building consists of a steel frame with exterior concrete block bearing walls. Column lines are at 25 ft-0 in. along the 150 ft length of the building. Main girder spans are 28 ft-0 in. Open web steel joists at 4 ft-0 in. spacing and 25 ft-0 in. span are used to support the roof structure, which is lightweight concrete poured on a corrugated steel deck. The long walls of the building have large window openings with the girders bearing between them on 8 in. thick unreinforced solid concrete block walls. The short walls of the building are 8 in. thick unreinforced hollow concrete block bearing walls and are without openings except for an exit on one side. All exterior walls have a 4 in. facing of brick, but no structural use was made of it. Interior partitions are nonload bearing 8 in. hollow block walls. The floor is a 6 in. concrete slab with wire mesh reinforcement poured at grade on a base course of 6 in. crushed rock. The wall foundations are simple strip footings 3 ft-6 in. below grade as specified by the Chicago Building Code. Spread footings (5 ft by 5 ft) were designed for the columns.

The small basement area of the basic building has 8 in. concrete block walls except for the 10 in. R/C exterior wall. The overhead first floor is an 11-1/2 in. concrete slab spanning between the basement walls and center partition wall. It was designed for continuity over the center wall.

The selection of the structural system was based on anticipated economy with the use of steel joists and concrete block walls. The basic structure, however, offers very little blast resistance.

R/C shelters were designed for two cases: first, the shelter was put at grade within the building occupying two adjacent office areas (see Fig. 4.2a) with the remaining building unaffected; second, the shelter was put below grade (immediately beneath the area of the above grade shelter) leaving the basic building essentially the same except for an access stairway (see Fig. 4.2b). Both shelters were designed for the dynamic effects of a 15 psi blast overpressure, and it is assumed that they can take any reasonable conventional loading.

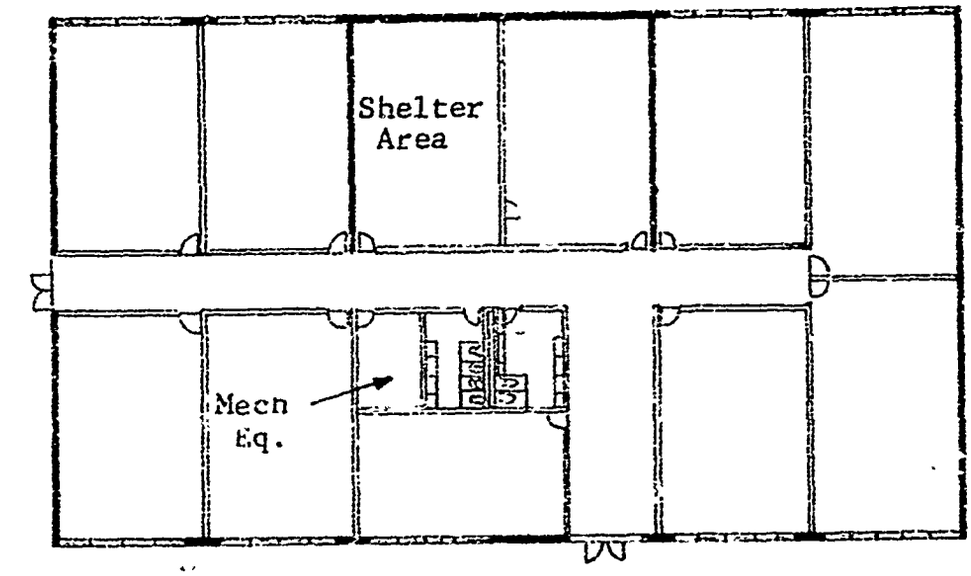

Fig. 4.2a Building with Shelter at Grade
(Plan and Elevation)

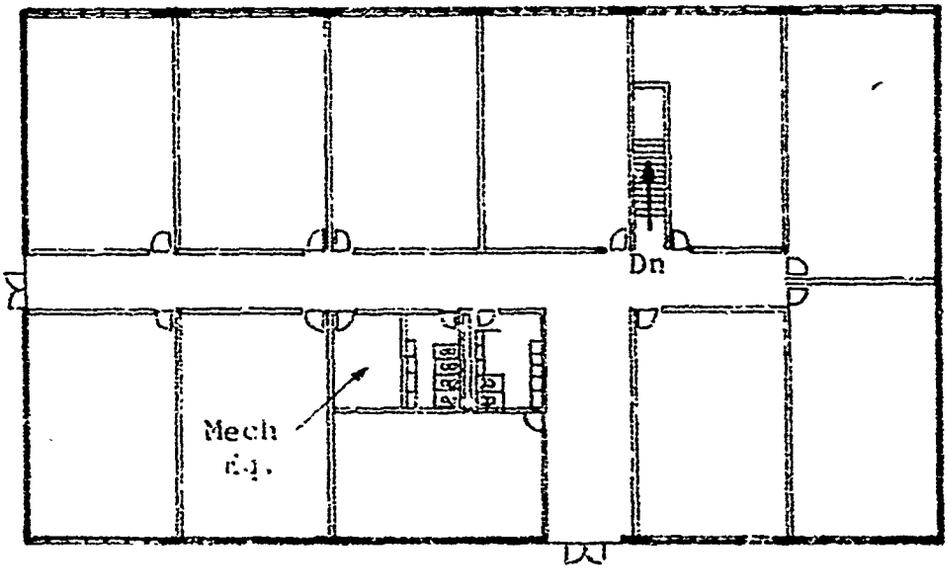

Fig. 4.2b Building with Blast Shelter Below Grade (Plan)

The shelter top slab was designed as two simply supported two-way slabs. A R/C partition wall serves to support one long edge of both slabs. The shelter walls were designed for dynamic effects as one-way slabs spanning from top of footing to the top slab. The following concrete thicknesses were used (see Fig. 4.3a and 4.3b):

	At Grade Shelter	Below Grade Shelter
Top slab	15 in.	15 in.
Peripheral walls	12 in.	10 in. (12 in. on exposed side)
Interior wall	12 in.	12 in.
Floor slab	6 in.	6 in.
Stairwell walls	-	8 in.

The at grade shelter also serves as part of the structural system of the building under conventional use. Adjacent roof joists and girders bear on the shelter walls, and the top slab serves as roof for the two offices it spans, eliminating the columns, girders and joists normally used.

Concrete strength of 3000 psi at 28 days and reinforcing steel of 40,000 psi minimum yield point were used. Structural steel is A36, but high strength 50,000 psi yield joists were used. Soil bearing pressure was assumed to be 2500 psf allowable. For blast effects, ultimate strength design after the methods presented in Ref. 1 was used. Elastic design procedure was used for the conventional building design. Structural details for the shelters are shown in Fig. 4.4.

4.6 DESIGN ASSUMPTIONS

4.6.1 Weapons Effects

The peak incident overpressure used in the design of the shelters was 15 psi. This corresponds approximately to the following weapons (see Ref. 5):

Weapon (surface burst)	Shelter distance to ground zero
1 MT	1.6 miles
20 MT	4.4 miles

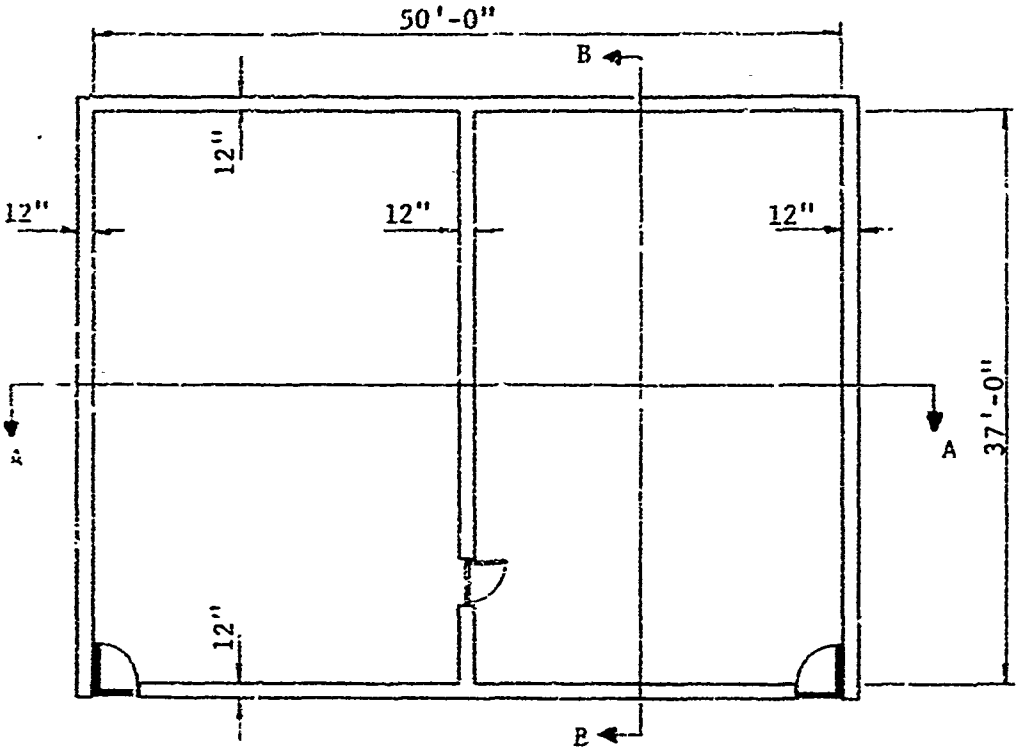

Fig. 4.3a At Grade Shelter Plan

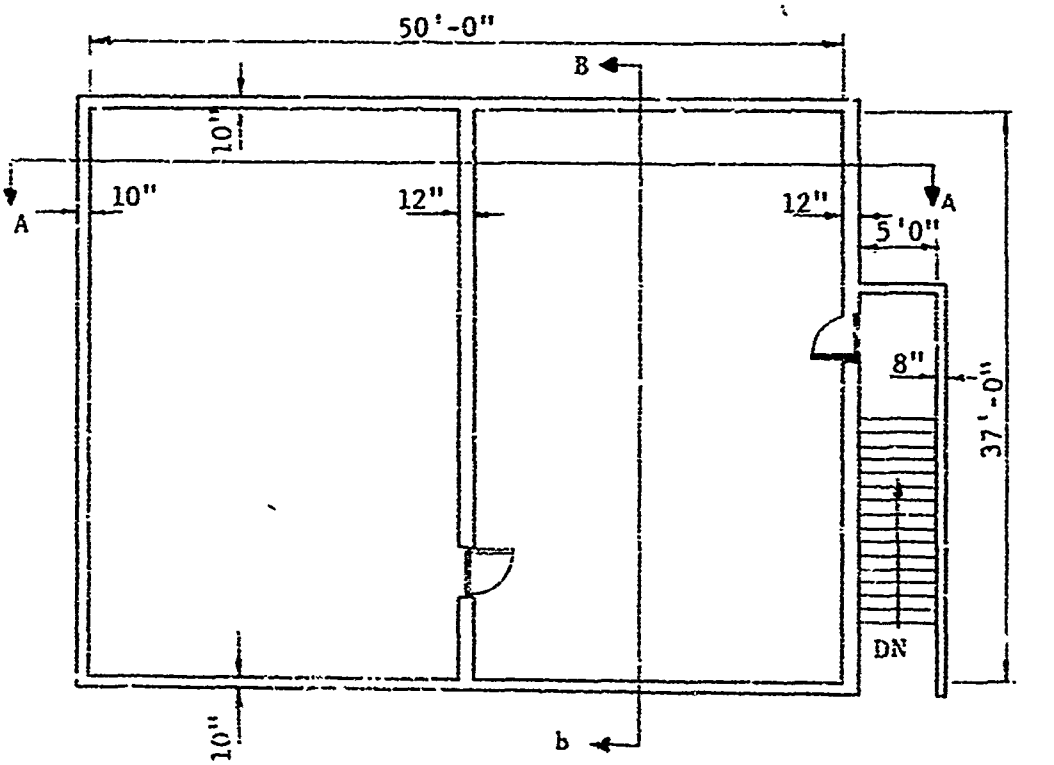

Fig. 4.3b Below Grade Shelter Plan

SCALE

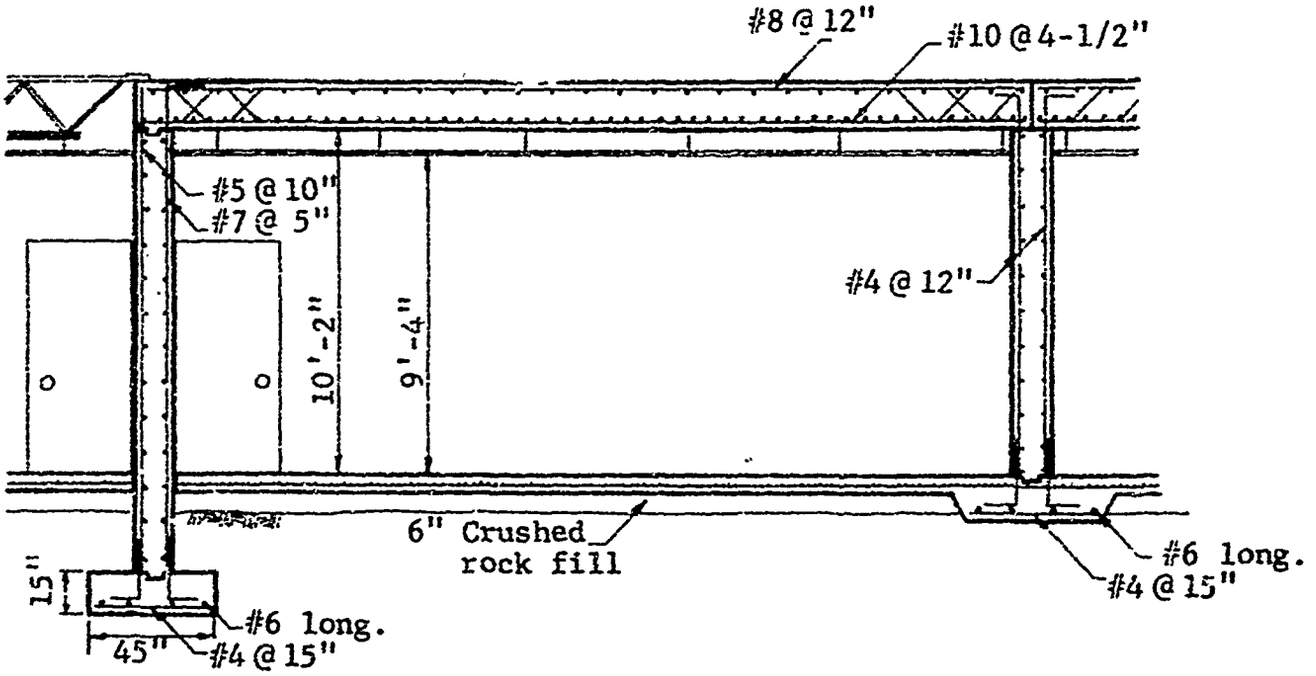

Fig.4.4a Section A-A, at Grade Shelter

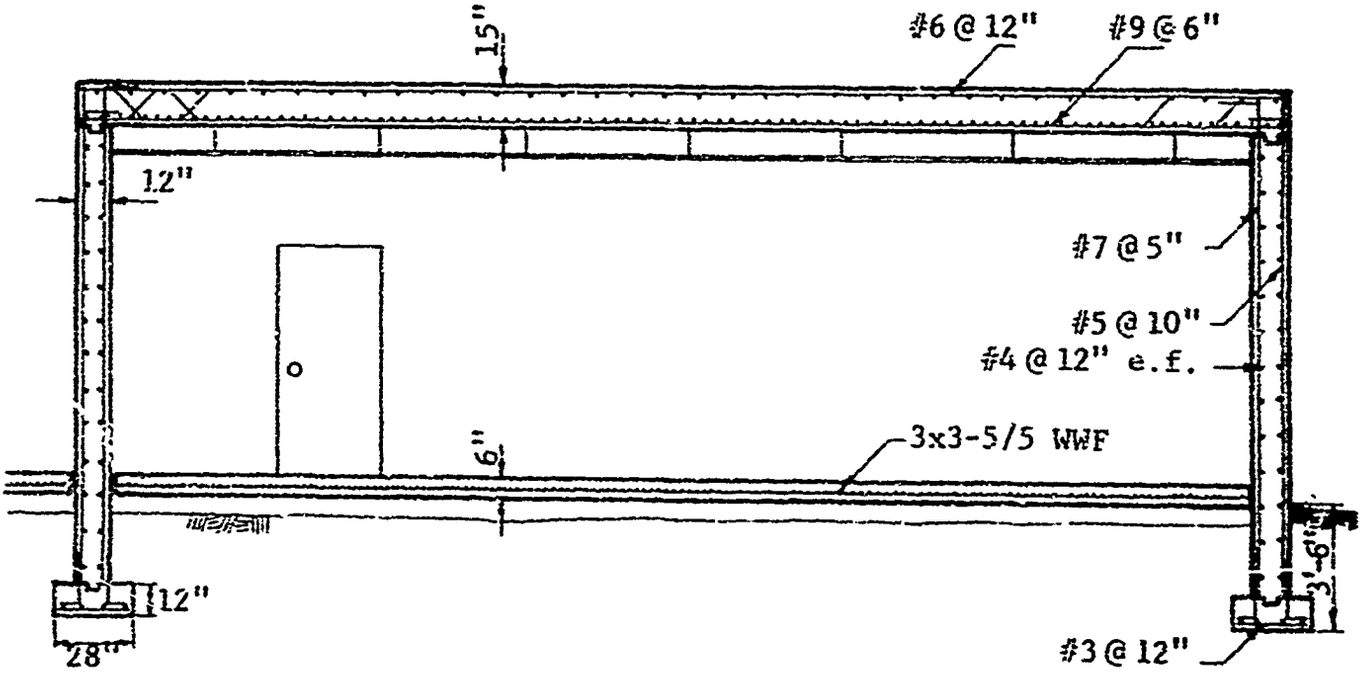

Fig.4.4b Section B-B, at Grade Shelter

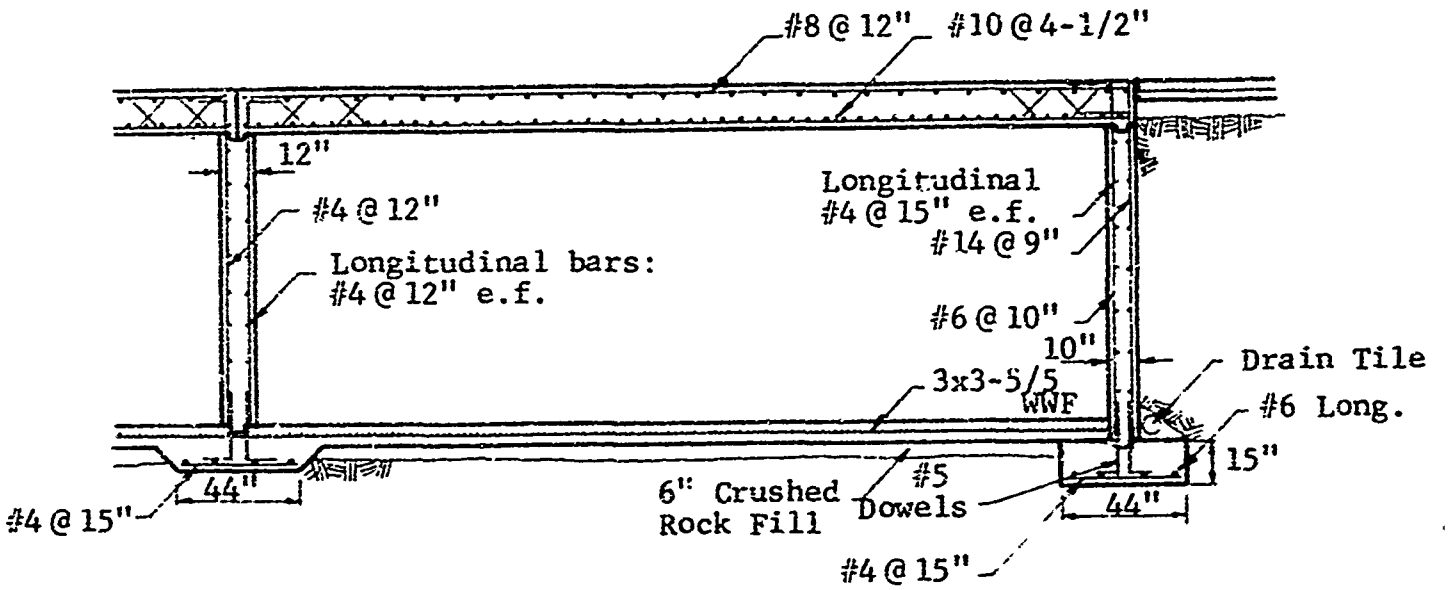

Fig.4.4c Section A-A, below Grade Shelter

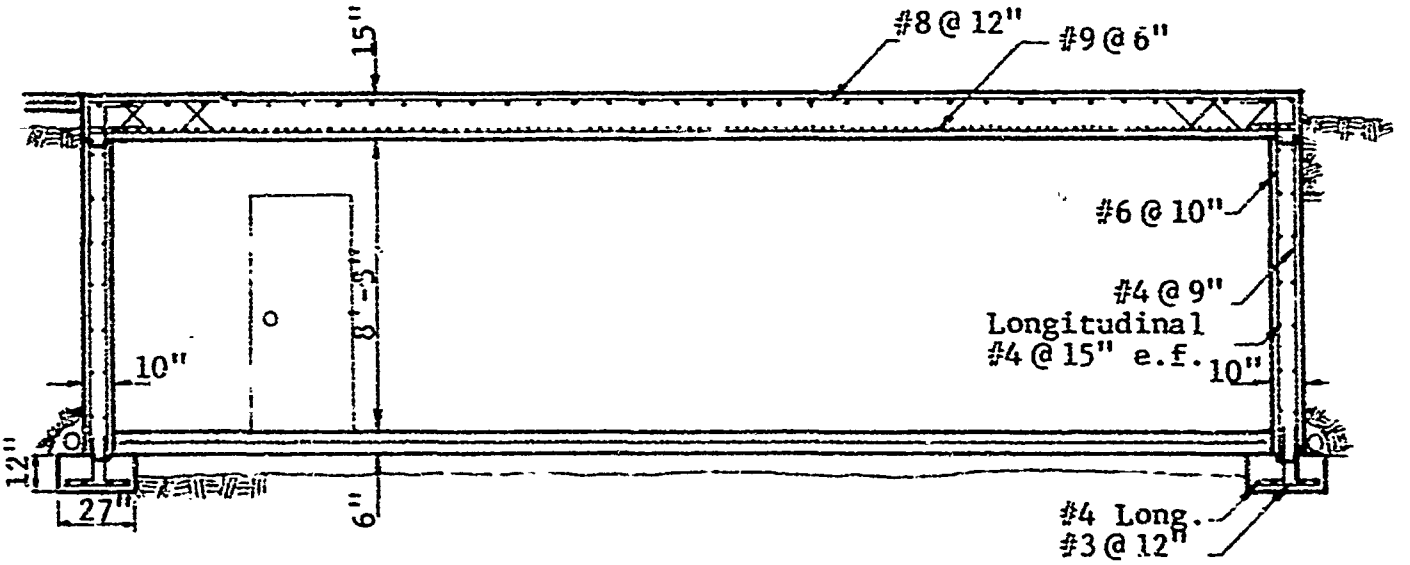

Fig. 4.4d Section B-B, below Grade Shelter

The initial radiation from the above weapons is such that the thickness of the shelter walls based on structural requirements is sufficient protection. Fallout radiation protection with PF = 115 for the above grade and PF = 120 for the below grade shelter is provided.

4.6.2 Mechanical

(a) Summer outside air design temperatures:
95°F dry bulb, 75°F wet bulb

(b) Summer outside relative humidity: 40 percent

(c) Winter outside air design temperature: 10°F

(d) Heat loss (BTU):

	Walls	Roof	Floor	Ventilation	Glass
Basic building	71,000	100,000	23,000	330,000	129,000
At grade shelter	18,600	33,200	2,500	240,000	-
Below grade shelter	5,500	-	2,500	240,000	-

(e) Inside shelter temperatures: 70°F winter, 100 percent outside air summer (no air conditioning)

(f) Fire protection: Local code requirements

4.6.3 Structural

(a) Applicable Codes

ACI Building Code Requirements for Reinforced Concrete (ACI 318-71)

Chicago Building Code, 1972

Specification for the Design, Fabrication and Erection of Structural Steel for Buildings, AISC, 1969.

Specifications for the Design and Construction of Load Bearing Concrete Masonry, NCMA, 1968.

(b) Assumed Material Properties

28 day concrete compressive strength, f'_c = 3,000 psi
Minimum yield for reinforcing bars, f_y = 40,000 psi
Minimum yield for structural steel, f_y = 36,000 psi
Minimum yield for steel joists, f_y = 50,000 psi
Allowable soil bearing pressure, p = 2,500 psf

(c) Assumed Dynamic Material Properties

Concrete compressive strength, f'_{dc} = 3,750 psi

Minimum yield for reinforcing steel, f_{dy} = 52,000 psi

Allowable dynamic soil bearing pressure: twice static allowable plus free field overpressure (see Ref. 1, pp 9-14).

4.7 COST ESTIMATES

The following is a summary of the cost estimates for the four designs. Costs are based on current Chicago area construction and include all costs, material, labor, etc. A detailed cost breakdown follows the summary (see Table 4.1).

	Basic Building	Basic Building with Basement	Building with Shelter at Grade	Building with Below Grade Shelter
1. Earthwork and structural	51,317	68,187	74,256	81,858
2. Architectural	74,276	75,943	71,774	75,502
3. Mechanical	57,160	59,536	67,960	72,136
4. Electrical	22,620	25,930	37,620	40,930
Total	$205,373	$229,596	$251,610	$270,426
Cost/sq ft	$16.30	$15.89	$19.97	$18.71

4.8 SHELTER SURVIVABILITY

Survivability estimates were made for personnel using the above grade shelter, the below grade shelter, the unprotected (normal) basement and the conventional building without a basement. Results are included in Fig. 4.5. Analysis of the above grade shelter revealed that collapse of the walls precedes roof slab collapse; thus, the survivability estimate is somewhat lower for the above grade shelter as compared to the below grade shelter where the overhead slab strength governs.

It will be noted that there is not a great deal of difference in protection afforded by the conventional building to prone or standing people provided they are uniformly distributed.

TABLE 4.1 COST ESTIMATES

Description	Unit	Price	Basic Building Quantity	Basic Building Cost	Basic Building with Basement Quantity	Basic Building with Basement Cost	Building with Shelter at Grade Quantity	Building with Shelter at Grade Cost	Building with Shelter below Grade Quantity	Building with Shelter below Grade Cost
Earthwork and Structural										
1. Excavation, backfill and greding	cu yd	2.75	545	1,499	2,200	6,050	757	2,068	2,200	6,050
2. Concrete (formwork included)	cu yd	67.00	278	18,626	384	25,728	486	32,562	461	30,887
3. Reinforcing bars - Grade 40	lbs	0.21	1,373	288	13,402	2,814	81,932	17,206	67,995	14,279
4. Welded wire fabric:										
3x3 - 5/5	sq ft	0.24	12,600	3,024	12,600	3,024	12,600	3 024	12,600	3,024
6x6 - 10/10	sq ft	0.06	12,600	756	12,600	756	12,600	756	12,600	756
5 Structural steel	lbs	0.21	31,005	6,511	31,005	6,511	23,845	5,007	31,005	6,511
6. Bearing plates and anchor bolts				205		205		167		205
7. Open web steel joists (16K5)	lbs	0.18	21,300	3,834	21,300	3,834	18,200	3,276	21,300	3,834
8. Steel joist accessories				1,271		1,271		1,129		1,271
9. Corrugated, galvanized, steel roof deck	sq ft	0.39	12,600	4,914	12,600	4,914	10,750	4,193	12,600	4,914
10. Concrete block walls:										
8 in. hollow block	sq ft	1.60	4,810	7,696	6,492	10,387	1,442	2,307	4,677	7,483
8 in. solid block	sq ft	1.65	820	1,353	820	1,353	740	1,221	790	1,304
11. 6 in. crushed stone base course for grade slabs	cu yd	5.75	233	1,340	233	1,340	233	1,340	233	1,340
TOTAL				$51,317		$68,187		$74,256		$81,858
Architectural										
1. Concrete block partitions, 8 in.	sq ft	1.60	6,720	10,752	6,720	10,752	5,110	8,176	6,740	10,784
2. Interior doors, 3 ft-0 in. by 6 ft-8 in. (including hardware)	ea.	300.00	14	4,200	16	4,800	15	4,500	16	4,800
3. Roof:										
2-1/2 in. lightweight concrete	cu yd	35.00	77	2,695	77	2,695	77	2,695	77	2,695
1-1/2 in. rigid insulation	sq ft	0.30	12,600	3,780	12,600	3,780	12,600	3,780	12,600	3,780
5 ply tar and gravel roofing	sq ft	0.32	12,600	4,032	12,600	4,032	12,600	4,032	12,600	4,032
Precast concrete coping	lin ft	2.60	470	4,230	470	4,230	470	4,230	470	4,230
Roof drainage (drains, pipes, copper flashing)				2,722		2,722		2,722		2,722
4. Brick veneer, 4 in.	sq ft	2.90	5,630	16,327	5,630	16,327	5,782	16,768	5,467	15,854
5. Entranceway:										
15 ft by 9 ft-6 in. glass with two doors	ea.	1,600.00	1	1,600	1	1,600	1	1,600	1	1,600
10 ft by 9 ft-6 in. glass with two doors	ea.	1,200.00	1	1,200	1	1,200	1	1,200	1	1,200
6. Suspended ceiling system	sq ft	0.85	12,600	10,710	12,600	10,710	12,600	10,710	12,600	10,710
7. Premolded expansion joint, 1/2 in. by 6 in. around floor perimeter	lin ft	0.26	468	122	550	143	468	122	550	143
8. Windows:										
6 ft by 19 ft-6 in.	ea.	345.00	9	3,105	9	3,105	7	2,415	9	3,105
6 ft-0 in. by 22 ft-0 in.	ea	350.00	4	1,400	4	1,400	4	1,400	4	1,400
9. Asphalt floor tile (including base)	sq ft	0.36	12,600	4,536	14,500	5,220	12,600	4,536	14,500	5,220
10. Painting (interior)	sq ft	0.15	19,100	2,865	21,512	3,227	19,250	2,888	21,512	3,227
TOTAL				$74,276		$75,943		$71,774		$75,502

Description	Basic Building	Basic Building with Basement	Building with Shelter at Grade	Building with below Grade Shelter
Mechanical Equipment				
1. 40 ton air conditioning unit	28,000	28,000	28,000	28,000
2. Ductwork	8,500	8,500	8,500	8,500
3. Diffusers and registers	1,000	1,000	1,000	1,000
4. Temperature controls	2,000	2,000	2,000	2,000
5. Exhaust fans	3,500	3,500	4,100	4,100
6. Exhaust hood or shaft	-	-	400	1,300
7. 1-1/2 hp emergency air handling unit	-	-	2,500	2,500
8. Emergency fresh air intake	-	-	600	1,200
9. CBR filters	-	-	5,900	5,500
10. Plumbing system	6,600	6,600	6,600	6,600
11. 1/3 hp sump pump, basin and drain tile	-	1,296	-	1,296
12. Sprinkler system	7,560	8,640	7,560	8,640
TOTAL	$57,160	$59,536	$67,960	$72,136
Electrical Equipment				
1. Lighting fixtures	11,490	13,890	11,490	13,890
2. Outlets, switches, telephone hookups	3,530	4,440	3,530	4,440
3. Wiring, control panels, distribution	7,600	7,600	7,600	7,600
4. 15kW emergency generator	-	-	15,000	15,000
TOTAL	$22,620	$25,930	$37,620	$40,930

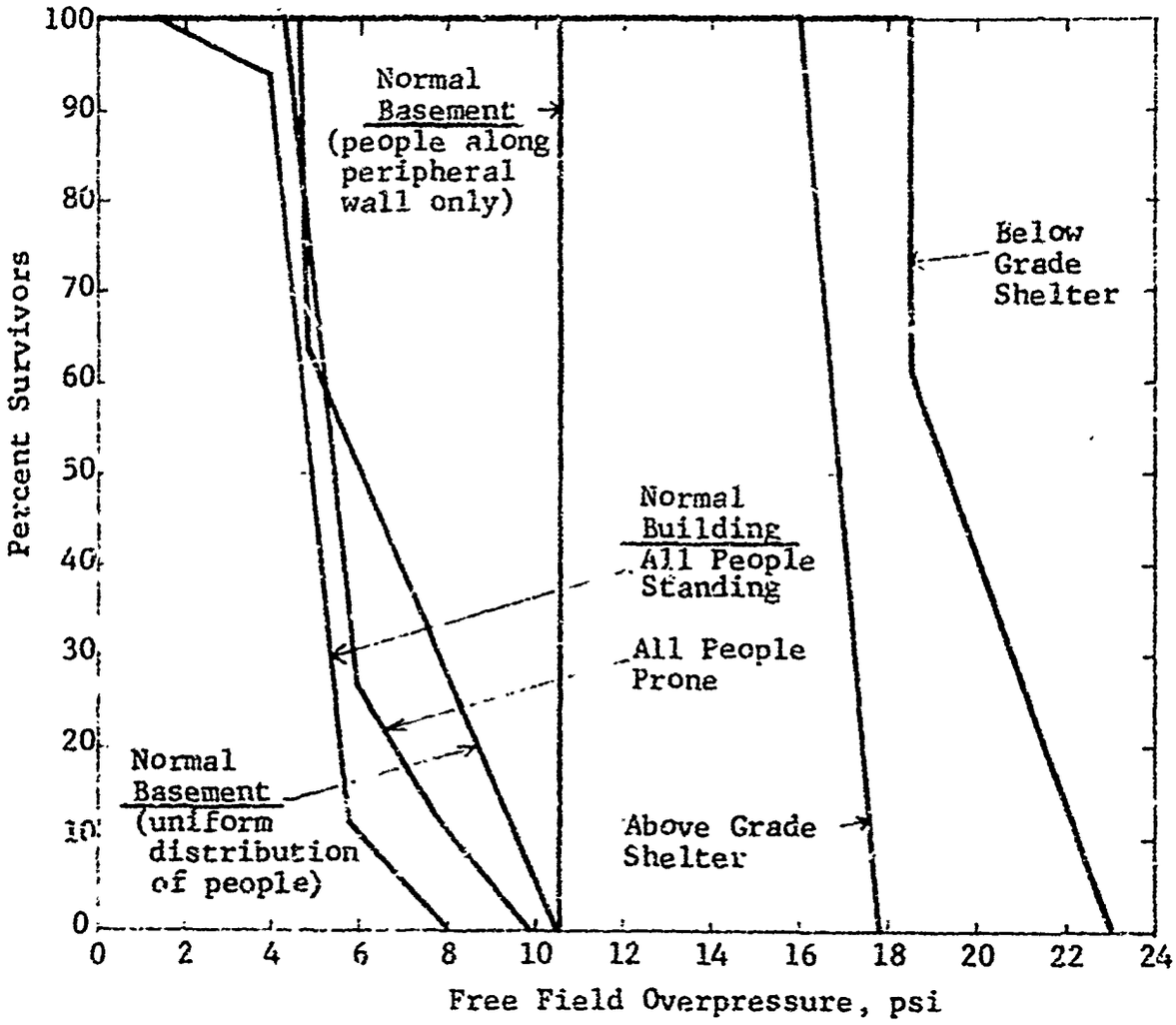

Fig. 4.5 Shelter Survivability Estimates

The Median Lethal Overpressure (MLOP) for people in the basement is 6.0 psi while that for upstairs is 4.9 psi when people are standing and 5.4 psi when they are prone. This is a relatively small basement with concrete block walls and a simply supported overhead slab which responds primarily in one-way action. It was designed for a minimum live load of 75 psf. Such a slab is not capable of developing a great deal of membrane action and when failing catastrophically becomes the primary cause of casualties. However, should these people be located along the peripheral walls, in prone or sitting positions, then the corresponding MLOP is 10.5 psi.

Such a large improvement is not possible for the upstairs portion by simply moving people around. The primary casualty mechanism upstairs is translation which is aided by the substantial percentage of window openings. This is followed fairly closely by debris from the breakup of the building. It will be noted that peripheral walls and interior partitions all consist of concrete masonry.

4.9 COST COMPARISON AND SUMMARY

Four cost comparisons were made for the two sheltering variations:

(1) total building cost per square foot of building
(2) shelter cost increment per square foot of building
(3) shelter cost per square foot of shelter
(4) shelter cost increment per square foot of shelter

The first comparison showed that the above grade shelter building is 7 percent more expensive per square foot than the below grade shelter building. This cost differential is magnified when the shelter cost increment over the comparable unprotected building is considered. The cost increment over the total building area was 30 percent greater for the above grade shelter over the below grade shelter. The actual shelter costs per square foot of shelter were compared and are given as:

Above grade shelter - $24.99/sq ft of shelter
Below grade shelter - $22.07/sq ft of shelter

On this basis the incremental shelter costs per square foot of shelter are computed as:

Above grade shelter: $24.99 - $16.30 = $8.69/sq ft of shelter
Below grade shelter: $22.07 - $15.89 = $6.18/sq ft of shelter

The survivability of either shelter variation was compared and showed the below grade shelter having an estimate mean lethal overpressure of 18.5 psi while the above grade shelter was at 16.5 psi.

In summary, the below grade shelter variation appears to be a better alternative with respect to cost and survivability than an above grade shelter.

REFERENCES

1. Newmark, N. M. and Haltiwanger, J. D., Principles and Practices for Design of Hardened Structures, Air Force Design Manual, Air Force Special Weapons Center, Kirtland AFB, New Mexico, Report SWC-TDR 62-138, December 1962.

2. Building Code Requirements for Reinforced Concrete, American Concrete Institute, ACI 318-72, Detroit, 1972.

3. Chicago Building Code, 1972

4. Manual of Steel Construction, 7th Edition, American Institute of Steel Construction, New York, 1971.

5. The Effects of Nuclear Weapons, Atomic Energy Commission, 1962.

6. Murphy, H. L., Feasibility Study of Slanting for Combined Nuclear Weapons Effects, Vol. I and II, Stanford Research Institute, October 1970.

CHAPTER 5

ANALYSIS OF SPECIAL PERMANENT AND EXPEDIENT SHELTERS

5.1 INTRODUCTION

An investigation of a set of eight shelters was performed to determine their usefulness with respect to direct nuclear weapons effects produced by megaton (MT) range nuclear weapons. These included special permanent and expedient shelters. Special permanent shelters are defined as those which may be constructed by private individuals or groups with direct effects and/or fallout radiation protection in mind. This may include a concrete block basement shelter, a wooden lean-to basement shelter or a small neighborhood shelter separate from adjoining dwellings. Such shelters are more permanent than expedient shelters. Expedient shelters refers to structures which can be erected with minimal cost, effort and time expenditure and requiring only rudimentary skills. Of the eight shelters investigated, five were designed primarily for fallout protection; the remaining three were planned for limited blast resistance in addition to fallout protection.

All eight shelters considered here were designed previously and are completely described in several references mentioned below. To facilitate discussion, a list of these shelters with identifying letters is given:

* A Unreinforced concrete block (Ref. 4)
* B Plywood lean-to (Ref. 1)
* C Plywood rigid frame (Ref. 1)
* D Reinforced concrete block (Ref. 1)
** E Aboveground timber A-frame earth covered (Ref. 4)
** F Outside semimounded plywood box (Ref. 4)
* G 480 person austere community fallout shelter (Ref. 2)
** H Underground wood-grate roof (Ref. 3)

---

* Special Permanent Shelter

** Expedient Shelter

Sketches, reproduced from the listed references, are included at the end of this chapter (see Figs. 5.1 through 5.8).

Shelters A, B, C and D are all planned as basement shelters for typical single family housing. Shelters E and F are also intended for a single family use, but are not associated with a particular house, rather, they are to be located outside, separate from a residence. Shelters G and H are larger scale shelters intended for community use.

The four basement shelters presented a problem, because their protection level may depend to a great extent on the nature of the structure enclosing them. Typical single family housing may be estimated as being able to withstand at most 2 to 3 psi overpressures before collapse occurs. Higher overpressures will clear the aboveground structure from the site. At this point no attempt was made to consider the interaction of the shelter and the house. The basement shelters, for the purpose of blast analysis were assumed to be located essentially in a free field environment. For initial nuclear radiation effects, however, the basement walls and below grade location were considered in estimating attenuation factors. The four remaining shelters were independent of other structures, except for debris from possible neighboring buildings.

5.2 SHELTER EVALUATION

5.2.1 Blast

As a first step in evaluating the effectiveness of these shelters in protecting occupants, their blast resistance was investigated. Only shelters B, C and D were specifically designed for resistance to blast, while the others are primarily fallout shelters.

In estimating the blast resistance, two overpressure levels were considered: first, the overpressure resulting in moderate damage to the shelter structure, and second, the overpressure causing complete collapse. Moderate damage is defined to occur at an overpressure level which leaves the shelter standing, however considerably weakening it with respect to further loading. Large scale

cracking of concrete block walls, failure of several wood joists, support loosening, and large deflections are indicative of a state of moderate damage. Although the structure remains standing a repeated load of similar or smaller magnitude may be sufficient to cause partial collapse. Complete collapse refers to an overpressure magnitude which essentially levels the shelter.

These two overpressure levels are determined to guide the evaluation of people survivability since debris (from the breakup of the shelter and parent structure) and translation of shelterees by blast winds are important casualty-producing mechanisms. At the first overpressure level, i.e., when the shelter experiences moderate damage, no casualties are expected. At the second, significant casualties may be produced due to the breakup of the shelter and subsequent translation of occupants.

Estimates of the strength of these shelters were made difficult by the nature of the structures and materials involved. The strength of a wooden frame is very much dependent on the particular wood used. Blast response of hollow concrete block walls such as in Shelter A or double wyth sand-filled walls as in G, or reinforced concrete block walls as in D, also presented some difficulties. For all shelters considered, a great deal depends on the connections and how soundly they are designed and then actually built. Based on current methodology, Table 5.1 lists the estimated blast resistance of the eight shelter types.

As is apparent from the table, shelters originally designed for fallout protection provide comparatively minimal blast resistance, at most up to the 3 psi. Also, it is evident, that at the above collapse ranges all shelters would no longer be able to provide satisfactory fallout protection, while at the moderate damage range fallout protection will still be essentially intact.

Table 5.1

EXPEDIENT SHELTER BLAST RESISTANCE

Shelter		Overpressure Levels (psi)	
		Moderate Damage	Collapse
A	roof	2.0	4.0
	walls	1.0	2.0
B	roof	10.0	13.0
C	lean-to wall	3.0	10.0
D	walls	6.0	10.0
E	roof	2.2	3.0
F	roof	1.6	2.2
G	roof	4.0	5.0
	walls	2.0	3.0
H	roof	1.0	1.8

5.2.2 Initial Nuclear and Thermal Radiation

For all of the shelters, sufficient thickness and density is provided to attenuate initial nuclear radiation to a level where no casualties are expected within the overpressure range where most damage occurs. Also, complete shielding from the thermal pulse is provided for the shelter occupants.

5.3 PERSONNEL SURVIVABILITY

Survivability in these shelters is a function of several casualty producing mechanisms. Basically, casualties can be anticipated with debris impacts on the shelter occupants with the collapse of the shelter structure. In addition casualties with translation of the occupants in the blast wind must also be considered. No casualties are expected prior to the collapse of the shelter structure. Thus, the overpressure levels shown in Table 5.1 are in themselves a good indication of the survivability potential of the shelters.

With the initial collapse of shelter G (480 person community fallout shelter) at 2 psi some casualties are expected. However,

the main problem with this shelter is expected to be the translation of the surviving occupants along with the building debris. Being exposed above grade to the blast wind, translation with impacts on the ground or with building debris would be the major danger as the structure and occupants are swept from the site. Overpressures of interest are in the range of 6 to 10 psi. Above 10 psi no survivors can be expected.

People translation will also represent a significant proportion of the casualties for the earth covered A-frame shelter E, since as originally planned, the shelter is located above grade with only an earth radiation shield. Collapse of the structure, as noted in Table 5.1, would occur at 3 psi. Debris pileup on the shelter occupants will have some probability of causing casualties, however, at higher overpressures, in the range of 8 to 10 psi, the shelter debris and occupants will be scattered by the wind with negligible probabilities of survival.

Shelter F, the partially buried plywood box, can expect collapse of the roof structure at 2.2 psi free field overpressure. Burial of the occupants at this level could cause some casualties. Higher overpressures could cause collapse of the roof sufficiently violent to seriously endanger the occupants. Being only partly buried, the possibility of being swept by the blast winds is also a factor.

The wood-grate roof shelter H, although failing at the lowest overpressure of the eight shelters, 1.8 psi, has an advantage over the other outdoor structures, that is, it is entirely below grade. Flexural failure of the roof structure, although producing significant casualties would still provide some protection to the shelter occupants remaining shielded beneath the collapsed structure. Translation by the blast wind would not be nearly as important a factor as in the other three exposed or partly exposed shelters. Thus, a small percentage of occupants may be expected to survive at relatively high overpressures, possibly in the range of 12 to 16 psi.

Survivability in the basement shelters A, B, C and D is not affected by the problem of people translation as it is for the outdoor shelters. Primarily, casualties will occur with impact of the shelter debris on the occupants.

For the unreinforced concrete block shelter A, an overpressure of 5 to 6 psi is required so that the brittle failure of the block walls and their ensuing short distance translation result in sufficiently severe impact velocities to cause fatalities.

Shelters B, C and D, which are the only ones of the eight expedient shelters which were designed for blast offer the most protection with complete protection up to 10, 13 and 10 psi, respectively. Several psi higher, and the violent collapse of the structure on the shelter occupants will preclude any possibility of survival.

In estimating the survivability for the basement shelters the effect of the enclosing structure was neglected. However, the debris from this and neighboring structures may present the major hazard to people in these shelters because of the possibility of fire. It is conceivable that, although able to resist blast over 10 psi, the three basement blast shelters are left completely vulnerable to fire, not only from a burning debris pile, but also from the shelter itself burning. In this event, unless evasive action is taken, no survivors can be expected. The major concern is that burning debris at overpressure levels much lower than the nominal strength of the shelters will make the originally attractive wooden and block shelters completely useless. The increased blast resistance would not protect the occupants from fire at low overpressures. At higher overpressures, debris from neighboring structures may also be a factor. In addition, the outdoor shelters are not invulnerable to the same effects, however the danger to them appears to be of lesser importance.

Based on the above described investigations, the estimates of people survivability in the various shelters are shown in Fig. 5.9. The effect of fire is not included in these estimates as no reasonable analytic evaluation could be made. As discussed above, the fire problem may well be the critical one for the basement shelters.

REFERENCES

1. Brotherson, D. E., Wright, R. N., and Pecora, S. D., Limited Blast Resistance in Houses, University of Illinois, Contract OCD-PS-64-201, Champaign, Urbana, Illinois, December 1968.

2. Dembo, M. M. and Baldwin, D. B., Design and Evaluation of 480 Person Austere Community Fallout Shelter, Protective Structures Development Center, Fort Belvoir, Virginia, June 1967.

3. Expedient Community Fallout Shelter - Wood Grate Roof Below Ground, Protective Structures Development Center, Fort Belvoir, Virginia, May 1964.

4. Longinow, A. and Stepanek, O., Civil Defense Shelter Options for Fallout and Blast Protection (Single Purpose), IITRI Project J6115, June 1968.

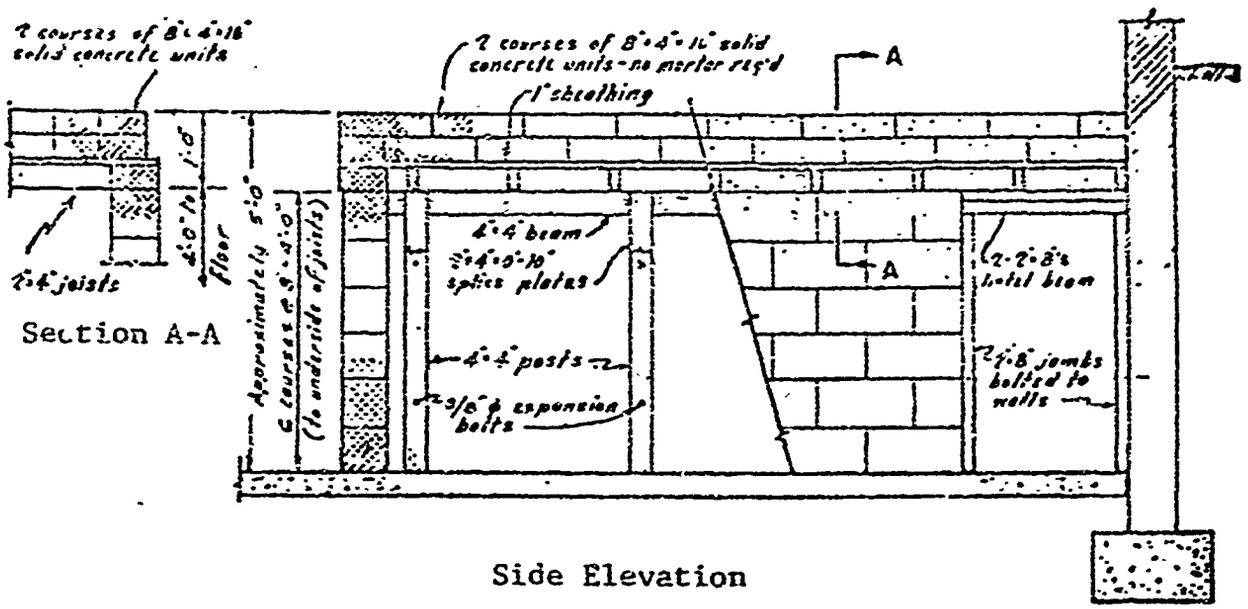

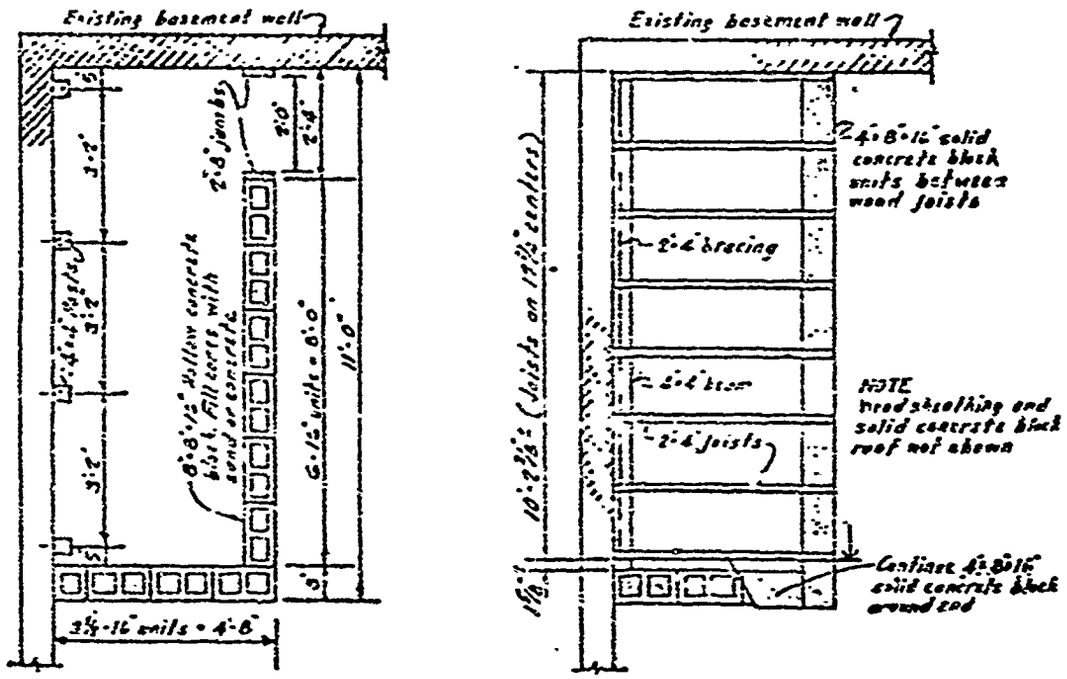

Fig. 5.1 Shelter A, Unreinforced Concrete Block

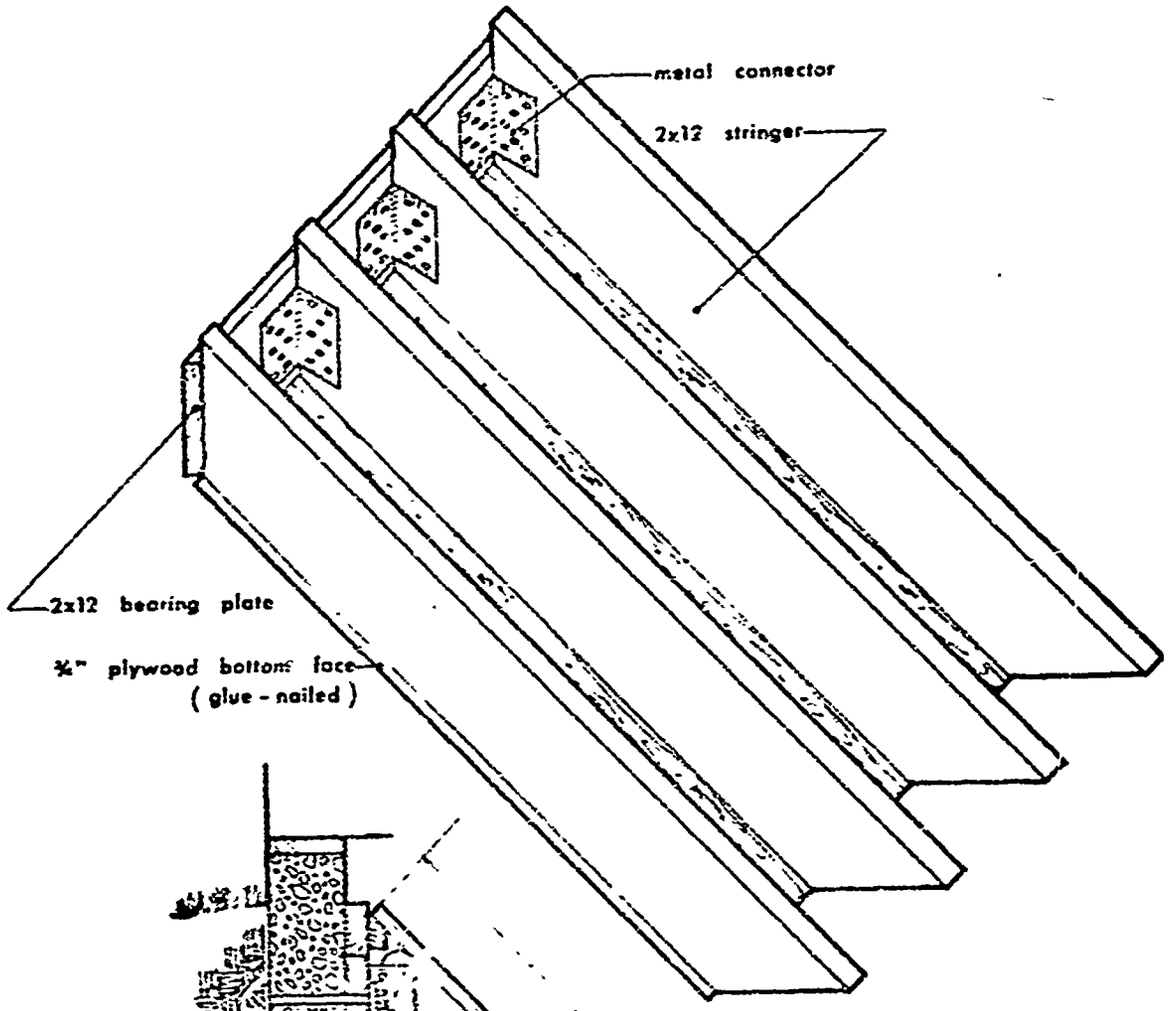

a. 4' Module

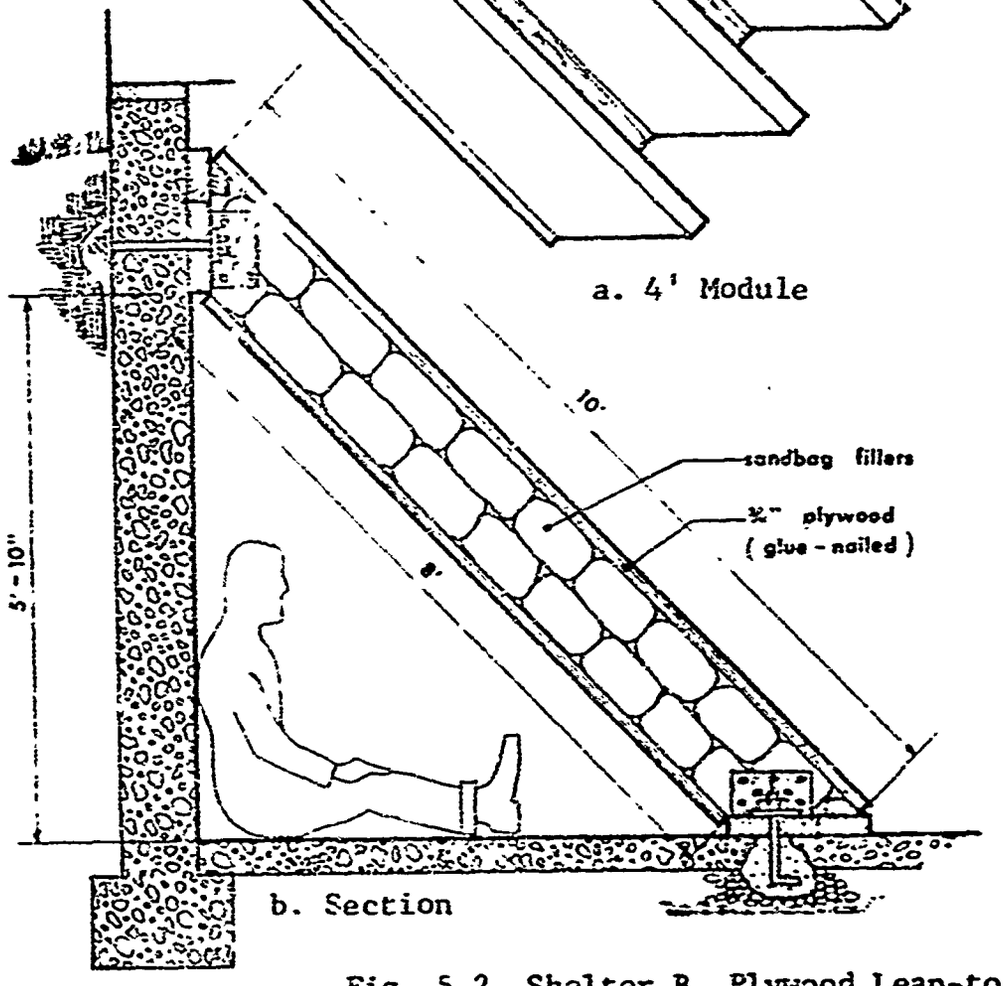

b. Section

Fig. 5.2 Shelter B, Plywood Lean-to

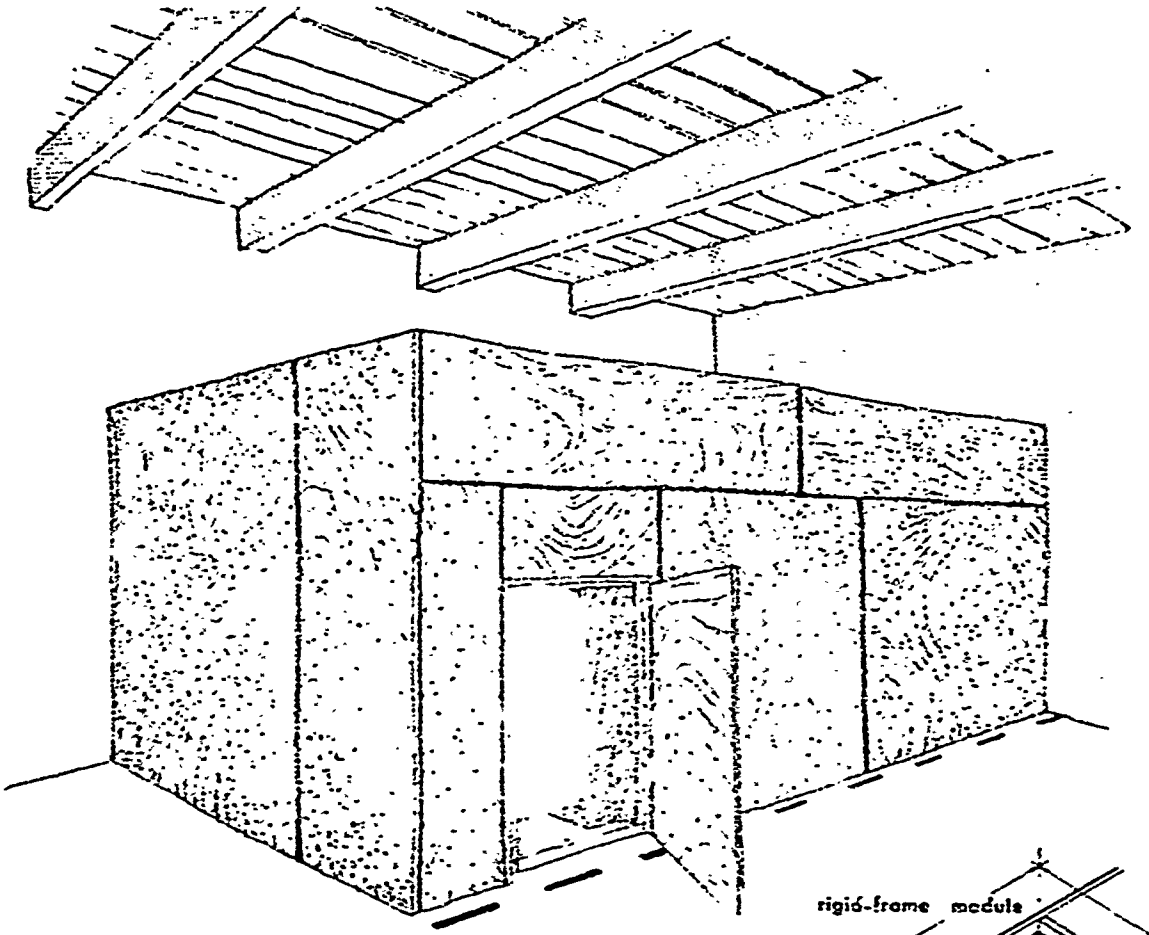

a. Isometric

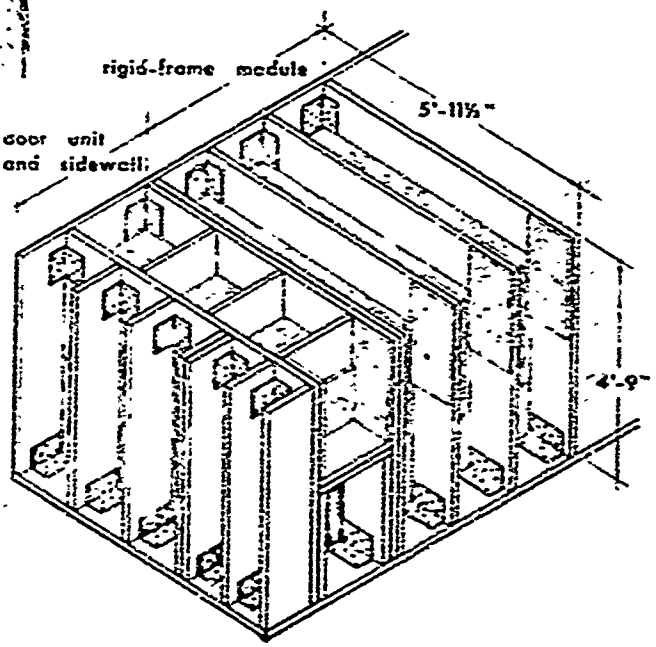

b. Frame

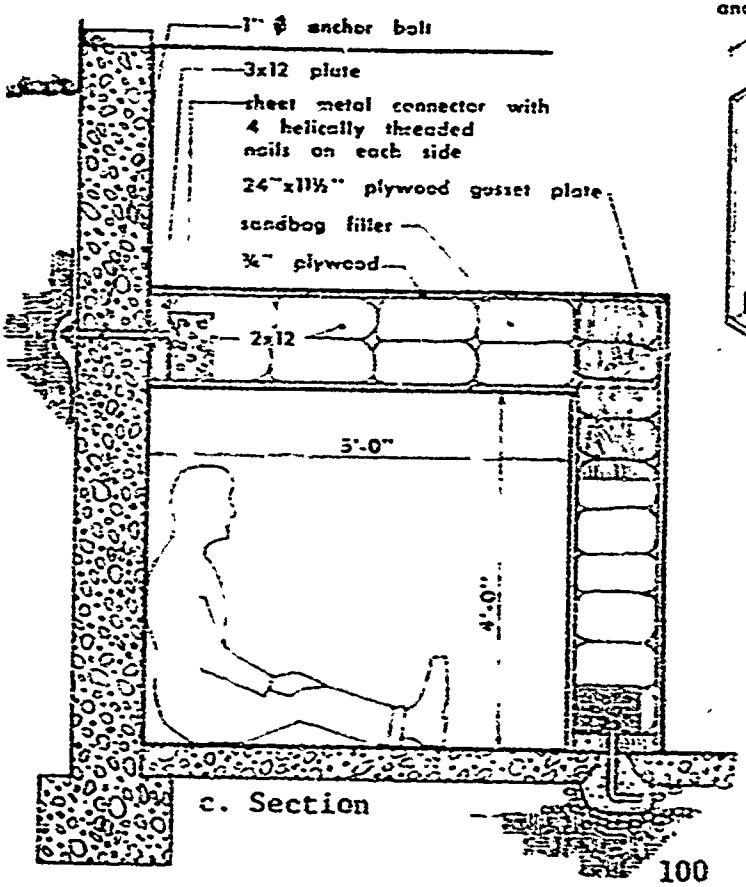

c. Section

Fig. 5.3 Shelter C, Plywood Rigid Frame

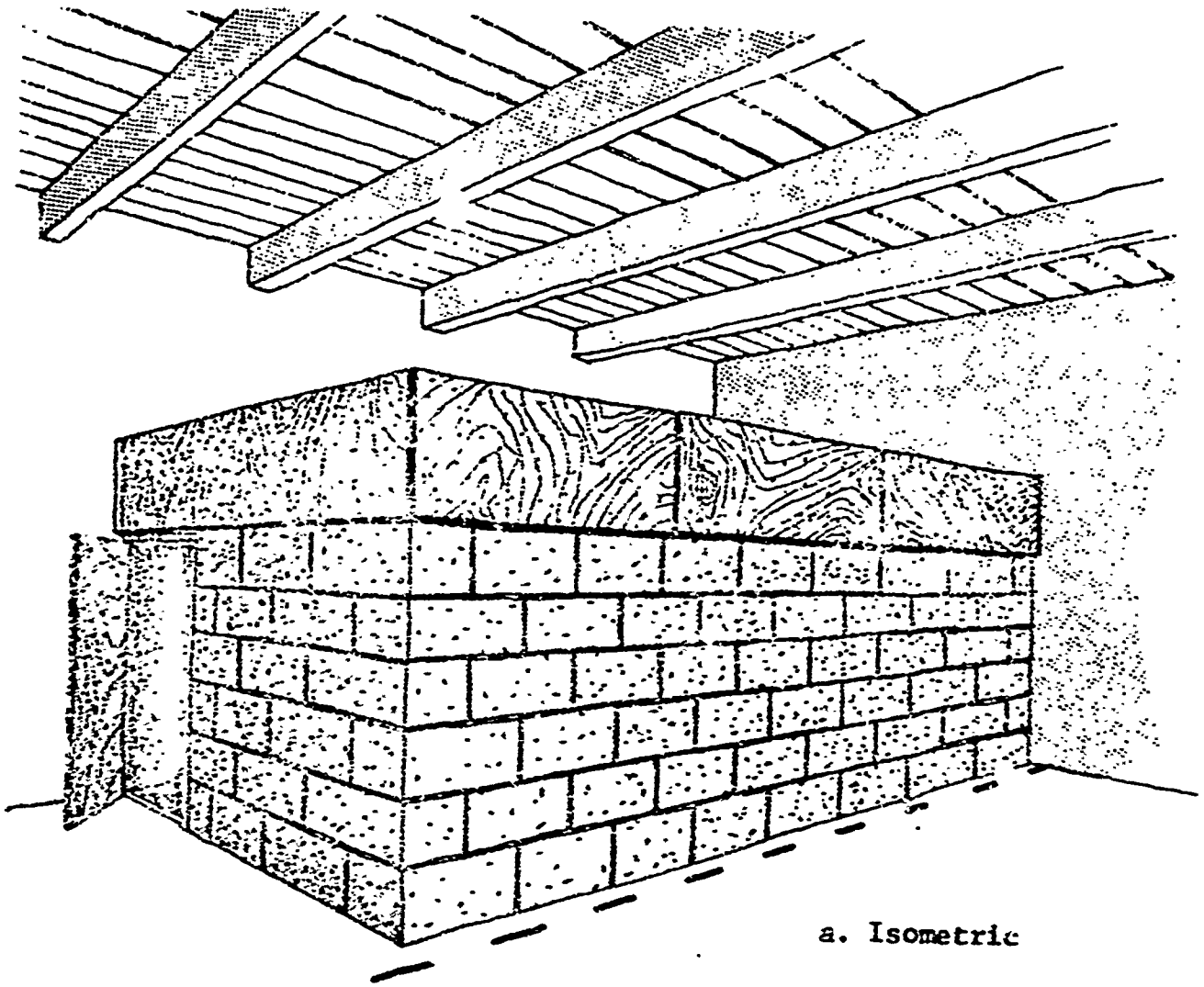

a. Isometric

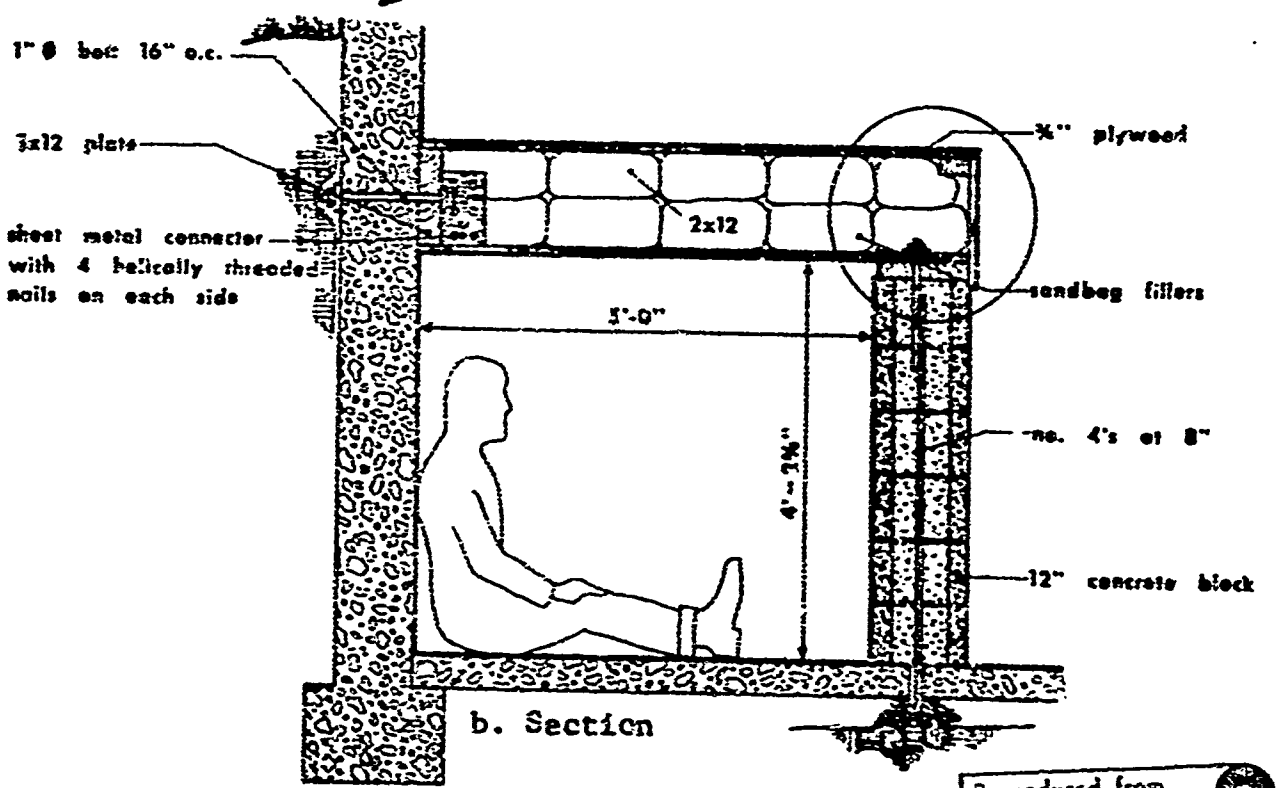

b. Section

Fig. 5.4 Shelter D, Reinforced Concrete Block

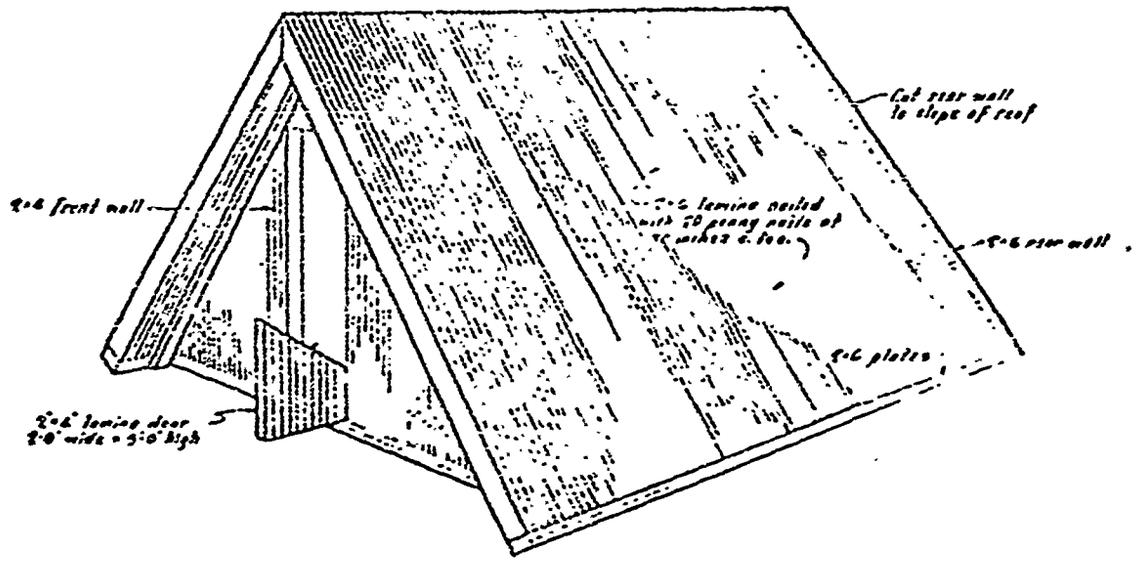

a. Perspective View

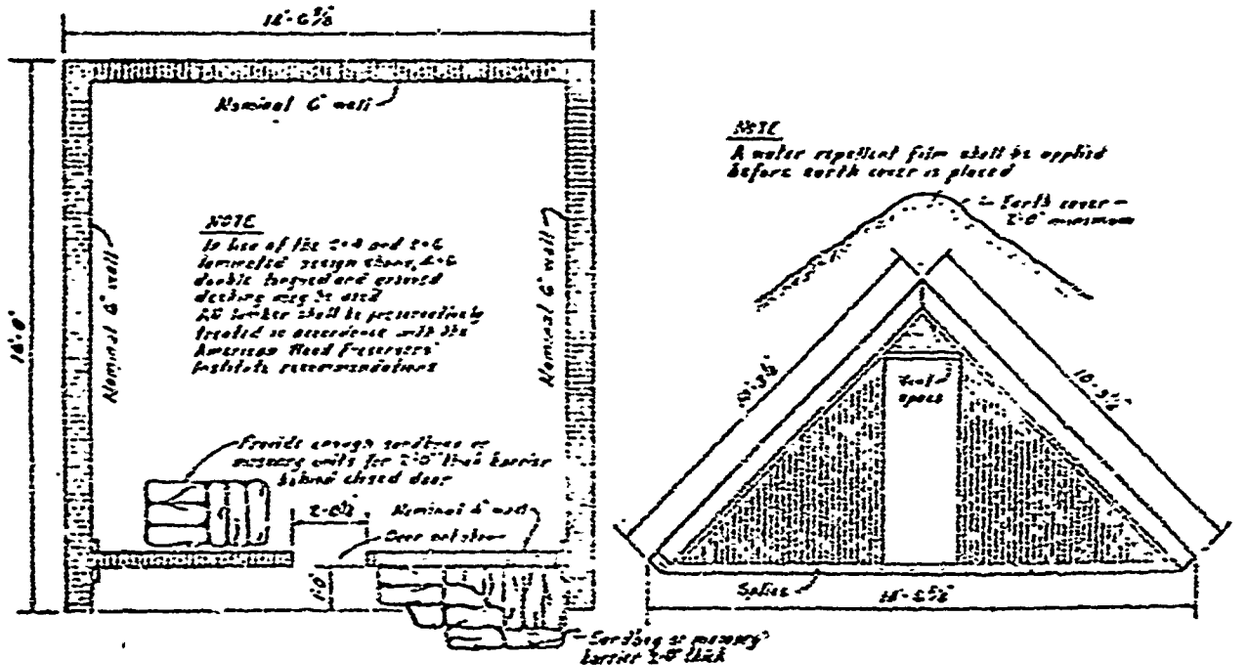

b. Floor Plan

c. Front Elevation

Fig. 5.5 Shelter E, Aboveground A-Frame, Earth Covered

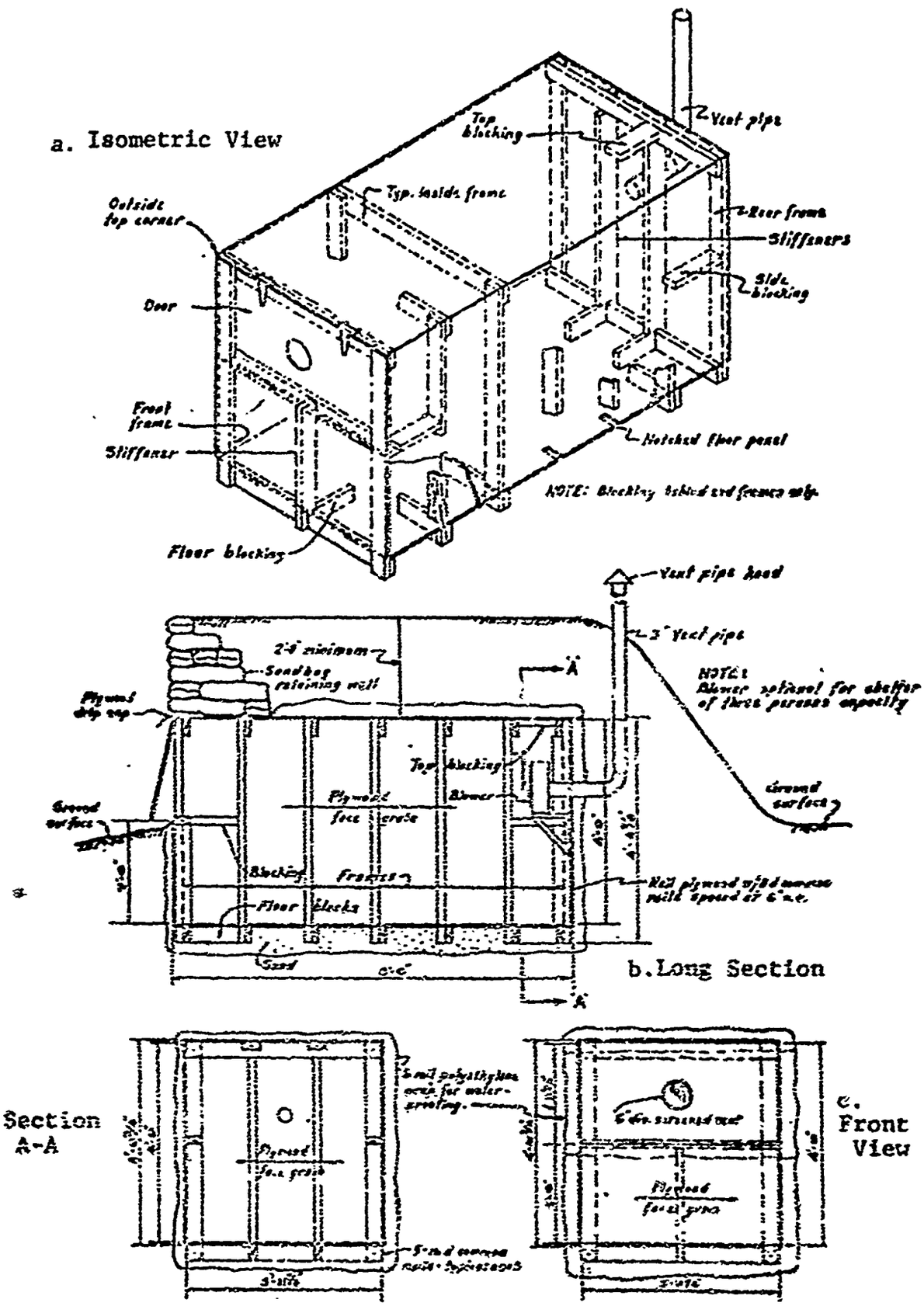

Fig. 3.6 Shelter F, Outside Semimounded Plywood Box

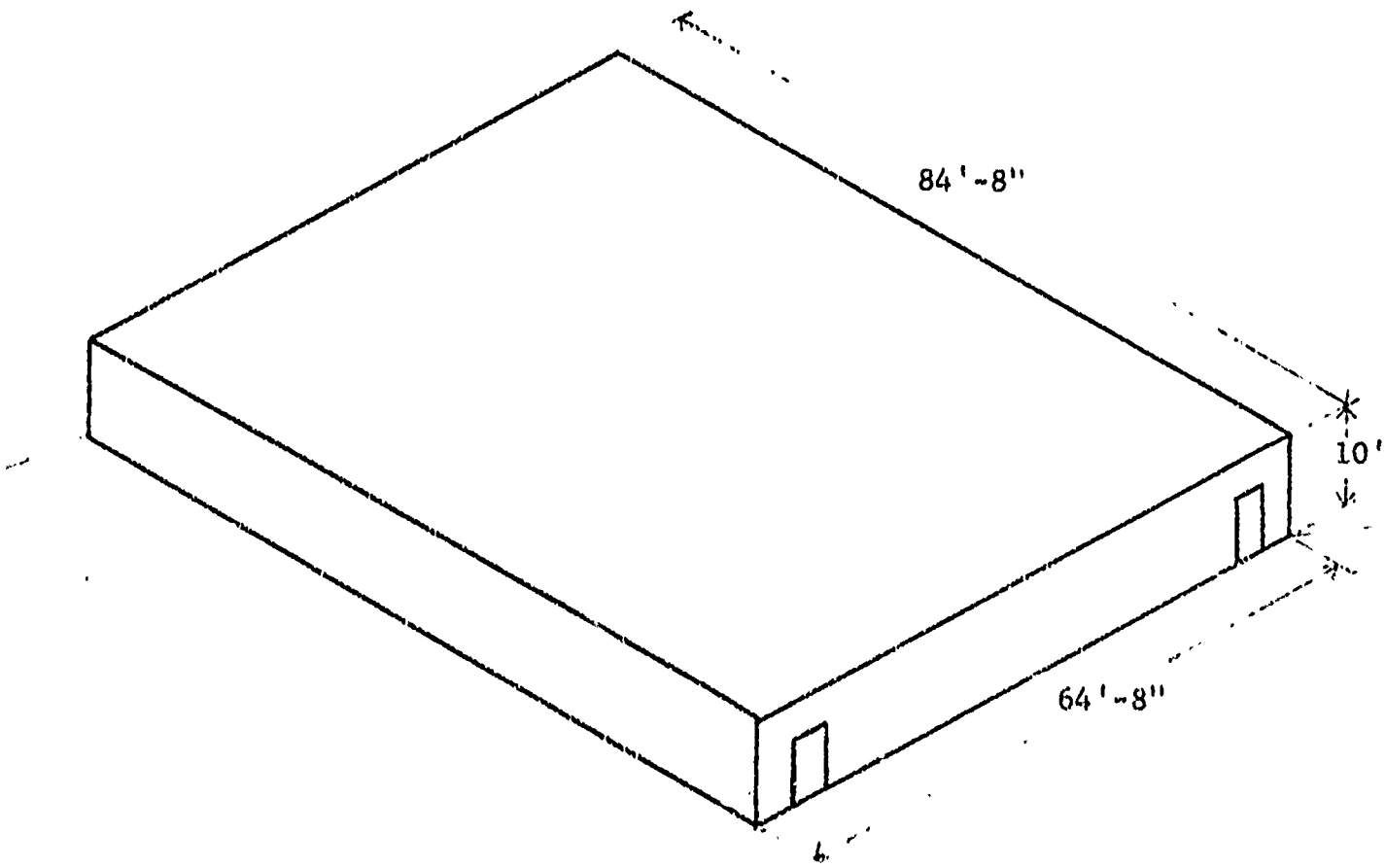

Fig. 5.7 Shelter G, 480 Person - Austere Community Fallout Shelter

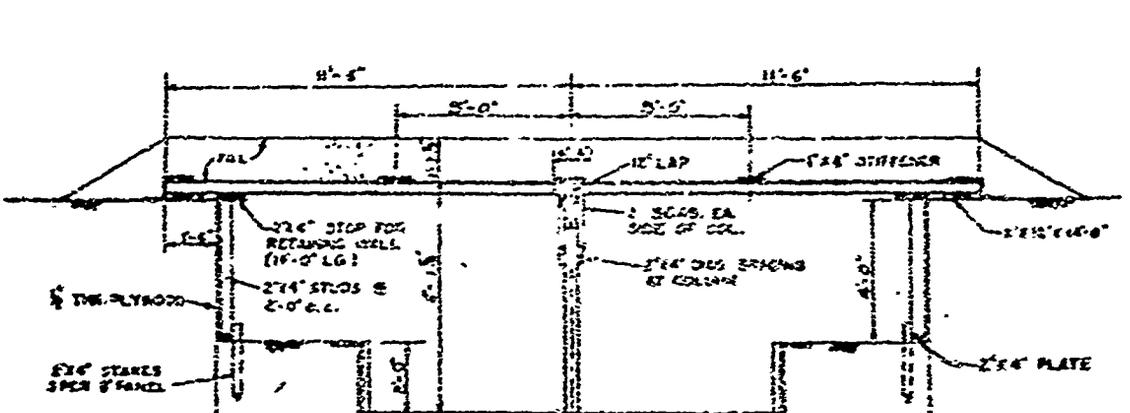

Section A-A

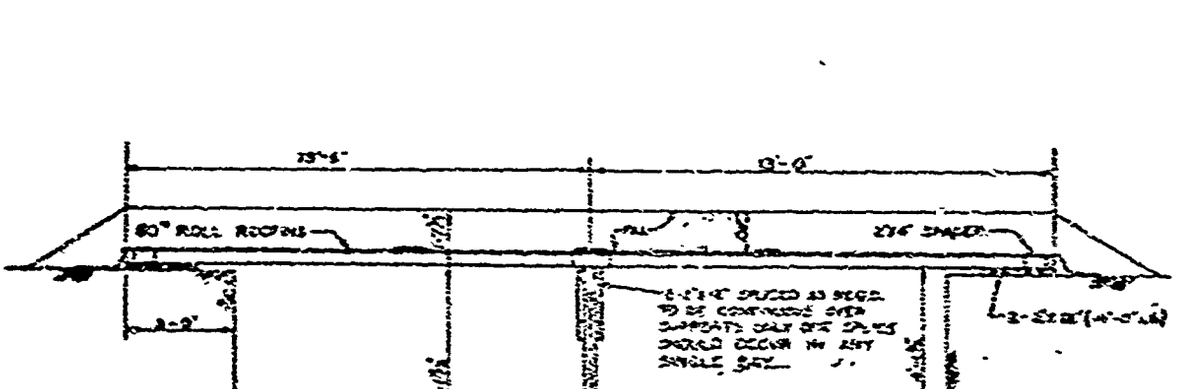

Section B-B

Fig. 5.8 Shelter H, Underground Roof Crate Roof Shelter

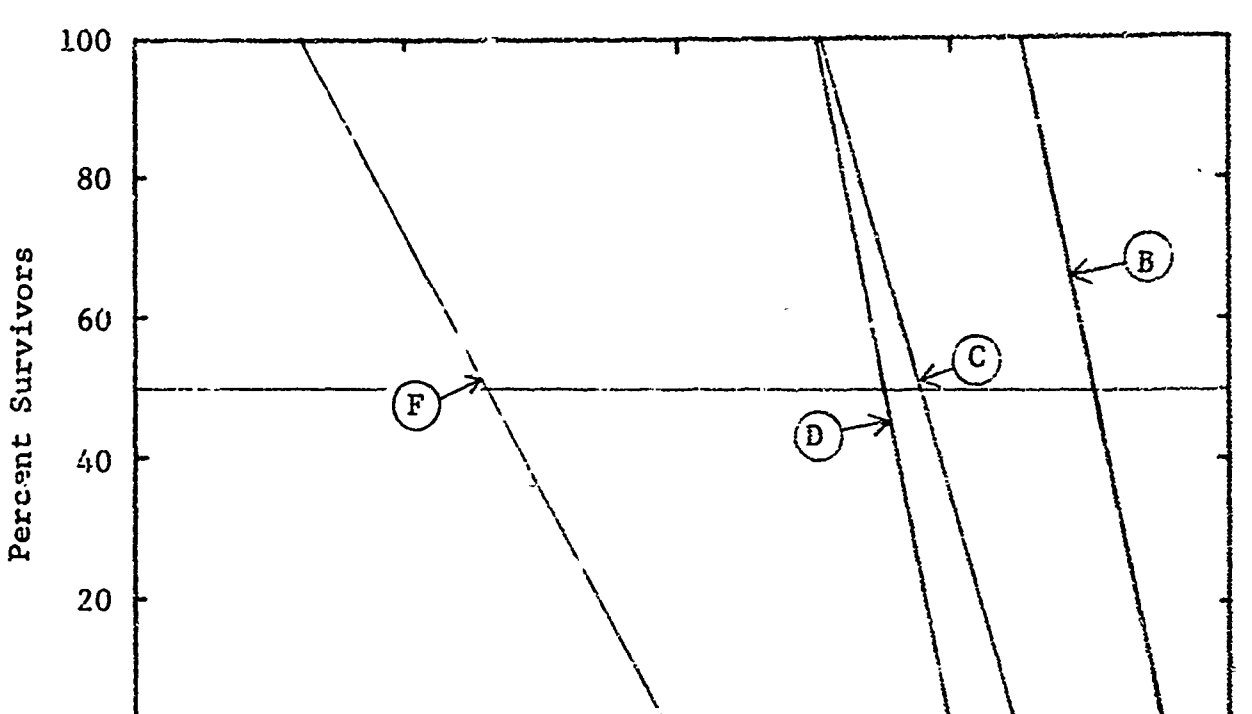

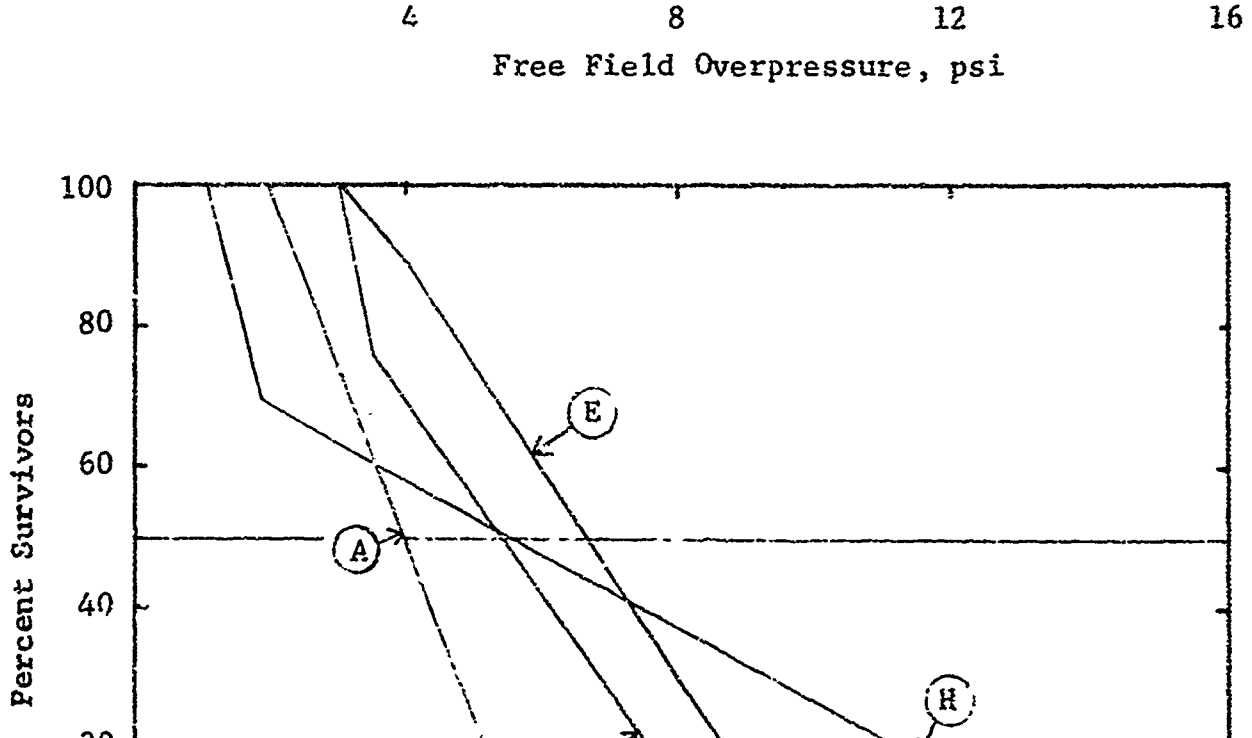

Fig. 5.9 Shelter Survivability Estimates

CHAPTER 6

CONCLUSIONS AND RECOMMENDATIONS

6.1 INTRODUCTION

By far the major portion of the effort reported herein was devoted to the task of developing a rational simulation model capable of predicting the survivability (relative safety) of people located in conventional (NFSS) buildings when exposed to the direct effects of nuclear weapons. Two models were produced. The first is a complete simulation process which uses a fair number of different routines which form the overall computational system. The second is simply an operational version of the first model which uses previously computed results that were run off for suitably large ranges of pertinent parameters. The operational version was developed to reduce computational costs and turnaround time in performing operational level survivability analyses on large numbers of "typical" buildings. The first model applies to unique situations requiring detailed modeling and to specific sensitivity analyses. The second applies to more standard situations for which it produces results quickly and economically. Both programs are currently operational on the University Computing Company (UCC) UNIVAC 1108 computational system.

The simulation process applies adequately to low and high rise framed (reinforced concrete and steel) buildings with "weak" exterior walls, i.e., buildings which do not produce significant quantities of casualty level debris when interacting with the blast wave. It applies reasonably well to buildings with "strong" exterior walls providing that overturning is not a problem, and to load-bearing buildings prior to the collapse of the load-bearing walls.

This model represents a substantial improvement over that of the original SEP code (Ref. 1) both in its range of applicability and ease of operation. To date it is the only simulation model which is capable of evaluating the survivability of people

relative to very specific hazards, i.e., the prompt effects of nuclear weapons. It can be readily extended to consider the survivability of people subject to hazards such as tornados, hurricanes and earthquakes. Operational analysis methods for dealing with such effects are currently very limited and where they do exist they are used for evaluating physical damage and never people survivability in the sense used herein.

Since the computational process necessarily takes into account the damage that a given building experiences, this model can certainly be used to perform damage assessment studies and therefore should be used for this purpose by agencies engaged in this activity.

With appropriate modification of blast loading data, the basic computational algorithm may be used in evaluating explosives safety and thus for establishing reliable safety criteria in separating munitions storage igloos from inhabited structures.

6.2 NECESSARY IMPROVEMENTS TO THE SIMULATION MODEL

Although the model is operational and is capable of producing results which are distinctly more reliable than anything in the past, it should nonetheless be considered as a first order, preliminary effort. As described in the preceding chapters of this report, the model has some distinct drawbacks which can and should be remedied. These are the following.

1. Blast loading prediction
2. Translation casualty dose prediction
3. Debris casualty dose prediction
4. Prompt nuclear radiation dose prediction

The first three items really define a single problem since they all deal with the secondary blast effects which occur approximately at the same time. People translation followed by impact, and debris-people interaction in a high velocity blast wind environment are coupled by the fact that motion in each case is produced by the same agent during approximately the same time interval. It should therefore be treated as a single event

which considers both the impact of people on hard surfaces and the impact of debris on people. Currently this is treated as two separate problems, i.e., translation effects and debris effects. Also, the debris casualty prediction process ignores the variation in the relative motion between people and debris. The translation casualty process ignores the interaction between individual occupants as in a crowded room. The consequence of these assumptions is that in many situations the former results represent a lower bound and the latter an upper bound of survivability than would ordinarily be expected. Just how much variation exists in any one case can only be crudely estimated at this time.

A significant portion of an algorithm which provides the basis for studying the plane problem currently exists. It will be recalled that routines for the first two of the items listed above have been prepared in the course of this effort (see Appendixes A and B). An adequate debris translation routine has also been developed and exercised (see Chapter 3). Before a useable, operational algorithm based on these routines can be produced it will be necessary to exercise each of them on a suitably large sample of representative case studies. Such an effort is important since it provides the means for isolating important problem parameters such as categories and content of required data, data accuracy requirements, integration times, limitations of results, etc. Further, it will also be necessary to exercise the combined simulation model on a detailed sensitivity basis. Only by this means can a reliable operational version be produced. It is recommended that such an effort be undertaken.

The prompt nuclear radiation dose prediction routine needs to be revised since original data are no longer current and new data are available. For KT range weapon yields this effect can be a significant casualty producer.

6.3 INCREASING THE SCOPE OF THE SIMULATION MODEL

6.3.1 Load-Bearing Buildings and Shielding Effects

As mentioned previously this model applies directly to framed buildings (i.e., buildings whose exterior walls and interior partitions are weaker than the supporting frame), as long as overturning of the structure as a whole does not pose a problem. Load-bearing buildings experience partial or total collapse when their exterior walls are breached. Results of this model are valid for fully load-bearing up to the point of exterior wall failure. If the load-bearing building in question has an interior frame then the applicability of results is correspondingly extended.

The problem is that this model does not contain a rational, automatic routine for predicting casualties in a mass debris environment as would be expected during the collapse of a load-bearing building. Such a routine should be formulated since many of the NFSS buildings fall in the fully or partial load-bearing category.

As far as blast effects are concerned, the analysis process assumes that the building being analyzed is located in the open and sufficiently far away from neighboring buildings such that no shielding is produced. For most cases of interest this assumption will produce conservative results, i.e., a lower bound on survivability. If results of numerous buildings are compared on a relative basis then this assumption is certainly adequate. However, it would be useful to determine to what extent such shielding is capable of increasing survivability in representative extreme cases.

6.3.2 Categorization of Survivors

The current simulation model predicts numbers of survivors in the immediate postevent period and includes those persons who are expected to survive (live) at least one week after the event provided that certain basic rescue operations are carried out.

Conversely, casualties include direct fatalities and those persons who are expected to become fatalities within a short period of time after the event.

By this definition survivors include two groups of people, i.e., those who experience no physical trauma and those who experience a wide spectrum of injuries from which they are expected to recover to some level of normality. Such injuries may be slight or incapacitating and will include combinations of shock, cuts, bruises, lacerations, broken limbs, damage to internal organs, burns, broken eardrums, blindness, recoverable levels of radiation illness, etc. Subsequent survival and recovery of this subcategory of people will depend on the extent to which postattack rescue operations are capable of removing them from hazardous places and to areas conducive to recovery. This may but does not necessarily include medical attention beyond that of basic first aid.

It will be recalled that "injured" survivors, who may be fully mobile or temporarily incapacitated, may be located in upper stories of buildings with damaged stairwells, basements with blocked exits, etc. Such areas may be subject to a wide spectrum of postevent hazards including fires, smoke, noxious gases, etc. Results reported herein assume that "basic" rescue operations are carried out. Should this not be the case then the number of survivors reported may be significantly reduced. Generally, the extent of this reduction in any one case will depend on the number of injured and the type and intensity of the postattack environment in the immediate vicinity of the shelter. To measure the extent of the possible reduction, it is first necessary to have the capability for separating survivors in two categories, i.e., the injured and uninjured. Since rescue operations are not expected to be always effective or even possible in some cases, it is important to have the means for predicting at least the lower and the upper bound on the total survivors.

Although casualty data are currently limited, it is felt that what exists is nonetheless capable of being categorized to separate survivors in relevant injured and uninjured categories. An attempt to do so in a crude fashion has already been made in connection with the JEP code (Ref. 1). It is recommended that currently available casualty data be reviewed and categorized giving a reasonable definition to the class of injured personnel. The more refined dose prediction models described earlier will be the basis for determining what classes of data are important, to what levels of accuracy and what limitations can be put on final results.

6.4 CAPABILITIES IN RELATED AREAS

The current simulation model has the capability of being applied in several other, related areas as described in the following paragraphs.

6.4.1 Damage Assessment and Munitions Safety

As mentioned previously, the model makes direct use of the physical state of buildings and therefore is capable of performing damage assessment studies in addition to people survivability. Since several agencies of the Federal Government perform damage assessment studies as part of their normal function, it would be useful if this model (or a suitable version of it) was employed for this purpose. This is the first model which has the capability of studying the problem in detail and therefore can be used as a basis for introducing uniformity into this field.

The basic algorithm contained within the body of this computer program also has the capability of being instrumental in establishing or verifying quantity-distance standards for the manufacture, handling and storage of munitions. To make this an operational model for this purpose, free-field environments as produced by munitions would need to be defined and introduced within the body of this model. Current analytic approaches to this problem are described in Refs. 2 and 3.

6.4.2 Natural Disaster Effects

Effects of natural disasters such as earthquakes, hurricanes and tornados have always posed a serious problem to cities and rural communities. Past events indicate that depending on the type of hazard and the given geographic area, every building can be susceptible to some level of damage. Injuries and fatalities are not uncommon. It is a matter of duration, distribution and intensity of a given effect as compared to how well the various buildings were designed to anticipate it in terms of effects mitigation and protection to occupants.

The problem of natural hazard effects mitigation has currently received some impetus and a fair amount of activity has been generated in a number of different areas. However, it appears that the emphasis is mostly on the reduction of physical damage and only indirectly on people survivability. Explicit evaluation of people survivability in existing buildings when exposed to specific natural disaster effects is not being considered at this time.

Although the simulation model described herein is specifically geared to prompt nuclear weapon effects people survivability evaluation, to a significant degree, it is also applicable for evaluating numbers of survivors when exposed to certain natural hazard environments provided that their loading effects can be defined. It will be recalled that in its most basic form this simulation model consists of a set of dose prediction routines which use nuclear effects in conjunction with simulated personnel to predict intensities of each dose experienced. These are then compared with casualty data to predict the state of personnel. In a seismic or wind (hurricane or tornado) environment (if we ignore floods) casualties in buildings are produced due to translation and debris. The latter is probably more significant in most cases. Therefore casualty data contained in the model apply directly. Provided that intensities, distributions and durations of wind and seismic loading and corresponding debris environments can be defined then casualties can be estimated.

The current blast wind loading model (see Appendix B) is now capable of predicting dynamic wind pressure distributions on the interior of buildings for a given free field wind environment and is especially suited for long duration, high velocity winds as occur in hurricanes.

Although this model is the closest thing available for estimating casualties due to natural hazard effects, a fairly significant effort would be required to develop an operational model for this purpose. Such an effort is nevertheless recommended since it would provide a useful adjunct to studies which are purely physical damage oriented.

6.4.3 Distribution of Blast Initiated Debris

Chapter 3 of this report describes the results of a study which was conducted in support of fire experiments. The corresponding model has the capability of determining local debris piles in terms of composition and distribution in substantial detail. It offers an opportunity for defining and understanding the problem of blast-fire interaction as this influences survivors in the postattack environment. This is the most rational model available at this time and should be applied to more typical situations.

REFERENCES

1. Feinstein, D. I., et al, Personnel Casualty Study, IIT Research Institute for Office of Civil Defense, July 1968.

2. Fugelso, L. E., et al, "A Computation Aid for Estimating Blast Damage from Accidental Detonation of Stored Munitions," General American Research Division, General American Transportation Corporation, Niles, Illinois. Proceedings of the Fourteenth Annual Explosives Safety Seminar, Department of Defense Explosives Safety Board, November 1972.

3. Feinstein, D. I., "Fragmentation Hazards to Unprotected Personnel, for Department of Defense Explosives Safety Board, Contract DAHC 04-69-C-0056, IIT Research Institute Project J6176, January 1972.

APPENDIX A

TRANSLATION SURVIVABILITY MODEL

A.1 INTRODUCTION

When subjected to blast winds produced by the explosion of a nuclear weapon, people located in buildings or in the open may be translated and impacted resulting in injury or mortality. The purpose of this appendix is to describe the analytic process which predicts people survivability in a blast wind environment.

The problem of people translation is primarily one of impact with the horizontal plane (ground surface, building floor) or a vertical surface such as a wall. Also, in taller buildings, should interior walls and other obstacles be cleared by the blast wind, a person could be swept off the building resulting in horizontal or vertical impact. Application of appropriate fatality criteria (described herein) to impacts determined by the mechanics of the rigid body model results in estimates of the probable lethality of translation.

The survivability model is in the form of a computer simulation of the process involving seven subroutines listed as follows:

1. MAIN Program
2. Subroutine TUMBLE
3. Subroutine PRESSJ
4. Function KNOCK
5. Subroutine IMPACT
6. Function HHIT
7. Function WBHIT

The MAIN program reads in data, coordinates the computational process and prints out results. TUMBLE is a plane rigid body translation model which simulates the trajectory of a person translated by the blast winds and determines impact velocities experienced. Subroutine PRESSJ provides the necessary free field

blast loading which is reduced in magnitude by the ratio of window to wall area of the room being analyzed. Function KNOCK provides such ratios. Subroutine IMPACT calls the two fatality criteria routines WBHIT (whole body impact) or HHIT (head impact) to relate the actual impacts computed in TUMBLE to determine the probability of survival.

The simulation model is operational. However it is expected to be modified in two respects. First, subroutine TUMBLE which simulates a person by means of a single rigid block is to be replaced by one which considers an articulated model. Such a model was developed and is described at the end of this appendix. Second, the blast loading routine is to be replaced by a more realistic model. Such a model was also developed and is described in Appendix B of this report. Subroutine PRESSJ which computes the time-dependent free field loading was developed previously (Ref. 7) and is not included in this appendix.

The remainder of this appendix describes the various routines listed above.

A.2 TRANSLATION MODEL AND MECHANICS

This section describes subroutine TUMBLE, which comprises the rigid body mechanics used to model the translation process.

A simple rigid block free to translate and rotate in two dimensions is used to represent a man. The rectangular block is defined by four corner points, shown in Fig. A.1 along with typical data for the average man. Points 1 and 2 in Fig. A.1 define the feet, points 3 and 4 define the head. The dashed line in the figure indicates front and back sides (points 2 and 3 defining the front).

The rigid block is subjected to blast loading and subsequent contact forces produced by impact with horizontal and vertical surfaces. Blast loading consists of diffraction, drag and lift forces. The manner in which the diffraction loading is applied is illustrated in Fig. A.2 in which $P_i (i=1,4)$ are pressures acting at the corner points.

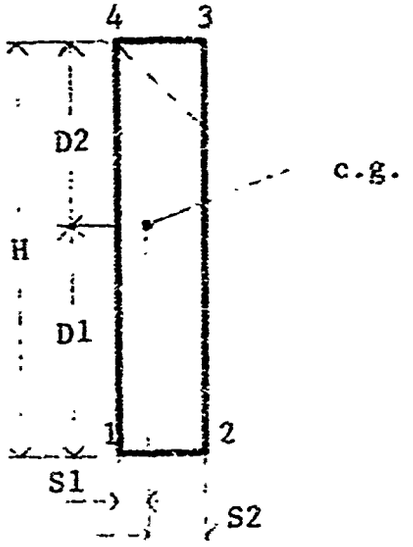

Weight	165 lbs
Height, H	5.77 ft
Height to c.g., D_1	3.20 ft
S_1	0.29 ft
S_2	0.625 ft
Width (out of plane)	1.56 ft
Moment of inertia	8.58 (lb-sec^2-ft)

Fig. A.1 Rigid Body Model

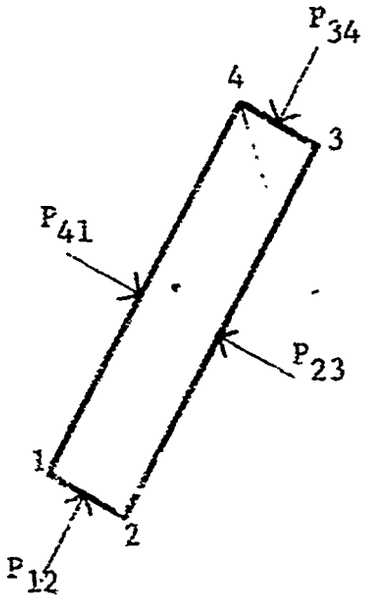

$$P_{12} = 1/2(P_1 + P_2)\cdot(S_1 + S_2)\cdot W$$
$$P_{23} = 1/2(P_2 + P_3)\cdot H\cdot W$$
$$P_{34} = 1/2(P_3 + P_4)\cdot(S_1 + S_2)\cdot W$$
$$P_{41} = 1/2(P_4 + P_1)\cdot H\cdot W$$

Fig. A.2 Pressure Force Notation

They are averaged as indicated and corresponding forces are assumed to act at the center of each lateral surface. The net effect of this loading vanishes once the shock clears around the block. For simplicity, the manner in which this loading is treated here may be replaced by a single impulse as discussed in Appendix B.

Drag and lift forces are applied as shown in Fig. A.3 and are defined as follows:

$D = q(t)\ A_d(\theta)$ Drag force

$L = q(t)\ A_\ell(\theta)$ Lift force

where $q(t)$ is the dynamic pressure of the flow and A_d and A_ℓ are position dependent drag and lift areas which are expressed as follows:

$$A_d = A_{dmin} + (A_{dmax} - A_{dmin}) \sin^2(\theta - \frac{\pi}{2})$$

$$A_\ell = A_{\ell max} \sin(2\theta - \pi)$$

A_{dmin}, A_{dmax} and $A_{\ell max}$ are respectively the minimum drag area, the maximum drag area and the maximum lift area of the rigid block. They are obtained by multiplying the actual areas of appropriate drag and lift coefficients. Variations of drag and lift area ratios with orientation is illustrated in Fig. A.4. For the geometry given in Fig. A.1 the basic area values are given as follows:

$A_{dmin} = 1.2$ sq ft

$A_{dmax} = 9.0$ sq ft

$A_{\ell max} = 2.5$ sq ft

As shown in Fig. A.3, the drag force is assumed to act at the center of the projected area. Its eccentricity (Δ) is

$$\Delta = (\frac{H}{2} - D_1)\cos\theta + \frac{1}{2}(S_1 - S_2)\sin\theta$$

The lift force is assumed to act at the center of gravity (c.g.) and therefore has no associated eccentricity.

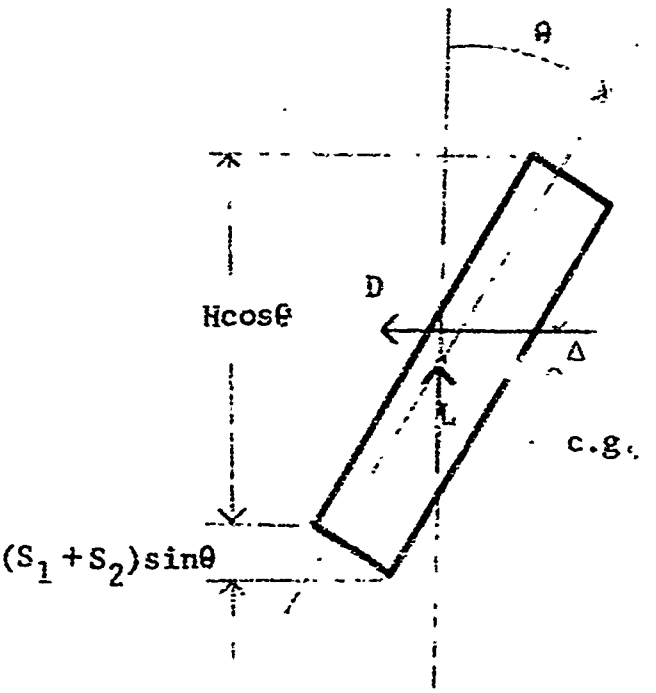

Fig. A.3 Drag and Lift Forces

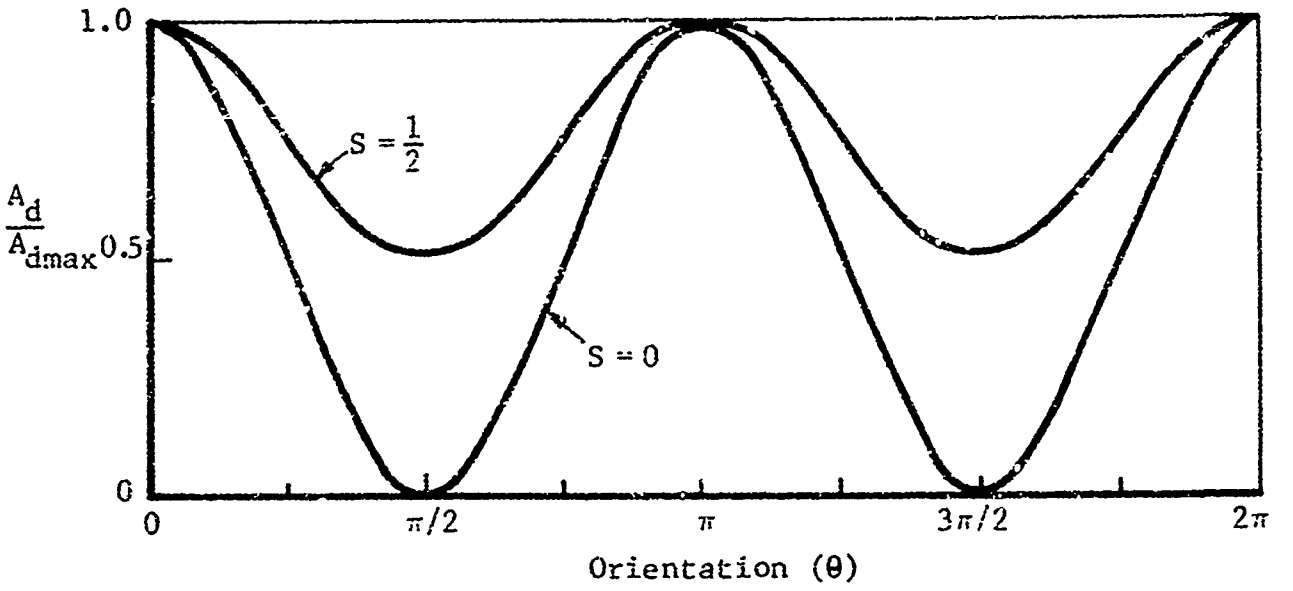

a. Variation in Drag Area Ratio

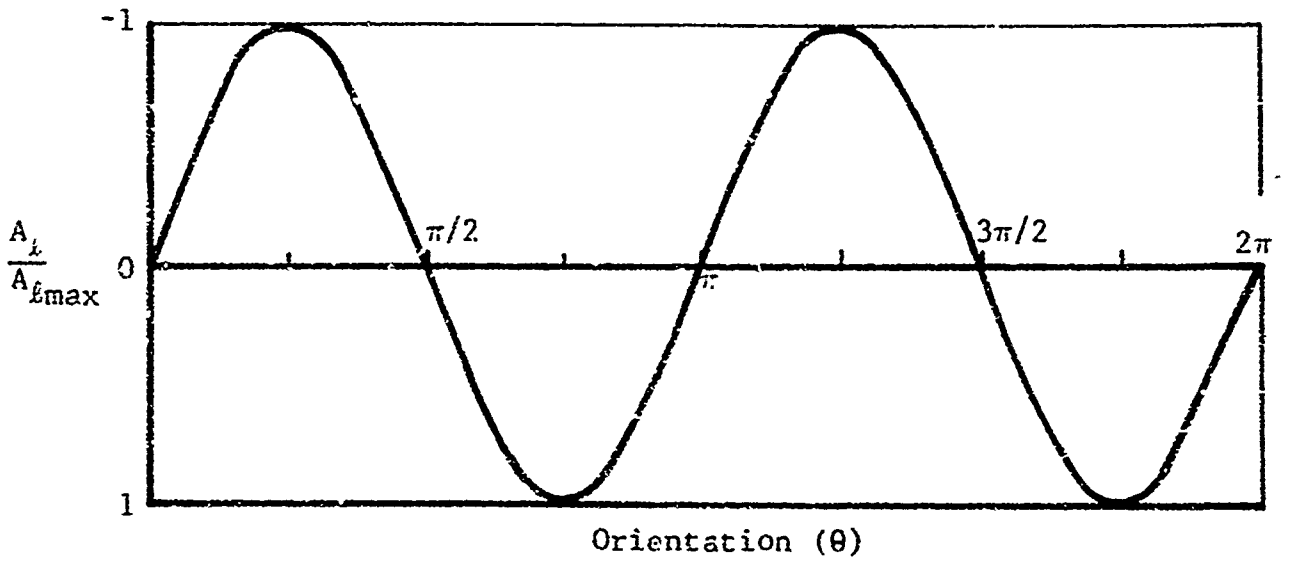

b. Variation in Lift Area Ratio

Fig. A.4 Variations in Drag and Lift Areas with Orientation

The final set of forces which may act on the man are contact forces which occur on impact with either a horizontal or a vertical surface. These contact forces are broken down into the horizontal (H) and vertical (V) components acting at the four corner points of the block.

The following forces apply (where the subscript i refers to the specific point in contact: i = 1,2,3 or 4):

For contact with floor:

$$V_i = -KL\ y_i \qquad y_i < 0 \quad \text{and} \quad \dot{y}_i < 0$$
$$= -Ku\ y_i \qquad y_i < 0 \quad \text{and} \quad \dot{y}_i \geq 0$$
$$= 0 \qquad y_i > 0$$
$$H_i = \mu V_i \cdot (|\dot{x}_i|/\dot{x}_i)$$

For contact with wall:

$$H_i = KL(x_i - x_w) \qquad x_i > x_w \quad \text{and} \quad \dot{x}_i > 0$$
$$= Ku(x_i - x_w) \qquad x_i > x_w \quad \text{and} \quad \dot{x}_i \leq 0$$
$$= 0 \qquad x_i < x_w$$
$$V_i = \mu H_i \quad (|\dot{y}_i|/\dot{y}_i)$$

where

- x_w - coordinate of the wall
- KL - spring constant for loading
- Ku - spring constant for unloading
- μ - coefficient of friction

The numerical values for KL, Ku and μ are estimated as:

$$KL = 1.65 \times 10^5 \text{ lb/ft}$$
$$Ku = 1.65 \times 10^3 \text{ lb/ft}$$
$$\mu = 0.25$$

A free body diagram of the rectangular block model showing all forces is shown in Fig. A.5.

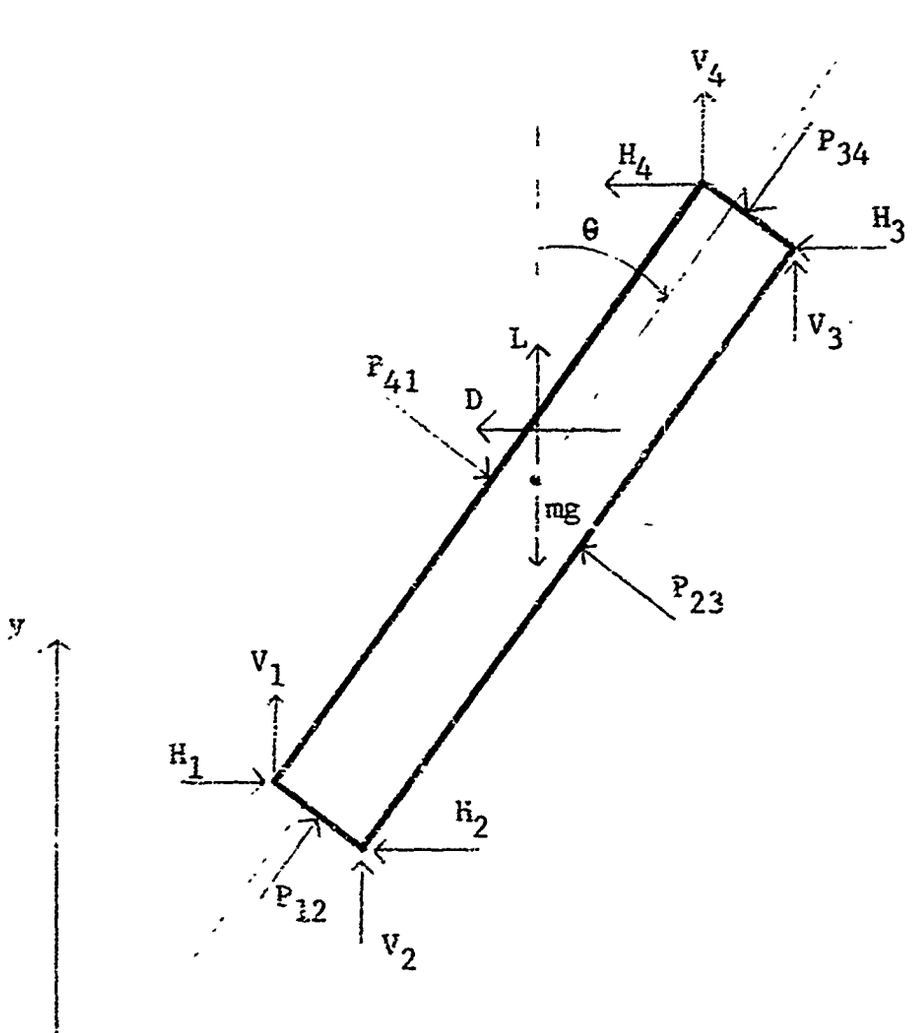

Fig. A.5 Tumbling Man -- Free Body

The governing equations for computing the trajectory of the block are given as follows:

$$M\ddot{x} = -D-H_1-H_2-H_3-H_4 + P_{12}\sin\theta - P_{23}\cos\theta - P_{34}\sin\theta + P_{41}\cos\theta$$

$$M\ddot{y} = L + V_1 + V_2 + V_3 + V_4 + P_{12}\cos\theta + P_{23}\sin\theta - P_{34}\cos\theta - P_{41}\sin\theta - mg$$

$$\begin{aligned} I\ddot{\theta} = {} & -D\Delta + H_1(D_1\cos\theta - S_1\sin\theta) + H_2(D_1\cos\theta + S_2\sin\theta) \\ & - H_3(D_2\cos\theta - S_2\sin\theta) - H_4(D_2\cos\theta + S_1\sin\theta) \\ & + V_1(D_1\sin\theta + S_1\cos\theta) + V_2(D_1\sin\theta - S_2\cos\theta) \\ & - V_3(D_2\sin\theta + S_2\cos\theta) - V_4(D_2\sin\theta - S_1\cos\theta) \\ & - P_{12}((S_2-S_1)/2) - P_{23}(H/2-D_1) \\ & + P_{34}((S_2-S_1)/2) + P_{41}(H/2-D_1) \end{aligned}$$

These, and the previous equations given form the basis of subroutine TUMBLE. The routine accepts data on room geometry (length and height), story height, story length and location and position (standing, prone) of the occupant being analyzed. For a given blast loading, which is applied as described previously, the routine computes the trajectory of the occupant keeping track of his impact velocities with horizontal and/or vertical surfaces. These velocities are then compared with casualty criteria as described in the following section.

Figure A.6 illustrates a typical output of this routine. In this example a building occupant located (standing) at the extreme end of a room having a length of 60 ft is subjected to a blast loading at the 8 psi range produced by a 1 MT weapon. Interior partitions (see Fig. A.6) are assumed to have yielded and therefore do not represent an obstruction. The occupant, subjected to the free field tumbles, impacts on the skull and comes to rest at the window sill at the opposite end of the room.

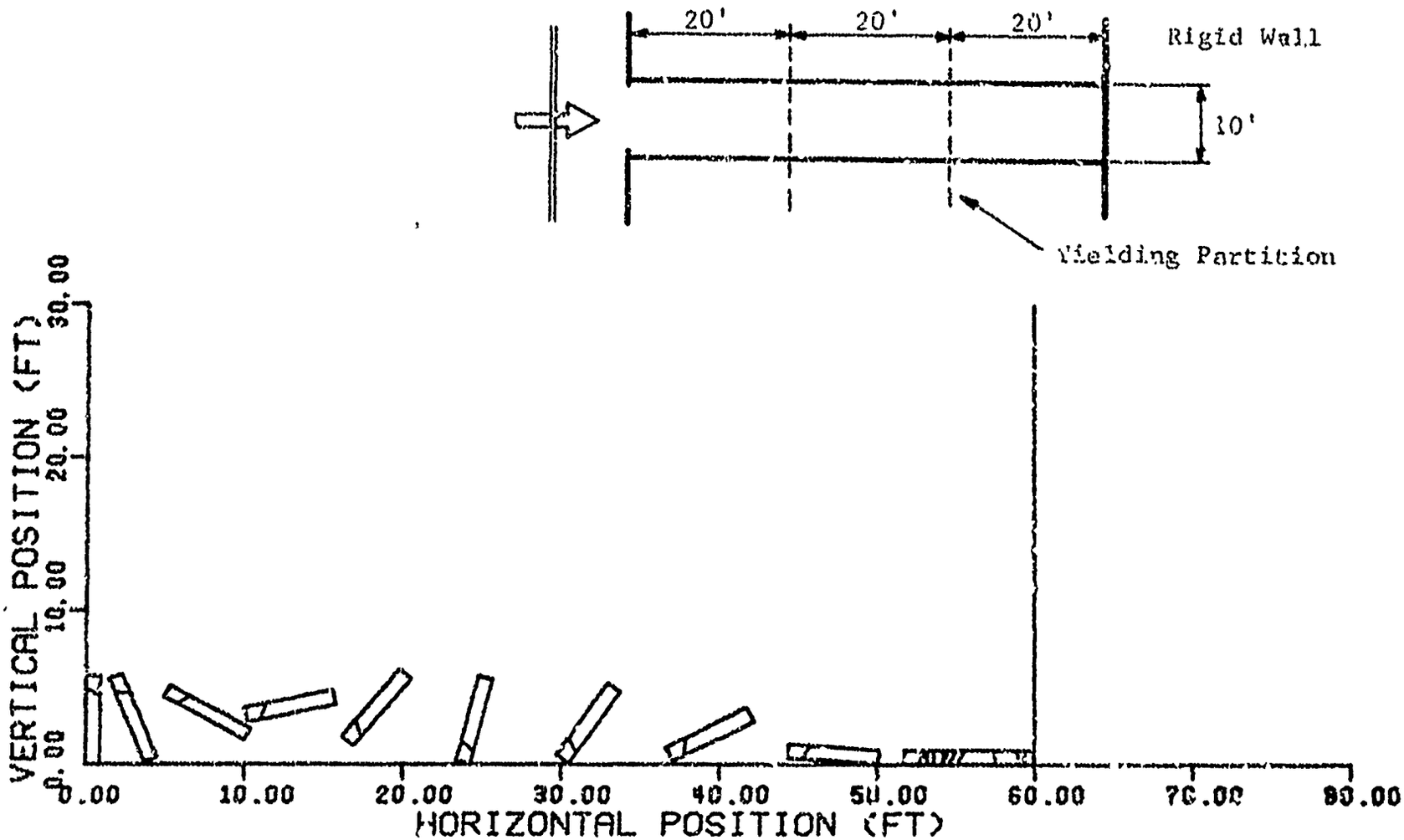

RUN 18: 8.0 PSI BLAST TRAJECTORY OF MAN; ΔT=0.10 SEC

Fig. A.6 Sample Trajectory Plot

A.3 CASUALTY CRITERIA

The mechanics of people translation are related to survivability, through fatality criteria based on impact velocity. These fatality criteria are incorporated in three routines, Subroutine IMPACT, Function HHT and Function WBHIT. IMPACT is called by TUMBLE whenever the trajectory computations indicate an impact has occurred. It then classifies the impacts as either head or whole body and then calls either HHIT or WBHIT to determine the probability of mortality for that impact.

Because of data limitations, no consideration, at present, is given to nonfatal injuries, and only two means of inflicting fatalities are employed: fatal skull fractures and fatal whole body impacts.

Every impact encountered during the translation and rotation of a person is subject to some probability of mortality. Medical data from Refs. 8 and 9 were used to obtain the fatality criteria curve of Fig. A.7. . Table A-1 gives several points from these two curves.

Table A-1

IMPACT VELOCITIES AND PROBABILITIES OF MORTALITY

	Probability of Mortality (%)	Head Impact Velocity ft/sec	Whole Body Impact Velocity ft/sec
Mostly safe	0	10	10
	10	13	21
	50	18	54
Nearly	100	23	138

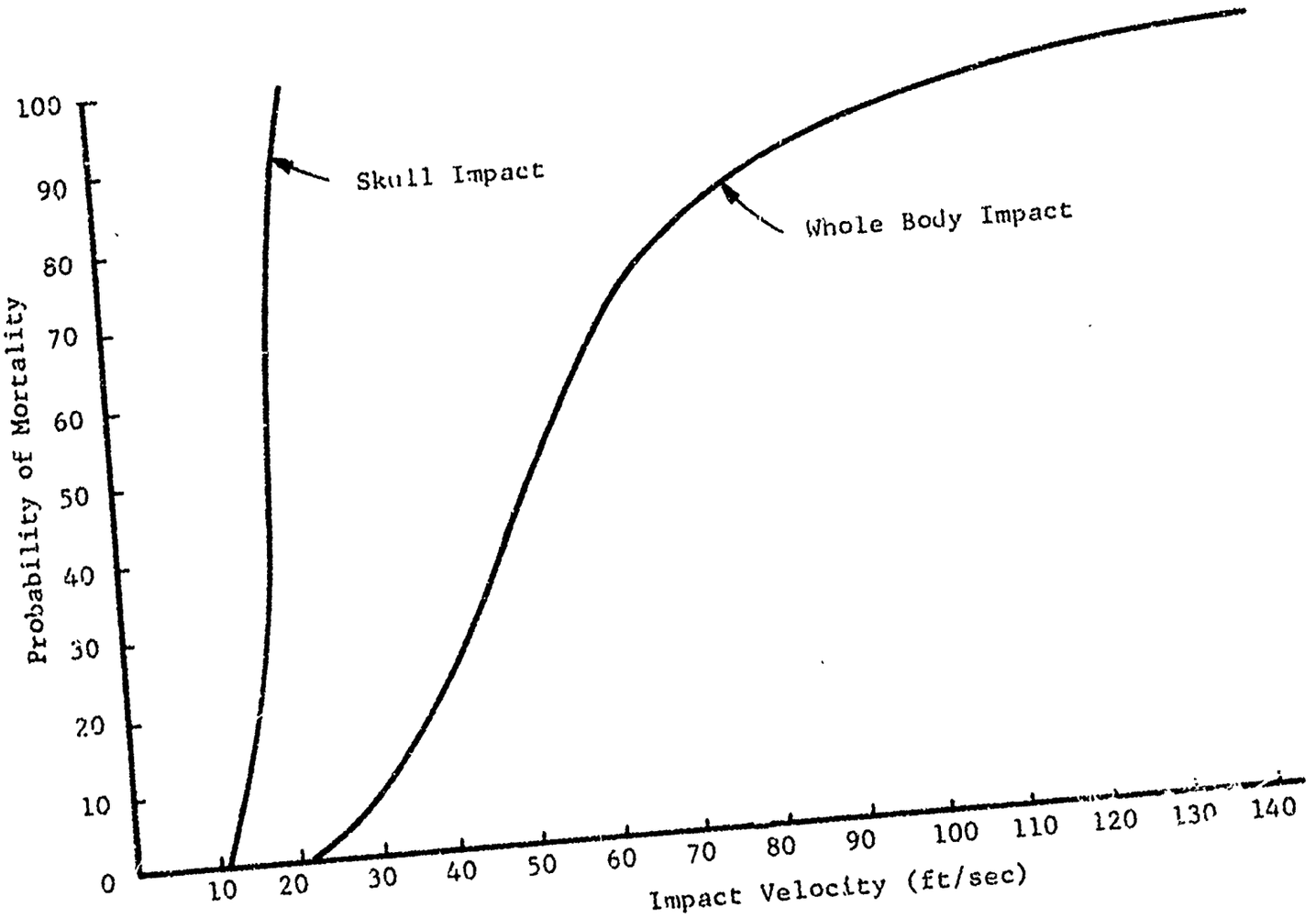

Fig. A.7 Impact Fatality Criteria

With the rigid block model, impacts are of two types: either a foot impact with points 1 or 2 encountering a hard surface, or head impacts with points 3 or 4 encountering a hard surface. A third possibility is that of a literal whole body impact occurring with either points 1 and 4 or points 2 and 3 impacting simultaneously. Thus, the model being a rigid block admits no body impacts, only point impacts, and a means of distinguishing between a head impact and a whole body impact becomes necessary. The distinction is tentatively based on the angle of impact, so if the axis of the rigid block is less than 10 deg off the impacted surface whole body criteria are used to determine the probability of mortality. In this case an average of the normal c.g. velocity and the normal head velocity is used as the impact velocity in the fatality curves. For angles greater than 10 deg pure head impact is assumed and the skull fracture fatality curves apply using the normal impact velocity.

Impacts on the feet (either point 1 or point 2) are more difficult to handle satisfactorily, primarily due to the simplicity of the model and the lack of biomedical data. Tentatively, the following approach has been taken: for foot impacts where the axis at the rectangular block is less than 30 deg from the impacted surface, whole body impact is assumed. The impact velocity is taken as an average of the normal foot velocity and the normal c.g. velocity. For impacts at angles greater than 30 deg whole body criteria are again applied, however, the velocity is halved for the purpose of reducing the severity. These subjective estimates regarding foot impacts are being used until more authoritative data become available.

In all impact cases, velocity normal to the impacted surface is used to enter the fatality curves. The effect of the velocity component parallel to the hard surface is not known but it is not expected to be as critical as the normal velocity.

A.4 SURVIVABILITY IN BUILDINGS

The rigid body translation mechanics and the impact fatality criteria as described above were used in developing a computerized model of blast translation survivability for people in buildings. In its present form the output of the computer code gives expected percent survivors in the building for a given free field overpressure and weapon size.

Three means of fatality are considered:

(1) collision with the floor
(2) collision with interior walls
(3) collision with ground after free fall from higher floors of buildings.

The existing survivability model operates in the context of a given single room. That is, it uses the translation model in conjunction with the fatality criteria to estimate the chances of a man surviving a blast wind in the room. The survivability function for an entire building may be found by either of two methods. First, the survivability in each distinct room in the building may be found and a weighted average used to estimate the total survivability. Second, a representative room may be chosen and the survivability of this room used as an estimate of the entire building. Both approaches have been used, however the second method, because of economic considerations (i.e., computation time), has been favored.

The survivability model operates on a room with the input parameters as shown in Fig. A.8. The length of the room is based on either actual length or a representative length. The length parameter determines where the back wall, which represents a vertical hard surface, is located. However, if the overpressure input is such that all walls are expected to fail no such vertical obstruction remains for the man to impact. In this event, the man can be blown off the building and survivability depends upon surviving free fall to the ground.

The width of the room and the window width dimensions are important in defining the shading that the front wall on either side of the window opening can provide. The blast jet, on entering the room, is assumed to have a form as shown in Fig. A.9 (Ref. 7)..

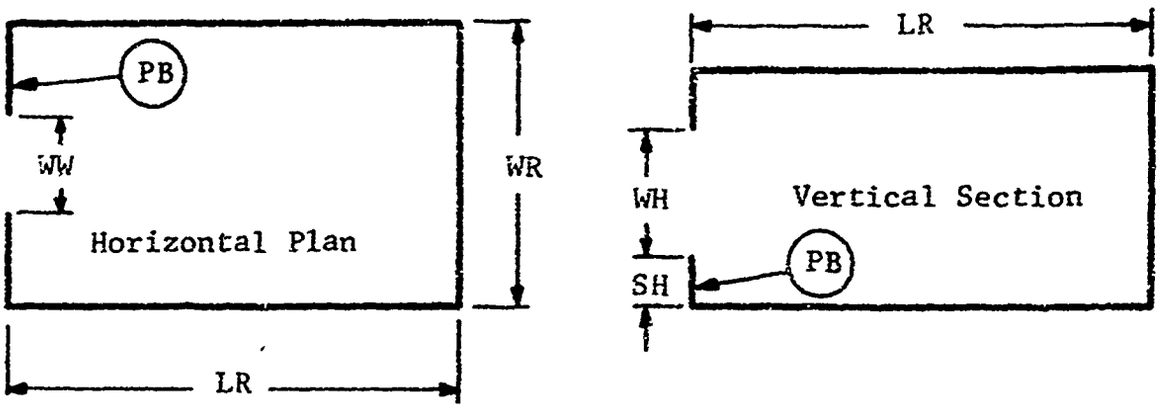

LR: Length of Room
WR: Width of Room
WH: Window Height
WW: Window Width
SH: Sill Height
PB: Failure Overpressure of Front Wall

Fig. A.8 Reference Room

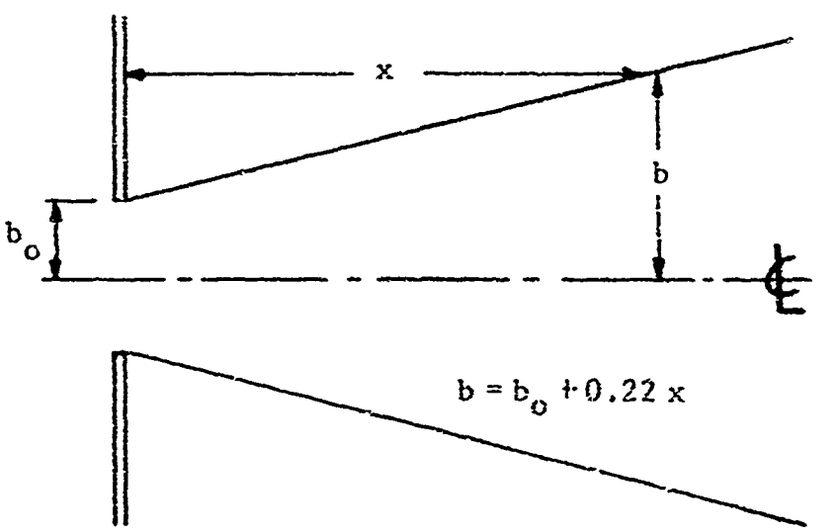

Fig. A.9 Assumed Jet Profile

Persons located outside the blast jet are safe with respect to translation. Thus for a narrow window in relation to total room width, considerable area of the room may be unaffected by the blast jet.

The exterior wall also provides shading because of the window sill. The shading is similar to that provided by the side walls as the relationship shown in Fig. A.9 can be applied in both vertical and horizontal planes. Typical sill heights, however, are such that shading is provided only to people initially prone.

The loading of a person inside of a room is at present considered as a free field loading knocked down as a function of window percentage. Figure A.10 shows the relationship used in function KNOCK to modify the free field loading.

This is a temporary measure. A blast loading routine was developed in the course of this study but was not sufficiently exercised to be included within the body of the people survivability code described herein. The new blast filling routine is described in Appendix B.

The protection provided by the front wall depends of course, on whether that wall is standing or not. Thus the input of the expected front wall failure overpressure, PB, defines the upper limit to overpressures for which occupants in the room can receive some beneficial effects from the wall. On exceeding the value of PB the front wall is "removed" and all occupants of the room exposed. Figure A.11 shows the shading which is included in the model for overpressures lower than PB.

To estimate the survivability in a room, the area is subdivided into three sections and the rectangular block model of a person is started at the center of each of the three sections. The rigid body translation model is called to execute the main trajectory in a blast wind and it calls the fatality criteria on encountering an impact to determine theprobability of mortality for that impact. These probabilities are applied only to those people subject to the blast, if, that is, those persons are not in the "safe" shaded areas.

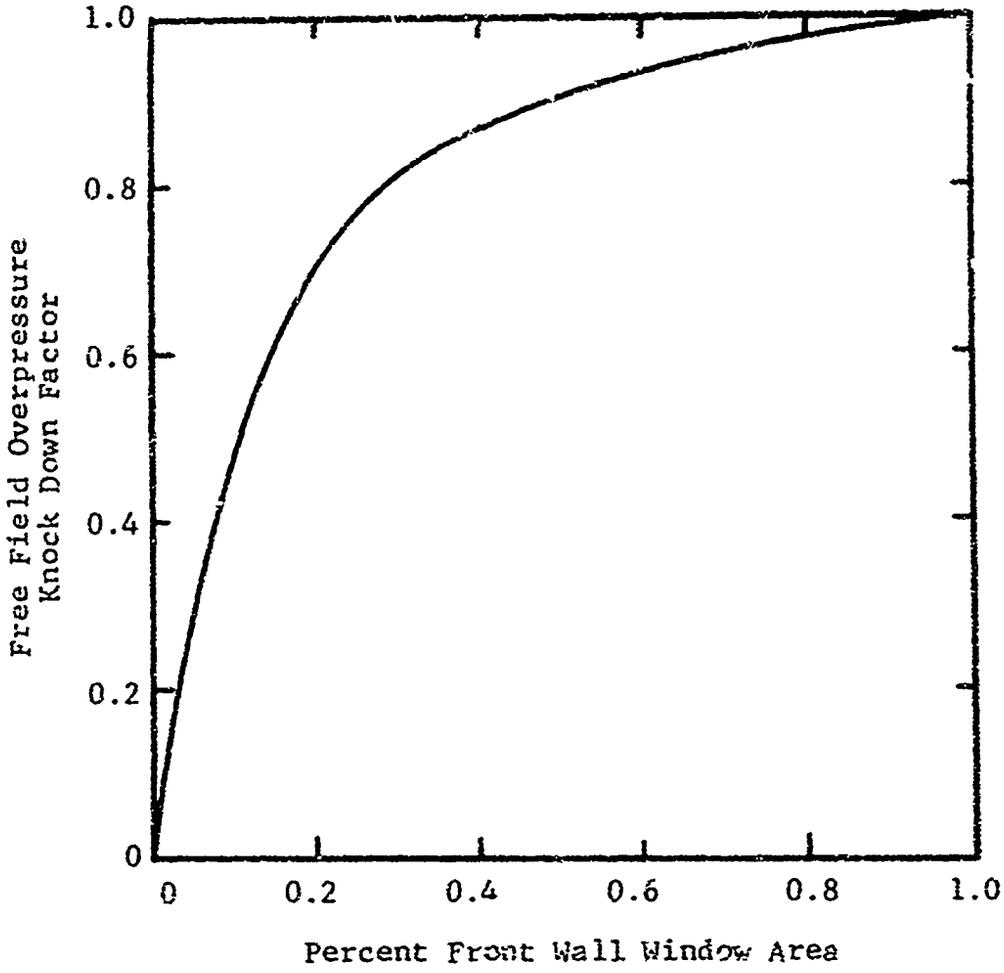

Fig. A.10 Overpressure Reduction Curve Based on Aperture Percentage (Refs. 12,13)

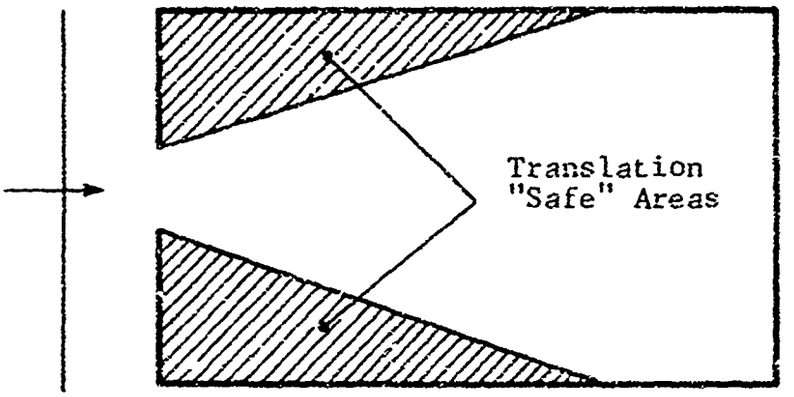

Horizontal Plan with Side Wall Shielding

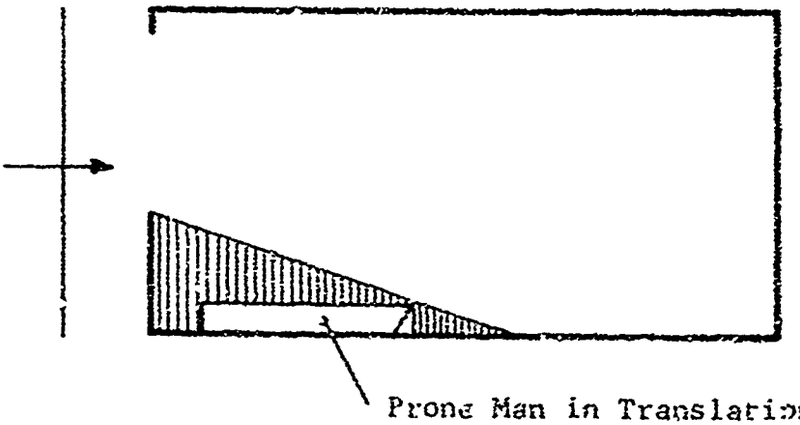

Vertical Section with Sill Shielding

Fig. A.11 Shielding from the Blast Jet

During the course of the rigid body displacement several impacts, each with their own probability of mortality, may occur. For each succeeding impact the kill probability is applied to those people surviving the previous impacts. For example, three impacts each with a probability of mortality equal to 0.50 would result in a (0.5)(0.5)(0.5) = 0.125 probability of survival. The final probability of surviving a specific translation process is applied to the percentage of people within a particular section who are affected by the blast jet.

A.5 SURVIVABILITY ON UPPER FLOORS

In tall weak walled buildings, typical of modern high rise office structures, the blast wind can be expected to clear each floor of all contents, including interior partitions, furniture and people. Depending on the overpressure and width of the structure, the percentage of occupants which will be swept clear of the structure varies. For floors higher than the third, all those people swept off a building will be mortalities because of the ensuing free fall. With the assumption of uniform distribution of people over the entire floor area the curves in Figs. A.12 and A.13 were drawn using the rigid block translation model. For a given building width (range from 40 ft to 200 ft) the percentage of people swept off the building for a given overpressure may be found. The curves show that the initially prone people stand a much better chance of remaining within the comparatively safe structure.

For typical high rise building widths of 60 or 70 ft, an overpressure of 5 psi will clear all standing personnel, while an overpressure of 10 psi is necessary to clear all prone personnel.

These two sets of data are necessarily idealized and represent an extreme case of buildings with "weak walls" and ignore the presence of columns, sills, building cores, elevator and stairwell) and possible shear walls.

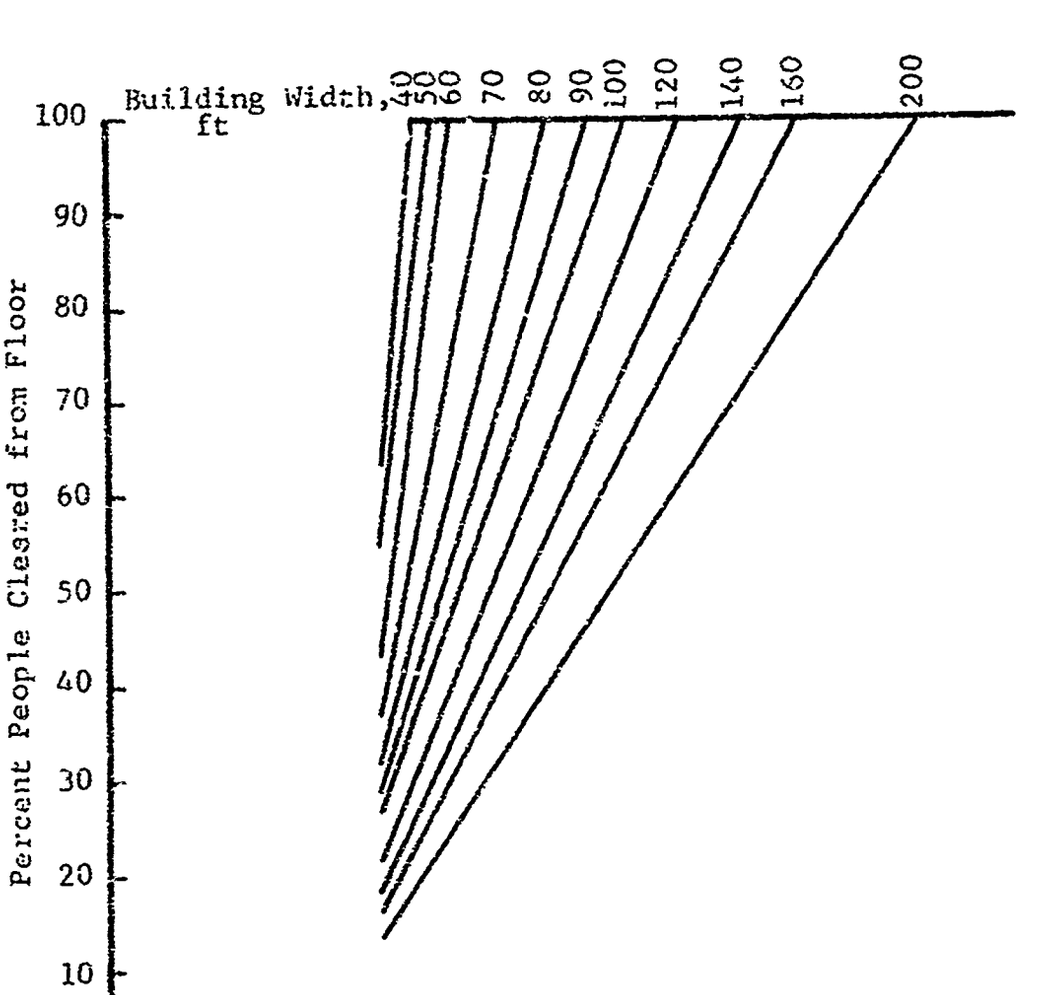

Fig. A.12 Building Clearance Estimates
People Initially Standing

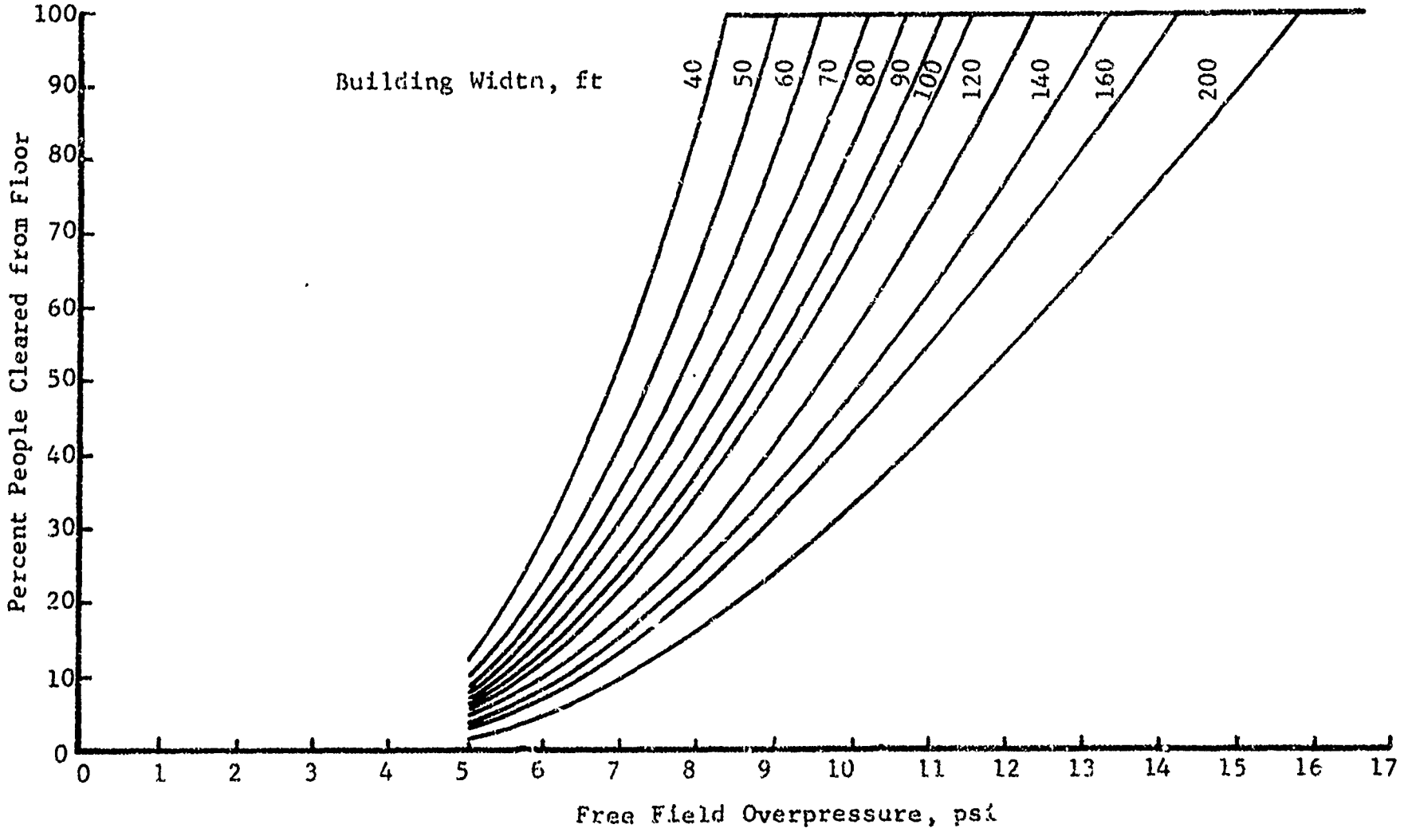

Fig. A.13 Building Clearance Estimates People Initially Prone

A.6 PROGRAM DOCUMENTATION

A.6.1 MAIN Program

A.6.1.1 Flow Chart

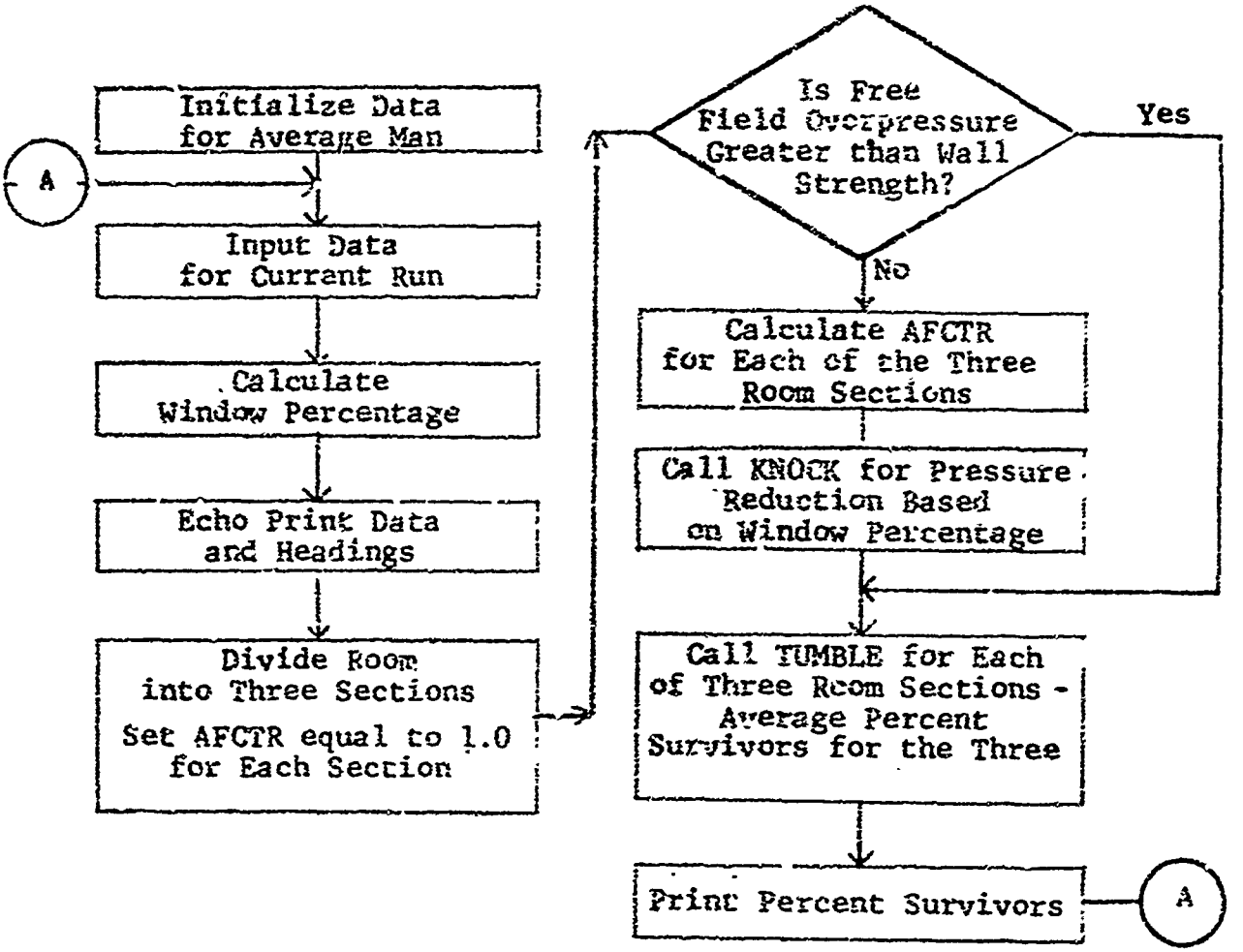

A.6.1.2 MAIN Program - Dictionary

ADMIN	minimum drag area in ft^2
ADMAX	maximum drag area in ft^2
AIMAX	lift area in ft^2
H	height of man (ft)
I	moment of inertia of man ($lb\text{-}sec^2$ ft)
D1	height to c.g. of man (ft)

S1	distance to c.g. from back (ft)
S2	c.g. to frontforce distance (ft)
W	width of man (ft)
KL	loading spring constant for floor impact (lb/ft)
KU	unloading spring constant for floor impact (lb/ft)
MU	floor coefficient of friction
KLW	loading spring constant for wall impact (lb/ft)
KUW	unloading spring constant for wall impact (lb/ft)
MUW	wall coefficient of friction
RUN	identifying run number
ICODE	standing or prone code; if standing ICODE≠0, if prone ICODE=0
YIELD	weapon yield in MT
PO	free field overpressure (psi)
PBREAK	pressure for failure of wall (psi)
DTI	initial time step (prior to first impact)(sec)
DTC	time step during contact with either floor or walls (sec)
DTF	time step otherwise (sec)
DTO	output time increment (sec)
TF	maximum time for trajectory calculation (sec)
LR	length of room (ft)
WR	width of room (ft)
SH	sill height (ft)
WW	window width (ft)
WH	window height (ft)
RH	room height (ft)
PWI	percentage windows
TH	angle of axis of man to vertical
THO	initial angle TH; either 0 (standing or 1.57079 (90 deg)(prone)
SAVE	percentage survivors for input overpressure
XA	third length of the room (ft)
XW	distance to wall initially (ft)
AFCTR	fraction of area susceptible to blast (for each of three sections)
A	total area of a section (ft^2)
X1,Y1	coordinates of point 1 on rigid block man

A.6.1.3 MAIN Program Notes

(1) Built in data:

H = 5.77 ft	W = 1.36 ft
D1 = 3.20 ft	ADMIN = 1.2 ft^2
S1 = 0.29 ft	ADMAX = 9.0 ft^2
S2 = 0.625 ft	ALMAX = 2.5 ft^2

KL = KLW = 165,000 lb/ft

KU = KUW = 1650 lb/ft

MU = MUW = 0.25

I = 8.58 lb-sec^2 ft

(2) Input data - four data cards required:

Variable	Format
RUN, ICODE	2I5
YIELD, PO, PBREAK	3F10.0
DTI, DTC, DTF, DTO, TF	5F10.0
LR, WR, SH, WW, WH, RH	6F10.0

Any number of complete data sets may be run at one time.

If man initially prone, ICODE=0

If man initially standing, ICODE≠0

(3) For integration time steps, sufficiently small increments must be used especially for DTI and DTC.

DTI should be small in order to get initial peak loading.

DTC should be small so that the impact may be properly accounted.

If DTC is too great the man may sink deep into floor and then spring out again very unrealistically.

DTI	0.0001 preferable	0.002 maximum advisable
DTC	0.0001 preferable	0.002 maximum advisable
DTF	0.0005 preferable	0.005 maximum advisable

TF should be on the order of 4 sec.

(4) The room is divided into three sections numbered as follows:

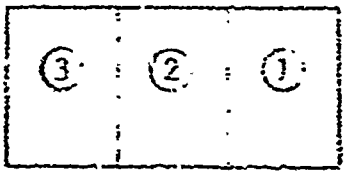

AFCTR(1) is percentage (expressed as decimal fraction) of area of section 1 affected by blast.

AFCTR(2), AFCTR(3) similarly.

This is calculated by expansion of jet approximation:

$$y = b_o + 0.22\ x$$

where y is half width at any point and b_o is half width at x=0. If man is initially prone further shielding occurs because of sill height.

(5) While wall remains standing (PO.LT.PBREAK) shielding is calculated. Also the overpressure is knocked down as a function of window percentage.

A.6.2 Function KNOCK - Dictionary and Notes

X window fraction as input to function

PO outside free field overpressure

Y knockdown factors for each tenth fraction windows

XI tenth window fraction

YI knockdown factor for X

(1) Y array is from knockdown curve given in Fig. A.10.. y values are factors for window percentage equals 0., 0.1, 0.2, 0.3, 0.4, ... etc.

(2) Program interpolates input window fraction linearly between known (Y) knockdown values for each tenth.

A.6.3 Subroutine TUMBLE - Notes

(1) For flow chart of routine see Appendix B.

(2) Differences between this version and flow charted version are:

plotting option removed

Subroutine IMPACT called to determine survivability

A.6.4 Subroutine PRESSJ - Notes

See previous documentation in Ref. 7; no changes.

4.6.5 Subroutine IMPACT

A.6.5.1 Flow Chart

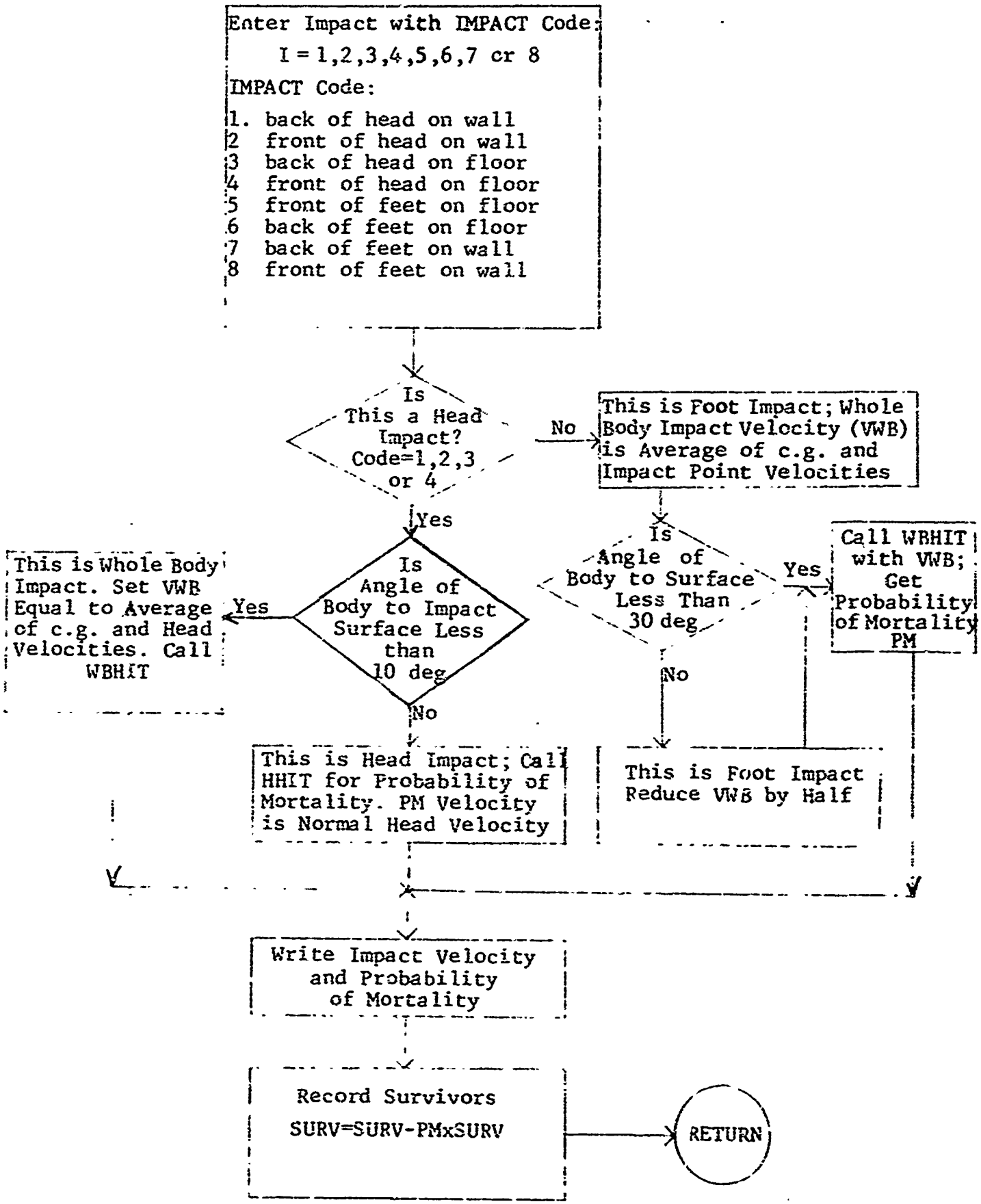

A.6.5.2 Subroutine IMPACT - Notes

(1) This routine calls the two injury criteria routine WBHIT or HHIT depending on whether impact is treated as a whole body hit or a head hit.

(2) All foot impacts are considered whole body impacts, however, for impacts at a sufficient angle to the impacting surface (>30 deg) the severity is reduced by halving the whole body impact velocity. This procedure is an interim one until sufficient data becomes available.

(3) The whole body impact velocity is considered as the average between the c.g. velocity and the impact point velocity. All velocities are those components of total velocity which are normal to the impacting surface.

(4) Survivors are recorded by successively subtracting the percent killed from the previous number of survivors. For each new run the TUMBLE routine initializes SURV to 1.0.

A.6.6 Function HHIT - Notes

(1) Mortality curve for head impacts is called with the impacting velocity.

(2) Curve is a linear interpolation between the following values:

Velocity	Probability of Mortality (%)
10.0	0
13.0	10
18.0	50
23.0	100

A.6.7 Function WBHIT - Notes

(1) This is mortality curve for whole body impact and is called with the impacting velocity.

(2) The probability of mortality is found from

$$Y \text{ (probability units)} = -5.155 + 2.541 \times \ln(v)$$

A.6.8 Program Listing

The following pages are a listing of the FORTRAN computer code described above.

A.7 ARTICULATED MODEL

A.7.1 Introduction

A significant refinement in the rigid block translation model is the introduction of neck and hip joints. A computerized model of this articulated man has been developed and briefly exercised during the course of this effort. This section of the appendix describes the model.

The introduction of joints at the hip and neck has greatly increased the ability to predict the nature and severity of impacts and to identify parts of the body subject to injury. However, since computation time has increased by several factors over the simple rigid block approach, this model at present remains only a research tool.

A.7.2 Description

The articulated man consists of three links representing his lower limbs, trunk and head with hinge points at their junction. Figure A.14 shows the model at some general position with appropriate data based on values for a "typical" man. The hinge points at the hips and neck are not completely free to rotate, rather they have associated with the restraining moments M3 and M5. The value of these resisting moments, M3 and M5, for the hip and neck joints respectively are chosen as functions of angle in Figs. A.15 and A.16. The data for the hip joint was found in Ref. 9 while Ref. 10 had the neck rotation data. These relationships between moment and angle are at best crude estimates of the response of the joints.

As more realistic descriptions become available these will be incorporated in the model.

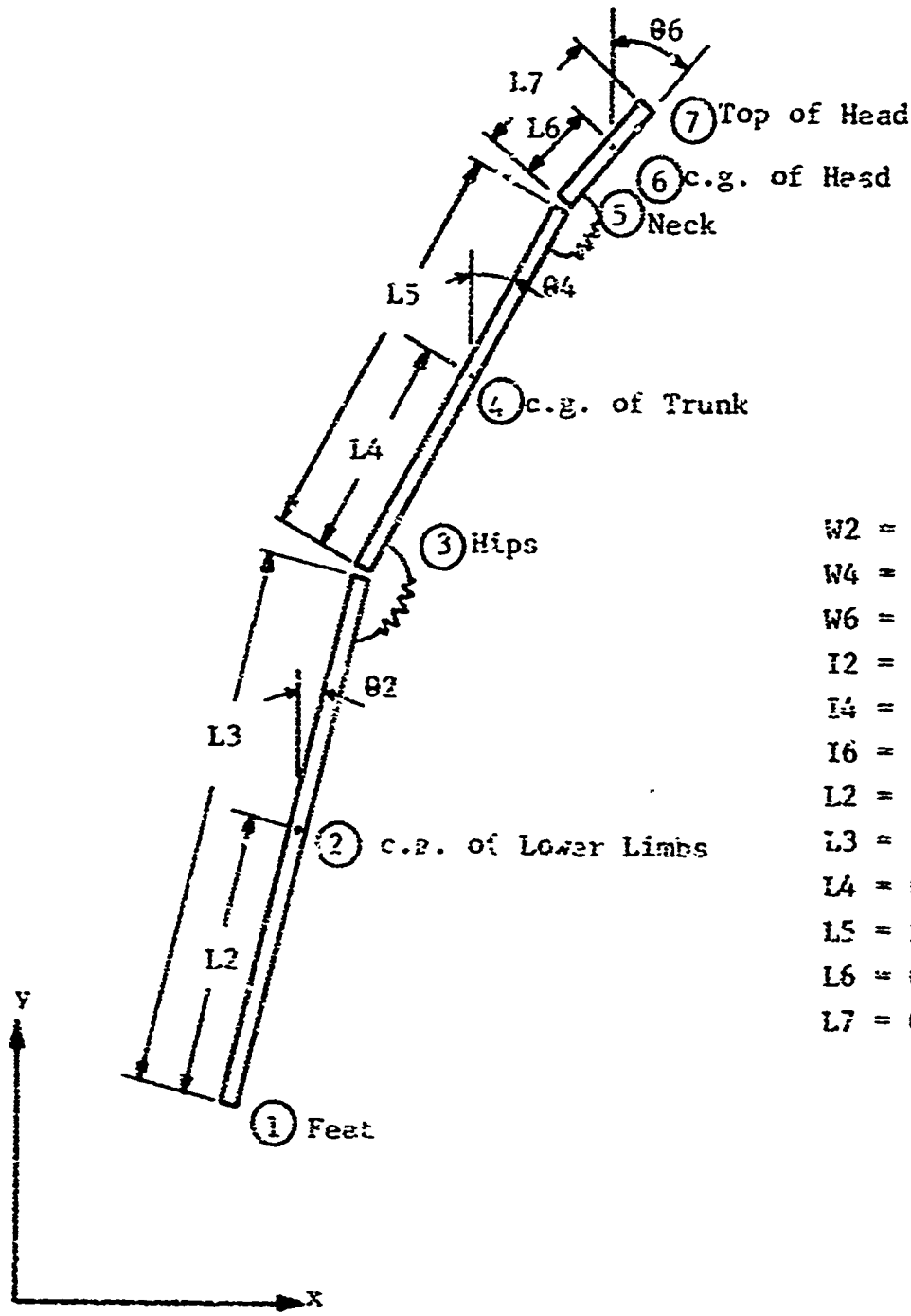

Data

W2 = 56.92 lbs
W4 = 96 69 lbs
W6 = 11.39 lbs
I2 = 1.67 lb-ft-sec^2
I4 = 1.14 lb-ft-sec^2
I6 = 0.03 lb-ft-sec^2
L2 = 1.83 ft
L3 = 3.01 ft
L4 = 0.99 ft
L5 = 2.01 ft
L6 = 0.37 ft
L7 = 0.75 ft

Fig. A.14 Articulated Man Model

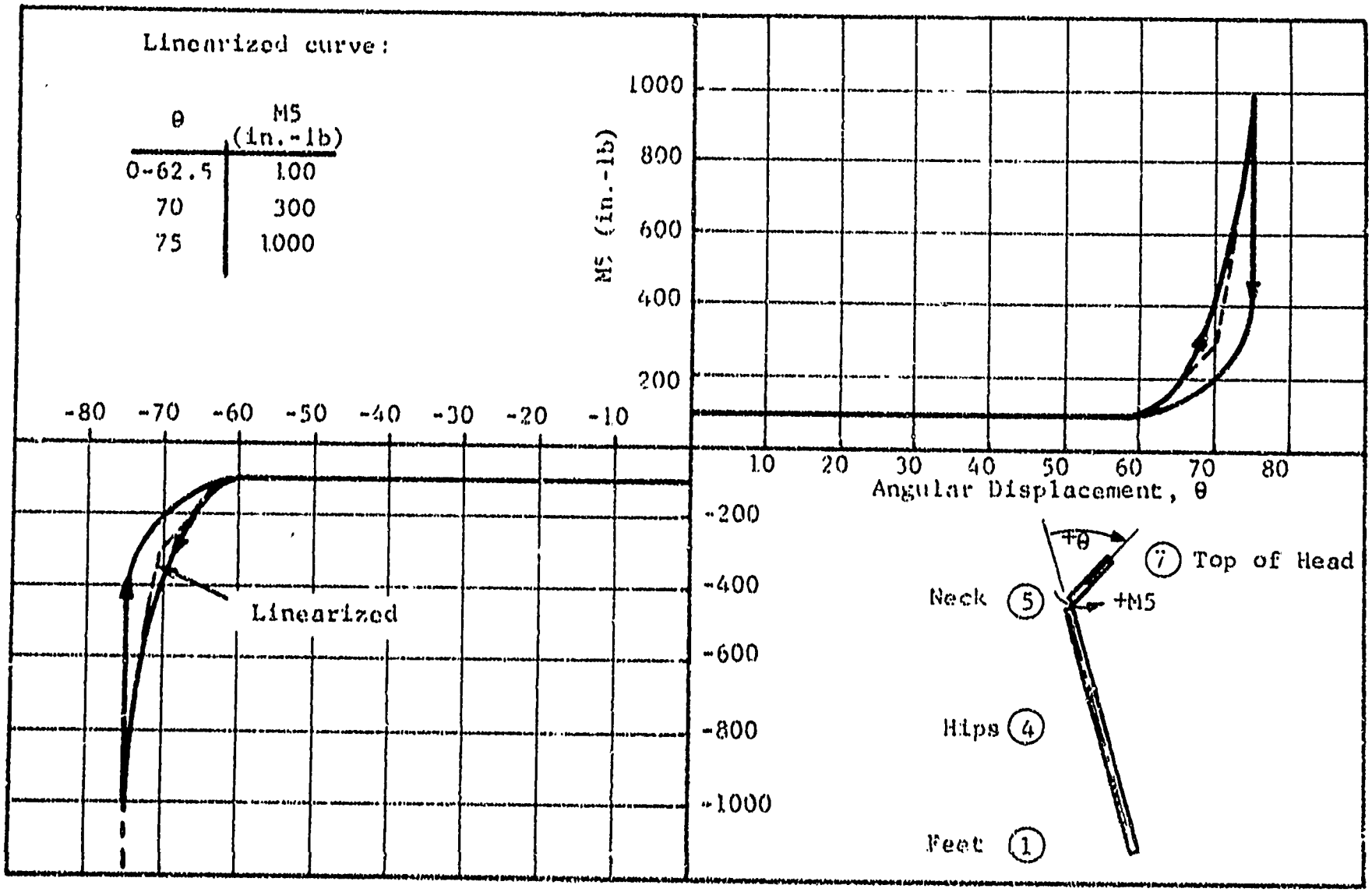

Fig. A.15 Resisting Moment MS for Neck Rotation

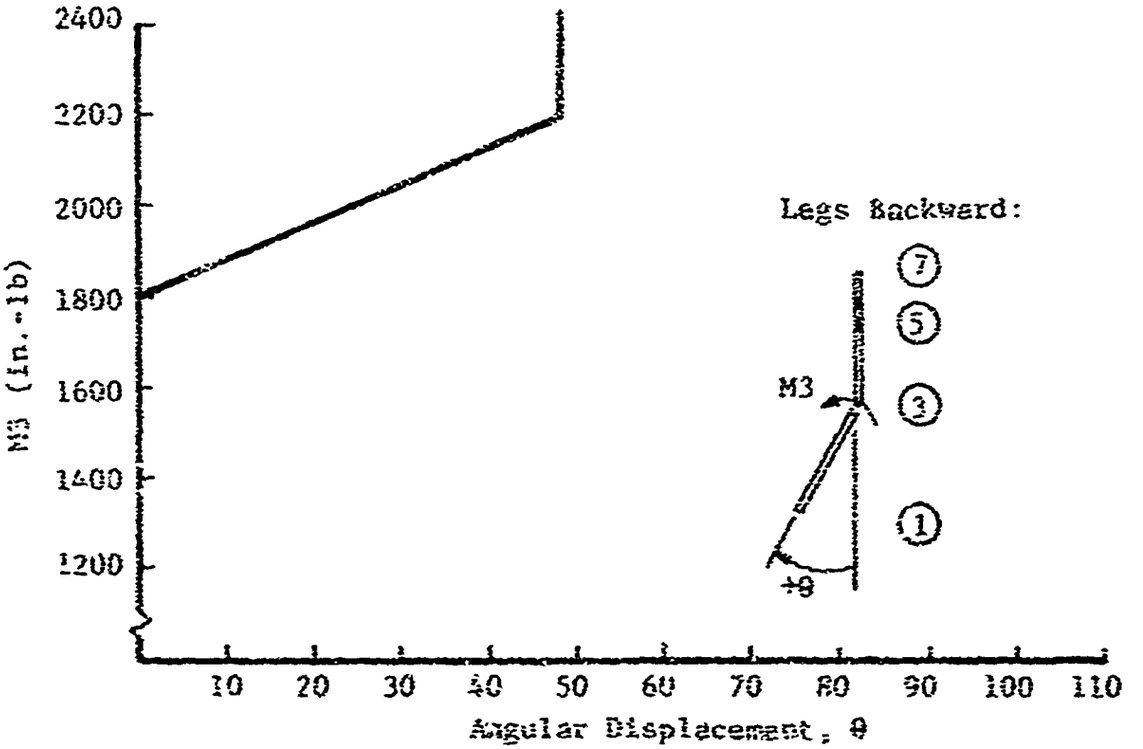

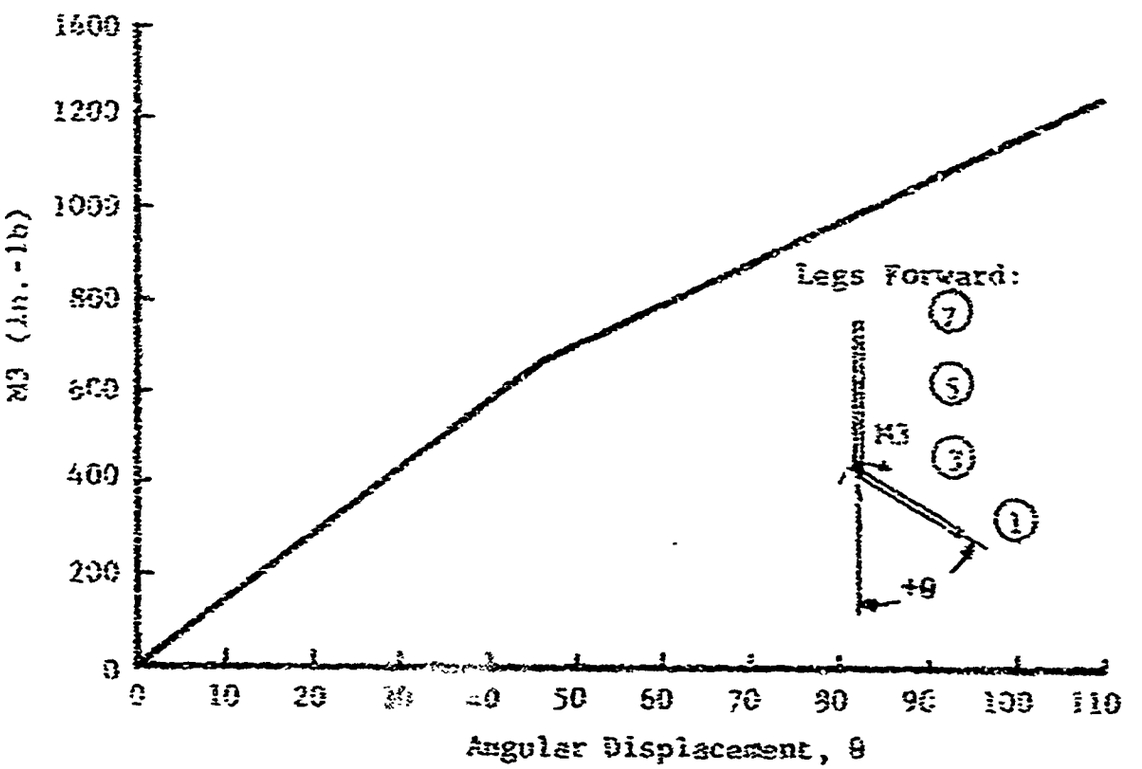

Fig. A.16 Resisting Moment M3 for Hip Rotation (Forward and Backward)

A.7.3 Development of Governing Equations

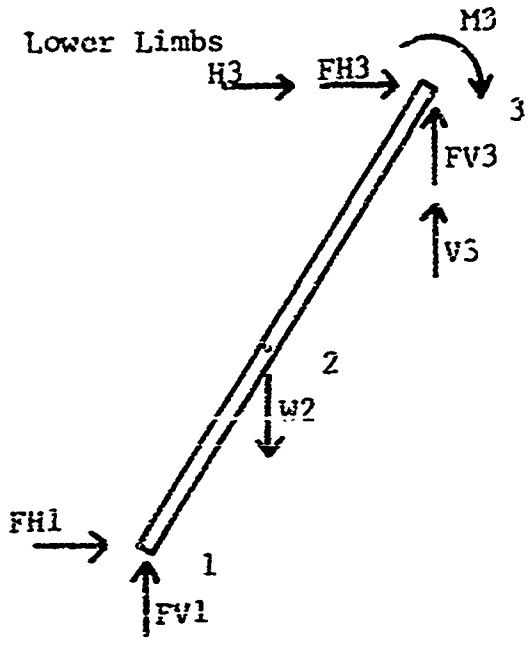

(1) $FH1 + FH3 + H3 = W2/g\ \ddot{x}2$

(2) $FV1 - W2 + FV3 + V3 = W2/g\ \ddot{y}2$

(3) $-FH1 \cdot L2 \cdot \cos\theta2 + FV1 \cdot L2 \cdot \sin\theta2 + H3 \cdot (L3-L2) \cdot \cos\theta2 + FH3 \cdot (L3-L2)\cos\theta2$
$-V3 \cdot (L3-L2) \cdot \sin\theta2 - FV3 \cdot (L3-L2) \cdot \sin\theta2 + M3 = I2 \cdot \ddot{\theta}2$

(4) $x2 = L2 \cdot \sin\theta2 + x1$

(5) $y2 = L2 \cdot \cos\theta2 + y1$

(6) $x3 = (L3-L2) \cdot \sin\theta2 + x2$

(7) $y3 = (L3-L2) \cdot \cos\theta2 + y2$

(8) $\dot{x}2 = L2 \cdot \dot{\theta}2 \cdot \cos\theta2 + \dot{x}1$

(9) $\dot{y}2 = -L2 \cdot \dot{\theta}2\ \sin\theta2 + \dot{y}1$

(10) $\dot{x}3 = (L3-L2)\ \dot{\theta}2\ \cos\theta2 + \dot{x}2$

(11) $\dot{y}3 = -(L3-L2)\ \dot{\theta}2\ \sin\theta2 + \dot{y}2$

(12) $\ddot{x}2 = L2 \cdot \ddot{\theta}2\ \cos\theta2 - L2 \cdot (\dot{\theta}2)^2\ \sin\theta2 + \ddot{x}1$

(13) $\ddot{y}2 = -L2 \cdot \ddot{\theta}2\ \sin\theta2 - L2 \cdot (\dot{\theta}2)^2\ \cos\theta2 + \ddot{y}1$

(14) $\ddot{x}3 = L3 \cdot \ddot{\theta}2\ \cos\theta2 - L3 \cdot (\dot{\theta}2)^2\ \sin\theta2 + \ddot{x}1$

(15) $\ddot{y}3 = -L3 \cdot \ddot{\theta}2\ \sin\theta2 - L3 \cdot (\dot{\theta}2)^2\ \cos\theta2 + \ddot{y}1$

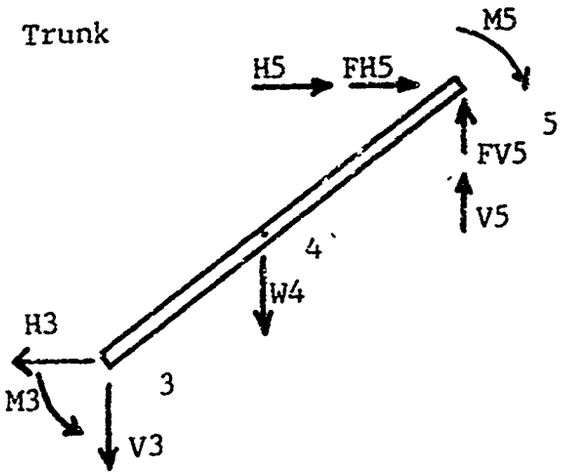

(16) $-H3 + H5 + FH5 = W4/g\ \ddot{x}4$

(17) $-V3 - W4 + V5 + FV5 = W4/g\ \ddot{y}4$

(18) $H3 \cdot L4 \cdot \cos\theta4 - V3 \cdot L4 \cdot \sin\theta4 - M3 + H5 \cdot (L5-L4) \cdot \cos\theta4 + FH5 \cdot (L5-L4) \cdot \cos\theta4 - V5 \cdot (L5-L4) \cdot \sin\theta4 - FV5(L5-L4) \cdot \sin\theta4 + M5 = I4 \cdot \ddot{\theta}4$

(19) $x4 = x3 + L4 \cdot \sin\theta4$

(20) $y4 = y3 + L4 \cdot \cos\theta4$

(21) $x5 = x4 + (L5-L4) \cdot \sin\theta4$

(22) $y5 = y4 + (L5-L4) \cdot \cos\theta4$

(23) $\dot{x}4 = \dot{x}3 + L4 \cdot \dot{\theta}4 \cdot \cos\theta4$

(24) $\dot{y}4 = \dot{y}3 - L4 \cdot \dot{\theta}4 \cdot \sin\theta4$

(25) $\dot{x}5 = \dot{x}4 + (L5-L4) \cdot \dot{\theta}4 \cdot \cos\theta4$

(26) $\dot{y}5 = \dot{y}4 - (L5-L4) \cdot \dot{\theta}4 \cdot \sin\theta4$

(27) $\ddot{x}4 = \ddot{x}3 + L4 \cdot \ddot{\theta}4\ \cos\theta4 - L4 \cdot (\dot{\theta}4)^2 \cdot \sin\theta4$

(28) $\ddot{y}4 = \ddot{y}3 - L4 \cdot \ddot{\theta}4\ \sin\theta4 - L4 \cdot (\dot{\theta}4)^2 \cdot \cos\theta4$

(29) $\ddot{x}5 = \ddot{x}3 + L5 \cdot \ddot{\theta}4\ \cos\theta4 - L5 \cdot (\dot{\theta}4)^2 \cdot \sin\theta4$

(30) $\ddot{y}5 = \ddot{y}3 - L5 \cdot \ddot{\theta}4\ \sin\theta4 - L5 \cdot (\dot{\theta}4)^2 \cdot \cos\theta4$

Head

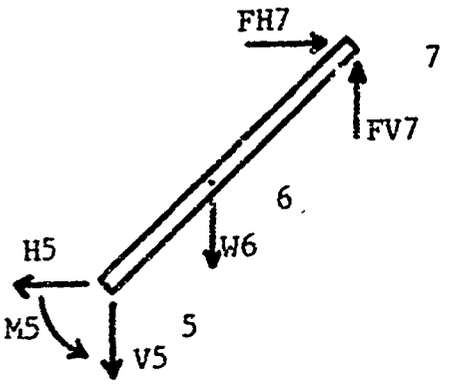

(31) $-H5 + FH7 = W6/g\ \ddot{x}6$

(32) $-V5 - W6 + FV7 = W6/g\ \ddot{y}6$

(33) $H5 \cdot L6 \cdot \cos\theta6 - V5 \cdot L6 \cdot \sin\theta6 - M5 + FH7(L7-L6) \cdot \cos\theta6$
$-FV7 \cdot (L7-L6) \cdot \sin\theta6 = I6 \cdot \ddot{\theta}6$

(34) $x6 = x5 + L6 \cdot \sin\theta6$

(35) $y6 = y5 + L6 \cdot \cos\theta6$

(36) $x7 = x6 + (L7-L6) \cdot \sin\theta6$

(37) $y7 = y6 + (L7-L6) \cdot \cos\theta6$

(38) $\dot{x}6 = \dot{x}5 + L6 \cdot \dot{\theta}6 \cdot \cos\theta6$

(39) $\dot{y}6 = \dot{y}5 - L6 \cdot \dot{\theta}6 \cdot \sin\theta6$

(40) $\dot{x}7 = \dot{x}6 + (L7-L6) \cdot \dot{\theta}6 \cdot \cos\theta6$

(41) $\dot{y}7 = \dot{y}6 - (L7-L6) \cdot \dot{\theta}6 \cdot \sin\theta6$

(42) $\ddot{x}6 = \ddot{x}5 + L6 \cdot \ddot{\theta}6 \cdot \cos\theta6 - L6 \cdot (\dot{\theta}6)^2 \cdot \sin\theta6$

(43) $\ddot{y}6 = \ddot{y}5 - L6 \cdot \ddot{\theta}6 \sin\theta6 - L6 \cdot (\dot{\theta}6)^2 \cdot \cos\theta6$

These governing equations can be reduced to a set of 19 simultaneous equations in 19 unknowns, the unknowns being the accelerations and the reactions at the hinge points.

Unknowns: $\ddot{x}1, \ddot{y}1, \ddot{x}2, \ddot{y}2, \ddot{x}3, \ddot{y}3, \ddot{x}4, \ddot{y}4, \ddot{x}5, \ddot{y}5,$
$\ddot{x}6, \ddot{y}6, \ddot{\theta}2, \ddot{\theta}4, \ddot{\theta}6, H3, V3, H5, V5$

The equations may be expressed in matrix form as

$[C][A] = [R]$ where the matrices C, A and R are:

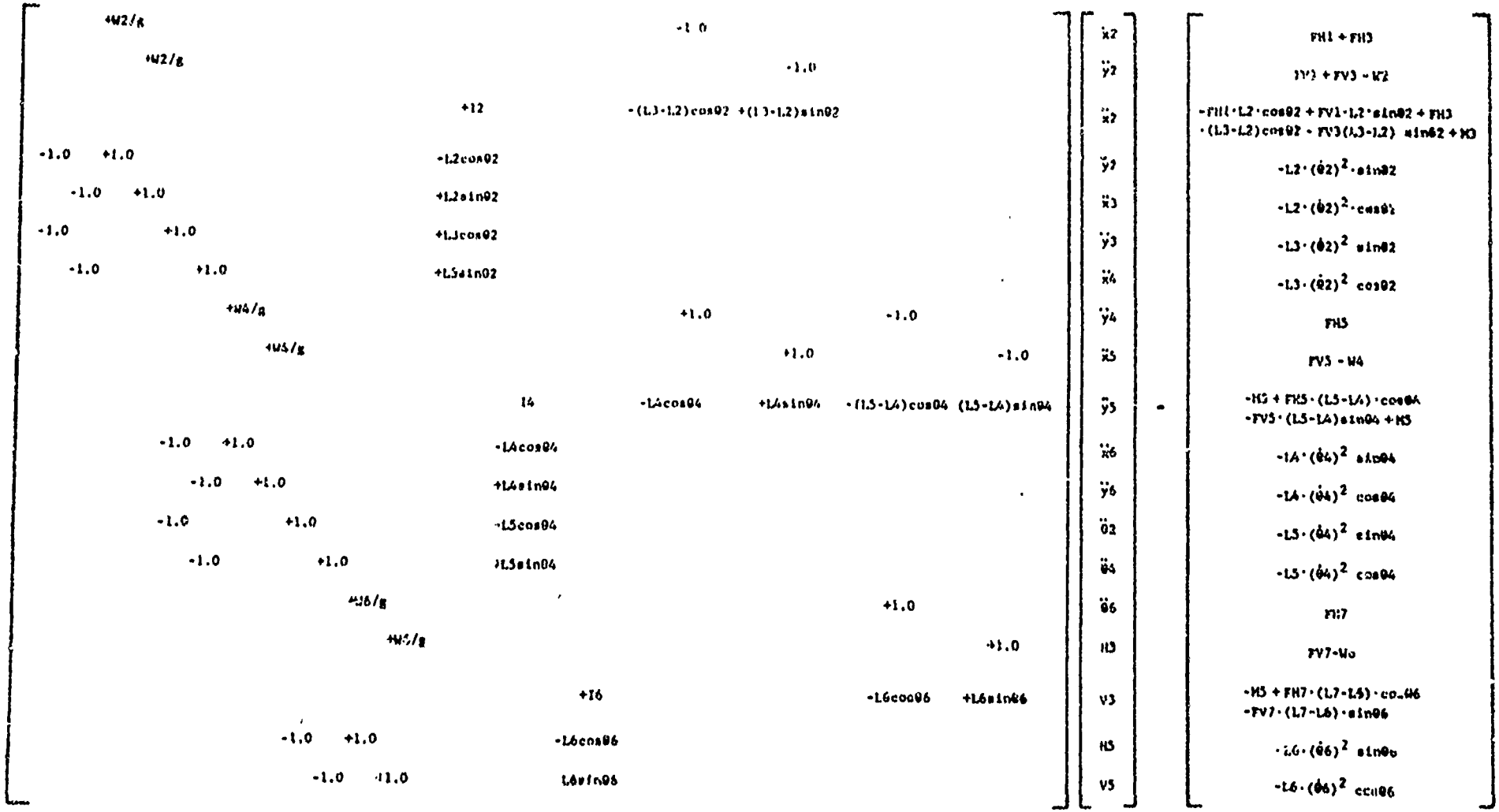
+M2/g
+M2/g
-1.0
+1.0
-1.0
+1.0
-1.0
+1.0
-1.0
+1.0
+M4/g
+M5/g
-1.0
+1.0
-1.0
+1.0
-1.0
+1.0
-1.0
+1.0
+M6/g
+M7/g
-1.0
+1.0
-1.0
+1.0
+I2
-L2cos02
+L2sin02
+L3cos02
+L5sin02
I4
-L4cos04
+L4sin04
-L5cos04
+L5sin04
+I6
-L6cos06
L6sin06
-1.0
+1.0
-(L3-L2)cos02
+1.0
+(L3-L2)sin02
+1.0
-L4cos04
+1.0
+L4sin04
-1.0
-(L3-L4)cos04
-1.0
(L5-L4)sin04
+1.0
-L6cos06
+1.0
+L6sin06
x2
y2
x2
y2
x3
y3
x4
y4
x5
y5
x6
y6
θ2
θ4
θ6
h3
v3
h5
v5
FH1 + FH3
FV1 + FV3 - W2
-FH1·L2·cosθ2 + FV1·L2·sinθ2 + FH3
·(L3-L2)cosθ2 - FV3(L3-L2) sinθ2 + M3
-L2·(θ̇2)2·sinθ2
-L2·(θ̇2)2·cosθ2
-L3·(θ̇2)2 sinθ2
-L3·(θ̇2)2 cosθ2
FH5
FV5 - W4
-M5 + FH5·(L5-L4)·cosθ4
-FV5·(L5-L4)sinθ4 + M5
-L4·(θ̇4)2 sinθ4
-L4·(θ̇4)2 cosθ4
-L5·(θ̇4)2 sinθ4
-L5·(θ̇4)2 cosθ4
FH7
FV7-W6
-M5 + FH7·(L7-L5)·cosθ6
-FV7·(L7-L6)·sinθ6
-L6·(θ̇6)2 sinθ6
-L6·(θ̇6)2 cosθ6

A.7.4 Results

In the brief exercising that has been done with the model, a number of observations were made. It was found that it is now possible to identify different parts of the body for impact; that is, impact on the head, shoulders, thorax, hips, and legs can be distinguished along with associated impact velocities. Thus as data on the severity of various types of impacts become available, a reasonable estimate of injury or fatality can be made.

Figure A.17 shows a sketch of two different runs. Both cases have a loading of 0.75 psi applied horizontal on projected area, similar to a steady dynamic pressure. In the top case the load is applied on the upper part of the man's body, simulating a man standing behind a window sill. The lower case has the load applied over the entire projected area.

In the top case the first impact is on the head at 12.3 ft/sec followed by an impact on the shoulders at 8.4 ft/sec. The lower case is the more interesting with a shoulder impact of 10.7 ft/sec immediately followed by a head impact of 20.8 ft/sec, which is nearly 100 percent fatal. In other words, after impacting on the shoulders, the head swung with much greater velocity into the floor. A rigid block model would result in an initial head impact of approximately 13 ft/sec which has very little chance of causing fatality. The introduction of the two hinge points resulted in greatly differing survivability estimates.

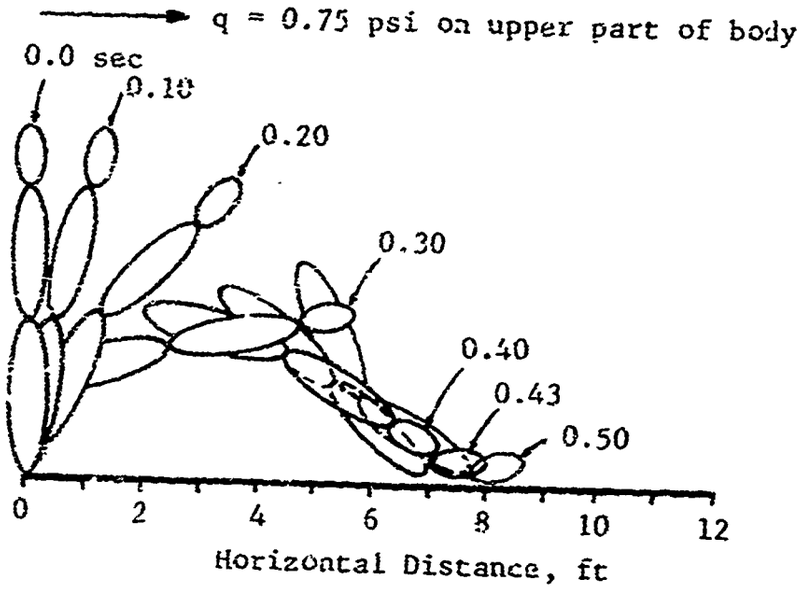

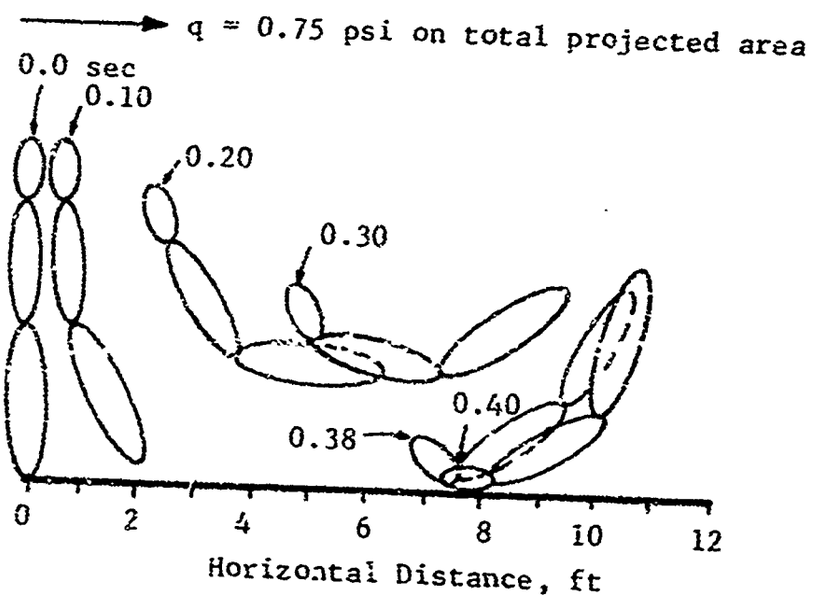

Fig. A.17 Trajectory of Articulated Tumbling Man

```
      DATA ADMIN,ADMAX,ALMAX/1.2,9.0,2.5/
      DATA WT,  H,D1,S1,S2,W/165.,     5.77,3.2,0.29,0.625,1.56/
      REAL KL /165000./,KU /1650./,MU /0.25/
      REAL KLW/165000./,KUW/1650./,MUW/0.25/
      REAL LR,LS
      REAL KNOCK
      REAL I/8.58/
      INTEGER RUN
      DIMENSION AFCTR(3)
      COMMON/BLK1/X1,Y1,X2,Y2,X3,Y3,X4,Y4
      COMMON/BLK3/ WT,I,H,D1,S1,S2,W
      COMMON/BLK4/ KL,KU,MU,KLW,KUW,MUW
      COMMON/BLK5/ ADMIN,ADMAX,ALMAX,TH
      COMMON/BLK6/ DTI,DTC,DTF,DTO,TF
      COMMON/BLK7/ SURV
    1 READ(5,10,END=100) RUN,ICODE
      READ(5,11)  YIELD,PO,PBREAK
      READ(5,11) DTI,DTC,DTF,DTO,TF
      READ(5,11) LR,WR,SH,WW,WH,RH
   10 FORMAT(2I3)
   11 FORMAT(8F10.0)
      PWI=(WW*WH)/(WR*RH)*100.
      TH=0.
      THO=TH
      WRITE(6,5) RUN
    5 FORMAT('1 RUN NUMBER',I3//)
      WRITE(6,6) YIELD,PO
    6 FORMAT(' YIELD:',F6.1,' FREE FIELD OVERPRESSURE:',F5.1)
      WRITE(6,34) PBREAK
   34 FORMAT(' EXTERIOR WALL FAILURE PRESSURE:',F6.1,' PSI')
      IF(ICODE.EQ.0) GO TO 3
      WRITE(6,7)
      GO TO 33
    3 WRITE(6,8)
      TH=1.57079632
      THO=TH
    7 FORMAT(/'  MAN STANDING')
    8 FORMAT(/'  MAN PRONE')
   33 WRITE(6,9) LR,WR,SH,WW,WH,RH,PWI
    9 FORMAT(//' ROOM LENGTH  (FT)',F10.2/' ROOM WIDTH   (FT)',F10.2/
     1 ' SILL HEIGHT  (FT)',F10.2/' WINDOW WIDTH (FT)',F10.2/
     2' WINDOW HEIGHT(FT)',F10.2/' ROOM HEIGHT  (FT)',F10.2/
     3' PER CENT WINDOWS ',F10.2//)
      WRITE(6,22) DTI,DTC,DTF,DTO,TF
   22 FORMAT(/' DTI (SEC)',F8.4/' DTC (SEC)',F8.4/' DTF (SEC)',F8.4/
     1        ' DTO (SEC)',F8.4/                   ' TF  (SEC)',F8.4//)
      WRITE(6,13)WT,KL,    H,KU,    S1,MU,    S2,KLW,ADMIN,D1,KUW,ADMAX,
     1 I,MUW,ALMAX
   13 FORMAT(//
     1' WEIGHT (LBS)  ',F8.2,4X'KL  (LB/FT)',E8.3/
     2' HEIGHT (FT)   ',F8.2,4X'KU  (LB/FT)',E8.3/
     3' S1     (FT)   ',F8.2,4X'MU          ',E8.3/
     4' S2     (FT)   ',F8.2,4X'KLW (LB/FT)',E8.3,4X'ADMIN (FT2)',E8.3/
```

```
     5' D1      (FT)    ',F8.2,4X'KUW (LB/FT)',E8.3,4X'ADMAX (FT2)',E8.3/
     6' I (LB SEC2 FT)',F8.2,4X'MUW          ',E8.3,4X'ALMAX (FT2)',E8.3/)
      SAVE=0.
      XA=LR/3.
      XW=LR/6.
      LS=0.44*XA
      DO 12 K=1,3
   12 AFCTR(K)=1.
      IF(PO.GT.PBREAK) GO TO 50
      PWI=PWI/100.
      FJ=KNOCK(PWI,PO)
      BW=WW
      A=XA*WR
      DO 30 J=1,3
      FW=BW+LS
      IF(FW.GT.WR) GO TO 35
      ARE=(FW+BW)*XA/2.
      AFCTR(4-J)=ARE/A
   30 BW=FW
      GO TO 37
   35 XE=(WR-BW)/0.44
      A1=XE*(WR+BW)/2.
      A2=WR*(XA-XE)
      AFCTR(4-J)=(A1+A2)/A
   37 IF(TH.LE.0.) GO TO 50
      DO 40 J=1,3
      B=J*XA-SH/0.22
      IF(B.GT.0.) GO TO 41
      AFCTR(4-J)=AFCTR(4-J)-WW*XA/A
   40 CONTINUE
      GO TO 50
   41 AFCTR(4-J)=AFCTR(4-J)-(XA-B)*WW/A
   50 DO 70 JJ=1,3
      TH=THO
      A1=0.
      Y1=(S1+S2)*SIN(TH)
      CALL TUMBLE(PO,YIELD,XW)
      XW=XW+0.33333*LR
   70 SAVE=SAVE+33.33333*(1.-AFCTR(JJ)+SURV*AFCTR(JJ))
      WRITE(6,47) SAVE
   47 FORMAT(/' AVERAGE PER CENT SURVIVORS!',F6.1)
      GO TO 1
  100 STOP
      END
```

```
      REAL FUNCTION KNOCK(X,PO)
      DIMENSION Y(11)
      DATA(Y(I),I=1,11)/0.,.474,.704,.807,.867,.904,.933,.959,.978,.989,
     1 1.0/
      DO 1 I=1,11
      XI=FLOAT(I-1)/10.
      J=I
      IF(X-XI)3,2,1
    1 CONTINUE
    2 YI=Y(J)
      GO TO 4
    3 YI=Y(J)-10.*(XI-X)*(Y(J)-Y(J-1))
    4 KNOCK=YI*PO
      RETURN
      END



      SUBROUTINE TUBBLE(PO,YIELD,XW)
      COMMON/BLK1/ X1,Y1,X2,Y2,X3,Y3,X4,Y4
      COMMON/BLK2/ XD1,YD1,XD2,YD2,XD3,YD3,XD4,YD4,XD,YD
      COMMON/BLK3/ WT,I,H,D1,S1,S2,W
      COMMON/BLK4/ KL,KU,MU,KLW,KUW,MUW
      COMMON/BLK5/ ADMIN,ADMAX,ALMAX,TH
      COMMON/BLK6/ DTI,DTC,DTF,DTO,TF
      COMMON/BLK7/ SURV
      REAL I,KL,KU,MU,KLW,KUW,MUW
      YR=0.
      SURV=1.0
      T=0.
      TC=T
      TS=T
      IR=0
      IF(TH.GT.1.) Id=1
      JB=1
      KB=0
      LB=0
      XD=0.
      YD=0.
      THD=0.
      V=0.
      DT=DTI
      S=W/2.
      CALL PRESSJ(PO,YIELD,PT,V0,S,PR,TS,PS,TB,PB,Z)
      X=X1+S1*COS(TH)+D1*SIN(TH)
      Y=D1*COS(TH)+S2*SIN(TH)
      TD=(S1+S2)/V0
    5 ST=SIN(TH)
      CT=COS(TH)
      D2=W-D1
      X1=X-D1*ST-S1*CT
      X2=X-D1*ST+S2*CT
```

```
      X3=X+D2*ST+S2*CT
      X4=X+D2*ST-S1*CT
      Y1=Y-D1*CT+S1*ST
      Y2=Y-D1*CT-S2*ST
      Y3=Y+D2*CT-S2*ST
      Y4=Y+D2*CT+S1*ST
      XD1=XD+THD*(-D1*CT+S1*ST)
      XD2=XD+THD*(-D1*CT-S2*ST)
      XD3=XD+THD*(+D2*CT-S2*ST)
      XD4=XD+THD*(+D2*CT+S1*ST)
      YD1=YD+THD*(+D1*ST+S1*CT)
      YD2=YD+THD*(+D1*ST-S2*CT)
      YD3=YD+THD*(-D2*ST-S2*CT)
      YD4=YD+THD*(-D2*ST+S1*CT)
      IF((JB.GT.0).AND.((Y3.LE.YR).OR.(Y4.LE.YR))) GO TO 101
      IF(JB.GT.0) GO TO 102
      IF((Y3.GT.YR).AND.(Y4.GT.YR)) GO TO 101
      WRITE(6,30)
   30 FORMAT (//37H HEAD CONTACT WITH HORIZONTAL SURFACE)
      IF((Y3.LT.YR).AND.((Y4.GE.YR).OR.(YD3.LE.YD4))) GO TO 23
      V4=(YD4**2+XD4**2)**.5
      WRITE (6,20) YD4,V4,XD,YD,THD,V
      CALL IMPACT(3)
   20 FORMAT (//33H NORMAL HEAD CONTACT VELOCITY   =E10.3/33H TOTAL HEAD
     1 CONTACT VELOCITY    =E10.3/33H HORIZONTAL C G CONTACT VELOCITY=E1
     20.3/33H VERTICAL C G CONTACT VELOCITY  =E10.3/33H ROTATIONAL CONTA
     3CT VELOCITY    =E10.3/33H RESULTANT C G CONTACT VELOCITY =E10.3)
      IB=1
      GO TO 101
   23 V3=(YD3**2+XD3**2)**.5
      WRITE (6,20) YD3,V3,XD,YD,THD,V
      CALL IMPACT(4)
      IB=1
      GO TO 101
  102 IB=0
  101 IF((JB.GT.0).AND.((Y1.LE.YR).OR.(Y2.LE.YR))) GO TO 103
      IF(JB.GT.0) GO TO 104
      IF((Y1.GT.YR).AND.(Y2.GT.YR)) GO TO 103
      WRITE(6,37)
   37 FORMAT (//37H FOOT CONTACT WITH HORIZONTAL SURFACE)
      IF((Y1.LT.YR).AND.((Y2.GE.YR).OR.(YD1.LE.YD2))) GO TO 41
      V2=(YD2**2+XD2**2)**.5
      WRITE (6,38) YD2,V2,XD,YD,THD,V
      CALL IMPACT(8)
   38 FORMAT (//33H NORMAL FOOT CONTACT VELOCITY   =E10.3/33H TOTAL FOOT
     1 CONTACT VELOCITY    =E10.3/33H HORIZONTAL C G CONTACT VELOCITY=E1
     20.3/33H VERTICAL C G CONTACT VELOCITY  =E10.3/33H ROTATIONAL CONTA
     3CT VELOCITY    =E10.3/33H RESULTANT C G CONTACT VELOCITY =E10.3)
      JB=1
      GO TO 103
   41 V1=(YD1**2+XD1**2)**.5
      WRITE (6,38) YD1,V1,XD,YD,THD,V
      CALL IMPACT(7)
```

```
      JB=1
      GO TO 103
  104 JB=0
  103 IF((KB.GT.0).AND.((X3.GE.XW).OR.(X4.GE.XW))) GO TO 105
      IF(KB.GT.0) GO TO 106
      IF((X3.LT.XW).AND.(X4.LT.XW)) GO TO 105
      WRITE (6,31)
   31 FORMAT (//35H HEAD CONTACT WITH VERTICAL SURFACE)
      IF((X3.GT.XW).AND.((X4.LE.XW).OR.(XD3.GE.XD4))) GO TO 32
      V4=(YD4**2+XD4**2)**.5
      WRITE (6,20) XD4,V4,XD,YD,THD,V
      CALL IMPACT(1)
      KB=1
      GO TO 105
   32 V3=(YD3**2+XD3**2)**.5
      WRITE (6,20) XD3,V3,XD,YD,THD,V
      CALL IMPACT(2)
      KB=1
      GO TO 105
  106 KB=0
  105 IF((LB.GT.0).AND.((X1.GE.XW).OR.(X2.GE.XW))) GO TO 33
      IF(LB.GT.0) GO TO 107
      IF((X1.LT.XW).AND.(X2.LT.XW)) GO TO 33
      WRITE (6,34)
   34 FORMAT (//35H FOOT CONTACT WITH VERTICAL SURFACE)
      IF((X1.GT.XW).AND.((X2.LE.XW).OR.(XD1.GE.XD2))) GO TO 35
      V2=(YD2**2+XD2**2)**.5
      WRITE (6,38) XD2,V2,XD,YD,THD,V
      CALL IMPACT(6)
      LB=1
      GO TO 33
   35 V1=(YD1**2+XD1**2)**.5
      WRITE (6,38) XD1,V1,XD,YD,TH,V
      CALL IMPACT(5)
      LB=1
      GO TO 33
  107 LB=0
   33 IF(T.LT.TO) GO TO 7
      V1=(XD1**2+YD1**2)**.5
      V2=(XD2**2+YD2**2)**.5
      V3=(XD3**2+YD3**2)**.5
      V4=(XD4**2+YD4**2)**.5
    6WRITE (6,6) T,XD,YD,THD,V,X1,X2,X3,X4,Y1,Y2,Y3,Y4,XD1,XD2,XD3,XD4,
    1YD1,YD2,YD3,YD4,V1,V2,V3,V4
    6 FORMAT(//E11.3,4E10.3//E21.3,3E10.3/E21.3,3E10.3//(E21.3,3E10.3))
      IF(T.LT.5..AND.T.GT..5) GO TO 19
      TO=TO+DTO
    7 IF(SURV.LE.0.0) GO TO 19
      IF(T.LE.TO+TB) GO TO 10
      Y1T=Y1+YD1*DT
      Y2T=Y2+YD2*DT
      Y3T=Y3+YD3*DT
```

```
      Y4T=Y4+YD4*DT
      X1T=X1+XD1*DT
      X2T=X2+XD2*DT
      X3T=X3+XD3*DT
      X4T=X4+XD4*DT
      IF((Y1.LE.YR).OR.(Y2.LE.YR).OR.(Y3.LE.YR).OR.(Y4.LE.YR).OR.(Y1T.LE
     1.YR).OR.(Y2T.LE.YR).OR.(Y3T.LE.YR).OR.(Y4T.LE.YR).OR.(X1T.GE.XW).O
     2R.(X2T.GE.XW).OR.(X3T.GE.XW).OR.(X4T.GE.XW)) GO TO 9
      DT=DTF
      GO TO 10
    9 DT=DTC
   10 IF(T.GT.TF) GO TO 19
      T3=T-X/VO
      CALL PRESSD(QT,TQ,XD)
      PT=144.*QT*(ADMIN+(ADMAX-ADMIN)*(SIN(TH-1.5707963))**P)
      PL=144.*QT*ALMAX*SIN(2.*TH-3.1415927)
      TP=T-X1/VO
      IF(TP.LT.TS) GO TO 14
      CALL PRESS(P1,TP)
   11 TP=T-X2/VO
      IF(TP.LT.TO+TD) GO TO 15
      CALL PRESS(P2,TP)
   12 TP=T-X3/VO
      IF(TP.LT.TO+TD) GO TO 16
      CALL PRESS(P3,TP)
   13 TP=T-X4/VO
      IF(TP.LT.TS) GO TO 17
      CALL PRESS(P4,TP)
      GO TO 18
   14 P1=0.
      IF(TP.GE.0.) P1=PS+(PR-PS)*(TS-TP)/TS
      GO TO 11
   15 P2=0.
      IF(TP.GE.TD) P2=(TP-TD)*P3/TB
      GO TO 12
   16 P3=0.
      IF(TP.GE.TD) P3=(TP-TD)*PS/TB
      GO TO 13
   17 P4=0.
      IF(TP.GE.0.) P4=PS+(PR-PS)*(TS-TP)/TS
   18 P12=72.*(P1+P2)*LE(S1+S2)
      P23=72.*(P2+P3)*W*H
      P34=72.*(P3+P4)*W*(S1+S2)
      P41=72.*(P4+P1)*W*H
      V1=0.
      V2=0.
      V3=0.
      V4=0.
      IF((Y1.LT.YR).AND.(YD1.LE.0.)) V1=-KL *(Y1-YR)
      IF((Y1.LT.YR).AND.(YD1.GT.0.)) V1=-KU *(Y1-YR)
      IF((Y2.LT.YR).AND.(YD2.LE.0.)) V2=-KL *(Y2-YR)
      IF((Y2.LT.YR).AND.(YD2.GT.0.)) V2=-KU *(Y2-YR)
      IF((Y3.LT.YR).AND.(YD3.LE.0.)) V3=-KL *(Y3-YR)
```

```
      IF((Y3.LT.YR).AND.(YD3.GT.0.)) V3=-KU *(Y3-YR)
      IF((Y4.LT.YR).AND.(YD4.LE.0.)) V4=-KL *(Y4-YR)
      IF((Y4.LT.YR).AND.(YD4.GT.0.)) V4=-KU *(Y4-YR)
      H1=0.
      H2=0.
      H3=0.
      H4=0.
      IF((X1.GT.XW).AND.(XD1.GT.0.)) H1=KLW*(X1-XW)
      IF((X2.GT.XW).AND.(XD2.GT.0.)) H2=KLW*(X2-XW)
      IF((X3.GT.XW).AND.(XD3.GT.0.)) H3=KLW*(X3-XW)
      IF((X4.GT.XW).AND.(XD4.GT.0.)) H4=KLW*(X4-XW)
      IF((X1.GT.XW).AND.(XD1.LE.0.)) H1=KUW*(X1-XW)
      IF((X2.GT.XW).AND.(XD2.LE.0.)) H2=KUW*(X2-XW)
      IF((X3.GT.XW).AND.(XD3.LE.0.)) H3=KUW*(X3-XW)
      IF((X4.GT.XW).AND.(XD4.LE.0.)) H4=KUW*(X4-XW)
      IF((H1.EQ.0.).AND.(XD1.NE.0.)) H1=MU *V1*XD1/ABS(XD1)
      IF((H2.EQ.0.).AND.(XD2.NE.0.)) H2=MU *V2*XD2/ABS(XD2)
      IF((H3.EQ.0.).AND.(XD3.NE.0.)) H3=MU *V3*XD3/ABS(XD3)
      IF((H4.EQ.0.).AND.(XD4.NE.0.)) H4=MU *V4*XD4/ABS(XD4)
      IF((V1.EQ.0.).AND.(YD1.NE.0.)) V1=-MUW*H1*YD1/ABS(YD1)
      IF((V2.EQ.0.).AND.(YD2.NE.0.)) V2=-MUW*H2*YD2/ABS(YD2)
      IF((V3.EQ.0.).AND.(YD3.NE.0.)) V3=-MUW*H3*YD3/ABS(YD3)
      IF((V4.EQ.0.).AND.(YD4.NE.0.)) V4=-MUW*H4*YD4/ABS(YD4)
      ST=SIN(T)
      CT=COS(T)
      XDD=(32.174/WT)*(+FD-H1-H2-H3-H4+P12*ST-P23*CT-P34*ST+P41*CT)
      YDD=(32.174/WT)*(FL+V1+V2+V3+V4+P12*CT+P23*ST-P34*CT-P41*ST+WT)
     DTHDD=(1./I)*(+FD*((H/2.-D1)*CT+.5*(S1-S2)*ST)+H1*(D1*CT-S1*ST)+H2*
     1(D1*CT+S2*ST)-H3*(D2*CT-S2*ST)-H4*(D2*CT+S1*ST)+V1*(D1*ST+S1*CT)+V
     22*(D1*ST-S2*CT)-V3*(D2*ST+S2*CT)-V4*(D2*ST-S1*CT)-P12*(S2-S1)/2.-P
     323*(H/2.-D1)+P34*(S2-S1)/2.+P41*(H/2.-D1))
      T=T+DT
      XD=XD+DT*XDD
      YD=YD+DT*YDD
      THD=THD+DT*THDD
      V=(XD**2+YD**2)**.5
      X=X+DT*XD
      Y=Y+DT*YD
      TH=TH+DT*THD
      GO TO 5
   10 IP=0
      WRITE(6,300) IP,SURV
  300 FORMAT(/' SURVIVAPILITY AT',I3,' PSI=',F6.3//)
      RETURN
      END
```

```
      SUBROUTINE PRESSJ(PO,YIELD,TC,VO,S,PR,TS,PS,TB,PB,Q)
C
C  VO IS THE SHOCK VELOCITY IN AIR
C  S IS THE MINIMUM DISTANCE FOR CLEARANCE OF A PACE ON FLAT PLATE
C  PR IS THE PEAK REFLECTED OVERPRESSURE
C  TS IS THE TIME OF INCREASED OVERPRESSURE
C  PS IS THE OVERPRESSURE AT TIME TS
C  TB IS THE TIME FOR PRESSURE BUILDUP BEHIND PLATE
C  PB IS THE OVERPRESSURE AT TIME TB
C  Q IS THE PEAK DYNAMIC PRESSURE
C  VA IS THE PEAK AIR VELOCITY
C
      DIMENSION KIND(6,10),NRANGE(10),P(6,10),C2(6,10),C3(6,10),V(10),C1
     1(6,10)
      DATA(KIND(1,J),J=1,8)/1,1,1,2,1,2,1,1/
      DATA(KIND(2,J),J=1,5)/1,1,2,2,1/
      DATA(KIND(3,J),J=1,8)/1,2,1,2,2,1,1,2/
      DATA(KIND(4,J),J=1,7)/1,1,2,2,1,2,1/
      DATA(KIND(5,J),J=1,2)/1,2/
      DATA(KIND(6,J),J=1,6)/1,1,2,1,1,1/
      DATA(NRANGE(I),I=1,6)/8,5,8,7,2,6/
      DATA(P(1,J),J=1,8)/2.,15.,35.,75.,220.,300.,900.,2000./
      DATA(P(2,J),J=1,5)/2.,9.8,30.,1500.,4000./
      DATA(P(3,J),J=1,8)/2.,3.,20.,30.,100.,300.,500.,4000./
      DATA(P(4,J),J=1,7)/2.,22.,40.,110.,280.,1700.,5000./
      DATA(P(5,J),J=1,2)/2.,200./
      DATA(P(6,J),J=1,6)/2.,10.,30.,200.,500.,4000./
      DATA(C1(1,J),J=1,8)/.94127992,1.1628274,1.0832833,-2.1896237,10.63
     13722,-3.5715442,38.497531,57.468645/
      DATA(C1(2,J),J=1,5)/.07391036,.10057667,-4.4409313,23.490011,.5199
     19155/
      DATA(C1(3,J),J=1,8)/.125,-2.3415881,.35607458,.34285702,-9.269/949
     1,.0040662,.7534693,68.131084/
      DATA(C1(4,J),J=1,7)/.25521219,.44409885,6.8534444,-24.211087,1.389
     1618,19.985486,.00853424/
      DATA(C1(5,J),J=1,2)/.02446584,.14168432/
      DATA(C1(6,J),J=1,6)/4.0237673,5.2468309,3.4743932,.42904355,.52706
     1715,.89097957/
      DATA(C2(1,J),J=1,8)/-.06469880,-.14275098,-.11757965,1.0499078,-.6
     10360648,1.3617450,-.80154185,-.85425236/
      DATA(C2(2,J),J=1,5)/.43615142,.30073985,1.3757287,-6.1312383,-.121
     1336683/
      DATA(C2(3,J),J=1,8)/1.,.1,5032479,.34469537,-.42775009,3.7176161,.0
     1376594,.19598924,-15.363012/
      DATA(C2(4,J),J=1,7)/.34374251,.1693199,-3.7469502,9.1911457,.05549
     1113,-5.0649923,.67807190/
      DATA(C2(5,J),J=1,2)/.22826899,-1.0923874/
      DATA(C2(6,J),J=1,6)/-.33047502,-.44739151,-1.5451558,.15002969,.11
     1691892,.05362128/
      DATA(C3(1,J),J=1,8)/0.,0.,0.,-.15072543,0.,-.16150803,0.,0./
      DATA(C3(2,J),J=1,5)/0.,0.,-.13063109,.37362382,0./
      DATA(C3(3,J),J=1,8)/0.,-.24087817,0.,.10820813,-.33868201,0.,0.,.8
     18453218/
```

```
      DATA(C3(4,J),J=1,7)/0.,0.,.49767470,-.04839391,0.,.33310964,0./
      DATA(C3(5,J),J=1,2)/0,,.11203606/
      DATA(C3(6,J),J=1,6)/0.,0.,.16603774,0.,0.,0./
      IF(P0.EQ.PP0) GO TO 13
      PP0=P0
      IF(P0.GE.2..AND.P0.LE.10000.) GO TO 11
      GO TO 16
   11 DO 2 K=1,4
      KK=NRANGE(K)-1
      I=1
    6 IF(P0.GE.P(K,I).AND.P0.LE.P(K,I+1)) GO TO 5
      IF(P0.GT.P(K,I+1)) GO TO 8
      GO TO 5
    8 IF(I.LT.KK) GO TO 7
      I=I+1
      GO TO 5
    7 I=I+1
      GO TO 8
    5 IKIND=KIND(K,I)
      GO TO(3,4),IKIND
    3 A=C1(K,I)
      B=C2(K,I)
      V(K)=A*P0**B
      GO TO 2
    4 A=C1(K,I)
      B=C2(K,I)
      C=C3(K,I)
      Y=1.+B*ALOG(P0)+C*ALOG(P0)*ALOG(P0)
      V(K)=EXP(Y)
    2 CONTINUE
      IF(P0.GE.100.) GO TO 14
      V(7)=0.
      V(8)=0.
      V(1)=1.0-V(2)
      GO TO 15
   14 V(3)=1.-V(1)-V(2)
   15 V(6)=V(4)*1.
      V(5)=V(5)*100.
      GO TO 17
   13 IF(YY.EQ.YIELD) GO TO 9
   17 TC=V(6)*YIELD**(1./3.)
      YY=YIELD
      V1=1126.*(1.+4.*EXP(-102.9))**.5
      PR=2.*P0*(102.9+4.*P0)/(102.9+P0)
      TS=3.*S/V0
      TAU=TS/TC
      E=EXP(-TAU)
      W=P0*(V(1)*(E**V(3))+V(2)*(E**V(4))+V(7)*(E**V(5)))*(1.0-TAU)
      TB=2.*TS
      TAU=TB/TC
      E=EXP(-TAU)
      PB=P0*(V(1)*(E**V(3))+V(2)*(E**V(4))+V(7)*(E**V(5)))*(1.0-TAU)
      W=2.5*P0*P0/(102.9+P0)
```

```
      VA=1126.*(5.*P0/102.9)/(1.+6.*P0/102.9)**.5
      RETURN
      ENTRY PRESS(OVERP,T)
      IF(T.LT.0.) GO TO 10
    9 TAU=T/TC
      E=EXP(-TAU)
      OVERP=P0*(V(1)*(E**V(3))+V(2)*(E**V(4))+V(7)*(E**V(5)))*(1.0-TAU)
      RETURN
   10 OVERP=0.0
      RETURN
   16 WRITE(6,12)
   12 FORMAT(49HOPEAK OVERPRESSURE NOT WITHIN LIMITS OF EQUATIONS)
      RETURN
      ENTRY PRESSD(DT,T,XD)
      IF(T.LT.0.) GO TO 18
      TDTC=T/(1.1+.04*P0)*TC)
      DT=(0/VA**2)*(VA*(1.-TDTC)*EXP(-TDTC)-XD)*ABS(VA*(1.-TDTC)*EXP(-TD
     1 )-XD)
      RETURN
   18 DT=0.
      RETURN
      END



      SUBROUTINE IMPACT(I)
      COMMON/BLK1/ X1,Y1,X2,Y2,X3,Y3,X4,Y4
      COMMON/BLK2/ XD1,YD1,XD2,YD2,XD3,YD3,XD4,YD4,XD,YD
      COMMON/BLK7/ SURV
      DATA HH,FM/1.0,2.75/
      GO TO (10,20,30,40,50,60,70,80),I
   10 IF((X4-X1).GT.HH) GO TO 11
      VWB=(XD4+XD)/2.
      PM=WBHIT(VWB)
      WRITE(6,12) VWB,PM
      GO TO 100
   11 PM=HHIT(XD4)
      WRITE(6,13) XD4,PM
      GO TO 100
   20 IF((X3-X2).GT.HH) GO TO 21
      VWB=(XD3+XD)/2.
      PM=WBHIT(VWB)
      WRITE(6,12) VWB,PM
      GO TO 100
   21 PM=HHIT(XD3)
      WRITE(6,13) XD3,PM
      GO TO 100
   30 IF((Y1-Y4).GT.HH) GO TO 31
      VWB=(YD4+YD)/2.
      PM=WBHIT(VWB)
      WRITE(6,12) VWB,PM
      GO TO 100
```

```
   31 PM=WHIT(YD4)
      WRITE(6,13) YD4,PM
      GO TO 100
   40 IF((Y2-Y3).GT.HH) GO TO 41
      VWB=(YD3+YD)/2.
      PM=WBHIT(VWB)
      WRITE(6,12) VWB,PM
      GO TO 100
   41 PM=WHIT(YD3)
      WRITE(6,13) YD3,PM
      GO TO 100
   50 VWB=(XD1+XD)/2.
      IF(ABS(Y3-Y2).LT.FH) VWB=VWB/2.
      PM=WBHIT(VWB)
      WRITE(6,12) VWB,PM
      GO TO 100
   60 VWB=(XD2+XD)/2.
      IF(ABS(Y1-Y4).LT.FH) VWB=VWB/2.
      PM=WBHIT(VWB)
      WRITE(6,12) VWB,PM
      GO TO 100
   70 VWB=(YD1+YD)/2.
      IF(ABS(X1-X4).LT.FH) VWB=VWB/2.
      PM=WBHIT(VWB)
      WRITE(6,12) VWB,PM
      GO TO 100
   80 VWB=(YD2+YD)/2.
      IF(ABS(X3-X2).LT.FH) VWB=VWB/2.
      PM=WBHIT(VWB)
      WRITE(6,12) VWB,PM
  100 SURV=SURV-PM*SURV
   12 FORMAT(/' WHOLE BODY IMPACT VELOCITY=',E10.3/
     1       '   PROBABILITY OF MORTALITY=',F6.3//)
   13 FORMAT(/' HEAD IMPACT VELOCITY=',E10.3/
     1       ' PROBABILITY OF MORTALITY=',F6.3//)
      RETURN
      END
```

```
      FUNCTION WBHIT(VV)
      V=ABS(VV)
      IF(V-21.) 1,3,3
    1 WBHIT=0.
      RETURN
    3 IF(V-138.) 2,4,4
    4 WBHIT=1.0
      RETURN
    2 PROBIT=-5.155+2.541*ALOG(V)
      XX=5.-PROBIT
      X=ABS(XX)
      KK=1
      SUMT=1.
      SUMT2=1.
      FCTR=1.
      DO 50 K=2,30,2
      FCTR=-FCTR*K/2.
      SUMT=SUMT+X**K/(2.**(K/2)*FCTR*(K+1))
      IF(ABS(SUMT-SUMT2).LE..001) GO TO 55
   50 SUMT2=SUMT
   55 IF(XX.LT.0.)  KK=-1
      WBHIT=.5-KK*SUMT*X*.398942
      RETURN
      END
```

```
      FUNCTION HHIT(VV)
      V=ABS(VV)
      IF(V.LE.10.) GO TO 31
      IF(V.LE.13.) GO TO 32
      IF(V.LE.18.) GO TO 33
      IF(V.LE.23.) GO TO 34
      HHIT=1.
      RETURN
   31 HHIT=0.
      RETURN
   32 HHIT=0.03333*V-0.33333
      RETURN
    3 HHIT=0.08*V-0.94
      RETURN
   34 HHIT=0.098*V-1.264
      RETURN
      END
```

A.7.5 Articulated Man Routine - Flow Diagram for Main Program and Forrran Listing

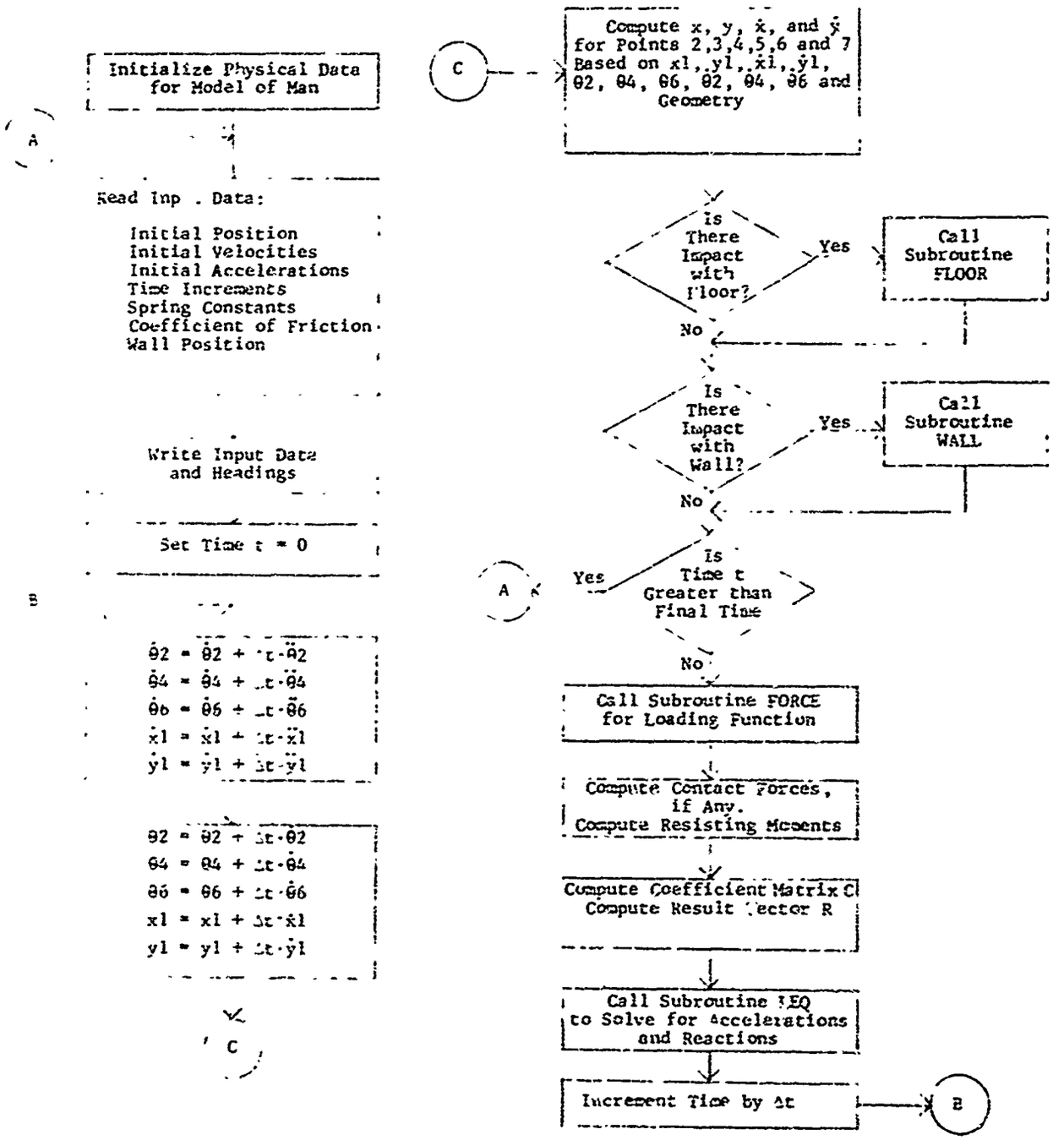

```
      DIMENSION X(7),Y(7),XD(7),YD(7),XDD(7),YDD(7)
      DIMENSION TH(6),THD(6),THDD(6)
      DIMENSION FH(7),FHI(7),FHW(7)
      DIMENSION FV(7),FVI(7),FVF(7)
      DIMENSION F(7),W(7),SI(6),CO(6)
      DIMENSION C(19,19),B(19,1)
      DIMENSION L(7),LL(7)
      COMMON/BLK1/ X,XD,Y,YD,T
      COMMON/BLK3/LL,TH
      INTEGER W,F
      REAL L,LL,M3,M5,I2,I4,I6,KL,KU,MU
      DATA W2,W4,W6,I2,I4,I6/56,92,96,69,11,39,1,67,1,14,0.03/
      DATA LL/0.,1.83,3.01,0.99,2.01,0.37,0.75/
      G=32.2
    1 READ(5,2,END=900) IRUN
    2 FORMAT(I2)
      READ(5,10)(TH(I),I=2,6,2),X(1),Y(1),TF,DT,DTO
   10 FORMAT(8F10.0)
      READ(5,10) XD(1),YD(1),XDD(1),YDD(1)
      READ(5,9) KL,KU,MU
    9 FORMAT(3F10.0)
      READ(5,11)(F(J),J=1,7,2)
   11 FORMAT(4I1)
      READ(5,3) XW
    3 FORMAT(F10.0)
      WRITE(6,17) IRUN
   17 FORMAT('1',' RUN NUMBER:',I2//)
      WRITE(6,15) X(1),KL,Y(1),KU,XW,MU,TH(2),TF,TH(4),DT,TH(6),DTO
   15 FORMAT(' X1    (FT)',F9.2,6X'KL (LB/FT)',E10.4/
     1       ' Y1    (FT)',F9.2,6X'KU (LB/FT)',E10.4/
     2       ' XW    (FT)',F9.2,6X'MU         ',E10.4/
     3       ' TH2 (RAD)',E9.3,6X'TF   (SEC)',F7.4/
     4       ' TH4 (RAD)',E9.3,6X'DT   (SEC)',F7.4/
     5       ' TH6 (RAD)',E9.3,6X'DTO  (SEC)',F7.4///)
      DO 12 J=2,6,2
      THD(J)=0.
   12 THDD(J)=0.
      WRITE(6,13)
   13 FORMAT(19X'X1'7X'X3'7X'X5'7X'X7'6X'XD1'6X'XD3'6X'XD5'6X'XD7'
     1 6X'TH2'6X'TH4'6X'TH6'/19X'Y1'7X'Y3'7X'Y5'7X'Y7'6X'YD1'6X'YD3'
     2 6X'YD5'6X'YD7'5X'THD2'5X'THD4'5X'THD6'//)
      L(2)=LL(2)
      L(3)=LL(3)-LL(2)
      L(4)=LL(4)
      L(5)=LL(5)-LL(4)
      L(6)=LL(6)
      L(7)=LL(7)-LL(6)
      T0=0.
      T=0.
   50 DO 51 J=2,6,2
      THD(J)=THD(J)+DT*THDD(J)
      TH(J)=TH(J)+DT*THD(J)
      SI(J)=SIN(TH(J))
```

```
      SI(J+1)=SI(J)
      CO(J)=COS(TH(J))
   51 CO(J+1)=CO(J)
      XD(1)=XD(1)+DT*XDD(1)
      YD(1)=YD(1)+DT*YDD(1)
      X(1)=X(1)+DT*XD(1)
      Y(1)=Y(1)+DT*YD(1)
      DO 52 I=2,7
      X(I)=X(I-1)+L(I)*SI(I)
      Y(I)=Y(I-1)+L(I)*CO(I)
      XD(I)=XD(I-1)+L(I)*THD(I)*CO(I)
   52 YD(I)=YD(I-1)-L(I)*THD(I)*SI(I)
      IF(T.LT.TO) GO TO 53
      WRITE(6,200) T,(X(I),I=1,7,2),(XD(I),I=1,7,2),(TH(I),I=2,6,2)
      WRITE(6,201)(Y(I),I=1,7,2),(YD(I),I=1,7,2),(THD(I),I=2,6,2)
  200 FORMAT(F12.4,4X,11E9.4)
  201 FORMAT(16X,11E9.4/)
      TO=TO+DTO
   53 DO 30 J=1,7,2
      IF((F(J).EQ.1).AND.(Y(J).LT.0.)) GO TO 30
      IF(F(J).EQ.1) GO TO 35
      IF(Y(J).GE.0.) GO TO 30
      CALL FLOOR(J)
      F(J)=1
      GO TO 30
   35 F(J)=0
   30 CONTINUE
      DO 40 J=1,7,2
      IF((W(J).EQ.1).AND.(X(J).GT.XW)) GO TO 40
      IF(W(J).EQ.1) GO TO 45
      IF(X(J).LE.XW) GO TO 40
      CALL WALL(J)
      W(J)=1
      GO TO 40
   45 W(J)=0
   40 CONTINUE
      IF(Y(7).LT.0.) GO TO 1
      IF(T.GT.TF) GO TO 1
      CALL FORCE(FHI,FVI,M3,M5)
      IF((M5.GT.999.).OR.(M5.GT.999.)) GO TO 1
      DO 70 J=1,7,2
      IF(Y(J).GE.0.) FVF(J)=0.
      IF((Y(J).LT.0.).AND.(YD(J).LT.0.)) FVF(J)=-KL*Y(J)
      IF((Y(J).LT.0.).AND.(YD(J).GT.0.)) FVF(J)=-KU*Y(J)
      IF(X(J).LE.XW. FHW(J)=0.
      IF((X(J).GT.XW).AND.(XD(J).GT.0.))FHW(J)=-KL*(X(J)-XW)
      IF((X(J).GT.XW).AND.(XD(J).LT.0.))FHW(J)=-KU*(X(J)-XW)
      FH(J)=FHI(J)+FHW(J)-MU*FVF(J)*XD(J)/ABS(XD(J))
   70 FV(J)=FVI(J)+FVF(J)-MU*FHW(J)*YD(J)/ABS(YD(J))
      DO 22 I=1,19
      DO 22 J=1,19
   22 C(I,J)=0.
      C(4,1)=-1.0
      C(6,1)=-1.0
      C(5,2)=-1.0
```

```
C(7,2)=-1.0
C(1,3)=W2/G
C(4,3)=1.0
C(2,4)=C(1,3)
C(5,4)=1.0
C(6,5)=1.0
C(11,5)=-1.0
C(13,5)=-1.0
C(7,6)=1.0
C(12,6)=-1.0
C(14,6)=-1.0
C(8,7)=W4/G
C(11,7)=1.0
C(9,8)=C(8,7)
C(12,8)=1.0
C(13,9)=1.0
C(15,9)=-1.0
C(14,10)=1.0
C(19,10)=-1.0
C(15,11)=W6/G
C(18,11)=1.0
C(16,12)=C(15,11)
C(19,12)=1.0
C(3,13)=I2
C(10,14)=I4
C(17,15)=I6
C(1,16)=-1.0
C(8,16)=1.0
C(2,17)=-1.0
C(9,17)=1.0
C(8,18)=-1.0
C(15,18)=1.0
C(9,19)=-1.0
C(16,19)=1.0
C(4,13)=-LL(2)*CO(2)
C(5,13)=LL(2)*SI(2)
C(6,13)=-LL(3)*CO(2)
C(7,13)=LL(3)*SI(2)
C(11,14)=-LL(4)*CO(4)
C(12,14)=LL(4)*SI(4)
C(13,14)=-LL(5)*CO(4)
C(14,14)=LL(5)*SI(4)
C(18,15)=-LL(6)*CO(6)
C(19,15)=LL(6)*SI(6)
C(3,16)=(LL(2)-LL(3))*CO(2)
C(10,16)=C(11,14)
C(3,17)=(LL(3)-LL(2))*SI(2)
C(10,17)=C(12,14)
C(18,18)=(LL(4)-LL(5))*CO(4)
C(17,18)=C(18,15)
C(10,19)=(LL(5)-LL(6))*SI(4)
C(17,19)=C(19,15)
B(1,1)=FH(1)+FH(3)
B(2,1)=FV(1)+FV(3)-W2
B(3,1)=FV(1)*LL(2)*SI(2)-FH(1)*LL(2)*CO(2)+FH(3)*(LL(3)-LL(2))*
```

```
     1CO(2)-FV(3)*(LL(3)-LL(2))*SI(2)+M3
      B(4,1)=-LL(2)*THD(2)**2*SI(2)
      B(5,1)=-LL(2)*THD(2)**2*CO(2)
      B(6,1)=-LL(3)*THD(2)**2*SI(2)
      B(7,1)=-LL(3)*THD(2)**2*CO(2)
      B(8,1)=FH(5)
      B(9,1)=FV(5)-W4
      B(10,1)=FH(5)*(LL(5)-LL(4))*CO(4)-FV(5)*(LL(5)-LL(4))*SI(4)+M5-M3
      B(11,1)=-LL(4)*THD(4)**2*SI(4)
      B(12,1)=-LL(4)*THD(4)**2*CO(4)
      B(13,1)=-LL(5)*THD(4)**2*SI(4)
      B(14,1)=-LL(5)*THD(4)**2*CO(4)
      B(15,1)=FH(7)
      B(16,1)=FV(7)-W6
      B(17,1)=FH(7)*(LL(7)-LL(6))*CO(6)-FV(7)*(LL(7)-LL(6))*SI(6)-M5
      B(18,1)=-LL(6)*THD(6)**2*SI(6)
      B(19,1)=LL(6)*THD(6)**2*CO(6)
      CALL LEQ(C,5,19,1,19,19,DET,KDET)
      XDD(1)=B(1,1)
      YDD(1)=B(2,1)
      XDD(2)=B(3,1)
      YDD(2)=B(4,1)
      XDD(3)=B(5,1)
      YDD(3)=B(6,1)
      XDD(4)=B(7,1)
      YDD(4)=B(8,1)
      XDD(5)=B(9,1)
      YDD(5)=B(10,1)
      XDD(6)=B(11,1)
      YDD(6)=B(12,1)
      THDD(2)=B(13,1)
      THDD(4)=B(14,1)
      THDD(6)=B(15,1)
      W3=B(16,1)
      V3=B(17,1)
      W5=B(18,1)
      V5=B(19,1)
      T=T+DT
      GO TO 50
  910 STOP
      END
```

```
      SUBROUTINE WALL(J)
      COMMON/BLK1/ X,XD,Y,YD,T
      DIMENSION X(7),XD(7),Y(7),YD(7)
      WRITE(6,10) J,T,X(J),Y(J),XD(J),YD(J)
   10 FORMAT(/' ******  POINT',I2,' IMPACT ON WALL AT T=',F7.4,
     1'SEC   X=',E9.4,' Y=',E9.4,' ,XD=' E9.4,' ,YD=',E9.4)
      RETURN
      END



      SUBROUTINE FLOOR(J)
      COMMON/BLK1/ X,XD,Y,YD,T
      DIMENSION X(7),XD(7),Y(7),YD(7)
      WRITE(6,10) J,T,X(J),Y(J),XD(J),YD(J)
   10 FORMAT(/' ******  POINT',I2,' IMPACT ON FLOOR AT T=',F7.4,
     1'SEC   X=',E9.4,' Y=',E9.4,' ,XD=',E9.4,' ,YD=',E9.4)
      RETURN
      END



      SUBROUTINE FORCE(FHI,FVI,M3,M5)
      COMMON/BLK3/ LL,TH
      REAL M3,M5,LL
      DIMENSION FHI(7),FVI(7),LL(7),TH(6)
      F=100.
      F2=0.
      F4=LL(5)*COS(TH(4))*F
      F6=LL(7)*COS(TH(6))*F/3.
      FHI(1)=F2/2.
      FHI(3)=FHI(1)+F4/2.
      FHI(7)=F6/2.
      FHI(5)=FHI(7)+F4/2.
      DO 10 J=1,7,2
   10 FVI(J)=0.
      THN=ABS(TH(4)-TH(6))
      IF(THN.LT.1.09083) GO TO 30
      IF(THN.LT.1.22173) GO TO 31
      IF(THN.LT.1.309) GO TO 32
      WRITE(6,33)
   33 FORMAT(/' **** NECK BREAKS'//)
      M5=1000.
      RETURN
   30 M5=F.3333
      GO TO 40
   31 M5=127.3236*THN-130.5551
      GO TO 40
   32 M5=668.424*THN-791.633
```

```
40 IF((TH(6)-TH(4)).LT.0.) M5=-M5
   THH=TH(4)-TH(2)
   IF(THH.LT.0.) GO TO 50
   IF(THH.LT..785398) GO TO 51
   IF(THH.LT.1.919862) GO TO 52
   WRITE(6,53)
53 FORMAT(/' **** HIP BREAKS'//)
   M3=1000.
   RETURN
51 M3=58.967*THH
   RETURN
52 M3=42.4413*THH+20.8333
   RETURN
50 THH=ABS(THH)
   IF(THH.LT..837758) GO TO 54
   WRITE(6,53)
   M3=1000.
   RETURN
54 M3=-38.79*THH-150.
   RETURN
   END
```

```
C**********                                                          LEG 0001
C  LEG    *                                                          LEG 0002
C**********                                                          LEG 0003
C                                                                    LEG 0004
   SUBROUTINE LEG(A,B,NEQS,NSOLNS,IA,IB,DET,KDET)                    LEG 0005
C                                                                    LEG 0006
C  SOLVES THE LINEAR SYSTEM 'AX=Y'                                   LEG 0007
C  THERE ARE 'NEQS' EQUATIONS AND 'NSOLNS' SOLUTION VECTORS,         LEG 0008
C  THE DETERMINANT IS RETURNED IN THE FORM 'DET*10.**KDET'           LEG 0010
C                                                                    LEG 0011
   DIMENSION A(IA,1),B(IB,1)                                         LEG 0012
   DATA LOGFAT,FAT,THIN/20.1,E+20,1.E-20/                            LEG 0013
C                                                                    LEG 0014
   NSIZ = NEQS                                                       LEG 0015
   NBSIZ = NSOLNS                                                    LEG 0016
   DET=1.0                                                           LEG 0017
   KDET = 0                                                          LEG 0018
   DO 1 I=1,NSIZ                                                     LEG 0019
   BIG=A(I,1)                                                        LEG 0020
   IF(NSIZ-1)50,50,51                                                LEG 0021
51 DO 2 J=2,NSIZ                                                     LEG 0022
   IF(ABS(BIG)-ABS(A(I,J))) 3,2,2                                    LEG 0023
 3 BIG=A(I,J)                                                        LEG 0024
 2 CONTINUE                                                          LEG 0025
   DO 4 J=1,NSIZ                                                     LEG 0026
 4 A(I,J)=A(I,J)/BIG                                                 LEG 0027
   DO 41 J=1,NBSIZ                                                   LEG 0028
41 B(I,J)=B(I,J)/BIG                                                 LEG 0029
   DET=DET*BIG                                                       LEG 0030
42 IF(ABS(DET).LT.FAT) GO TO 60                                      LEG 0031
   DET = DET*THIN                                                    LEG 0032
```

```
      KDET = KDET+LOGFAT                                                LE. 0033
      GO TO 1                                                           LE. 0034
   60 IF(ABS(DET).GT.THIN) GO TO 1                                      LE. 0035
      DET = DET*FAT                                                     LE. 0036
      KDET = KDET-LOGFAT                                                LE. 0037
    1 CONTINUE                                                          LE. 0038
      NUMSYS=NSIZ-1                                                     LE. 0039
      DO 14 I=1,NUMSYS                                                  LE. 0040
      NN=I+1                                                            LE. 0041
      BIG=A(I,I)                                                        LE. 0042
      NBGRW=I                                                           LE. 0043
      DO 5 J=NN,NSIZ                                                    LE. 0044
      IF(ABS(BIG)-ABS(A(J,I))) 6,5,5                                    LE. 0045
    6 BIG=A(J,I)                                                        LE. 0046
      NBGRW=J                                                           LE. 0047
    5 CONTINUE                                                          LE. 0048
      IF(NBGRW-I) 7,10,7                                                LE. 0049
    7 DO 8 J=1,NSIZ                                                     LE. 0050
      TEMP=A(NBGRW,J)                                                   LE. 0051
      A(NBGRW,J)=A(I,J)                                                 LE. 0052
    8 A(I,J)=TEMP                                                       LE. 0053
      DET=-DET                                                          LE. 0054
      DO 9 J=1,NBSIZ                                                    LE. 0055
      TEMP=B(NBGRW,J)                                                   LE. 0056
      B(NBGRW,J)=B(I,J)                                                 LE. 0057
    9 B(I,J)=TEMP                                                       LE. 0058
   10 DO 13 K=NN,NSIZ                                                   LE. 0059
      PMULT=-A(K,I)/A(I,I)                                              LE. 0060
      DO 11 J=NN,NSIZ                                                   LE. 0061
   11 A(K,J)=PMULT*A(I,J)+A(K,J)                                        LE. 0062
      DO 12 L=1,NBSIZ                                                   LE. 0063
      B(K,L)=PMULT*B(I,L)+B(K,L)                                        LE. 0064
   12 CONTINUE                                                          LE. 0065
   14 CONTINUE                                                          LE. 0066
      DO 15 NCOLB=1,NBSIZ                                               LE. 0067
      DO 19 I=1,NSIZ                                                    LE. 0068
      NROW=NSIZ+1-I                                                     LE. 0069
      TEMP=0.0                                                          LE. 0070
      NXS=NSIZ-NROW                                                     LE. 0071
      IF(NXS) 18,17,16                                                  LE. 0072
   16 DO 18 K=1,NXS                                                     LE. 0073
      KK=NSIZ+1-K                                                       LE. 0074
   18 TEMP=TEMP+B(KK,NCOLB)*A(NROW,KK)                                  LE. 0075
   17 B(NROW,NCOLB)=(B(NROW,NCOLB)-TEMP)/A(NROW,NROW)                   LE. 0076
   19 CONTINUE                                                          LE. 0077
   15 CONTINUE                                                          LE. 0078
      DO 20 I=1,NSIZ                                                    LE. 0079
      DET=DET*A(I,I)                                                    LE. 0080
      IF(ABS(DET).LT.FAT) GO TO 61                                      LE. 0081
      DET = DET*THIN                                                    LE. 0082
      KDET = KDET+LOGFAT                                                LE. 0083
      GO TO 20                                                          LE. 0084
   61 IF(DET.GT.THIN) GO TO 20                                          LE. 0085
      DET = DET*FAT                                                     LE. 0086
      KDET = KDET-LOGFAT                                                LE. 0087
   20 CONTINUE                                                          LE. 0088
      RETURN                                                            LE. 0089
      END                                                               LE. 0090
```

REFERENCES

1. Newmark, N. M. and Haltiwanger, J. D., Principles and Practices for Design of Hardened Structures, Air Force Design Manual, Air Force Special Weapons Center, Kirtland AFB, New Mexico, Report SWC-TDR 62-138, December 1962.

2. Building Code Requirements for Reinforced Concrete, American Concrete Insd itute, ACI 318-72, Detroit, 1972.

3. Chicago Building Code, 1972

4. Manual of Steel Construction, 7th Edition, American Institute of Steel Construction, New York, 1971.

5. The Effects of Nuclear Weapons, Atomic Energy Commission, 1962.

6. Murphy, H. L., Feasibility Study of Slanting for Combined Nuclear Weapons Effects, Vol. I and II, Stanford Research Institute, October 1970.

7. Civil Defense Shelter Options: Deliberate Shelters, Vol. I and II, IITRI, December 1971.

8. White, C. S., The Nature of Problems Involved in Estimating the Immediate Casualties from Nuclear Explosions, CEX 71.1, Lovelace Foundation, July 1971.

9. White, C. S., et al, The Biodynamics of Airblast, Lovelace Foundation

10. Slowik, J., Power Driven Articulated Dummy, IITRI Project K6051, December 1965.

11. A Three-Dimensional Computer Simulation of a Motor Vehicle Crash Victim, Cornell Aeronautical Laboratory, July 1971.

12. Experimental Observation of Interior Pressures in Hollow Models - Blast Effects on Buildings and Structures Operation of Six Foot and Two Foot Shock Tubes, Final Test Report 5, Armour Research Foundation, D-087, March 1956.

13. Experimental Observations of Interior Pressures in Hollow Models (Part II) - Blast Effects on Buildings and Structures Operation of the Six Foot and Two Foot Shock Tubes, Final Test Report 7, Armour Research Foundation D-087, July 1956.

APPENDIX B

BLAST LOADING OF BUILDING OCCUPANTS

B.1 INTRODUCTION

When a weapon of known yield is detonated at a known distance from a building, the overpressure at the location of the building is known. For buildings located in the Mach region the distance from the burst will be large compared to the building dimensions, so that the radius of curvature of the shock front can be ignored, and the load on the building analyzed as though produced by a plane shock.

The incident shock is capable of penetrating deep into the interior of the building, since walls with openings are quite "transparent" to shock waves; for example, a 25 percent opening in a wall will transmit about 81 percent of the incident overpressure at the range of 14.7 psi. Following the penetrating shock waves is a jet flow pattern which seeks to equalize pressures on the exterior and interior. Pressure differences across walls may cause wall destruction, and the intense flow through openings may produce interior wind speeds high enough to propel occupants into obstacles, causing injury or fatality. The latter possibility arises because the interior wind persists long after the pressures have nearly equalized, thereby allowing time enough for the impulse imparted to the occupants to reach dangerous levels, if the wind speed is high enough.

The aim here, is to estimate these aerodynamic loads on the building and its occupants, taking into account the coupling between the flow and the changes in geometry caused by failing walls. This is attempted in the following sections, in which the simplest physically meaningful model with these features is presented. We begin by simplifying the building geometry in Section B.2, then discuss the assumed failure mode of the walls in Section B.3. After presenting the free field blast wave (Section B.4) and its interaction with the building exterior (Section B.5), we analyze the

shock penetration by a one-dimensional model (Section B.6) and the jet flow (Section B.7), which governs the filling phase. The governing parameters of the problem through the filling phase are collected and discussed in Section B.8, while Section B.9 discusses the steady state flow through the building.

The initial part of this effort was concerned with a detailed examination of 16 NFSS buildings described in Ref. 3. Their structural and geometric characteristics were examined in order to produce a realistic model for this category of buildings.

B.2 BUILDING GEOMETRY

For this effort, we consider only the case of an isolated building, neglecting the partial protection given by neighboring structures. Also, the shock is assumed incident in the plane of the building face, so that no horizontal crossflow is to be expected in the interior, except in the direction of shock motion; this also minimizes diffraction calculations on the exterior. Thus, the building is taken to be a two-dimensional array of chambers (rooms), with flow occurring only along a front-to-rear axis, the floors being uncoupled by crossflow.

The building is described mathematically (see Fig. B.1) by specifying its overall dimensions (BH,BW,BL), number of stories (NS), number of bays deep (NB), and number of bays wide (NW). A particular chamber is defined by giving its story index (j); its bay index (i) matches that of its rear wall, with walls being numbers 1, 2,... NB+1 from front to rear. Thus chambers 1 and NB+1 are the front and rear exteriors of the building respectively. Each chamber has values of length, width, height (RL_{ij},W_{ij},H_{ij}) specified, and each wall has the fraction of orifice (window) area/wall area (A_{ij}) specified.

Note that windows are not characterized by their positions in the wall, nor by their proportions -- only their area; this is done because it is judged that the dominant factor in determining wind speeds and durations is the ability of the pressure differences across any orifice to bodily transport the fluid through the opening, and thus geometric details of the flow are unimportant.

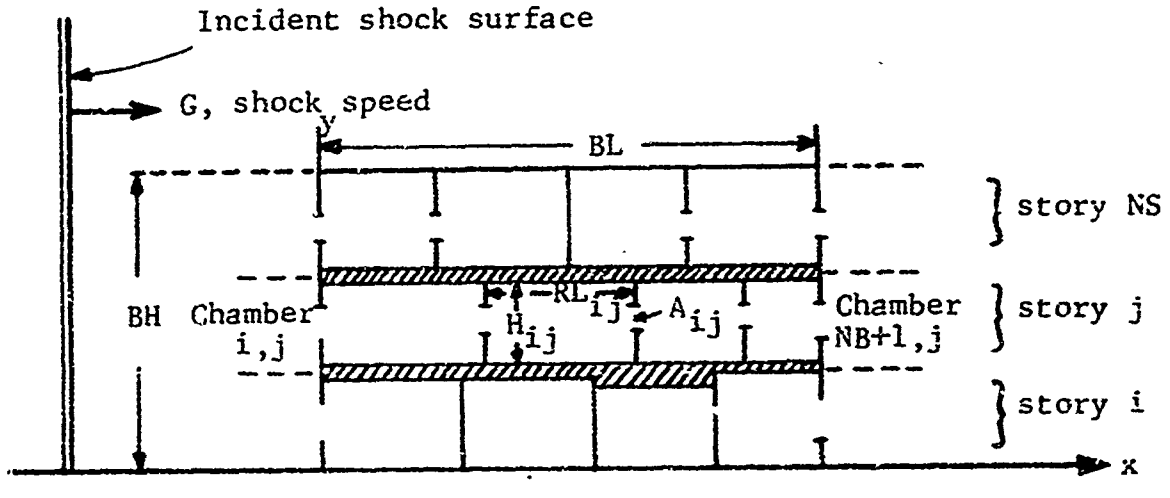

Fig. B.1 Nomenclature of Building Model (array repeats in plane normal to paper)

By prescribing the dimensions of each room separately, the model has great flexibility for describing the effects of area changes in the flow direction due to building frames, elevator shafts, etc. This feature also allows for the important effects on timing of wall failures due to the different rates of change of pressure in the room interiors, as discussed in Section B.7.

B.3 CONSIDERATION OF WALL FAILURE

The primary emphasis of this analysis is to develop a blast loading routine for studying the translation and impact of people located in upper stories of conventional buildings. The routine therefore applies to any building up to the overpressure level which produces total collapse. The class of buildings to which this routine is specifically applicable includes multistory framed construction in which the walls (interior and exterior) are primarily nonstructural and can therefore fail without producing building collapse. Because of the two-dimensional geometry assumed, pressure loads will advance along the same front throughout the lateral (width) dimension of the building, and fore-and-aft walls will see little or no pressure difference. So long as floors are not vastly different in distribution of interior partitions, the same statement can be made for pressure differences across floor slabs -- the pressure differences which do appear because of different retardation of the penetrating shock waves will be of very short duration, since the arrival times cannot be greatly different at a given station (x-coordinate) owing to the transparency of orifices to shock penetration. Thus, for any given room, we consider failure of only the end walls. Also, glass is ignored, and any glass panel is assumed to vanish upon arrival of the shock wave.

Our basic configuration of a failing wall is then a rectangular panel set at right angles to the flow direction, loaded by some pressure difference across it. The general case is simplified as follows:

(a) The pressure difference applied is considered uniform over the area of the wall; that is, the pressure relief around any opening in the wall is ignored.

(b) The wall is assumed to stand if the pressure difference is less than a known value, p_c (collapse overpressure).

(c) The wall is assumed to stand if the pressure difference, no matter how large, is not applied for a known minimum time, Δt_c (time to maximum response).

(d) When the wall fails, it does so in two steps; first, cracks appear instantaneously, removing some percentage of the effective wall area; second, the fractured wall segments fall to the floor under the action of gravity alone, removing the remaining effective flow-blocking area.

Thus, wall failure is characterized here by four parameters: p_c, Δt_c, A_d, and t_H, where A_d is the percentage effective area reduction at crack appearance, and t_H is the time required for the debris to fall to the floor.

This model is similar in spirit to that presented by Zaker (Ref. 1), in that it requires some total failure impulse, and takes into account the inertial resistance of the wall by requiring that the pulse duration exceed Δt_c. Zaker's T' corresponds directly to Δt_c, while his q_{av} corresponds to, but does not equal, p_c, unless it is desired to underestimate wall resistance in the interest of producing conservative results. Typical values of these, for a 10 ft by 16 ft nonload bearing cinderblock wall without orifices, are given by Sevin (Ref. 2);

q_{av} = 1.3 psi
T' = 61 msec

Since the static load-deflection curve for the wall requires 3 psi to achieve a deflection greater than 1 in., a more realistic value of p_c would lie between these two values, say at 2 psi. Since T' is the time duration of q_{av} required to produce the failure impulse, it should be shortened in proportion; that is, using Zaker's results requires:

$$p_c \Delta t_c = T' \, q_{av} = \text{failure impulse/unit area} \qquad \text{(B.1)}$$

Overall, this procedure should provide a slightly conservative result (because the wall may be counted as failed even if the pressure never reaches the maximum value of the static load-deflection curve), but should give correct order-of-magnitude values to the parameters in a very simple manner. This simplicity is a strong motive here, since each wall must be tested on each integration step of the interior pressure-time history calculation.

In summary, failure of the wall with index ij is assumed whenever

$$\left|p_{ij}(t) - p_{i-1,j}(t)\right| \geq p_c \text{ for a total time } \Delta t \geq \Delta t_c \qquad (B.2)$$

As the program is written, this Δt may be accumulated -- it need not be a continuous interval, but may be several intervals of time whose total length exceeds Δt_c. It is not anticipated that this difference will be significant, since the pressure variation in time tends to be monotonic, so that it is unlikely that the rise-fall-rise p(t) required to fail a wall in this mode will ever occur. The condition (Eq.(B.2)) is illustrated in Fig. B.2.

After the failure impulse has been delivered to the wall, failure is modeled by removing area from the wall as described in item (d) of the general case giving

$$A_e = A_{ij} + \left\{A_d + (1-A_{ij}-A_d)\ \tfrac{1}{2}\, g\, (t-\Delta t_{cij}-t_{oij})^2/H_{ij}\right\} 1(t^*) \qquad (B.3)$$

where A_e is the effective area of the orifice in wall ij at time t, $1(t^*)$ is the Heaviside step function, and $t^* = t - t_{oij} - \Delta t_{cij}$, with t_{oij} = time when pressure difference first exceeded p_c. This is illustrated in Fig. B.3.

B.4 FREE FIELD BLAST WAVE

Since we do not anticipate use of this analysis at overpressures much in excess of 30 psi, we employ Brode's shock model (Ref. 4) for the free field blast conditions. As noted at the end of this section, this same model can be used to fit the free field curves of Ref. 5.

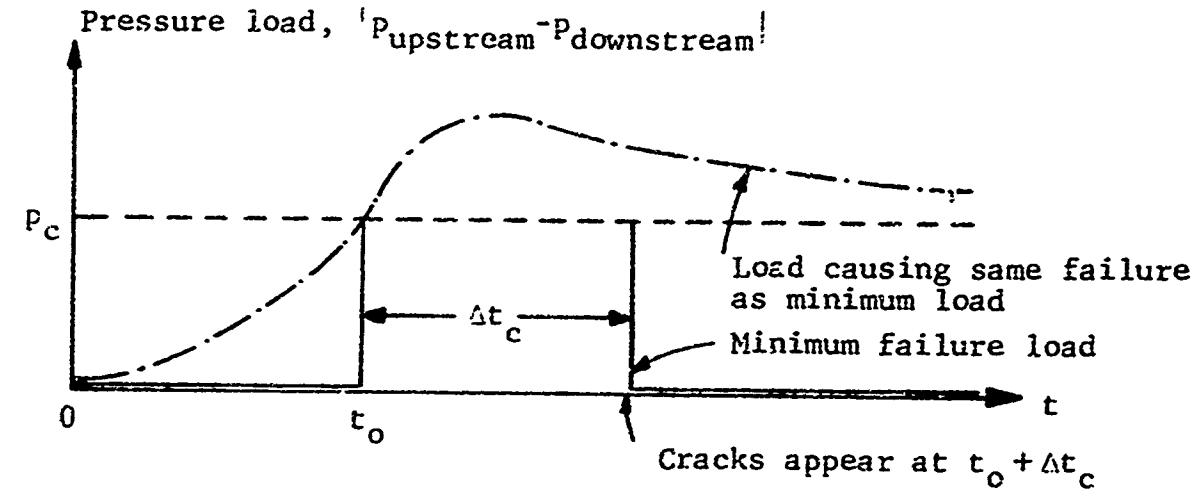

Fig. B.2 Failure Criterion

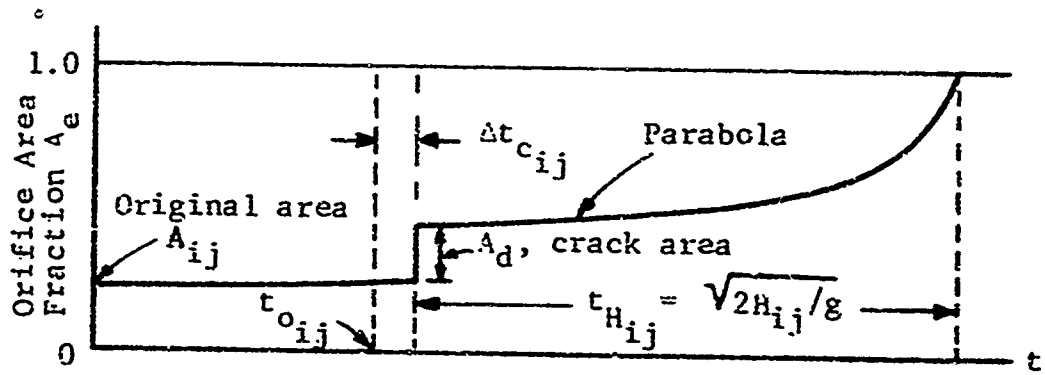

Fig. B.3 Failure Mode

Since we later use dimensionless variables for the jet flow calculation, Brode's equations are slightly rearranged here to make them dimensionless

$$p = p^+/p_1 \qquad \rho = \rho^+/\rho_1 \qquad T = T^+/T_1 \qquad q = q^+/a_1$$

where x^+ is the physical variable, and x_1 its value at ambient conditions; a_1 is ambient acoustic velocity; p, ρ, T, q are, respectively, absolute pressure, mass density, absolute temperature, and the flow speed of the air. In this notation, the static (side-on) pressure of the free field is given by

$$p(t) = 1 + (144\ OP/p_1)(1-\tau)(ae^{-\alpha\tau} + be^{-\beta\tau}) \tag{B.4}$$

where OP is the overpressure with $\tau = t/D_p^+$; time (t) being started at blast arrival, D_p^+ being the duration of the positive overpressure phase. The values given for the various coefficients in Eq. (B.4) may be written in approximate analytical forms when $0 \leq OP \leq 30$ psi.

$$\begin{aligned} D_p^+ &= 0.2555\ (OP)^{0.3455} \\ b &= 1-a = 0.08\ (OP)^{1/3} \\ \alpha &= -0.00268(OP)^2 + 0.1075(OP) - 0.0036 \\ \beta &= 2.24(OP)^{0.425} \end{aligned} \tag{B.5}$$

The same form may be given to the dynamic pressure of the wind in the free field

$$p_d(t) = Q_s(1-\omega)^2(0.88e^{-\delta\omega} + 0.12e^{-\phi\omega}) \tag{B.6}$$

where Q_s is the dynamic pressure just behind the shock, and may be obtained from the Rankine-Hugoniot relations as

$$Q_s = XOP/(2\gamma + (\gamma-1)XOP) \tag{B.7a}$$

with $XOP = OP/(p_1/144)$ and γ = adiabatic index of air = 1.40;

$$\omega = \tau\, T_{ratio};\ T_{ratio} = D_p^+/D_a^+ = 0.82(OP)^{0.212} \tag{B.7b}$$

$$\delta = 0.357\ (OP)^{0.80} \qquad \phi = 5.33\ (OP)^{0.587}$$

Since an air particle undergoes no entropy change after passing through the free field shock, we may write for its equation of state in the subsequent motion

$$(p/p_1) = (\rho/\rho_1)^{\gamma} \exp\left(\frac{s_2-s_1}{c_v}\right) \tag{B.8}$$

where s_2 is the specific entropy behind the shock

$$\exp \frac{s_2-s_1}{c_v} = (1+XOP)/(\rho_2/\rho_1)$$

with

$$\rho_2 = 1 + 1/\left[\gamma/XOP + (\gamma-1)/2\right]$$

from the Rankine-Hugoniot relations. Now Eq. (B.8) can be used to evaluate $\rho(t)$ in the free field, and free field velocities may be obtained from $\rho(t)$ and $p_d(t)$

$$q(t) = (q^+/a_1) = \sqrt{2p_1p_d(t)/\rho_1\rho(t)}/a_1 = \sqrt{2p_d(t)/\gamma\rho(t)} \tag{B.9}$$

Equations (B.4), (B.6), (B.8) and (B.9) give all the variables in the free field as a function of time.

It should be noted that Eq. (B.9) ignores the compressibility of the air in the stagnation process, if this dynamic pressure is taken equal to the stagnation pressure which is measured by halting the flow; actually,

$$p^+_{stagnation} = 1/2\ \rho^+q^{+2}\left\{\frac{2}{\gamma M^2}\left[\left(1+\frac{\gamma-1}{2}M^2\right)^{\gamma/\gamma-1}-1\right]\right\}$$

for a steady compressible flow with Mach number M and an isentropic stagnation process. Since the difference between p^+_d and $p^+_{stagnation}$ is only 27 percent even at M=1, and we expect no Mach number, larger than one-half in the overpressure range considered, this distinction has been ignored.

The following is included only to list the precise transformation of the free field Eqs. (B.4) and (B.6) to the form given in Ref. 5. To get

$$p(t) = 1 + \left[XOP\ e^{-t/D^+_p}\right](1-t/D^+_p) \tag{B.10}$$

set parameters equal to:

$$b = 0; \quad a = 1.0; \quad \alpha = 1.0; \quad \beta = 0$$

The same thing may be done with $p_d(t)$ as

$$p_d(t) = Q_s(1-2t/D_p^+)^2 e^{-2t/D_p^+} \tag{B.11}$$

The parameter values which yield this expression are

$$T_{ratio} = 0.50$$
$$Q_s' = Q_s/0.88$$
$$\delta = 1.0$$
$$\phi = 100.$$

B.5 LOADING ON BUILDING; EXTERIOR DIFFRACTION

When a plane shock wave impinges on a solid object, the geometry and strength of the wave is modified by the flow behind the shock, which is in turn determined by the object's shape. If the object is porous, as in our case, this further complicates the problem of estimating the diffracted shock and its associated flow field. Since there is no analytical solution to this diffraction problem, it is necessary to construct a semiempirical analytical model; we do this here by retaining only those details which are judged to be absolutely necessary, and neglecting the remainder.

On the front of the building, the dominant features of the shock interaction will be that a reflected shock is formed with a strength and shape determined by the porosity of the front of the building. As time passes, expansion waves from the edge of the roof will reach this shock and weaken it, until it ultimately disappears. After it has been eroded away, the loading on the remaining walls of the building front will be nearly equal to the

stagnation pressure of the free field flow. This process is then characterized by

(a) the strength of the initial reflected shock, computed in Section B.6.

(b) the time for the reflected shock to be eroded to zero strength, called "diffraction clearing time." This we estimate following Ref. 5, which gives the value

$$t_d = 3(BH - y)/G_{ff} \tag{B.12}$$

where y = position aboveground, and G_{ff} = free field shock speed.

(c) the time variation of the pressure, entropy, and velocity during the diffraction clearing process. We follow the spirit of Ref. 5, but extend the model to include entropy and velocity by postulating linear time variations in each of these variables

$$p(t) = p_r - (p_r - p_{ff})t/t_d \tag{B.13}$$

$$\text{For } 0 \leq t \leq t_d \quad \frac{s-s_1}{c_v} = \frac{s_r-s_1}{c_v} - \left[\frac{s_r-s_1}{c_v} - \frac{s_2-s_1}{c_v}\right]\frac{t}{t_d} \tag{B.14}$$

$$q = q_r - (q_r - q_{ff})t/t_d \tag{B.15}$$

where subscript r refers to initial reflected shock, and ff to free field; s_2 is free field entropy, and s_1 is ambient entropy.

Also, in Eqs. (B.13), (B.14) and (B.15) the free field quantities are evaluated at $t = t_d$ from Eqs. (B.4), (B.8) and (B.9). The resulting diffraction model produces the curves in Fig. B.4. The three Eqs. (B.13), (B.14) and (B.15) are mutually inconsistent in that they do not satisfy the Rankine-Hugoniot relations for a single shock, but they are employed because it is not felt that any finer detail of the time variation is needed, since t_d will be very short ($\leq$ 100 msec) for reasonable buildings (buildings where the nearest free edge is under 50 ft away). This model differs from that of Ref. 5 in having the initial reflected shock of strength significantly less than the fully reflected shock, and also in specifying entropy and flow speed during the diffraction process.

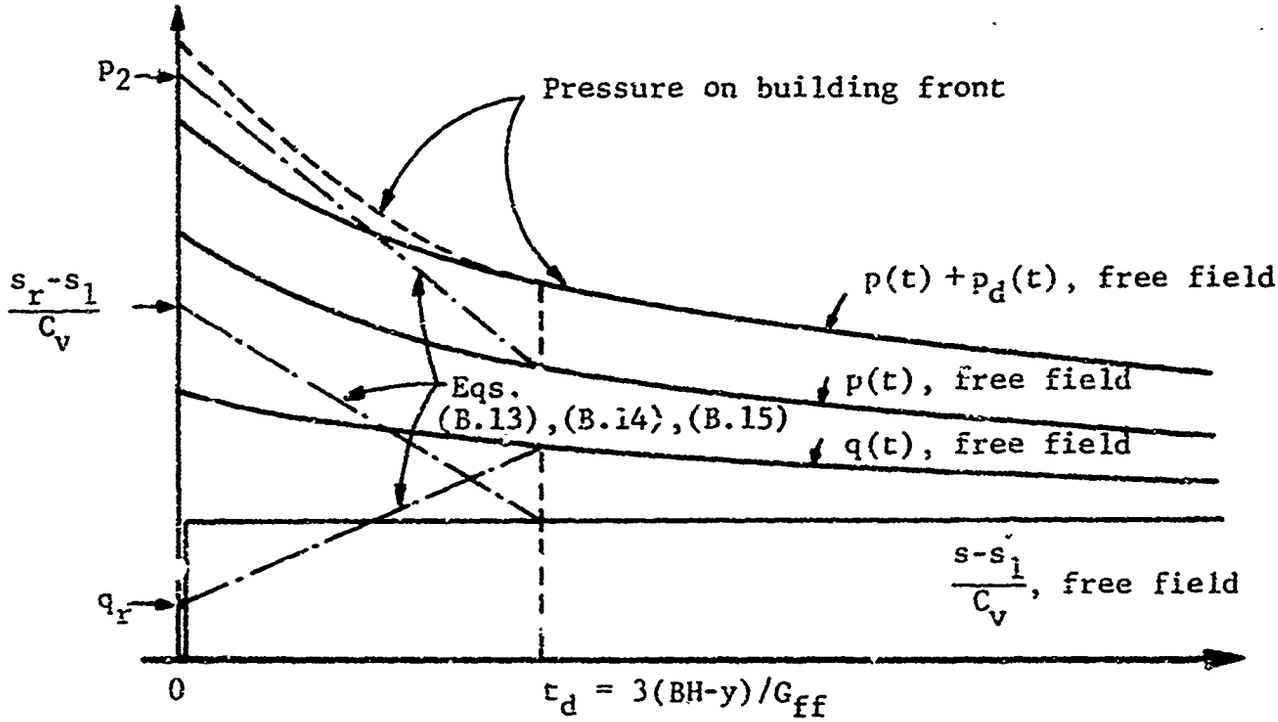

Fig. B.4 Diffraction Model on Building Front at Height y (t_d specified, and initial reflected shock values p_r, s_r, q_r computed by shock penetration analysis in Section B.6)

On the rear of the building, the first disturbance to arrive at any point may be a shock diffracted around the edge of the roof, moving vertically downward. The strength of this shock will be less than free field, since it is interacting with the expansion waves emanating from the roof edge. This shock's side-on pressure can create a shock in the building traveling back-to-front, that is, shock penetration can occur from both back and front of any floor. After some time has passed, this shock's overpressure will rise to the free field level, less a reduction due to the fact that the rear wall is in the wake of the building. The needed features for the rear diffraction model are then:

(a) the time of arrival to the diffracted shock at a height y, which we take to be the time required to traverse the distance over the building and down the back, moving at free field shock speed (thus neglecting the slightly lower speed of the diffracted shock)

$$t_A = BL/G_{ff} + (BH-y)/G_{ff} \tag{B.16}$$

(b) the strength of the diffracted wave, which we have taken to be 25 percent of the free field overpressure (no known data or theoretical estimate of strength of shock undergoing 90 deg diffraction)

$$p_{rear} = 1+0.25(OP)/(p_1/144) \tag{B.17}$$

(c) the diffraction clearing time, for the side-on pressure to reach free field

$$t_{dr} = 6(BH-y)/G_{ff} \tag{B.18}$$

(Reference 5 uses $4(BH-y)/G_{ff}$.)

(d) time variation of p,s,q during diffraction; this is taken to be linear for the first two, and q = 0 since the wake is forming during this period

For $t_A \leq t \leq t_A + t_{dr}$

$$p = p_{rear} + (p_{ff} - p_{rear})(t-t_A)/t_{dr} \tag{B.19}$$

$$\frac{s-s_1}{c_v} = \frac{s_{rear}-s_1}{c_v} + \left[\frac{s_2-s_1}{c_v} - \frac{s_{rear}-s_1}{c_v}\right](t-t_A)/t_{dr} \tag{B.20}$$

$$q = 0 \tag{B.21}$$

After the diffraction process is ended, we wish a realistic model of the wake which takes the porosity of the building into account, that is, which raises the wake pressure as the flow through the building increases. Without this feature, the interior wind speeds cannot be accurately calculated, so the extra complication compared to the simple model of Ref. 5 is necessary to our purpose.

A second complication in computation of the rear loading is the fact that the wave arrives at the top of the rear at time BL/C_{ff}, so that rigorously, the free field pressure, velocity, etc., should be evaluated at $t-BL/C_{ff}$, rather than at the current time t. We do not do that here because of the quasi-steady flow model described in Section B.7, which requires no time lag for consistency, and also because this will usually be a very small effect, less than 5 percent of either pressure or velocity. Thus, after diffraction clearing on the rear, conditions are given by

(e) static pressure variation is:

$$p = p_{ff}(t), \text{ from Eq. (B.4)} \tag{B.22}$$

(f) actual pressure applied on rear walls is lower than static free field pressure because of wake deformation

$$p_{rear}(t) = p_{ff}(t) - p_{wake}(t) \tag{B.23}$$

with the wake pressure reduction being estimated as

$$-p_{wake}(t) = \left[p_{dff}(t) - p_d^*(t)\right] C_d$$

with p_d^* being the dynamic pressure of the outflow from building interior, and c_d = drag coefficient, computed from the mass flow rate ($\dot{M}$) out the rear orifice

$$p_d^*(t) = \frac{\gamma}{2} \rho_{ff}(t) \left[\dot{M}(t)/\rho_{ff}(t)\, A_{ext}\right]^2 \operatorname{sgn}(\dot{M})$$

where the γ factor appears because of the nondimensional variables, and sgn($\dot{M}$) is the sign of $\dot{M}$. This factor is included to reflect the wake pressure reduction due to flow <u>into</u> the building rear. Combining these expressions gives

$$\text{For } t \leq t_A + t_{dr}: \quad p_{rear}(t) = p_{ff}(t) + C_d p_{dff}(t) - \frac{C_d}{2} \gamma \dot{M}|\dot{M}|/(\rho_{ff} A_{ext}^2) \qquad \text{(B.24)}$$

The exterior area, A_{ext}, is computed as the average area of one bay: $A_{ext} = BH \times BW/(NW \times NS)$, and $\dot{M}$ is the result of the interior flow computation of Section B.7.

The rear pressure given by Eq. (B.24) differs from the estimate of Ref. 5 for a solid building ($\dot{M} = 0$) because Ref. 5 estimates $C_d = -0.4$, which we have taken $C_d = -1.0$.

Now it can be seen that the driving force for the flow through the building is the difference in pressure between front and rear, which we have taken to be, after diffraction clearing

$$p_{driving} = p_{front}(t) - p_{rear}(t) = (1 - C_d)\, p_d(t) + C_d\, p_d^*(t)$$

and it is clear that the transience of the wind in the interior is reflected only by the p_d^* term; that is, without this term, the pressures would be fixed on front and rear by the blast profile alone, and it would make no difference to exterior loads whether the building had solid walls or no walls at all, while, in the real case, the pressure relief due to flow through the building can be quite significant. This is reflected by the two extreme cases:

(a) Solid Walls: $p_d^* = 0$, and the back-to-front difference depends only on the blast profile. The drag coefficient of Ref. 5, taken to be -1.0 here, is one way of introducing the influence of geometry on this difference, and should be included in any future work.

(b) No Walls: the building is an open tube, end-on to the shock, so the free field flow should penetrate without distortion. Our model demands that the front

of the tube have stagnation conditions, with

$$p = p_{ff} + p_{dff};\ q = 0$$

and that interior flow consist of steady isentropic expansion; thus, the emerging rear jet with

$$p = p_{ff},\ q = q_{ff}$$

will satisfy both the interior flow equations, and will have

$$p_d^* = \frac{\gamma}{2}\rho_{ff}\left[\frac{\rho_{ff}\sqrt{2p_{dff}/\gamma\rho_{ff}}\,A_{tube}}{\rho_{ff}\,A_{tube}}\right]^2 = p_{dff}$$

so that the wake pressure equal to free field is consistent, and therefore gives the steady flow (asymptotic) solution. This model is therefore unrealistic only in that it overloads the front wall by specifying stagnation pressure on its upstream face; all other pressures and velocities are free field.

The postulated rear loading corresponding to the free field case shown in Fig. B.4 is sketched in Fig. B.5.

B.6 SHOCK PENETRATION

Our aim here is to determine the approximate strength of the shock waves which penetrate into the building interior, given the incident shocks on front and rear described in Section B.5. The exact solution of this problem is exceedingly complex, since a complicated pattern of multiple shock appears at each orifice. We do not require complete details of this early time pattern, which vanishes rapidly; all that is necessary for assessing possible translation of occupants due to aerodynamic loading is a reasonable estimate of the strengths of the dominant shock waves. On this basis, we construct a simple one-dimensional model to estimate the strength of a single wave equivalent to the actual diffraction pattern of waves, and cite the detailed experimental confirmation of this model in Ref. 6. The cost and complexity of the exact solution can be inferred from Melichar's studies of a single chamber problem by numerical methods (Ref. 7).

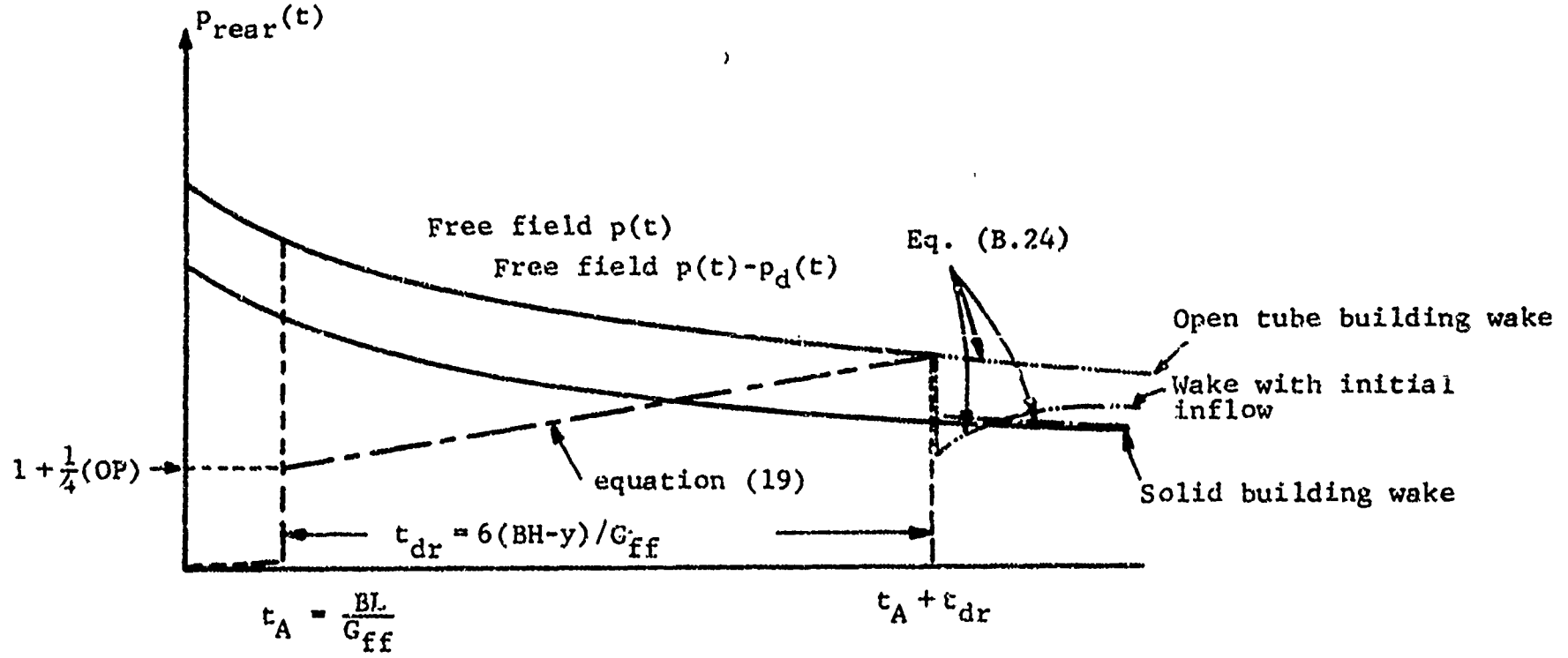

Fig. B.5 Rear Diffraction Pressure at Height y (t_A,t_{dr}, initial shock strength (1/4 OP) specified; wake dependent on solution of interior flow problem $C_d = -1.0$)

Our model is taken to be one-dimensional by the argument that the initial interaction of the incident shock and the exterior openings of the building can depend only on conditions immediately in front of the openings: there is no coupling between floors because the shock has penetrated before disturbances from adjacent floors can reach the orifice. Thus, the shock propagating through a floor behaves exactly as if it were in a tube during the first instants. Since this is precisely the case considered by Dadoni & Pandolfi (Ref. 6), their model is extended and used for the analysis, and their extremely good agreement between the measured strength of the head shock wave (indeed, the seeming absence of significant diffracted waves following the head shock wave) and the one-dimensionally predicted strength are taken as confirmation of the precision of this simple model.

The physical elements of this model are summarized in Fig. B.6, which shows the reflection-transmission process at an orifice in a tube of varying area across orifices, but constant between them. This latter feature is needed here to assess the amplifying effects due to flow blockage by building frames and thickness of floor slabs; these effects are significant for realistic geometry of buildings.

Our problem is to determine, for the tube in Fig. B.6a with area fractions α_o (orifice area/upstream cross-sectional area) and α_d (downstream cross-sectional area/upstream cross-sectional area), the transmitted shock state, $(\bar{p}_t, \bar{\rho}_t, q_t, \bar{T}_t)$, and the reflected shock state, given the incident shock strength, $\bar{p}_i$. We assume, following Ref. 6 that

(a) conditions are uniform in Ⓡ

(b) the jet is formed by isentropic expansion from state Ⓡ to pressure p_c.

(c) the contact region Ⓒ is uniform, so $p_c = p_t$. This is the same as demanding that the jet deceleration from Ⓙ to Ⓒ is isobaric, i.e., a constant pressure process.

(d) the transmitted shock region is uniform.

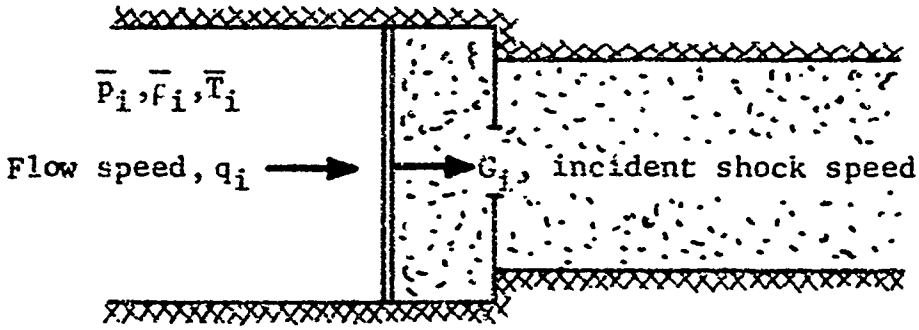

(a) Incident Shock

α_o = (area orifice)/(upstream area)

α_d = (area downstream)/(upstream area)

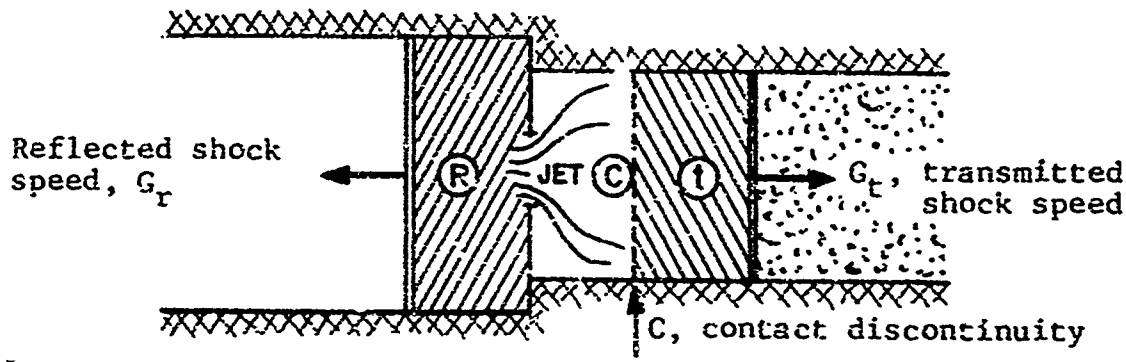

(b) Reflected and Transmitted Shocks

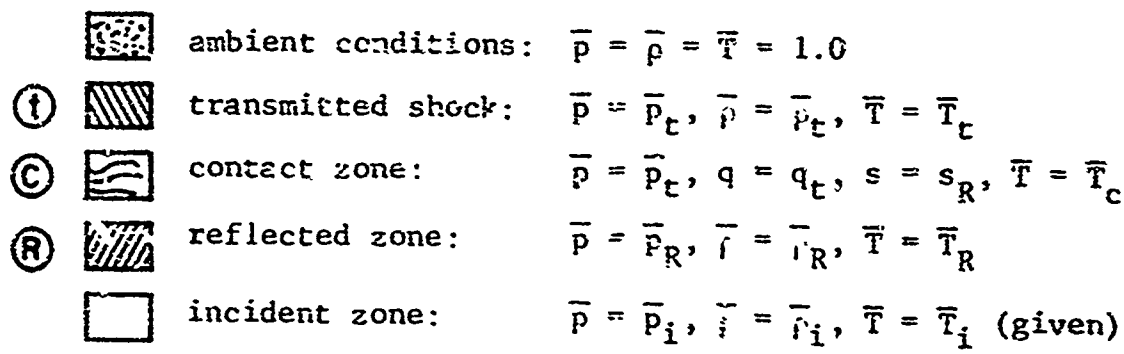

Fig. B.6 Shock Interaction with Orifice in Tube

With these assumptions, and the Rankine-Hugoniot relations, we may eliminate all the variables in © from the equations of flow, and obtain the following two relations

$$(N_R-1)(A_R/A_J)^2\, x^{\gamma+1/\gamma} - N_R\, x^{\gamma-1/\gamma} + 1 = 0 \qquad (B.25)$$

$$1/2Cx(f_2-x)^2 - f_2 = 0 \qquad (B.26)$$

where

$N_R = 1 + \frac{1}{2}(\gamma-1)\, M_R^2$; M = Mach number = q/a

A_R, A_J, A_t = cross-sectional areas upstream, in jet and downstream, respectively.

A_J = jet area at vena contracta = $C_c A_o$, with C_c = coefficient of contraction.

$x = \bar{p}_R/\bar{p}_t$

$C = (\gamma-1)\, M_R^2 N_R (A_R/A_t)^2 = (\gamma-1)\, M_R^2\, N_R\, \alpha_d^{-2}$

$f_2 = C_o(\bar{p}_R - x)^2/(\bar{p}_R + \mu^2 x)$

$C_o = \mu^2/(\gamma \bar{T}_R N_R)$

$\mu^2 = (\gamma-1)/(\gamma+1)$

Equations (B.25) and (B.26) are to be solved simultaneously for the unknowns x and $\bar{p}_R$, but the exponents of x make its elimination impossible, while M_R, N_R, and $\bar{T}_R$ all depend on $\bar{p}_R$ through the Rankine-Hugoniot relations. This compact form of the relations, however, allows us to dispense with the trial-and-error approach of Dadoni & Pandolfi, and perform instead the following systematic iteration

(a) Prescribe some value of $\bar{p}_R$ and solve the Rankine-Hugoniot relations for $M_R, N_R, \bar{T}_R$; the coefficients of x in Eq. (B.26) are then known.

(b) Solve Eq. (B.26) numerically for the correct x corresponding to this $\bar{p}_R$. Physically, this represents a solution for some orifice, but not necessarily the prescribed one.

(c) Calculate from Eq. (B.25) the exact orifice area corresponding to this $\bar{p}_R$, x solution. If it is not correct, make a linear adjustment of the trial $\bar{p}_R$ according to

$$\bar{p}_R' = \bar{p}_i + (\bar{p}_R - \bar{p}_i)(1-\alpha_o)/(1-\alpha_{ot}) \qquad (B.27)$$

where α_{ot} is the trial orifice area corresponding to $\overline{p}_R, x$ and where p_R' is the new trial value.

To compute the complete shock penetration pattern for a given floor, the possibility that the shock penetrating from the rear may arrive first must be considered. For our purposes it is sufficient to treat the rear diffracted shock as though it were incident in the plane of the rear wall, rather than at right angles to it, since the strength of this diffracted wave is known to no more precision than the error made in this geometric change. Then computation proceeds as outlined above.

The computation of the waves actually seen by occupants of the array of chambers on a given floor then proceeds as follows:

(a) Compute the incoming shocks from the front of the building, with each interior orifice having incident on it p_t of the previous orifice.

(b) Compute the arrival time of the shock at each orifice, based on the shock speed of the transmitted shock from the previous orifice:

$$t^f_{A_{ij}} = t^f_{A_{i-1,j}} + RL_{ij}/G^f_{t_{i-1,j}} \qquad (B.28)$$

where the f superscript refers to the shock coming from the front.

(c) Compute the arrival time of the wave diffracted around the rear of the building, using Eq. (B.16)

(d) Compute arrival times of shocks penetrating from the rear until the chamber is reached in which the shocks from front and rear meet.

After the chamber in which the front and rear shocks meet (confluent chamber) is identified, no further computation of the rear shock penetration is carried out, and chambers downstream are assumed to see only the shocks from the rear and their reflections. The rationale underlying this procedure is that each chamber can be expected to see at most the incoming shock and the shock reflected from the rear wall before the interaction of the jet flows into and out of the chamber with the shocks reduce the shock strength to a level where the shocks no longer contribute significantly to

the aerodynamic loading of occupants or structure. Essentially the same arguments hold for the confluent chamber; after the two shocks meet head-on and interact with each other, they meet the opposing jet flows and are weakened.

B.6.1 Shock Impulses on Occupants

Now that the shocks traversing each chamber are specified, we may estimate the aerodynamic load they exert on occupants. We take, for simplicity, the case of the occupant being a rectangular solid, with the shock incident parallel to one face of the solid, as in Fig. B.7. When the shock strikes this object, the front will be subjected to time-varying pressure during the diffraction process, and the rear will see the disturbance only after ℓ/G lag for the shock to overrun the whole object. We consider no spatial distribution of pressure on the front and rear, as we did for the building, because the times are so short here, and because the precision of this procedure is already compromised by the shape considered. Thus, back and front are assumed to "see" the pressure histories in Fig. B.7b where back and front have equal clearing times, $3w/G$, and the rear pressure (average over whole back face) starts with initial value zero. The net impulse/unit area applied to the solid will be the pressure difference between front and rear integrated up to the time when this difference goes to zero; this is just the area between the two curves in Fig. B.7b, and has the value

$$I = \frac{3}{2}\frac{\bar{P}_r + \bar{P}_i}{G} w + \frac{\bar{P}_i}{G} \ell = D_1^t w + D_2^t \ell \qquad (B.29)$$

This calculation is carried out once for the transmitted wave, and once for the reflected wave in each chamber, with the reflected wave impulse given a negative sign, yielding the final form

$$D_i = D_i^t - D_i^R$$

so that

$$I_{net} = D_1 w + D_2 \ell \qquad (B.30)$$

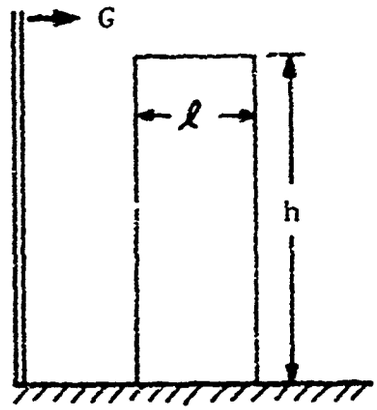

Fig. B.7a Shock Impulse Model

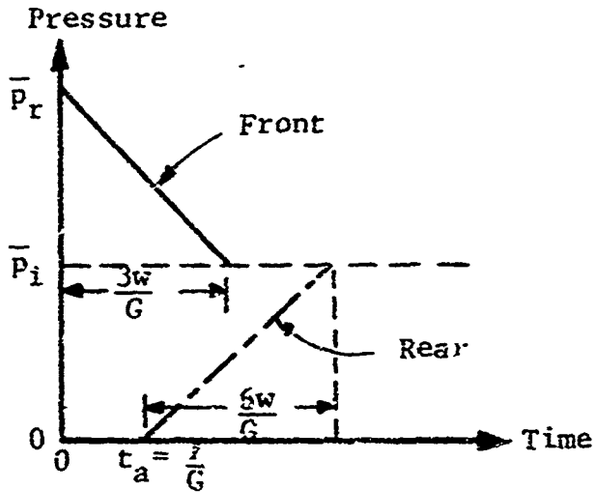

Fig. B.7b Diffraction Model for Shock Impulse

where D_1 and D_2 do not depend on ℓ or w, so that computation of these diffraction coefficients allows the effect of different orientations of the solid to be crudely taken into account, by assigning values to (ℓ,w,h). Since the reflected wave must be stronger than the incident wave in each chamber, the sign of the diffraction coefficients will be opposite to that of the shock speed. If the shock penetrates from the front, the net shock impulse will be directed to the front, and shocks incoming from the rear tend to propel the occupant to the rear. The velocities imparted by the shocks are significant ($\sim$ 5 fps) for overpressures $\leq$ 30 psi, but not sufficient by themselves to cause serious injury, and actually seem to represent a safety factor, since they tend to oppose the motion of the wind following the shock. Finally, the special case of the confluent chamber is treated as though the shock incoming from the rear is the reflected shock, and the same computation is carried out as in any other chamber.

B.6.2 Destruction of Walls by Shocks

According to our one-dimensional model, the wall containing the orifice (Fig. B.6) will see a pressure difference of $p_R - p_t$ across it until the reflected wave from the next orifice downstream returns to the downstream side of the wall, or an expansion wave reaches it from upstream. Because of the destruction of the returning reflected shock by the jet through the orifice, this wave is not expected to actually reach the wall; therefore, we prescribe the duration of this pressure difference to be twice the transit time of the transmitted wave into the next chamber

$$t_{dur_{ij}} = 2\left|t_{A_{ij}} - t_{A_{i+1,j}}\right| \qquad \text{(B.31)}$$

where $t_{dur_{ij}}$ is the time wall (ij) is exposed to the pressure difference. If this pressure difference and duration are sufficiently large, the wall fails by Eq.(B.2).

The various special cases of the confluent chamber's walls, the rear exterior wall, and walls without orifices are explained in

subsequent sections; they differ only in the manner in which duration is assigned to the shock load.

This completes the direct effects attributed to shock penetration; in summary, this analysis provides:

(a) Arrival times for the blast disturbance at various points in the building. The precision of these times is of some importance, because the buildup of pressure and wind speed in the interior is quite sensitive to them, as can be seen in the effect on wall failures, which require duration of load to exceed Δt_c.

(b) Shock impulses on occupants. Note that these do not include any dynamic pressure terms, because these terms are taken into account by the jet flow analysis of the next section. Including them here would double count them in the routine which computes translation of occupants.

(c) Wall failures. For most walls, the shock loads will be the most severe in the entire loading history, because the jet flows very rapidly equalize pressures across them. The exceptions are the special cases of confluent chambers and exterior walls, which may undergo more severe loading due to the jet flows.

B.7 CHAMBER FILLING BY JET FLOW

This portion of the analysis is the most complex in our model, yet is more severely simplified than any other; that is, while we retain many features of the exact solution, we neglect more than we retain.

The first simplifying assumption we make is that the filling process, that is, the increase of the chamber's pressure, density and temperature due to the jet flows, can be uncoupled from the shock penetration solution, except that the shock arrival times are used to switch on the jets. The fact that only the region behind the contact discontinuity can be reached by the jet flow is ignored, and we assume that the whole chamber has a uniform pressure, temperature, and density at each time step.

Specification of a spatially uniform density in the chamber forces us to specify the velocity as a function of position if mass is to be conserved in the chamber. If we demand only that the

velocity be in the x-direction and that it depend only on x, the result is a linear distribution of velocity from front-to-rear. This linear dependence of velocity on position is the simplest possible for conservation of mass, but it does violate the kinematic boundary condition at the two end walls of the chamber (that is, the air particles have a nonzero velocity normal to the end walls, so that, physically, this solution would mean air is penetrating the walls). This in turn can only be removed by making the velocity a function of (y,z) as well as x, that is, by prescribing some two- or three-dimensional structure to the velocity field in the room. For this first effort, the cost of incorporating such an analysis was not deemed proper, since we can globally conserve mass and energy with our present one-dimensional model, so we retain as our second assumption the specification that the velocity vector is given by

$$\vec{q} = \left\{q(x),0,0\right\} \tag{B.32}$$

which, along with the uniform density assumption, means

$$q(x) = q_f - (q_f - q_r)\ x/L \tag{B.33}$$

where q_f and q_r are the velocity at the front and rear walls respectively, and x is measured from the front of the chamber, which has length L.

This reduces our mathematical problem for each chamber to finding values for the unknowns (p,ρ,T,q_f,q_r), a total of five functions of time. The driving force which changes these values is the jet flow into the chamber, driven by the pressure differences across the orifice in the wall, so we next construct the jet flow model.

The flow across any orifice will be dictated by the two chambers which it separates, so only the pressures, etc., of these two chambers will appear in the equations for mass and energy flux through the orifice. The model for the jet which forms is the same as was used in Section B.6 for the connection between reflected and transmitted shocks, that is:

(a) The flow from the source (= higher pressure chamber) is isentropic to the jet. The point of origin of

the jet is taken at midchamber, where $q = 1/2(q_f+q_r)$.

(b) The flow from jet to midpoint in the recipient chamber is taken to be isobaric (constant pressure).

(c) The flow in (a) and (b) is quasi-steady, which means physically that the inertia of the air is neglected in the equation of motion. This is also equivalent to an infinite speed of sound, since each end of the jet is affected by the other instantaneously. So long as small time intervals are used in the analysis, this does not cause noticeable error.

(d) Because of the arrangement of the program, the velocities assigned to each chamber are those of the previous time step, which introduces a sort of numerical inertia into the problem, offsetting the effects of the quasi-steady assumption.

(e) The jet velocities cannot physically exceed the speed of sound, so a "sonic choke" is incorporated in this model. The effect of this is to maximize the mass flux of the jet.

The resulting governing equations for the jet are

$$q_{J_{ij}} = \sqrt{q_{s_{ij}}^2 + 2p_{s_{ij}}\left[1-(p_{r_{ij}}/p_{s_{ij}})^{(\gamma-1)/\gamma}\right]/\rho_{s_{ij}}(\gamma-1)} \qquad \text{(B.34a)}$$

if the flow is subsonic in the jet, and

$$q^*_{J_{ij}} = \sqrt{\left[q_{s_{ij}}^2 + 2T_{s_{ij}}/(\gamma-1)\right]\frac{\gamma-1}{\gamma+1}} \qquad \text{(B.34b)}$$

if the jet is sonic. In both expressions,

$$p_{s_{ij}} = \max\{p_{ij}, p_{i+1,j}\}$$
$$p_{r_{ij}} = \min\{p_{ij}, p_{i+1,j}\}$$

distinguish recipient (r) from source (s) chamber. The densities corresponding to the jet velocities are

$$\rho_{J_{ij}} = \rho_{s_{ij}}(p_{r_{ij}}/p_{s_{ij}})^{(\gamma-1)/\gamma} \qquad \text{(B.35a)}$$

$$\rho^*_{J_{ij}} = \rho_{s_{ij}}(a^{*2}_{J_{ij}}/a^2_{s_{ij}})^{1/\gamma-1} \qquad \text{(B.35b)}$$

Finally, the total mass flux into the chamber is then

$$\dot{M} = (\rho\, q_J)\, A_{ij} C_{c_{ij}} W_{ij} H_{ij} = (\rho q)_J\, \alpha_{o_{ij}} W_{ij} H_{ij} \tag{B.36}$$

and has dimensions of length squared because of the multiplication by the upstream wall area. The sign of $\dot{M}$ and q_J is positive if flow is from chamber i to i+1; negative for reverse flow.

Now that we have values for the flux through the orifices into a chamber, we need to estimate the effect on the state of the chamber. For the net mass flow, this is simple, since conservation of mass requires

$$\dot{\rho}_{ij} = d\rho_{ij}/dt = a_1 (\dot{M}_{in} - \dot{M}_{out})/V_{ij} \tag{B.37}$$

where V_{ij} is the volume of the chamber, $H_{ij} \times W_{ij} \times RL_{ij}$. To obtain pressure or temperature, something must be assumed about the thermodynamic process undergone by the particles after they enter or leave. In the case of particles leaving the chamber, the effect on the chamber is taken to be consistent with the isentropic formation of the jet:

(a) There is no significant flow between stories or side-to-side within the story.

(b) Outflow produces an isentropic expansion of the contents remaining in the chamber

$$\frac{\dot{p}_{ij}}{p_{ij}} = -\frac{\gamma \dot{\rho}_{ij}}{\rho_{ij}} = \frac{\gamma \dot{M}_{out} a_1}{\rho_{ij} V_{ij}} \tag{B.38}$$

(c) Inflow is "smeared out" over the entire chamber volume instantaneously as it enters. This has already been implicitly assumed for mass in Eq. (B.37). If the flow is energy conserving, this gives

$$\dot{p}_{ij}/p_{ij} = a_1 (T_{s_{ij}}/T_{ij}) \left(1 + [\gamma - 1] p_{ij}/p_{s_{ij}}\right) \dot{M}_{in}/(\rho_{ij} V_{ij}) \tag{B.39}$$

(d) The total pressure change instantaneously is the sum of the right-hand sides of Eqs. (B.38) and B.39)

$$\dot{p}_{ij}/p_{ij} = \frac{a_1 (T_{s_{ij}}/T_{ij}) \left(1 + [\gamma - 1] p_{ij}/p_{s_{ij}}\right) \dot{M}_{in} - \gamma \dot{M}_{out}}{\rho_{ij} V_{ij}} \tag{B.40}$$

Equations (B.36), (B.37) and (B.40) are essentially the forms used in the numerical computation, except that the mass flux terms $\dot{M}$ are written as FMF (front mass flux) and RMF (rear mass flux) so that, at each step of the computation, only RMF need be calculated, FMF having the same value as RMF of the previous chamber.

The actual computation consists of integrating Eqs. (B.36) and (B.40) by a fourth-order Runge-Kutta method, with the velocity assigned to the chamber at each subinterval being evaluated on the basis of the previous subinterval's mass flux values

$$q_{ij}(t+dt_n) = \frac{(FMF_{ij}(t+dt_{n-1}) - RMF_{ij}(t+dt_{n-1}))}{2\rho_{ij}(t+dt_{n-1})W_{ij}H_{ij}} \qquad (B.41)$$

where t is the time at the beginning of the integration step, and dt_n are the four Runge-Kutta subinterval steps: $\{dt_n\} = \{0, \Delta t/2, \Delta t/2, \Delta T\}$. This is the numerical inertia referred to above. After an integration step is completed, this time lag is wiped out before beginning the next step; this is done by calculating q_{ij} on the basis of the pressures assigned by the just-completed step. This process is iterative, since it involves determining a set of values q_{ij} which are consistent for every chamber of the floor j.

B.7.1 Wall Failure

During each integration step, the current size of the orifice is computed; if the wall has not yet failed, the pressure difference across the wall is tested, and, if it exceeds p_c, the time increment is added and retained for that wall. When the accumulated time exceeds Δt_c, the wall is counted as failed.

B.7.2 Approach to Steady State Flow

After all the chambers of the floor have filled, the flow through the floor is essentially steady, varying with the time scale of the free field. The chambers of the floor in this configuration will differ in pressure by an amount required to produce an isentropic jet at front and rear with equal mass fluxes; the sume of the pressure drops from front-to-rear on the floor will be such that the

wake pressure satisfies Eq. (B.24). This steady solution is not physically defensible, and arises only because of the assignment of a single pressure to the whole chamber, whereas in the actual flow, there is a pressure rise from the jet to the middle of the room into which it flows, due to the deceleration of the flow. This pressure rise is negligible in the filling calculation, because the room-to-room variation in pressure is much larger than this pressure rise, but it must be taken into account during the steady flow, at which time it is the same order as the room-to-room variation. Therefore, the steady flow which evolves from the filling calculation is nonphysical: the correct steady solution is analyzed in Section B.9.

If the governing Eqs. (B.36) and (B.40) are made fully dimensionless by factoring the area factors of the $\dot{M}$ terms, they may be put into the form

$$\dot{\rho}_{ij} = B_{ij}\left[\left(A_{J_{i-1,j}}/A_{J_{ij}}\right) F(i-1,j) - F(i,j)\right] \qquad \text{(B.42)}$$

$$\dot{p}_{ij} = B_{ij}\left[\left(A_{J_{i-1,j}}/A_{J_{ij}}\right) G(i-1,j) - G(i,j)\right] \qquad \text{(B.43)}$$

where

$B_{ij} = a_1 \alpha_{o_{ij}}/L_{ij}$; dimensions $(\text{time})^{-1}$

F, G = the dimensionless thermodynamic functions at the orifice whose indices appear. These functions contain only the pressure and density ratios, and no geometric terms.

It is clear that the geometry of each chamber is described by only two numbers in our model; the values of B_{ij} and $(A_{J_{i-1,j}}/A_{J_{ij}})$; the significance of the area ratio is obvious, but B_{ij} has been interpreted in two ways:

(a) $\alpha_{o_{ij}}/L_{ij} = A_{J_{ij}}/V_{ij}$; the area-to-volume ratio used as a separate parameter in BRL literature (Refs. 8 and 9). Only the dimension L_{ij} really plays a role in the one-dimensional model, however, so it is perhaps more pertinent to not introduce any implicit generality (application to two-dimensional or three-dimensional flows) by writing this as area-to-volume here.

(b) a_1/L_{ij} = time required for a pressure pulse to traverse the chamber in the flow direction, under ambient conditions. It is to be expected that the one-dimensional model will provide an estimate for filling time which is some multiple of this physically significant characteristic time. The α_{oij} factor indicates that filling time will in fact be some multiple of B_{ij}, inversely proportional to α_{oij}. The filling times given by Ref. 5, which are $2L_{ij}/G_{ff}$, contain this pressure dependence of G_{ff}, and scale dependence in the L_{ij} term, but lacks the area-volume ratio dependence, which accounts for orifice size.

In summary, our results have the same suggestive form as those of Refs. 5, 8 and 9, namely, we give filling times as multiples of a physically meaningful characteristic time, and we include also the scaling term of volume-to-area ratio.

B.8 SUMMARY AND DISCUSSION OF INPUTS GOVERNING DIMENSIONLESS NUMBERS

The dimensionless form of the chamber filling equations in Section B.7 makes it clear that the geometry of a chamber is characterized by only two numbers, B_{ij} and $(A_{J_{i-1,j}}/A_{J_{ij}})$, and therefore provides the most efficient way of choosing inputs to the program to uncover the full range of phenomena which the model possesses. Therefore, the dimensionless numbers governing the whole model are collected in Table B.1 so that the full set of inputs can be conveniently chosen.

The governing dimensionless numbers are specified in two ways; first, those which are input as data to the program (Input Dimensionless Numbers in the table), and those which are assigned values in the program itself (Arbitrary Program Constants in the table). As noted in the foctnote, this latter set is incorporated in such a way that the value may be changed if new data is found which suggests revision is needed, usually by the substitution of a single card in the program.

Each entry in the table is chosen so that it is both independent of the other dimensionless numbers (as required by the Buckingham Pi-Theorem) and so that its value has a simple physical meaning.

Table B.1

GOVERNING DIMENSIONLESS PARAMETERS

Phenomenon	Parameter	Input Dimensionless Number	Arbitrary Program Constants	Remarks
Blast:				
Yield	WY	WY		WY and XOP fix all other parameters, including durations D_p^+ and D_Q^+.
Pressure	OP	$OP/p_1 = XOP$		
Diffraction:				
Front	t_{df}		$t_{df} = 3(BH-y)/G_{ff}$	
Rear	t_{dr}		$t_{dr}/t_{df} = 2$	
	t_A^r	$BL/(BH-y)$	$t_A^r/t_{df} = \frac{1}{3}\left[1+\frac{BL}{BH-y}\right]$	Purely a geometric parameter because of model.
Initial rear shock strength	p_{or}		$p_{or}/OP = POR = 0.25$	
Wake pressure reduction	p_{wake}		$-p_{wake} = (p_{dff}-p_d^*)C_d$; $C_d = -1.0$	Both model and C_d values are arbitrary.
Wall Failure:	Δt_c	$\Delta t_c/t_{df}$		
	p_c	p_c/p_R^o		p_R^o is full-reflection pressure of incident blast
	A_d		$A_d = 0.15$	Percentage of wall removed by cracks
	t_H	$2H/(gD_p^{+2})$	$t_H = 2H/g$	Time for wall to vanish after cracks appear.
Shock penetration and chamber filling	t_F	$L/(a_1\alpha_o)t_{df}$		Estimate of fill time for chamber with one orifice.
Jets	A_j	$A_{J_{rear}}/A_{J_{front}}$		
		C_c		Vena contracta coefficient of contraction

Thus, the ratio of rear arrival time to diffraction clearing time indicates whether the blast reaches the rear in time to interact with the diffraction loads on the front (value of the ratio less than 1 indicates that it does), and the fact that the ratio becomes a purely geometry quantity in our model indicates that only the ratio BL/(BH-y) is significant in choosing overall configurations. Said in another way, the implication is that the same N-story configuration will have exactly the same solution whether it is placed on the ground or on top of a multistory building, so that, by analyzing a 10-story configuration, we obtain solutions for the same internal configurations for floors in one-story, two-story, etc., buildings. This is not a minor savings in light of the fact that office buildings do indeed tend to have the same internal configuration regardless of the number of stories (after two), and so do dormitory-apartment buildings, according to the NFSS data. Thus, the response of a whole city full of two to 10-story office buildings can be obtained from one 10-story run of program.

The next input variable, $\Delta t_c/t_{df}$, is a measure of whether or not the wall can fail before diffraction clearing occurs (value less than unity indicates it does), and therefore, whether the wall is subjected to significant load durations above free field overpressure. The same sort of interpretation is attached to p_c/p_R^o, which indicates with a value greater than unity whether or not there is any pressure possible capable of failing the wall; small values, of course, indicate that the wall is likely to be failed.

The final wall failure dimensionless number, $2H(gD_p^2)$, indicates by a value order unity that the blast has essentially passed over before the wall is removed from the flow, and therefore leads to the conclusion that the wall has been effective in protecting the occupants from free field winds even though it has failed structurally.

The filling dimensionless number, t_f/t_{df}, will have a value near unity in those cases where the filling process has been driven by the diffraction model pressures, rather than free field. If the

value is very much smaller than unity, the indication is that greater detail should be added to the diffraction model's time dependence; a value much larger than unity would imply that diffraction could be ignored, and filling computed from free field conditions.

B.9 STEADY STATE FLOW THROUGH THE BUILDING

The previous sections have analyzed the flows in the building during the early-time phases of blast loading, when the driving force was the large pressure differences between chambers. These pressure differences are reduced to small values as each chamber fills in its characteristic time t_F; since $t_F/D_p^+ \sim 0.001$, it is to be expected that the whole process will have ended for the building long before the blast loading has passed; that is, the whole filling process will pass in a time order of $NB \cdot t_F$, which is still much less than D_p^+, since $NB < 10$ in most cases.

After this time has passed, the character of the flow is much different, with the chambers no longer serving as significant sources and sinks of mass, but the flow being essentially steady, so that the algebraic continuity equation replaces the differential equations of filling ($\dot{M}_{ss_j}$ is the mass flux through story j)

$$\dot{M}_{ss_j} = \rho_{i-1,j}\, q_{i-1,j}\, H_{i-1,j}\, W_{i-1,j} = \rho_{ij}\, q_{ij}\, H_{ij}\, W_{ij} \qquad (B.44)$$

and the pressure differences between chambers will now be due solely to the dissipation occurring at the orifices

$$p_{front}(t) - p_{rear}(t) = \sum_{i=1}^{NB+1} \Delta p_{ij} \qquad (B.45)$$

where Δp_{ij} is the pressure drop across orifice ij due to dissipation.

The problem now is to determine an appropriate model for the dissipative pressure drops; once this is fixed, Eqs. (B.44) and (B.45) are sufficient to determine the flow, if we consider the fluid incompressible at this stage

$$\rho_{ij}(t) = \rho_{ff}(t) \qquad (B.46)$$

As emerges later, the velocities to be expected in the flow are a great deal smaller than sonic, so Eq. (B.46) is fully justified on physical grounds, and of great usefulness in simplifying the analysis.

The dissipation model, then, is the standard model of incompressible hydraulics, so we replace the momentum and energy equations with the modified Bernoulli equation

$$p/\rho g + 1/2\ q^2/g = p_{ff}/\rho g + q_{ff}^2/2g - h_L \qquad (B.47)$$

where h_L is the "head loss" due to dissipation between the free field source of the fluid particle and its present position; this loss is conventionally represented in terms of the velocity head multiplied by an experimentally determined loss coefficient

$$h_L = k_L q^2/2g \qquad (B.48)$$

Thus, our problem reduces to assigning realistic values to k_L for each orifice, since the losses in the room interiors are negligible compared to those of the orifice.

Consider, then, a single orifice, with upstream flow at speed q over an area A, which passes through an orifice of area A_o; the flow will have the general configuration shown in Fig. B.8. This flow has nonzero losses only because it is viscous, so these losses are represented as functions of orifice size (A_o/A), Reynolds' number $(q_J\sqrt{A_o}/\nu)$, with ν = kinematic viscosity of the flow, and orifice geometry. Values for standard geometries are presented in any hydraulics text.

The flow in Fig. B.8 differs in two respects from the idealized one-dimensional flow; first, in that a vena contracta forms, making the jet area, A_J, smaller than the geometric opening area, A_o; second, in that the flow is dissipative. Corrections for these two effects are made by introducing a coefficient of contraction, $C_c = A_J/A_o$ and a coefficient of velocity, $C_v = q_{Jactual}/q_{J\,C_v}$, where $q_{J\,C_v}$ is the speed of the jet if it has area A_J but dissipation is ignored.

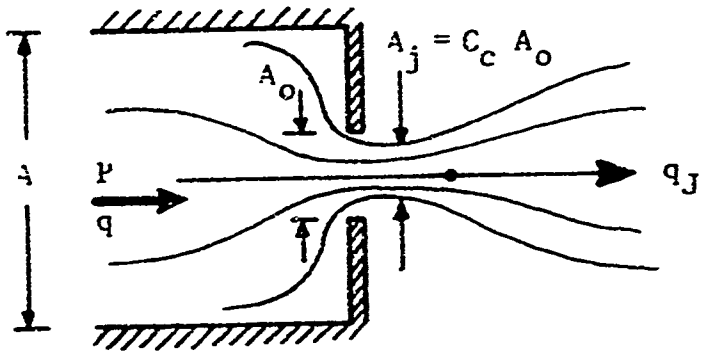

Fig. B.8 Orifice Flow

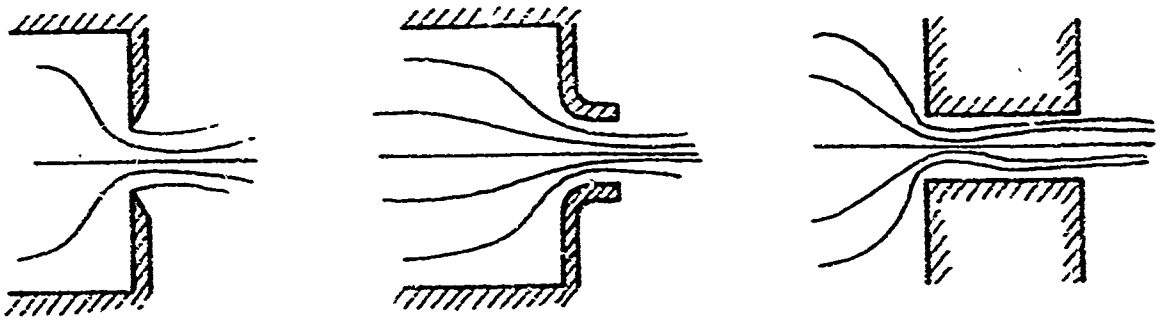

C_c	0.62	1.00	1.00
C_r	0.98	0.98	0.80
	sharp-edged	round-edged	short tube

Fig. B.9 Nominal Correction Coefficients

In terms of these coefficients, the head loss is

$$h_L = (p-p_{J_{act}})/\rho g + (q^2-q^2_{J_{act}})/2g$$
$$= + (1-A_J^2/A^2)(1-1/C_v^2)(q^2_{J_{act}}/2g) \qquad (B.49)$$

At large Reynolds numbers (greater than 10^4; typical value for a 2 ft window with 100 fps velocity is 10^6), these coefficients are independent of Reynolds number, and depend only on the size and geometry of the orifice. Values for a few standard geometries are given in Fig. B.9. If we arrange Eq. (B.49) into a more convenient form, based on upstream velocity (chamber velocity) we get (using Eqs. (B.44) and (B.46)

$$h_L = -(A^2/[C_c A_o]^2 - 1)(1-1/C_v^2)(q^2/2g) \qquad (B.50)$$

and we can then write, using Eq. (B.24) for the pressure in the wake of the building (see Fig. B.10)

$$h_L^{1-2} = \frac{P_{ff}-P_2}{\rho g} + \frac{q_{ff}^2-q_2^2}{2g} = \frac{P_{ff}-\left[P_{ff}+C_d(P_{ff}-\frac{1}{2}\rho q_2^2)\right]}{\rho g} + \frac{q_{ff}^2-q_2^2}{2g}$$
$$= \frac{1}{\rho g}(1-C_d)(P_{dff}-P_{d2}) \qquad (B.51)$$

where

$$P_{d2} = \frac{1}{2}\rho q_2^2$$

Now Eqs. (B.45) and (B.50) give for this head loss

$$h_L^{1-2} = -\sum_{i=1}^{NB+1}(A^2/[C_c A_o]^2-1)_{ij}(1-1/C^2_{v_{ij}})(q^2_{i-1,j}/2g) \qquad (B.52)$$

if the dissipation occurring in the room exterior is ignored compared to that caused by the orifice, an assumption which should be justifiable. The flow through each story is now determined by solving the equation obtained by equating the right hand sides of Eqs. (B.51) and (B.52).

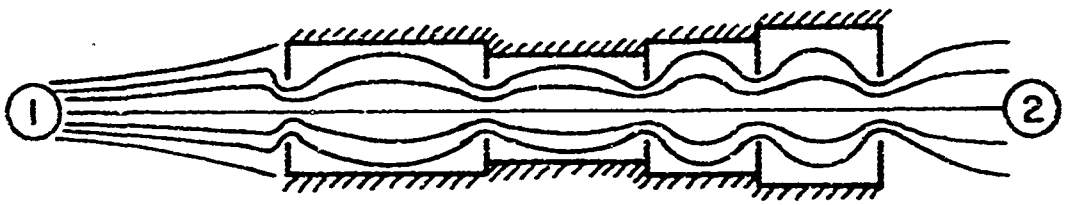

Fig. B.10 Flow through Story j

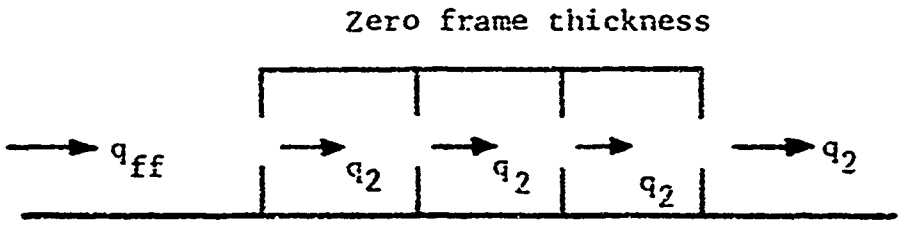

Fig. B.11 Flow through NB Identical Chambers

Example: Suppose we have the configuration shown in Fig. B.11, with all chambers having A/A_o = same value, so that continuity, Eq. (B.44) gives all chamber velocities $= q_2$, the wake velocity. If each orifice also has the same values of C_c and C_v, we get

$$(1-C_d)(p_{d_{ff}}-p_{d2}) = -(NB+1)\left(\frac{A^2}{[C_cA_o]^2}-1\right)\left(1-\frac{1}{C_v^2}\right)p_{d2}$$

from Eqs. (B.51) and (B.52) multiplied through by ρg. Thus

$$p_{d2} = \frac{1}{1+(NB+1)\dfrac{(1/C_v^2-1)(A^2/[C_cA_o]^2-1)}{(1-C_d)}}\,p_{dff} \qquad (B.53)$$

Equation (B.53) allows us to estimate the order of magnitude of the interior dynamic pressure as a fraction of the free field for some typical values of the parameters. Suppose that we consider

NB = 5 (typical 4- to 10-story office or dormitory)
A/A_o = 4 (typical of present architectural practice)

Our solution now is dependent on our precision in assigning values to <u>three</u> parameters: C_d, the wake drag coefficient; C_c and C_v, dependent on orifice details. The extreme choices of these yield:

(a) Most severe possible interior wind:

$C_d = -1$ (assumed in Section B.5)

$C_v = 0.98$

$C_c = 1.00$ Rounded edge in Fig. B.9

Then Eq. (B.53) gives

$$p_{d2} = p_{dff}/2.80 \qquad (B.54)$$

(b) Least possible interior wind:

$C_d = -0.40$ (assumed in Ref. 5)

$C_v = 0.80$

$C_c = 1.00$ Short tube in Fig. B.9

These values yield:

$$p_{d2} = p_{dff}/36.2 \qquad (B.55)$$

Thus the conclusion is, that, in light of the possibility that three parameters can be chosen plausibly and still give order-of-magnitude differences in the chamber p_d, there is little point at this time in any more refined analysis of this model until something more is known about the details of the orifice flows.

Although the actual geometry of the orifices which exist in a particular structure will control, to some extent, the late time interior velocity field we must of necessity establish some "most probable" values for these flow coefficients. Such an approach would be reasonable in many cases because such details of the geometry will either not be specified, or if known, their application to such an idealized model would be inconsistent with the neglect of other geometric features of the overall structure.

The exterior and interior building openings will generally not be of the round edge type. Rather they will be somewhere between those of the round edge type and the sharp edge type. Thus we have selected a value of 0.8 for C_c as being a most probable value. The short tube geometry is uncommon, especially in a series configuration. We have therefore selected a value of 0.98 for the most probable value of C_r. This value is realistic and represents a practical value for current applications of the flow model. Finally, a value of -1 for C_d is a better established value, especially for structures with sharp corners so that its use should also be adopted. Using these most probable values yields

$$p_{d2} = p_{d_{ff}}/3.4 \qquad \text{(B.56)}$$

Clearly the 3.4 multiplier is uncertain by perhaps a factor of 2, however it suggests that the more probable interior winds will be severe winds.

B.10 BLAST LOAD DISTRIBUTION IN UPPER STORIES (SAMPLE PROBLEM)

This section illustrates the use of the "Blast Loading Simulation Model" described previously, when applied to the solution of a typical problem. The subject building is illustrated in Fig. B.12. This is a long and narrow (38 ft), four-story office building which consists of a reinforced concrete frame and non-load bearing, nonarching masonry walls. All windows and door openings are 20 sq ft and represent 25 percent of wall area. Rooms are 16 ft along the short direction and 10 ft wide in plan. Bay width along the long direction is 12 ft. The objective of this problem is to illustrate some of the salient features of this simulation model by determining the distribution of dynamic pressure on the third story of this building when subjected to a 1 MT surface burst at the range of 14.7 psi (approximately 8400 ft). Input data required by the simulation model are the following:

Building Data

NB (number of bays (rooms) front to rear of building) = 3
NS (number of stories) = 4
NSB (initial story analyzed) = 3
NST (final story analyzed) = 3
NW (number of bays in the long direction) = 1
BL (building length) = 38 ft
BW (bay width in the long direction) = 12 ft
BH (building height) = 40

Room Data (Three Rooms)

Room 1 RL = 16 ft, W = 10 ft, H = 8 ft
Room 2 RL = 3 ft, W = 10 ft, H = 8 ft
Room 3 RL = 16 ft, W = 10 ft, H = 8 ft

Wall and Window Data (One wall type used)

PC (incipient collapse overpressure) = 2 psi
DTC (time to maximum wall response) = 20 ms
A_i (wall window area); A_1 = 20 sq ft, A_2 = 0 sq ft, A_3 = 0 sq ft, A_4 = 20 sq ft

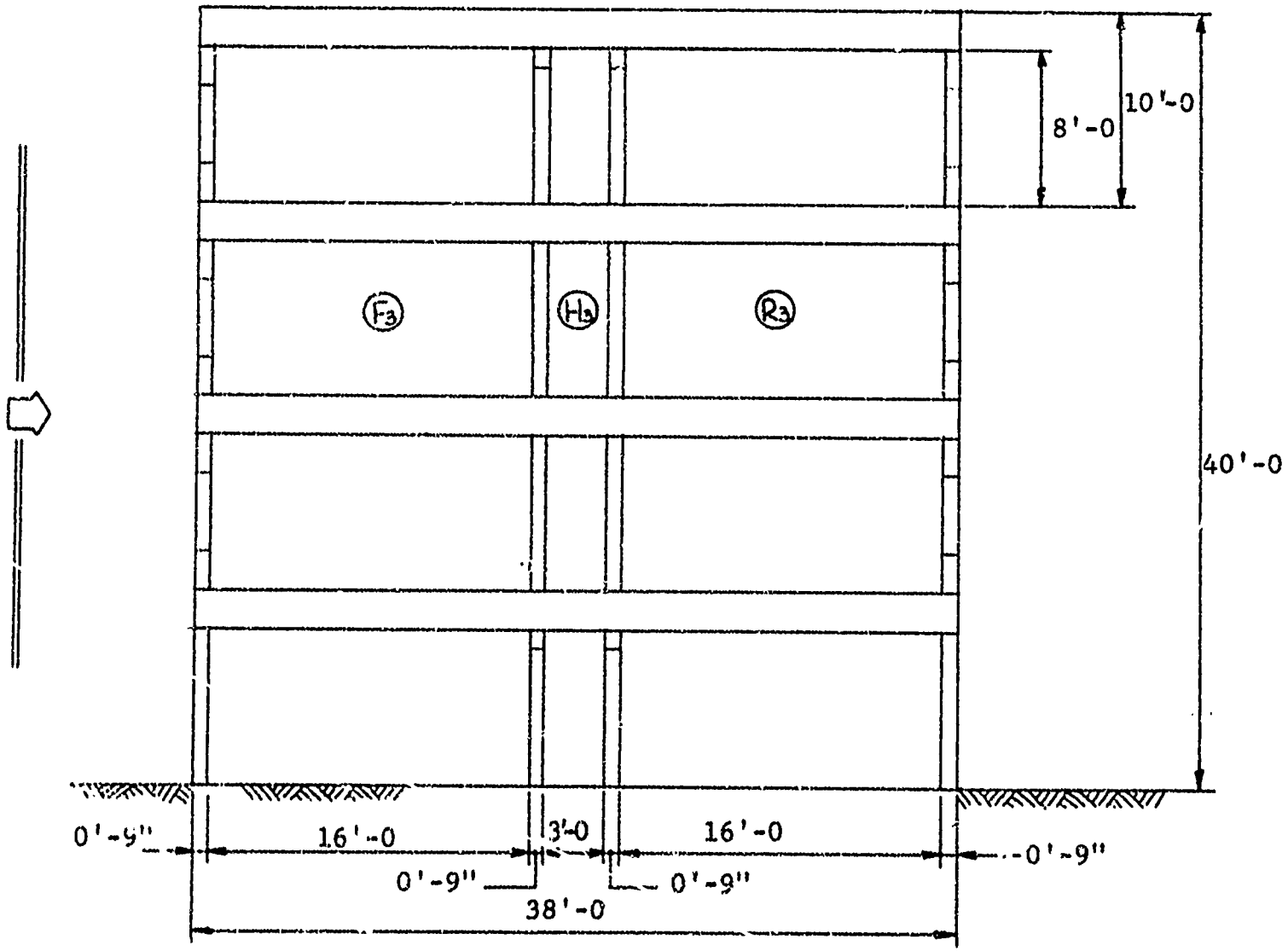

Fig. B.12 Sample Office Building (Elevation)

CC (coefficient of contraction) = 1.0

Weapon Environment Data

WY (weapon yield) = 1 MT
OP (incident free field overpressure) = 14.7 psi

Integration Times

TINC (time increment in filling integration) = 0.001 sec
TSTOP (total duration of filling integration) = 0.10 sec

Results of the analysis are plotted in Figs. B.13 and B.14. Figure B.13 gives the details of the filling phase in terms of average total overpressures. Figure B.14 provides the dynamic pressures in each of the three rooms.

We begin the analysis by surveying some of the pertinent dimensionless numbers given in Table B.1. For a 1 MT surface burst the positive phase duration for overpressure is 1.7 sec. With the free field shock speed of 1538 ft/sec, the diffraction time for the third floor at the front of the building, t_{df} = 29.25 ms, and at the rear, t_{dr} = 58.50 ms. With the reflection coefficient of 3 at this range, the ratio of p_c/p_r^o (incipient collapse overpressure/peak reflected pressure) is 0.0454, and the ratio of $\Delta t_c/t_{df}$ (maximum wall response time/diffraction clearing time) is 1/3. These two ratios indicate that shocks are fully capable of destroying the walls in the diffraction clearing phase. Very large values of p_c/p_r^o would imply no damage to walls in the loading process.

The value of $(t_H/D_p^+)^2$ is 0.172. This ratio of the time for the wall to vanish/positive phase duration indicates that walls will vanish (producing clear openings) about halfway through the positive phase duration.

The ratio of t_F/t_{df} (chamber fill time/diffraction clearing time) is 1.89 indicating that filling will occur at a sufficiently fast rate such that the diffraction model needs to be included in the simulation process.

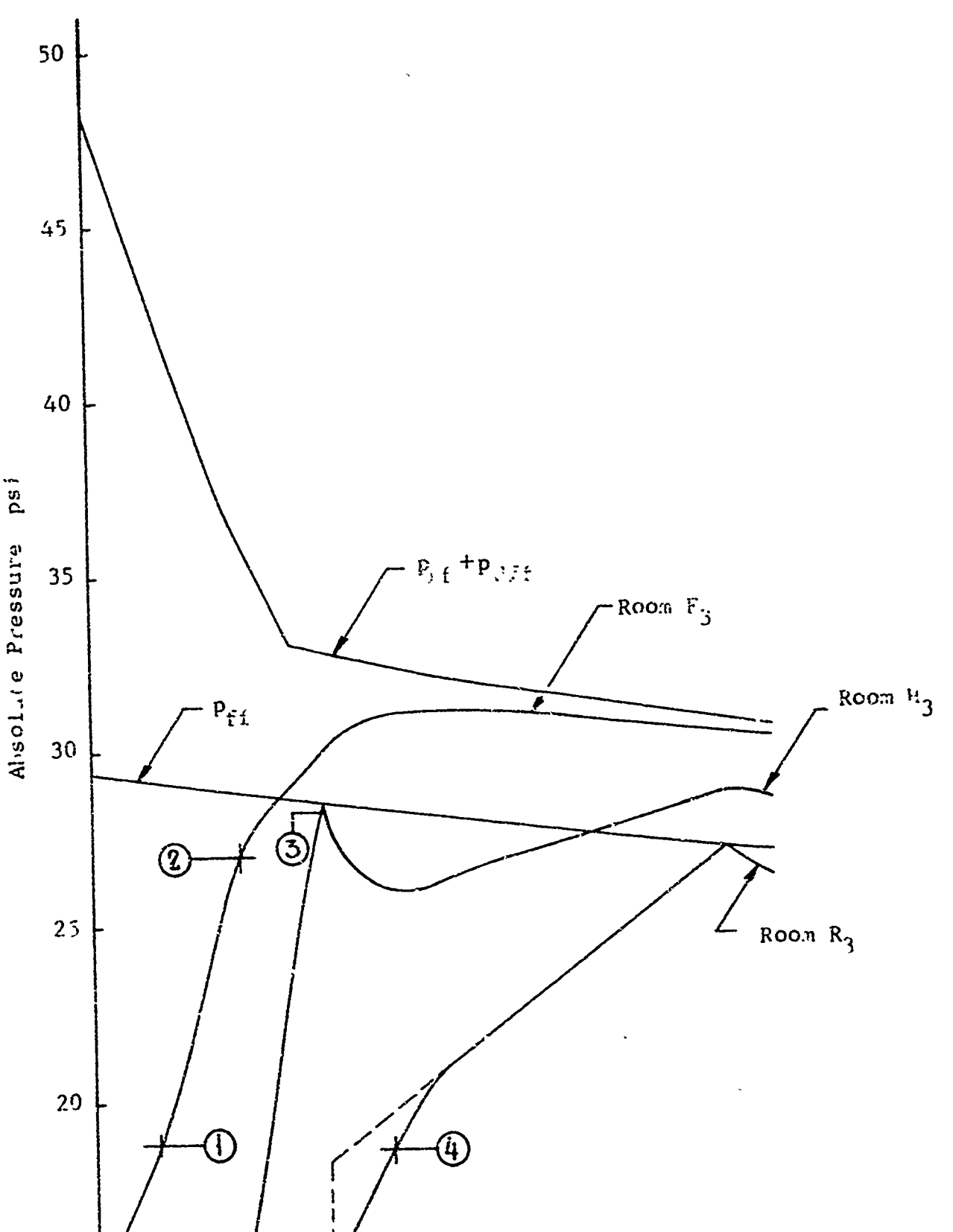

Fig. 8.13 Room Pressures (Filling Phase)

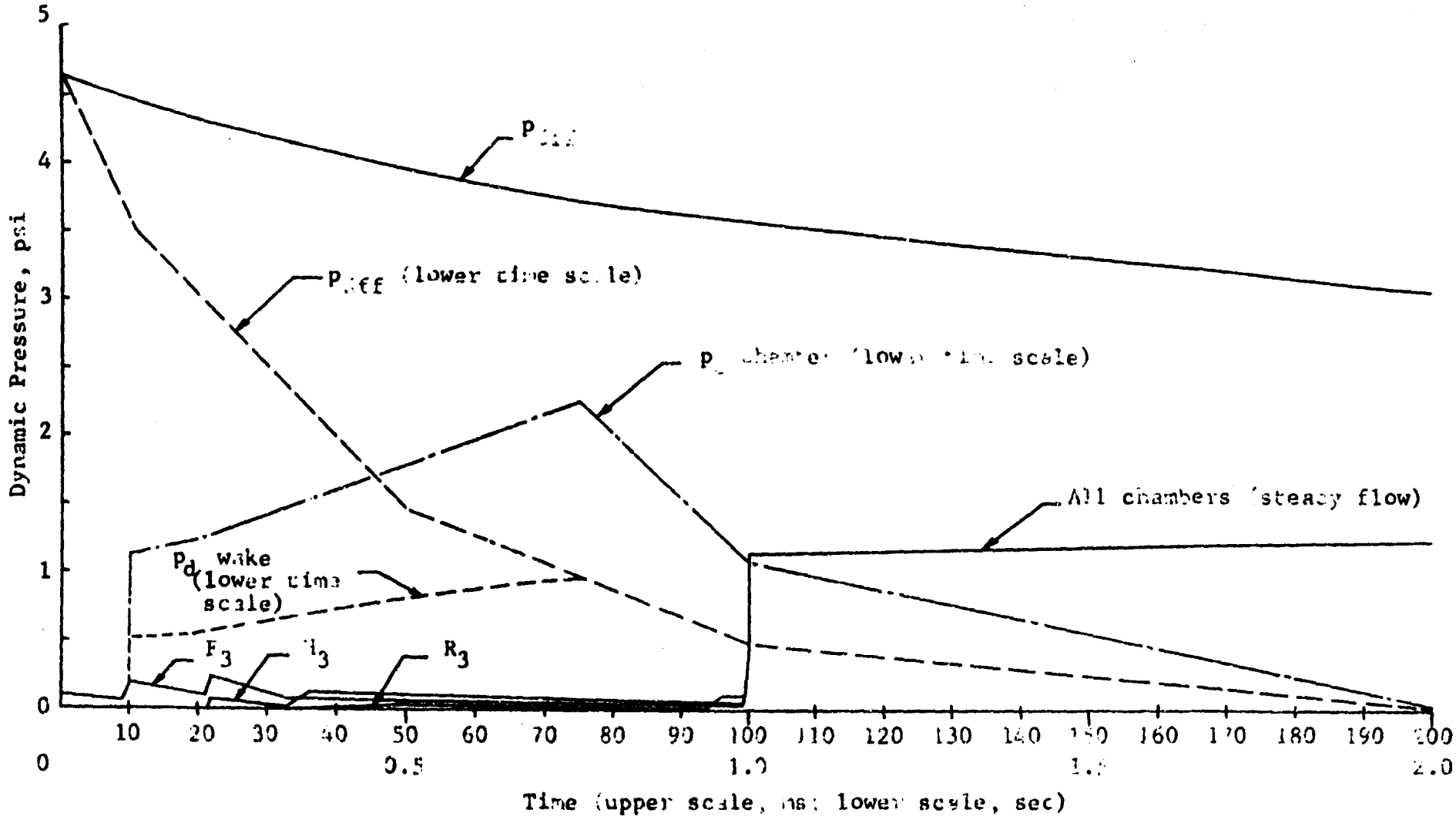

Note: Solid curves refer to upper time scale, dash and dash dot curves refer to lower time scale.

Fig. 2.14 Dynamic Pressure (Positive Phase)

This preliminary discussion provides a basis both for setting up the problem and for examining the results given in Figs. B.13 and B.14.

Figure B.14 illustrates the filling phase. Superimposed on the average results for each of the rooms are the external free field conditions of overpressure, dynamic and reflected pressure. Response (failure) times of each of the four walls are indicated by the circled numbers. In the absence of wall failures predicted by the shock analysis, room H_3 (hallway) would remain at atmospheric pressure since no door or window openings lead into it from adjoining rooms. Figure B.13 indicates that in fact flow into H_3 begins at 21.52 msec and the pressure has risen to nearly free field at 34 msec when the rear wall of this room fails (due to the fact that the pressure across wall 3 is above 2 psi after 24 msec, and the shock from the rear offers no counterpressure until 47.59 msec). When wall 3 fails, flow begins into the rear chamber (R3) from the front, a half millisecond before the inflow from the rear window begins; thus up to about 50 msec R3 has inflow from both directions.

Dynamic pressures during filling are given for the center station of each room in Fig. B.14, recalling that velocity varies linearly front-to-rear in the model used here, so dynamic pressures vary as quadratics in x. Accordingly, R_3 has a positive (rearward directed) dynamic pressure at room center at all times, because the positive inflow from the front is always larger than the negative inflow from the rear in this case. Clearly these dynamic pressures are negligible during filling, being both small in magnitude and of short duration. Even if it is noted that the actual flow near the front of the room is a jet concentrated over the orifice area (rather than spread over the room section as in this model), so that

$$p_{d_{jet}} \sim p_{d_{front}} / \alpha_o^2 \sim 16\, p_{d_{front}}$$

here, the impulse is negligible over a 100 msec duration.

After filling ends, the steady flowthrough model is used:

$$p_{d,ext_{ij}} = \frac{p_{ff}(t)}{1 + \frac{1}{1-C_d}\sum_{i=1}^{NB+1}\left(\frac{i}{C_{v,ij}^2} - 1\right)\left(\frac{A_{ext}}{A_{ij}}\right)^2\left(\frac{1}{\alpha_{e,ij}^2(t)} - 1\right)} \qquad (B.57)$$

$$p_{d_{ij}} = \left(\frac{A_{ext}}{A_{ij}}\right)^2 p_{d,ext_{ij}} \qquad (B.58)$$

Taking worst-case analysis, $C_v = 0.98$, $C_c = 1.0$ for all orifices and $C_d = 0.4$, we get the broken line curves in Fig. B.14 for $p_{dij}(t)$ after the filling phase ends. As can be seen the $A_{ext}/A_{ij} = (10x12)/(8x10) = 3/2$ factor in Eq.(B.58) causes the interior dynamic pressure to be 2.25 times free field after the walls have been completely removed (at $t_{wij} = \max_i\{t_{c,ij}\} + t_H \cong 75$ msec here), so that the flow blockage offered by the framing enhances wind speeds in the steady flow phase.

REFERENCES

1. Zaker, Thomas A., "Shock Tube Studies of Blast Pressures behind Frangible Wall Panels," Proc. Second Shock Tube Sympos., 28-43, AF SWR-TM-58-3 (1958)

2. Sevin, E., "A Comparison of Shock Tube and Field Test Data on the Pressure Buildup behind Frangible Walls," Proc. Second Shock Tube Sympos., 44-54, AF SWR-TM-58-3 (1958)

3. National Fallout Shelter Survey

4. Brode, Harold L., "Review of Nuclear Weapons Effects" Annual Rev. Nuc. Sci. 18, 153-202 (1968)

5. The Effects of Nuclear Weapons, Ed. Samuel Gladstone, AEC. Rev. Ed. (1964)

6. Dadoni, A. and Pandolfi, M., "Interaction of Traveling Shock Waves with Orifices inside Ducts," Intl. J. Mech. Sci. 13(1), 1-16 (1971)

7. Melichar, J., Airblast-Induced Aerodynamic Effects in Blast-Slanted Basement Shelters, Final Report to OCD, URS-692-3, Section 6, (1969)

8. Clark, R., "Pressure-Time History in a Chamber Subjected to Shock Wave Filling through an Orifice," Proc. Second Shock Tube Sympos., 101-117, AF SWR-TM-58-3 (1958)

9. "Information Summary of Blast Patterns in Tunnels and Chambers," 2nd Ed., Shock Tube Facility Staff, BRL; BRL Mem. Rept. 1390 (1962)

10. Vennard, J. K., Elementary Fluid Mechanics, 4th Ed., Wiley (1961)

APPENDIX C

SIMULATION MODEL OF PEOPLE SURVIVABILITY IN CONVENTIONAL BUILDINGS

C.1 INTRODUCTION

This appendix describes the computer program used for survivability estimates of existing conventional buildings. Basically it is a simplified version of several SEP code routines and the translation survivability routine described in Appendix A, in which parameters critical to the problem were identified and sufficient exercising of the detailed routines was accomplished to permit rapid, reliable estimates to be made from these results. Survivability to translation in the blast wind was found to be the most critical factor and thus was studied in greatest detail. The remaining sections of this appendix describe the various routines.

C.2 TRANSLATION SURVIVABILITY ROUTINE

C.2.1 Description

In the process of exercising the translation survivability model (see Appendix A) it was determined that for a specified weapon (in this case, a 1 MT surface burst), the translation survivability results could be treated as functions of overpressure and distance to a downwind vertical hard surface. A parametric study was undertaken utilizing the rigid block translation model (see Appendix A) with varying overpressure and distances to downwind walls (also including the possibility that no vertical obstructions remain). The results are presented in tabular form for people initially standing and prone (Tables C.1 and C.2).

The simplified translation model is essentially a table lookup with modifications for specific buildings because of walls, shading from blast, and room geometry (Appendix A). Areas in buildings are identified as having the following characteristics:

room length, room width, room height, sill height, window width, window height, wall failure pressure, and distance to downwind wall. For a total building any number of different areas may be identified and the survivability based on the average results (weighted proportionally to the area) for each separate area is obtained.

The model consists of four routines: MAIN program, subroutine TRANS, function KNOCK (see Appendix A), and subroutine SURVIV. The MAIN program reads the input data, calls subroutine TRANS, accumulates and averages the results, and outputs the average survivability estimate. Subroutine TRANS is the main body of the routine. It contains the table data, calculates shielding from the walls, reduces interior pressures by calling KNOCK, and obtains results from the tables by calling SURVIV. For each different area a uniform distribution of people is obtained by dividing the area into ten sectors and averaging results for people initially in each of these areas. Subroutine SURVIV is simply a table lookup with linear interpolation.

Table C-1

SURVIVABILITY FOR STANDING POSITIONS

OVERPRESSURE (PSI)	DISTANCE TO WALL (FT)													
	0	5	10	15	20	25	30	35	40	45	50	55	60	NO WALL
2	1.00	.92	1.00	1.00	1.00	1.00	1.00	1.00	1.00	1.00	1.00	1.00	1.00	1.00
3	1.00	.92	.96	.96	1.00	1.00	1.00	1.00	1.00	1.00	1.00	1.00	1.00	1.00
4	1.00	.96	.92	.91	1.00	1.00	1.00	1.00	1.00	1.00	1.00	1.00	1.00	1.00
5	1.00	.82	.81	.57	.68	.50	.75	.75	.75	.75	.75	.75	.75	.75
6	.70	.69	.69	.23	.36	.00	.50	.50	51	.51	.51	.51	.51	.51
7	.50	.49	.53	.11	.20	.03	.25	.25	.25	.25	.25	.25	.25	.49
8	.31	.26	.37	.06	.05	.06	.03	.04	.00	.00	.00	.00	.00	.47
9	.20	.20	.25	.00	.03	.03	.02	.02	.00	.00	.01	.00	.00	.23
10	.10	.13	.14	.00	.01	.00	.00	.00	.00	.00	.00	.00	.00	.00
11	.06	.08	.10	.00	.00	.00	.00	.00	.00	.00	.00	.00	.00	.00
12	.00	.03	.06	.00	.00	.00	.00	.00	.00	.00	.00	.00	.00	.00
13	.00	.02	.04	.00	.00	.00	.00	.00	.00	.00	.00	.00	.00	.00
14	.00	.01	.02	.00	.00	.00	.00	.00	.00	.00	.00	.00	.00	.00
15	.00	.01	.03	.00	.00	.00	.00	.00	.00	.00	.00	.00	.00	.00
16	.00	.00	.03	.00	.00	.00	.00	.00	.00	.00	.00	.00	.00	.00
17	.00	.00	.01	.00	.00	.00	.00	.00	.00	.00	.00	.00	.00	.00
18	.00	.00	.00	.00	.00	.00	.00	.00	.00	.00	.00	.00	.00	.00
19	.00	.00	.00	.00	.00	.00	.00	.00	.00	.00	.00	.00	.00	.00
20	.00	.00	.00	.00	.00	.00	.00	.00	.00	.00	.00	.00	.00	.00

Table C-2
SURVIVABILITY FOR PRONE POSITIONS

OVERPRESSURE (PSI)	DISTANCE TO WALL (FT)													
	0	5	10	15	20	25	30	35	40	45	50	55	60	NO WALL
2	1.00	1.00	1.00	1.00	1.00	1.00	1.00	1.00	1.00	1.00	1.00	1.00	1.00	1.00
3	1.00	1.00	1.00	1.00	1.00	1.00	1.00	1.00	1.00	1.00	1.00	1.00	1.00	1.00
4	1.00	1.00	1.00	1.00	1.00	1.00	1.00	1.00	1.00	1.00	1.00	1.00	1.00	1.00
5	1.00	1.00	1.00	1.00	1.00	1.00	1.00	1.00	1.00	1.00	1.00	1.00	1.00	1.00
6	1.00	1.00	1.00	1.00	1.00	1.00	1.00	1.00	1.00	1.00	1.00	1.00	1.00	1.00
7	1.00	1.00	.95	.87	.88	.94	1.00	1.00	1.00	1.00	1.00	1.00	1.00	1.00
8	1.00	1.00	.90	.74	.75	.89	.99	1.00	1.00	1.00	1.00	1.00	1.00	1.00
9	1.00	1.00	.69	.37	.38	.44	.50	.50	.50	.50	.55	.64	.75	1.00
10	1.00	1.00	.48	.00	.00	.00	.00	.00	.00	.00	.10	.29	.50	1.00
11	1.00	1.00	.24	.00	.00	.00	.00	.00	.00	.00	.05	.14	.25	1.00
12	1.00	.88	.00	.00	.00	.00	.00	.00	.00	.00	.00	.00	.00	1.00
13	1.00	.75	.00	.00	.00	.00	.00	.00	.00	.00	.00	.00	.00	.88
14	1.00	.50	.00	.00	.00	.00	.00	.00	.00	.00	.00	.00	.00	.75
15	1.00	.25	.00	.00	.00	.00	.00	.00	.00	.00	.00	.00	.00	.38
16	1.00	.13	.00	.00	.00	.00	.00	.00	.00	.00	.00	.00	.00	.00
17	1.00	.00	.00	.00	.00	.00	.00	.00	.00	.00	.00	.00	.00	.00
18	1.00	.00	.00	.00	.00	.00	.00	.00	.00	.00	.00	.00	.00	.00
19	1.00	.00	.00	.00	.00	.00	.00	.00	.00	.00	.00	.00	.00	.00
20	1.00	.00	.00	.00	.00	.00	.00	.00	.00	.00	.00	.00	.00	.00

C.2.2 Flow Chart for Subroutine TRANS

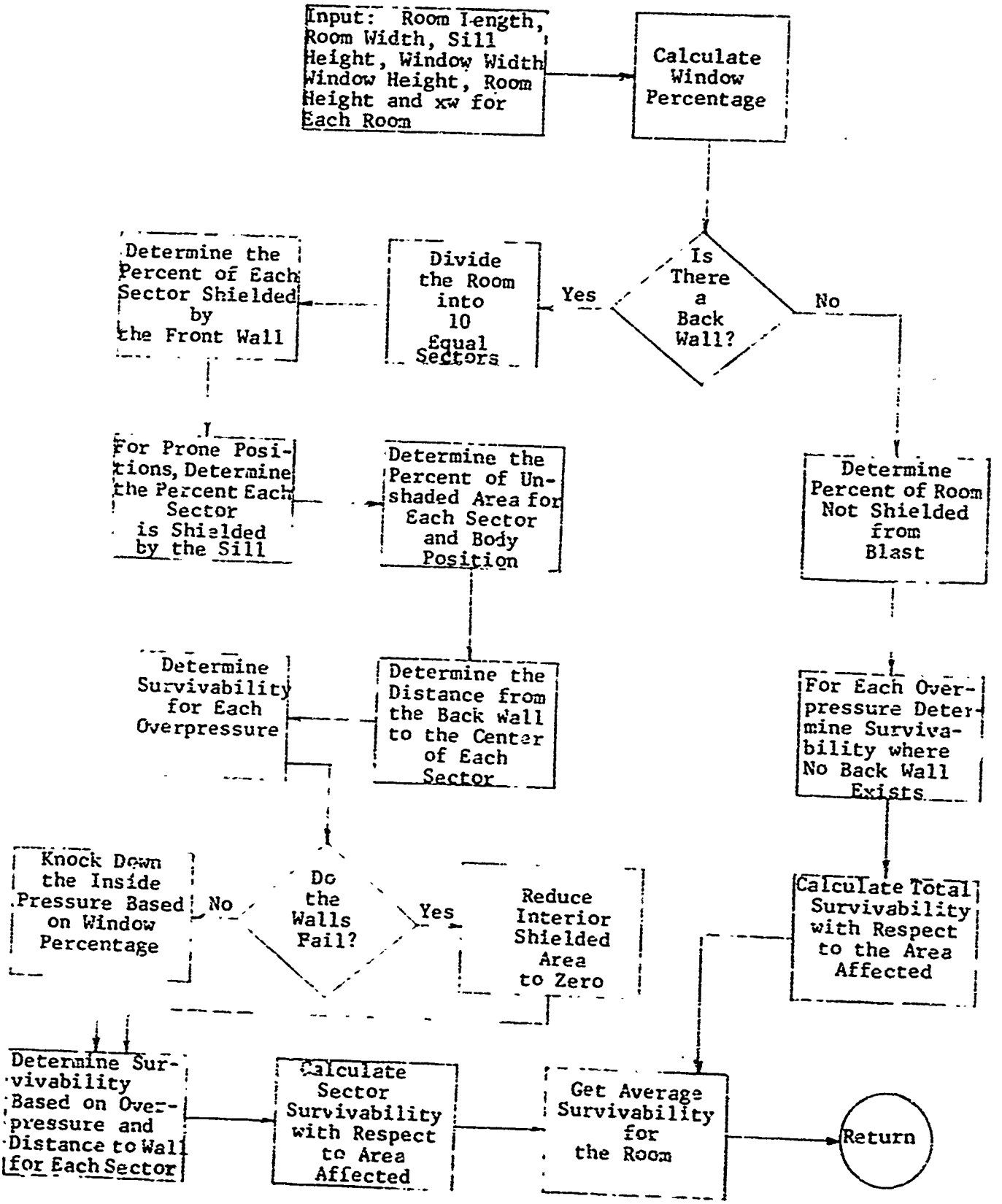

C.2.3 Translation Survivability Routine Listing

```
      MAIN PROGRAM
      DIMENSION NAME(13),FCTR(15),ST(20),PT(20),SRVST(20),SRVPR(20)
      REAL LR
100C  READ(5,2,END=500)(NAME(I),I=1,13)
    2 FORMAT(13A6)
      READ(5,11) N,(FCTR(I),I=1,N)
   11 FORMAT (I2,3X,15F5.0)
      DO 50 I=1,20
      ST(I)=0.
   50 PT(I)=0.
      WRITE(6,4)(NAME(I),I=1,13)
      WRITE(6,504)
  504 FORMAT(4X' FCTR'7X'LR'8X'WR'8X'SH'8X'WW'8X'WH'8X'RH'8X'PB'8X'XW')
      DO 20 J=1,N
      READ(5,12) LR,WR,SH,WW,WH,RH,PB,XW
   12 FORMAT(8F10.0)
      WRITE(6,505) FCTR(J),LR,WR,SH,WW,WH,RH,PB,XW
  505 FORMAT(//9F10.3)
      CALL TRANS(LR,WR,SH,WW,WH,RH,PB,XW,SRVST,SRVPR)
      SRVST(1)=100.
      SRVPR(1)=100.
      DO 30 K=1,20
      ST(K)=ST(K)+SRVST(K)*FCTR(J)
   30 PT(K)=PT(K)+SRVPR(K)*FCTR(J)
   20 CONTINUE
      WRITE(6,4)(NAME(I),I=1,13)
    4 FORMAT('1',13A6/)
      WRITE(6,77)
   77 FORMAT(' BLAST TRANSLATION SURVIVABILITY RESULTS'/////)
      WRITE(6,78)
   78 FORMAT('     FREE FIELD      PER CENT SURVIVORS'/
     1       '   OVERPRESSURE'/7X'(PSI)'7X'STANDING   PRONE'//)
      DO 90 J=1,20
      P=J
   90 WRITE(6,111) P,ST(J),PT(J)
  111 FORMAT(7X,F5.1,9X,F5.1,6X,F5.1)
      GO TO 1000
  500 STOP
      END
```

```
      SUBROUTINE TRANS(LR,WR,SH,WW,WH,RH,PB,XW,SRVST,SRVPR)
      DIMENSION SMX(19,14),SMXP(19,14),SRVST(20),SRVPR(20)
      DIMENSION AREA(50),AREAP(50),X(50),SRVIVE(50),SRVIVP(50)
      DATA((SMX(I,J),J=1,14),I=1,19) /1,,,9,13*1,,,925,,962,,957,11*1,,
     1 ,95,,923,,914,11*1,,,823,,806,,571,,66,,5,,752,,752,,755,,751,
     2 4*,755,,7,,695,,689,,229,,36,0,,,5*4,,505,6*,508,,5,,487,,527,
     3 ,114,,205,,029,,252,,252,5*,254,,449,,3,,278,,365,0,,,095,,058,
     4 ,032,,039,5*0,,,470,,2,,205,,253,0,,,031,,032,,017,,020,5*0,,
     5 ,25,,1,,131,,141,0,,,007,,005,,003,8*0,,,08,,102,0,,,003,,002,
     6 9*,,,029,,063,12*0,,,022,,044,12*0,,,014,,024,12*0,,,009,,020,
     7 12*0,,,004,,029,12*0,,,002,,015,53*0,/
      DATA((SMXP(I,J),J=1,14),I=1,19)/ 72*1,,,952,,869,,87/,,943,,996,
     1 9*1,,,904,,739,,753,,886,,992,9*1,,,691,,370,,377,,443,,496,3*,5,
     2 ,549,,643,,75,3*1,,,477,7*0,,,098,,296,,501,3*1,,,259,7*0,,,049,
     3 ,143,,25,,2*1,,,,75,11*0,,2*1,,,75,11*0,,,875,1,,,50,11*0,,,75,
     4 1,,,25,11*,,,375,1.0,,125,12*0,,1.0,13*0,,1.0,13*0,,1,,
     5 13*0,,1,,13*0,/
      COMMON/BLK1/ SMX,SMXP
      REAL KNOCK
      REAL LR
      PA=(,4*,1)/(,8*,8)
      IF(YA.LE.40.) GO TO 37
      AA=1.-(,8-,4)*(,8-,4)/(0.88*LR*WR)
      PLIMIT=1.
      P=1.
      DO 748 J=1,19
      P=PLIMIT+1.
      PLIMIT=P
      IF(P.GT.PB) AA=1.
      IF(P.LT.PB) P=KNOCK(PW,P)
      CALL SURVIVE(P,XW,SRV,SRVP)
      SRVST(J+1)=(1.-AA+SRV*AA)*100.
      SRVPR(J+1)=(1.-AA+SRVP*AA)*100.
  748 CONTINUE
      RETURN
   37 N=1
      DX=LR/2
      A1=.8*DX
      DO 5 K=1,,
      AREAP(K)=A1
    5 AREA(K)=A1
      J=0
      FW=.4
      BW=FW+0.44*DX
      IF(BW.GT.WR) GO TO 10
      DO 8 J=1,N
      AREA(J)=(FW+BW)*DX/2.
      AREAP(J)=AREA(J)
      FW=BW
      BW=FW+0.44*DX
      IF(BW.GT.WR) GO TO 10
    8 CONTINUE
      GO TO 11
```

```
 10 AREA(J+1)=A1-(WR-FW)*(WR-FW)/0.88
    AREAP(J+1)=AREA(J+1)
 11 J=0
    IF(SH/0.22.LT.DX) GO TO 70
    DO 60 J=1,N
    AREAP(J)=AREAP(J)-WW*DX
    IF((J+1)*DX*0.22).GE.SH) GO TO 70
 60 CONTINUE
 70 AREAP(J+1)=AREAP(J+1)-(SH-J*DX*0.22)*WW/0.22
    DO 80 J=1,N
    AREA(J)=AREA(J)/A1
 80 AREAP(J)=AREAP(J)/A1
    TEMP=WR+DX/2.
    DO 90 J=1,N
    X(J)=TEMP-DX
 90 TEMP=X(J)
    PI=IT=1.
    KK=0
    DO 100 J=1,19
    P=PI*IT+1.
    PI*IT=P
    SJ=0.
    SJMP=0.
    IF(P.GT.PB.AND.KK.EQ.0) GO TO 200
    IF(P.LT.P3) P=KNOCK(PWI,P)
    GO TO 93
200 DO 99 K=1,N
    AREA(K)=1.
 99 AREAP(K)=1.
    KK=1
 93 DO 110 I=1,N
    CALL SURVIV(P,X(I),SRV,SRVP)
    SRVIVE(I)=1.-AREA(I)+SRV*AREA(I)
    SRVIVP(I)=1.-AREAP(I)+SRVP*AREAP(I)
    SJ=SJ+SRVIVE(I)
110 SJMP=SJMP+SRVIVP(I)
    SRVRT(J+1)=SJ*100./N
    SRVPR(J+1)=SJMP*100./N
100 CONTINUE
    RETURN
    END
```

```
      SUBROUTINE SURVIV(P,X,SRV,SRVP)
      COMMON/BLK1/ SMX,SMXP
      DIMENSION SMX(19,14),SMXP(19,14)
      M1=P-1.0
      M2=M1+1
      IF(M1.LE.0) GO TO 99
      XM1=M1+1
      IF(X.GT.60.) GO TO 70
      K1=(X+5.)/5
      K2=K1+1
      XK1=K1*5.-5.
      SRV1 =SMX (M1,K1)+(X-XK1)/(5.)*(SMX (M1,K2)-SMX (M1,K1))
      SRV2 =SMX (M2,K1)+(X-XK1)/(5.)*(SMX (M2,K2)-SMX (M2,K1))
      SRV =SRV1 +(P-XM1)*(SRV2 -SRV1 )
      SRVP1=SMXP(M1,K1)+(X-XK1)/(5.)*(SMXP(M1,K2)-SMXP(M1,K1))
      SRVP2=SMXP(M2,K1)+(X-XK1)/(5.)*(SMXP(M2,K2)-SMXP(M2,K1))
      SRVP=SRVP1+(P-XM1)*(SRVP2-SRVP1)
      RETURN
70    SRV =SMX (M1,14)+(P-XM1)*(SMX (M2,14)-SMX (M1,14))
      SRVP=SMXP(M1,14)+(P-XM1)*(SMXP(M2,14)-SMXP(M1,14))
      RETURN
99    SRV=1.,
      SRVP=1.
      RETURN
      END
```

C.2.4 Translation Survivability Routine - Notes

MAIN Program: input variables

First card: Make of building

Second card: N - number of different areas within a building for which pertinent parameter S will be input ($N \leq 15$)

FCTR - array containing N values representing the fraction of the total survivability results attributable to each distinct area within the building

$$\left| \sum_{I=1,N} FCTR(I) = 1.0 \right|$$

Third and following cards (area parameter cards):

LR - length of room (ft)

WR - width of room (ft)

SH - height of window sill (ft)

WW - width of window (ft)

WH - height of window (ft)

RH - height of room (ft)

PB - failure overpressure of exterior wall (psi)

XW - distance to downwind wall; if XW > 60 ft then no wall is assumed.

A total of N area parameter cards are required in order with the FCTR array of the second card which prescribes the relative weight of the survivability results for each set of area parameters.

C.3 PROMPT NUCLEAR RADIATION MODEL

Sensitivity studies on the SEP code resulted in the survivability curves shown in Figs. C.1 through C.4. These curves apply to typical exterior walls over a range of window percentages. An interpolation routine for these curves was written.

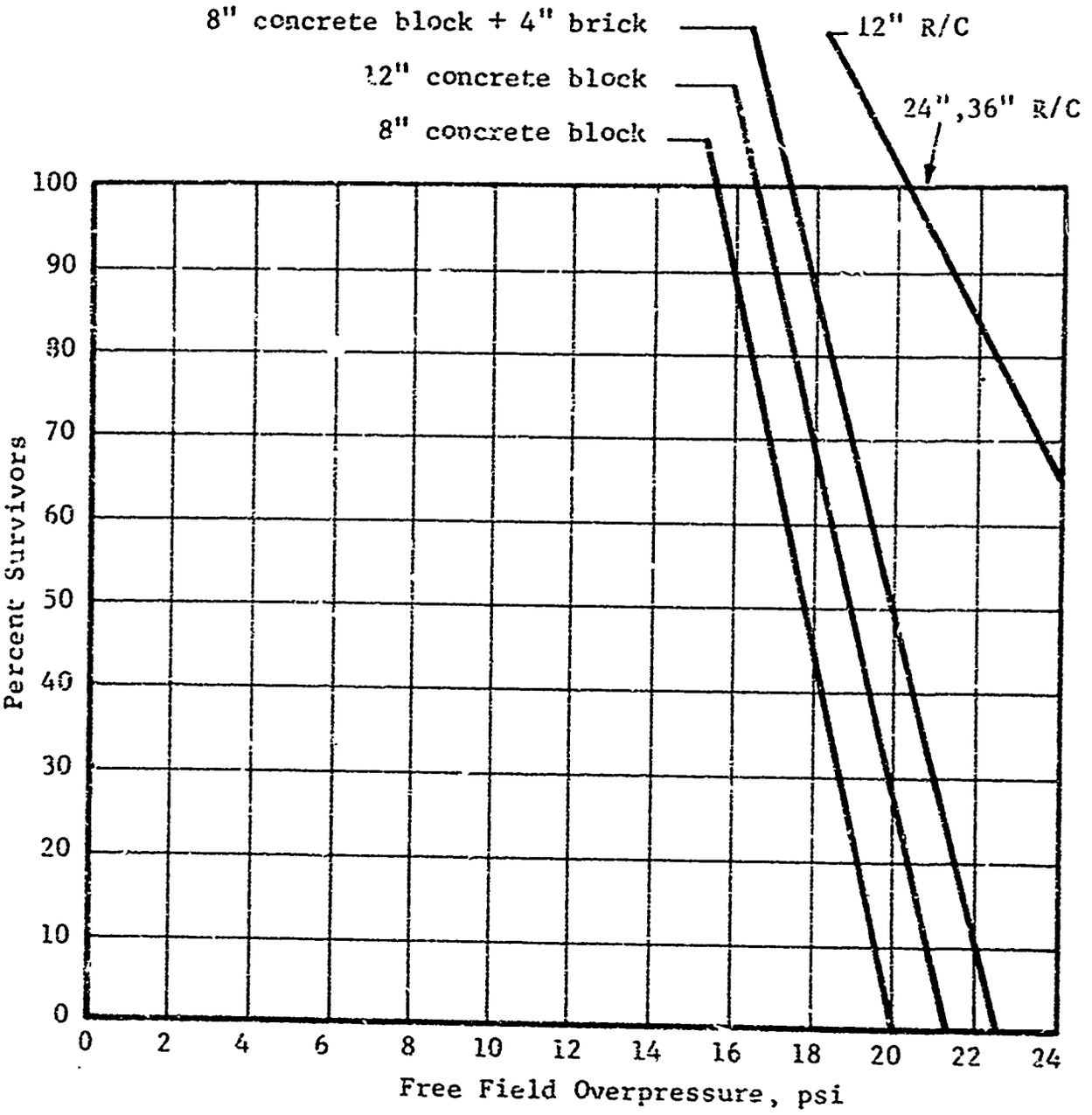

Fig. C.1 Variation of People Survivability with Overpressure (Ionizing Radiation 0 percent Windows)

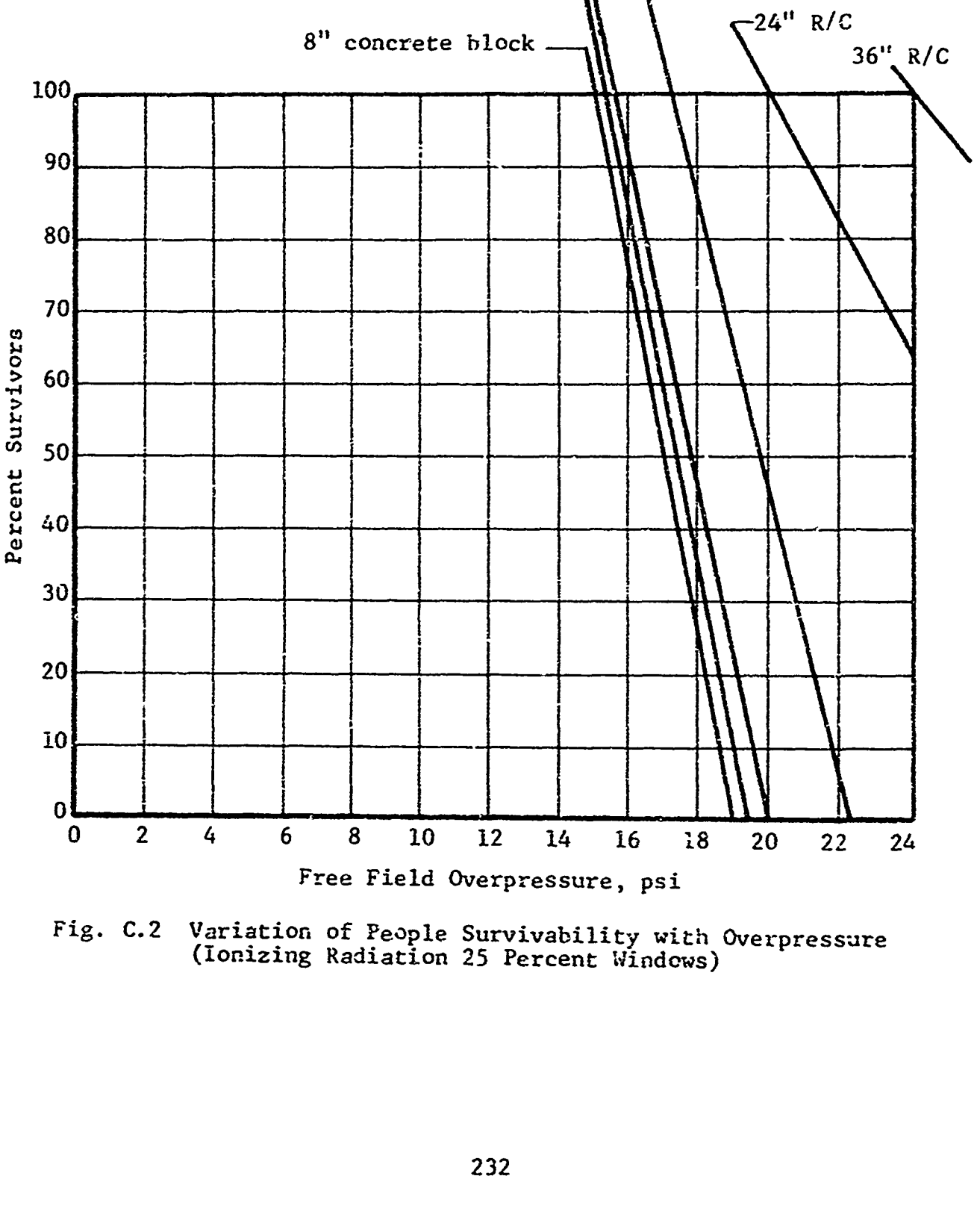

Fig. C.2 Variation of People Survivability with Overpressure (Ionizing Radiation 25 Percent Windows)

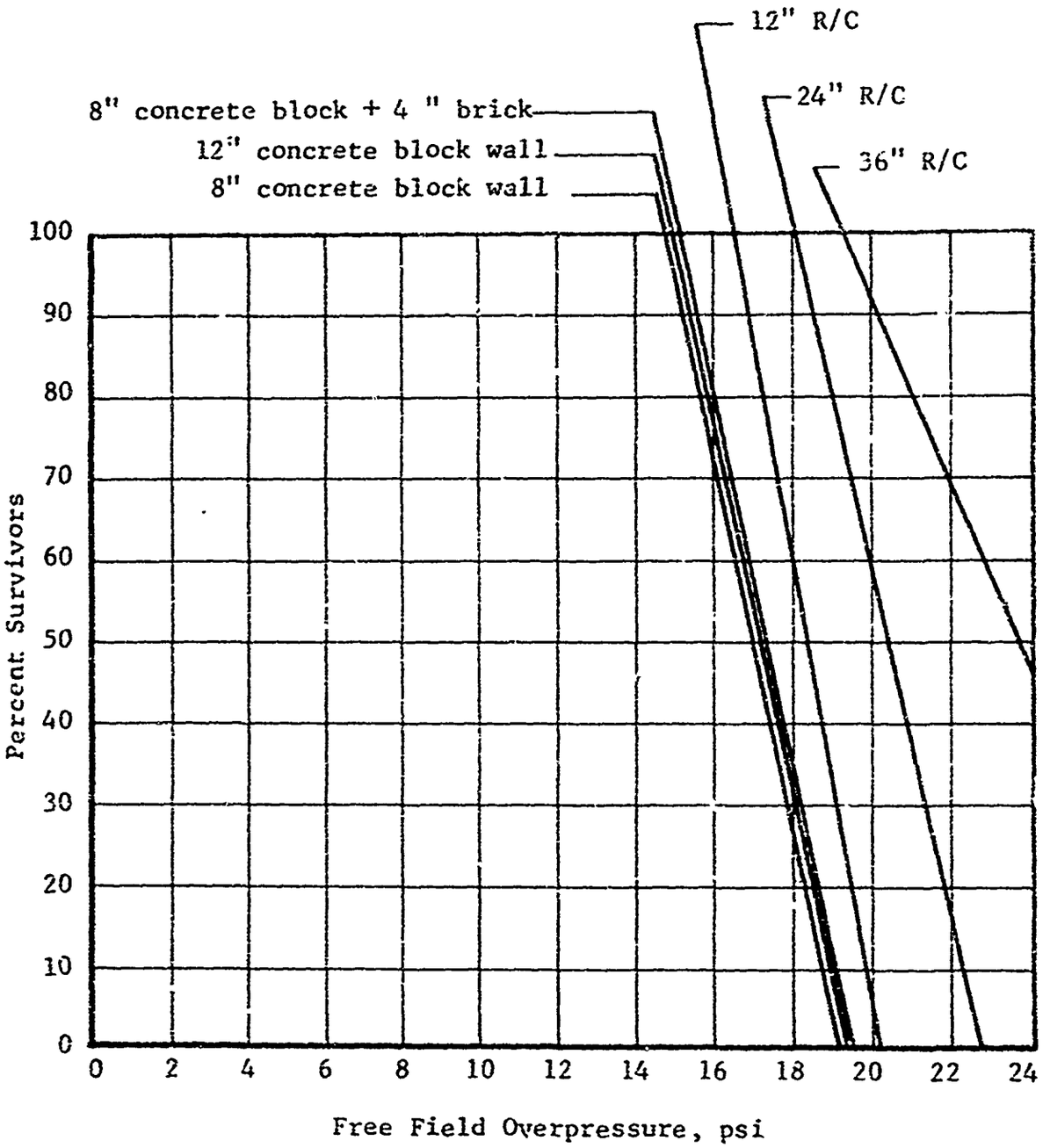

Fig. C.3 People Survivability with Overpressure (Ionizing Radiation 50 Percent Windows)

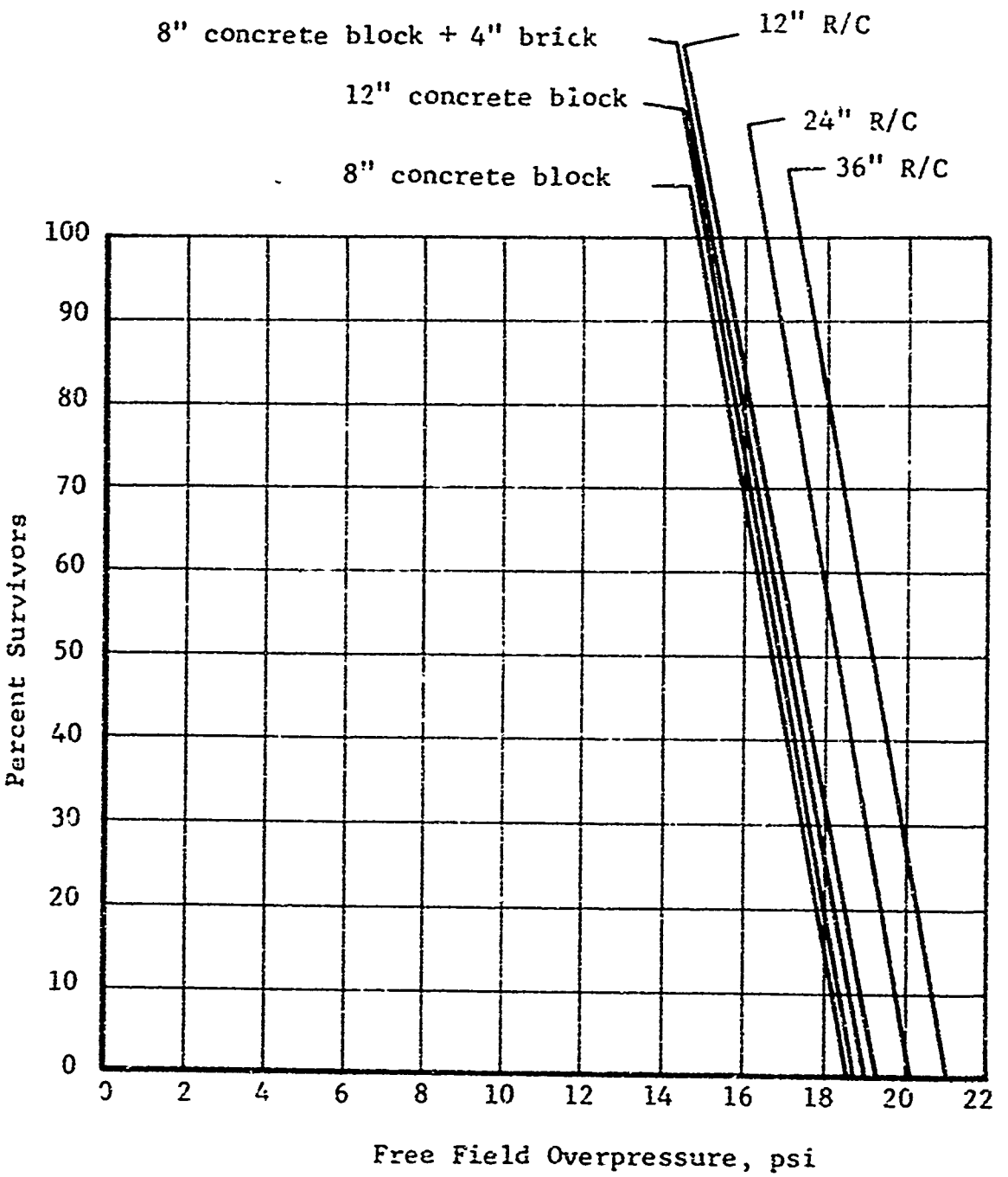

Fig. C.4 People Survivability with Overpressure (Ionizing Radiation 75 Percent Windows)

C.4 PRIMARY BLAST AND ACCELERATION

With regard to fatalities, primary blast and acceleration were found to be relatively inconsequential for typical buildings and were not included in survivability estimates. However, should injury criteria be considered both of these effects will need to be included.

C.5 DEBRIS MODEL

Debris results from the SEP code are used for the debris survivability model. Several parametric cases were run (see Fig. C.5) and many typical buildings can be assumed to fit one or a combination of these cases. Other buildings of markedly different characteristics are run independently on the SEP code. The debris survivability model is probably the least credible of all the routines, and it is hoped that continuing research into the problem, especially debris-people interaction, will resolve some of the uncertainties involved. The present routine represents the best estimates currently available.

C.6 THERMAL RADIATION MODEL

C.6.1 Description

During the parametric studies of the SEP code, it was determined that thermal radiation is not negligible, but neither is it a major mortality hazard. Due to the large amount of data required for operation of the code, a simplified thermal routine was implemented (Fig. C.6). Since the geometry of a ground level blast is very simple, the percentage of occupants of a building exposed to thermal radiation is easily determined. The parameter is based upon window size and outer room length, and was input to the routine along with sill height. Body area exposed was determined on the basis of sill height; exposed body area burned was based on the radiant exposure, and burn mortality was determined from the total body area burned. These data are identical to those currently used in the SEP code.

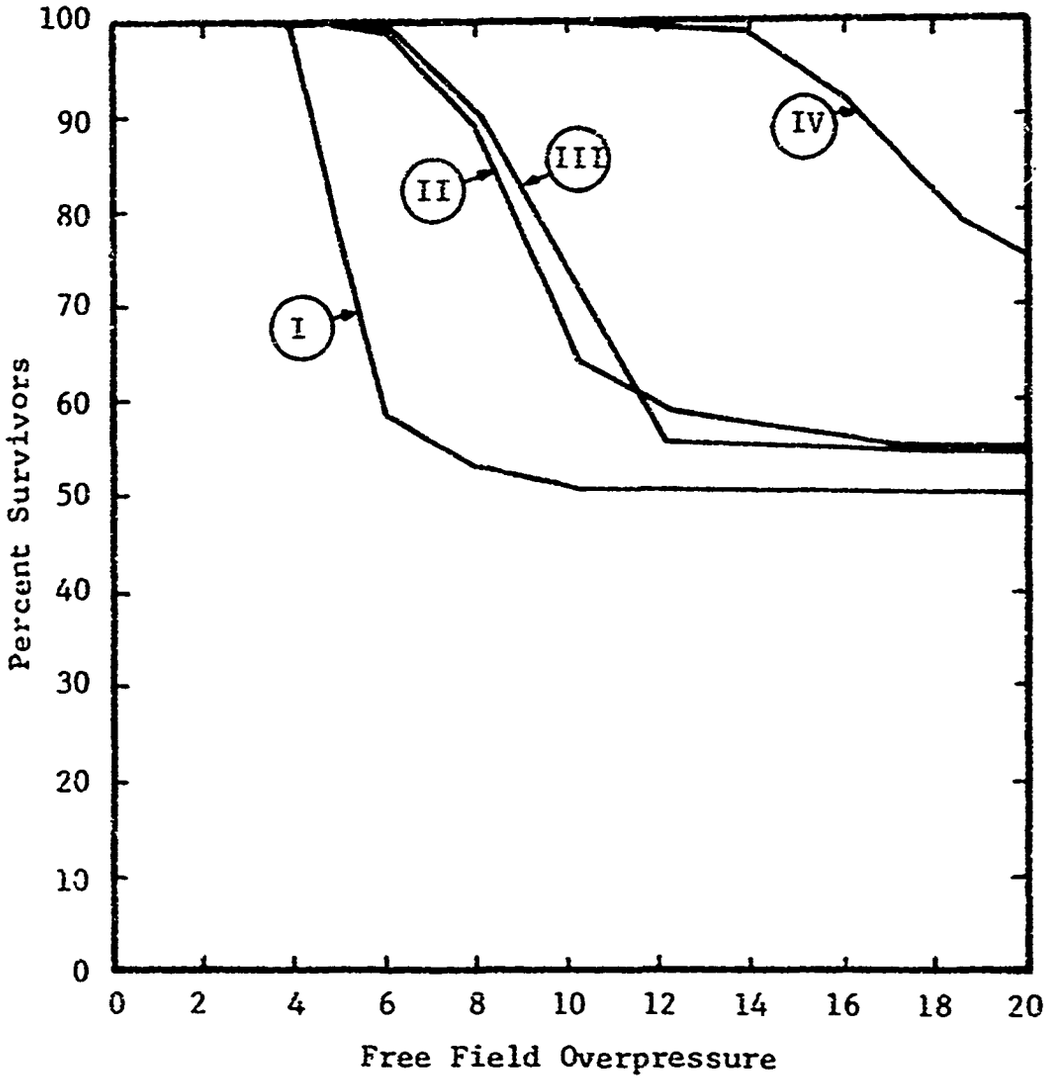

	I	II	III	IV
Inner room length	20 ft	20 ft	30 ft	30 ft
Outer room length	20 ft	30 ft	30 ft	20 ft
Wall height	10 ft	10 ft	12 ft	10 ft
Wall failure overpressure				
Outer Wall	5 psi	5 psi	8 psi	5 psi
Inner Wall	2 psi	2 psi	5 psi	2 psi
Fragment Size	Small	Large	Large	Very large

Fig. C.5 Debris Results

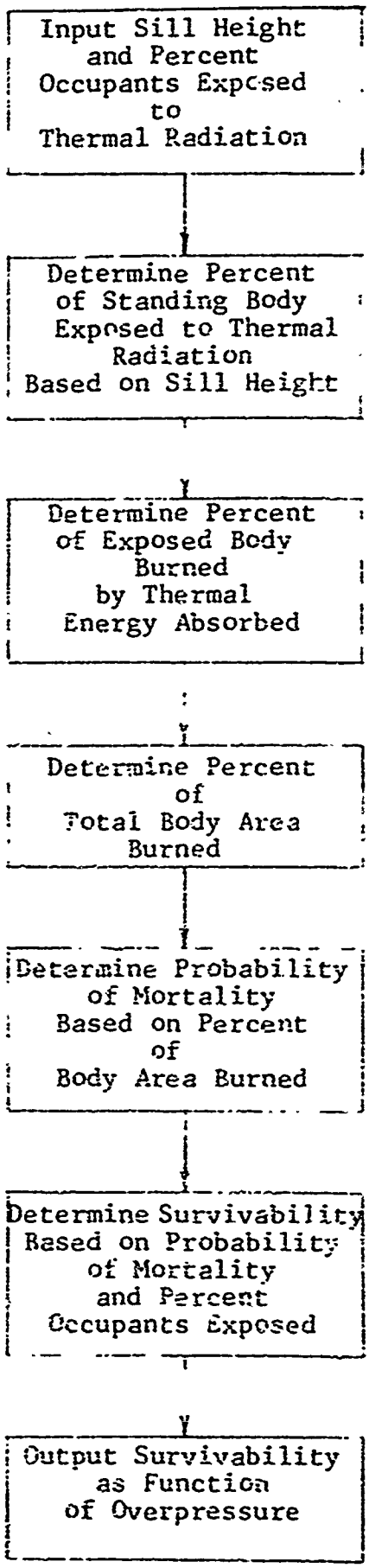

Fig. C.6 Flow Chart of Thermal Radiation Routine

C.6.2 Thermal Radiation Model - Listing

```
      DIMENSION TQ(19),NAME(10)
      DATA (TQ(N),N=1,19)/367.42,343.96,320.50,301.28,282.07,260.14,
     *238.14,215.90,193.47,176.41,159.35,143.20,127.05,106.52,
     *78.02,60.90,48.25,24.89,13.84/
   25 READ(5,2,END=1000)(NAME(N),N=1,10)
    2 FORMAT(10A6)
      READ(5,1)PERIX,SILHT
    1 FORMAT(2F10.3)
      WRITE(6,4)(NAME(N),N=1,10)
    4 FORMAT('1',10A6//1X,'THERMAL RADIATION SURVIVABILITY'//)
      WRITE(6,3)PERIX,SILHT
    3 FORMAT(/' PERCENT OCCUPANTS EXPOSED',F7.3//' SILL HEIGHT',F7.2)
      WRITE(6,4)(NAME(N),N=1,10)
      WRITE(6,5)
    5 FORMAT( 5(' '/),18X,'FREE FIELD',9X,'PERCENT'/17X,'OVERPRESSURE',
     *7X,'SURVIVORS'/)
      IF(SILHT.GT.5.76) GO TO 200
      PERBX=1.-(SILHT/5.76)
  200 PERBX=.4*PERBX
      DO 100 IL=1,19
      ENTRAN=.56*TQ(IL)
      IF(ENTRAN.LT.4.) GO TO 40
      IF (ENTRAN.GT.6.) GO TO 41
      BURN=8.35*ENTRAN-33.4
      GO TO 30
   41 IF(ENTRAN.GT.16.7) GO TO 42
      BURN=16.7
      GO TO 30
   42 BURN=1.3*ENTRAN-4.6
      IF(BURN.GT.100.) BURN=100.
      GO TO 30
   40 BURN=0.
   30 PERBAB=PERBX*BURN
      PERMOR=.6*PERBAB
      IF(PERBAB.GT.10.) PERMOR=1.4*PERBAB-8.
      IF(PERBAB.GT.20.) PERMOR=2.54*PERBAB-30.77
      IF(PERBAB.GT.33.) PERMOR=1.69*PERBAB-2.68
      IF(PERBAB.GT.49.) PERMOR=1.09*PERBAB+26.5
      IF(PERBAB.GT.60) PERMOR= .4*PERBAB+58.
      IF(PERBAB.GT.80.) PERMOR=100.
      PERSUR=100.-PERMOR*PERIX
      FFOP=21-IL
  100 WRITE(6,8)FFOP,PERSUR
    8 FORMAT(20X,F6.2,10X,F7.2/)
      GO TO 25
 1000 STOP
      END
```

C.6.3 Thermal Radiation Routine - Notes

Input Variables

First card: Name of building

Second card: PERIX - percentage of building occupants exposed to thermal pulse

SILHT - height of window sill (ft)

The variable PERIX is based on the fraction of the building area which is exterior rooms facing the blast. In addition, the fraction of window length as compared to total wall length on the exposed side of the building is included. The product of these two fractions expressed as a percentage is the percentage of people who are in direct line with the thermal pulse.

C.7 TOTAL SURVIVABILITY

Since survivability with respect to each hazard is determined separately for each overpressure level, the total survivability is taken as the product of the survivabilities for each hazard. Total survivability is determined for both standing and prone positions, and the results plotted as a function of free field overpressure at the building site.

PEOPLE SURVIVABILITY IN A DIRECT EFFECTS ENVIRONMENT AND RELATED TOPICS (Unclassified)
61 refs; 246 pp

Final Report

Contract DAHC 20-68-C-0126
DCPA Work Unit 1614D

IIT Research Institute
May 1973

ABSTRACT

This report describes a deterministic, computerized methodology for predicting the survivability (relative safety) of people located in conventional (NFSS) buildings when subjected to the direct effects of megaton range nuclear weapons. Individual effects considered include thermal radiation, prompt nuclear radiation, primary and secondary blast and debris. The computational process is described and illustrated by means of example problems.

Related topics include: distribution of blast-initiated debris, analysis of special permanent and expedient shelters relative to blast effects and a cost and survivability comparison of above- and below-grade shelters.

PEOPLE SURVIVABILITY IN A DIRECT EFFECTS ENVIRONMENT AND RELATED TOPICS (Unclassified)
61 refs; 246 pp

Final Report

Contract DAHC 20-68-C-0126
DCPA Work Unit 1614D

IIT Research Institute
May 1973

ABSTRACT

This report describes a deterministic, computerized methodology for predicting the survivability (relative safety) of people located in conventional (NFSS) buildings when subjected to the direct effects of megaton range nuclear weapons. Individual effects considered include thermal radiation, prompt nuclear radiation, primary and secondary blast and debris. The computational process is described and illustrated by means of example problems.

Related topics include: distribution of blast-initiated debris, analysis of special permanent and expedient shelters relative to blast effects and a cost and survivability comparison of above- and below-grade shelters.

PEOPLE SURVIVABILITY IN A DIRECT EFFECTS ENVIRONMENT AND RELATED TOPICS (Unclassified)
61 refs; 246 pp

Final Report

Contract DAHC 20-68-C-0126
DCPA Work Unit 1614D

IIT Research Institute
May 1973

ABSTRACT

This report describes a deterministic, computerized methodology for predicting the survivability (relative safety) of people located in conventional (NFSS) buildings when subjected to the direct effects of megaton range nuclear weapons. Individual effects considered include thermal radiation, prompt nuclear radiation, primary and secondary blast and debris. The computational process is described and illustrated by means of example problems.

Related topics include: distribution of blast-initiated debris, analysis of special permanent and expedient shelters relative to blast effects and a cost and survivability comparison of above- and below-grade shelters.

PEOPLE SURVIVABILITY IN A DIRECT EFFECTS ENVIRONMENT AND RELATED TOPICS (Unclassified)
61 refs; 246 pp

Final Report

Contract DAHC 20-68-C-0126
DCPA Work Unit 1614D

IIT Research Institute
May 1973

ABSTRACT

This report describes a deterministic, computerized methodology for predicting the survivability (relative safety) of people located in conventional (NFSS) buildings when subjected to the direct effects of megaton range nuclear weapons. Individual effects considered include thermal radiation, prompt nuclear radiation, primary and secondary blast and debris. The computational process is described and illustrated by means of example problems.

Related topics include: distribution of blast-initiated debris, analysis of special permanent and expedient shelters relative to blast effects and a cost and survivability comparison of above- and below-grade shelters.

UNCLASSIFIED

Security Classification

DOCUMENT CONTROL DATA - R & D

(Security classification of title, body of abstract and indexing annotation must be entered when the overall report is classified)

1. ORIGINATING ACTIVITY (Corporate author) IIT Research Institute 10 West 35th Street Chicago, Illinois 60616	2a. REPORT SECURITY CLASSIFICATION Unclassified 2b. GROUP

3. REPORT TITLE

PEOPLE SURVIVABILITY IN A DIRECT EFFECTS ENVIRONMENT AND RELATED TOPICS

4. DESCRIPTIVE NOTES (Type of report and inclusive dates)

Final Report

5. AUTHOR(S) (First name, middle initial, last name)

A. Longinow, G. Ojdrovich, L. Bertram, A. Wiedermann

6. REPORT DATE	7a. TOTAL NO. OF PAGES	7b. NO. OF REFS
May 1973	246	61

8a. CONTRACT OR GRANT NO. DAHC 20-68-C-0126 b. PROJECT NO. Work Unit 1614D c. d.	9a. ORIGINATOR'S REPORT NUMBER(S) J6144 9b. OTHER REPORT NO(S) (Any other numbers that may be assigned this report)

10. DISTRIBUTION STATEMENT

Approved for Public Release; Distribution Unlimited.

11. SUPPLEMENTARY NOTES	12. SPONSORING MILITARY ACTIVITY
	Defense Civil Preparedness Agency Washington, D.C. 20310

13 ABSTRACT

This report describes a deterministic, computerized methodology for predicting the survivability (relative safety) of people located in conventional (NFSS) buildings when subjected to the direct effects of megaton range nuclear weapons. Individual effects considered include thermal radiation, prompt nuclear radiation, primary and secondary blast and debris. The computational process is described and illustrated by means of example problems.

Related topics include: distribution of blast-initiated debris, analysis of special permanent and expedient shelters relative to blast effects and a cost and survivability comparison of above- and below-grade shelters.

DD FORM 1 NOV 68 1473 REPLACES DD FORM 1473, 1 JAN 64, WHICH IS OBSOLETE FOR ARMY USE.

UNCLASSIFIED

Security Classification